WL-TR-96-2019

ATARR UNCERTAINTY ANALYSIS

C. Halderman   M. Dunn

Calspan Corp
Advanced Technology Center
PO Box 400
Buffalo NY 14225

MARCH 1991

FINAL

DTIC QUALITY INSPECTED 4

19961011 120

NOTICE

WHEN GOVERNMENT DRAWINGS, SPECIFICATIONS, OR OTHER DATA ARE USED FOR ANY PURPOSE OTHER THAN IN CONNECTION WITH A DEFINITELY GOVERNMENT-RELATED PROCUREMENT, THE UNITED STATES GOVERNMENT INCURS NO RESPONSIBILITY OR ANY OBLIGATION WHATSOEVER. THE FACT THAT THE GOVERNMENT MAY HAVE FORMULATED OR IN ANY WAY SUPPLIED THE SAID DRAWINGS, SPECIFICATIONS, OR OTHER DATA, IS NOT TO BE REGARDED BY IMPLICATION, OR OTHERWISE IN ANY MANNER CONSTRUED, AS LICENSING THE HOLDER, OR ANY OTHER PERSON OR CORPORATION; OR AS CONVEYING ANY RIGHTS OR PERMISSION TO MANUFACTURE, USE, OR SELL ANY PATENTED INVENTION THAT MAY IN ANY WAY BE RELATED THERETO.

THIS REPORT IS RELEASABLE TO THE NATIONAL TECHNICAL INFORMATION SERVICE (NTIS). AT NTIS, IT WILL BE AVAILABLE TO THE GENERAL PUBLIC, INCLUDING FOREIGN NATIONS.

THE TECHNICAL REPORT HAS BEEN REVIEWED AND IS APPROVED FOR PUBLICATION.

CHRISTIAN E. RANDELL, Lt, USAF
Turbine Design Engineer
Turbine Engine Division

CHARLES D. MacARTHUR
Chief, Turbine Branch
Turbine Engine Divsion

RICHARD J. HILL
Chief of Technology
Turbine Engine Division
Aero Propulsion & Power Directorate

IF YOUR ADDRESS HAS CHANGED, IF YOU WISH TO BE REMOVED FROM OUR MAILING LIST, OR IF THE ADDRESSEE IS NO LONGER EMPLOYED BY YOUR ORGANIZATION PLEASE NOTIFY WL/POTT WPAFB OH 45433-7251 HELP MAINTAIN A CURRENT MAILING LIST.

COPIES OF THIS REPORT SHOULD NOT BE RETURNED UNLESS RETURN IS REQUIRED BY SECURITY CONSIDERATIONS, CONTRACTUAL OBLIGATIONS, OR NOTICE ON A SPECIFIC DOCUMENT.

REPORT DOCUMENTATION PAGE

1. AGENCY USE ONLY *(Leave blank)*	2. REPORT DATE Mar 91	3. REPORT TYPE AND DATES COVERED Final

4. TITLE AND SUBTITLE

ATARR Uncertainty Analysis

5. FUNDING NUMBERS
C: F33615-88-C-2825
PE: 62203F
PR: 3066
TA: 06
WU: 84

6. AUTHOR(S)

C. Halderman   M. Dunn

7. PERFORMING ORGANIZATION NAME(S) AND ADDRESS(ES)
Calspan Corp
Advanced Technology Ctr
PO Box 400
Buffalo NY 14225

8. PERFORMING ORGANIZATION REPORT NUMBER

9. SPONSORING/MONITORING AGENCY NAME(S) AND ADDRESS(ES)
Aero Propulsion & Power Directorate
Wright Laboratory
Air Force Materiel Command
Wright-Patterson AFB OH 45433-7251
POC: Lt Christian Randell, WL/POTT, WPAFB OH, 513-255-3150

10. SPONSORING/MONITORING AGENCY REPORT NUMBER

WL-TR-96-2019

11. SUPPLEMENTARY NOTES

12a. DISTRIBUTION/AVAILABILITY STATEMENT

Approved for public release; distribution is unlimited

12b. DISTRIBUTION CODE

13. ABSTRACT *(Maximum 200 words)*
The Wright-Patterson Air Force Base Advanced Turbine Aerothermal Research Rig (ATARR) is a short-duration, turbine stage testing facility. The ATARR facility is designed for a nominal 2-second run time. This long run time created the requirement for fast-acting shut-off valves to avoid over-heating the eddy brake system and other potential emergency situations. In addition, the ATARR facility will be used to test a wide variety of turbines, necessitating frequent modification to the main test section. Finally, one of the main applications of the ATARR facility will be aero-performance measurements.

14. SUBJECT TERMS

Uncertainity Analysis

15. NUMBER OF PAGES
154

16. PRICE CODE

17. SECURITY CLASSIFICATION OF REPORT Unclassified	18. SECURITY CLASSIFICATION OF THIS PAGE Unclassified	19. SECURITY CLASSIFICATION OF ABSTRACT Unclassified	20. LIMITATION OF ABSTRACT SAR

TABLE OF CONTENTS

Introduction

I.1 Description of the Wright-Patterson Air Force Base ATTAR Turbine Testing Facility

The Wright-Patterson Air Force Base Advanced Turbine Aerothermal Research Rig (ATARR) is a short-duration, turbine stage testing facility similar in configuration to the blowdown turbine facility at MIT's Gas Turbine Lab. Both facilities have common design goals, to match the corrected mass flow and speed of a typical turbine, and to match the proper non-dimensional parameters which influence heat transfer and pressure distributions across the stage. Despite the similarities there are some distinct differences between the two facilities. The ATARR facility is designed for a nominal 2 second run time as compared to MIT's 0.5 second. This long run time created the requirement for fast-acting shut-off valves to avoid over-heating the eddy brake system and other potential emergency situations. In addition, the ATARR facility will be used to test a wide variety of turbines, necessitating frequent modification to the main test section. Finally, one of the main applications of the ATARR facility will be aero-performance measurements, versus the heat transfer focus of the MIT facility.

I.2 The Different Roles of Short-Duration and Long-Duration Testing Facilities in Gas Turbine Research

The ATARR facility is substantially different from long-duration facilities. Since there are approximately 10,000 events a second (a rotor blade passing a nozzle guide vane), the flow appears to be in a quasi-steady state condition from the rotor standpoint. However, due to the short duration of a test, the flowpath remains in a condition which is close to being isothermal rather than the near adiabatic condition found in most long-duration facilities. The differences between these two thermodynamic processes have been estimated to be on the order of 1%[1] in the ATARR facility. The ATARR facility provides the ability to do controlled research on the complicated three-dimensional unsteady flow which occurs in turbines. But to use a short-duration facility only for verification of data taken in long-duration facilities is to under-utilize an impressive and valuable resource. It's ability to provide time-resolved measurements accurately and inexpensively can be used to complement the data obtained in long-duration facilities.

Since a turbine in the ATARR facility is dynamically similar to that component in its actual operating environment, the fluid flow and heat transfer results obtained in this facility are scaled versions of those in a real engine. The resulting measurements are much more representative of the heat transfer and fluid environment than data obtained in standard long-duration testing facilities where the proper non-dimensional fluid properties cannot all be

matched. However, representative measurements in all types of facilities come at some cost. In a long-duration rig the costs are extensive and the test instrumentation limited by the testing environment. A short-duration facility requires the development of fast-response instrumentation and the modification of many personal perceptions concerning short-duration testing.

In a long-duration rig, the efforts are aimed at developing average measurements which generally lead to a calculated efficiency. The use of efficiency as an evaluation criterion is not surprising since one of the standards by which engines are sold is overall efficiency. However, the fundamental fluid process which occurs in an engine is unsteady in nature. While the amalgamated number which represents the "efficiency" of an engine is one which could be used in fuel consumption calculations, it can not be traced backwards to tell how to improve the engine. Thus the difference between evaluation testing and development research on gas turbines. The single amalgamated efficiency is a measure of the present state of engine technology; it can not be used as a diagnostic tool. In a short-duration facility, (which can resolve the underlying unsteadiness associated with the turbine rotor), time-resolved measurements of the heat-flux and pressure can be made on the turbine components. These measurements when used in conjunction with computational codes have the potential of leading to significant improvements in engine performance.

I.3 Efficiency and its Dependence on the Testing Process

Efficiency is not the only topic of interest to manufactures and researchers, but this property, with others such as total thrust and specific fuel consumption, define the operation of the engine as a unit. Improved understanding of the heat flux and pressure distribution along engine components contributes to better understanding of component efficiency, which in turn improves the engine efficiency.

While the ATARR facility allows the study of turbulence, pressure and temperature profiles, and cooling on different turbine stage configurations, the overall efficiency of the stage is still an important parameter. Being able to measure the stage efficiency accurately is of great importance to the facility, not so much for the direct information it provides, but rather for the skill and documentation this task generates.

It is important to be able to efficiency accurately in the ATARR facility so that one can compare data obtained with those obtained in other test rigs. But tan associated benefit is that to obtain an efficiency measurement accurate to 0.25% requires measurements of temperature and pressure which are generally much more accurate. In addition, it requires a detailed knowledge of where the errors occurred in these measurements, and how they are propagated through the experiment to achieve the final result. To make any claim about efficiency measurements which

2

are accurate to 0.25% believable requires that the reduction process be well documented. Measuring efficiency accurately in the ATARR facility becomes the test of the facility and data reduction process integrity. This paper is a documentation of the different components which needed to be addressed in order to produce an efficiency accuracy of 0.25% (the definition is listed below in table I-1).

Table I-1

Definition of Efficiency Accuracy Goal for the ATARR Facility

The goal of the ATARR facility is to measure efficiency to ±0.25% of the true value within a 95% confidence limit. If η represents the turbine stage efficiency then the calculated efficiency is expected to reside within the range $\eta - \Delta\eta \leq \eta \leq \eta + \Delta\eta$ 95% of the time, where $\Delta\eta/\eta = 0.25\%$. Thus, $\Delta\eta = 2\sigma$, where σ represents the standard deviation of the measurements. All accuracies in this paper will be expressed as relative errors to the 95% confidence level.

Before proceeding with this paper it is important to note that the 0.25% level of accuracy desired may be overwhelmed by the relative inaccuracy which comes from comparing data from different facilities. As Guenette, Epstein and Ito[2] have shown, the only proper way of comparing efficiencies taken from different facilities is to "correct" the indicated efficiency to account for losses and obtain an efficiency measure which is independent of the test process. In long-duration test facilities uncooled turbines operate at conditions which are very close to being adiabatic, while short-duration facilities operate at conditions very close to being isothermal[3]. To compare measurements taken in these two facilities one has to correct for the fundamental differences in the process. Using Guenette's notation, the efficiency measured in any facility (assuming constant mass flow) is given by:

$$\eta = \frac{h_1 - h_2}{h_1 - h_{2,is}}$$

(I-1)

Where the subscripts 1 and 2 represent the conditions upstream and downstream of the stage, respectively and $h_{2,is}$ represents the resulting enthalpy of the fluid if it were to be expanded isentropically through the actual measured pressure ratio. To calculate the adiabatic efficiency one would have to account for all possible sources of energy loss in the turbine stage. This would include heat transfer effects and possible mass flow leakage through seals. This accounting process has to be done since any energy lost in this manner is not available to do work on the turbine. If these losses are labeled as Q then the adiabatic efficiency is:

$$\eta_{ad} = \frac{h_1 - h_2 - Q}{h_1 - h_{2,is}}$$

(I-2)

which is related to the indicated efficiency by:

$$\eta_{ad} = \eta - \frac{Q}{h_1 - h_{2,is}}$$

(I-3)

In general, long-duration facilities are assumed to have no heat losses (although this assumption has to be verified for each facility) and negligible mass flow losses implying that Q=0. If one could be convinced that the losses in a long-duration facility were indeed very small, then Q could be neglected and h_2 would become an adiabatic enthalpy downstream of the rotor $h_{2,ad}$ and the efficiency in a long-duration facility would be the same as the adiabatic efficiency[4]:

$$\eta_{ad} = \frac{h_1 - h_{2,ad}}{h_1 - h_{2,is}} \qquad (I-4)$$

In a short-duration facility, the indicated efficiency will be[5]

$$\eta_{ind} = \frac{h_1 - h_2}{h_1 - h_{2,is}} \qquad (I-5)$$

However, in this case there will be heat transfer because of the isothermal nature of the facility and h_2 would need to be corrected for these losses. Assuming that Q_{SD} represents the losses in the short duration facility, the stage efficiency would be:

$$\eta_{SD} = \frac{h_1 - h_2 - Q_{SD}}{h_1 - h_{2,is}} \qquad (I-6)$$

and the efficiency measured in a short-duration facility is related to the efficiency measured in an adiabatic facility by[6]:

$$\eta_{ad} = \eta_{SD} - \frac{h_{2,ad} - h_2 - Q_{SD}}{h_1 - h_{2,is}} \qquad (I-7)$$

Thus to convert an efficiency measurement in any testing facility to an adiabatic efficiency requires the knowledge of two of three variables: h_2, $h_{2,ad}$, of Q

To avoid the problem of trying to determine Q accurately in a short-duration facility, a second method, using the work extracted by the turbine, can determine the actual change in enthalpy across the stage.

$$W = h_1 - h_2 - Q_{SD} \qquad (I-8)$$

where Q_{SD} represents the available work lost due to labyrinth seal loss and heat transfer. Then W could replace the numerator in equation I-6. These two methods are commonly referred to as the thermodynamic method and the mechanical method for measuring efficiency. While the conceptual relationship between the adiabatic and isothermal efficiencies is easy to understand, the adiabatic flow enthalpy downstream of the rotor is not an easy thing to calculate accurately. Guenette et al. have shown that the correction needed for efficiency measurements in short-duration facilities is approximately 1% for a two second test duration[7]. Thus to make corrections for the different types of facilities requires an accurate knowledge of the adiabatic enthalpy.

4

I.4 Required Accuracy on Instrumentation as a Function of Stage Configuration for an Uncooled Adiabatic Turbine

To provide an idea of the instrumentation accuracy needed to achieve the efficiency accuracy listed in table 1-1, and how the stage configuration effects this accuracy, the simple case of an uncooled adiabatic (no losses) turbine will be examined. For this configuration the efficiency is given as:

$$\eta = \frac{1-\tau}{1-\Pi^{\frac{\gamma-1}{\gamma}}} \tag{I-9}$$

where η is the efficiency; γ is C_p/C_v for the gas at the turbine inlet (assumed to be constant across the stage); τ is the total temperature ratio across the turbine stage (defined as T_{t2}/T_{t1} where location 1 is upstream of the stage and location 2 is downstream). Π is the total pressure ratio defined in a similar manner P_{t2}/P_{t1}. Assuming that the uncertainties in the measurements are random and normally distributed, they can be propagated through to achieve the resulting uncertainty in efficiency using equation I-10.

$$\frac{\Delta\eta}{\eta} = [\sum_{i=1}^{n} ((\frac{\partial\eta}{\partial x_i})(\frac{x_i}{\eta})(\frac{\Delta x_i}{x_i}))^2]^{\frac{1}{2}} \tag{I-10}$$

(the subscript i refers to the ith variable). Doing the partial derivatives one gets:

$$\frac{\Delta\eta}{\eta} = [(C_\tau(\frac{\Delta\tau}{\tau}))^2 + (C_\Pi(\frac{\Delta\Pi}{\Pi}))^2 + (C_\gamma(\frac{\Delta\gamma}{\gamma}))^2]^{\frac{1}{2}} \tag{I-11}$$

where C_τ, C_Π and C_γ can be interpreted as the influence coefficients of that variable on the final efficiency uncertainty.

$$C_\tau = (\frac{-\tau}{1-\tau}) \; ; \; C_\Pi = (\frac{\gamma-1}{\gamma})(\frac{\Pi^{\frac{\gamma-1}{\gamma}}}{1-\Pi^{\frac{\gamma-1}{\gamma}}}) \; ; \; C_\gamma = \frac{\ln(\Pi)}{\gamma}(\frac{\Pi^{\frac{\gamma-1}{\gamma}}}{1-\Pi^{\frac{\gamma-1}{\gamma}}}) \tag{I-12}$$

A new variable (called the r factor in this paper) can be defined as:

$$r = \Pi^{\frac{\gamma-1}{\gamma}} \tag{I-13}$$

and then equations I-9 and I-12 can be rewritten as:

$$\eta = \frac{1-\tau}{1-r} \tag{I-14}$$

5

$$C_\tau = (\frac{-\tau}{1-\tau}) \; ; \; C_\Pi = (\frac{\gamma-1}{\gamma})(\frac{r}{1-r}) \; ; \; C_\gamma = \frac{\ln(\Pi)}{\gamma}(\frac{r}{1-r})$$

<div align="right">(I-15)</div>

To see how the instrument accuracies vary with stage configurations we can imagine the test turbines ranging in pressure ratios from 0.5 to 0.2, γ from 1.2 to 1.4, and efficiencies from 0.8 to 0.95. Using these values we find that r varies from about .63 to .89. Thus for different efficiencies we can find τ. If any one measurement was examined (consider τ as an example), and the others were ignored (which is the same as suggesting that they are perfectly accurate) then the accuracy of the instrument under consideration is:

$$\frac{\Delta\tau}{\tau} = [\frac{1}{C_\tau^2}]^{\frac{1}{2}} \frac{\Delta\eta}{\eta}$$

<div align="right">(I-16)</div>

To achieve an efficiency accuracy of 0.25%, the instrument can be no more inaccurate than the results listed below.
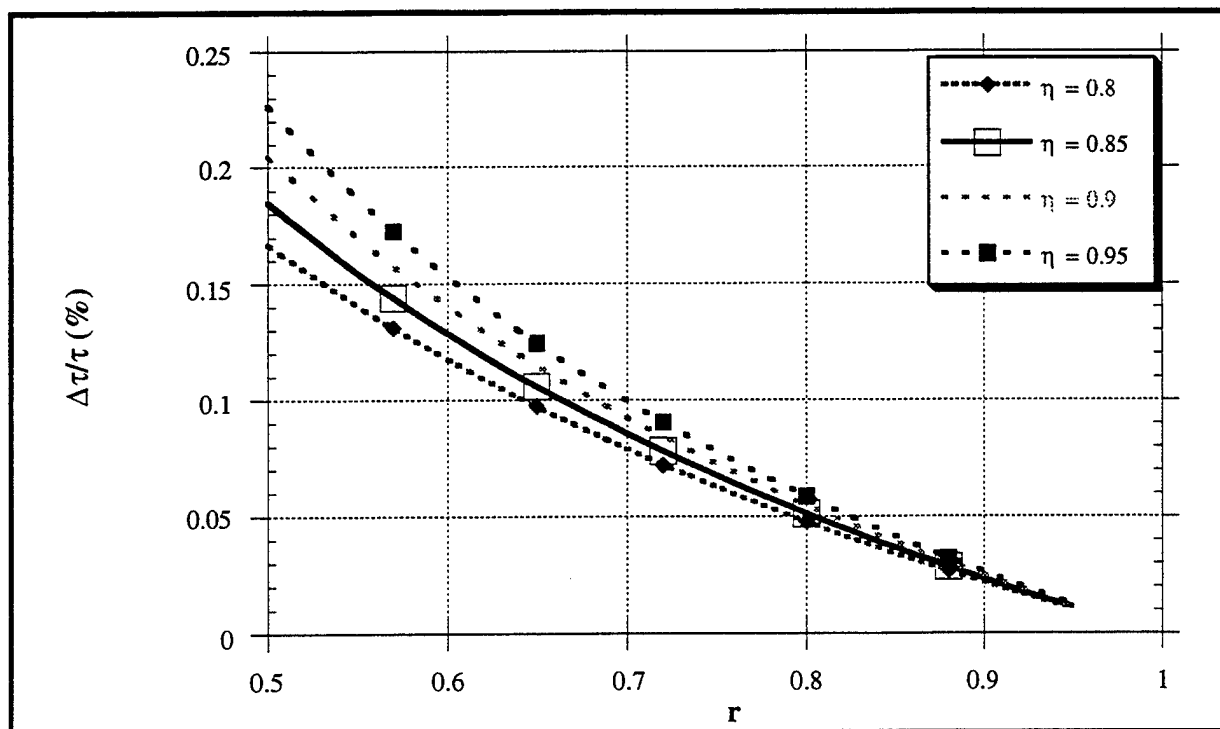
Figure I-1   Plot of $\Delta\tau/\tau$ versus r for Different Efficiencies
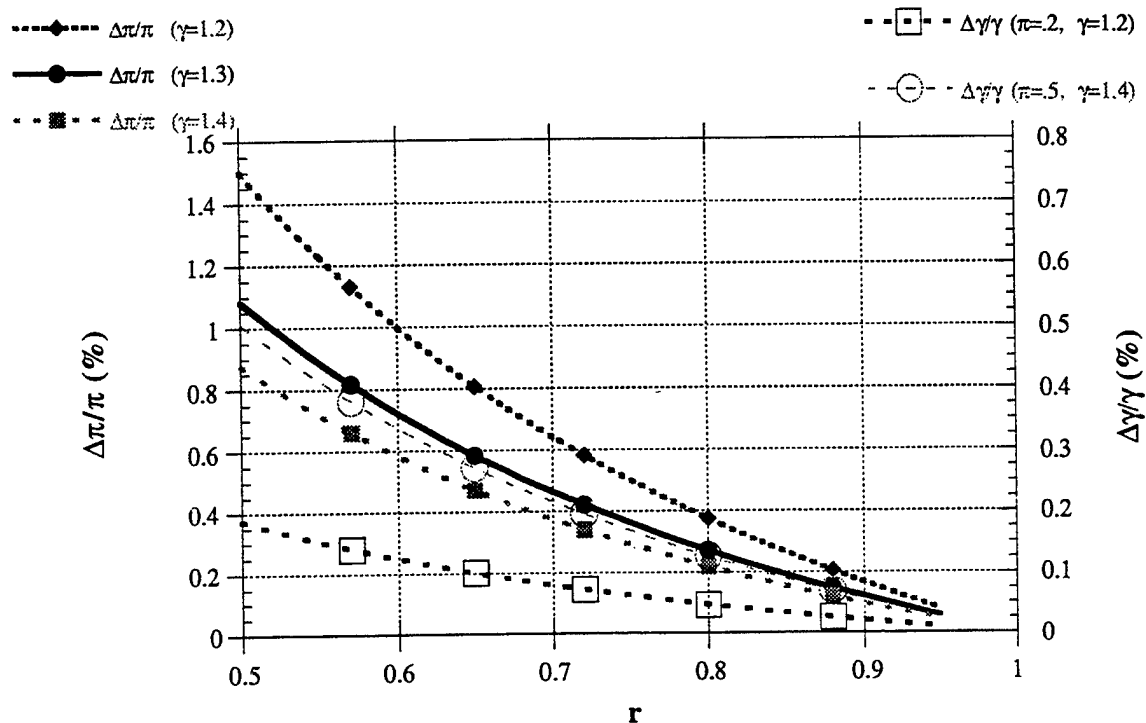
Figure I-2 Plot of $\Delta\pi/\pi$ and $\Delta\gamma/\gamma$ versus r for Different Parameters

As one can see in figure I-1, the required accuracy of the temperature ratio measurement varies dramatically with r. The low end of r corresponds to a high pressure ratio (0.2) and a high γ (1.4) test condition. For most modern turbines r is between .7 and .8. At this level there is not much of a dependency on the turbine efficiency, but to achieve a 0.25% accurate efficiency measurement τ has to be better then .075%. Since τ is really dependent on two measurements T_1, and T_2, if the accuracies of each of these measurements were equal, then the overall accuracy of the individual temperature measurement would be about .053% (.075% / $\sqrt{2}$). If one were to test a turbine at a higher value of r then each temperature measurement would need to be about .021% accurate, or at 550 °K, 0.1 °K accurate.

Better news is that the pressure ratio is not as important as the temperature ratio. In fact the influence coefficient is less than one for the pressure ratio so that a higher inaccuracy can be tolerated on the pressure measurements (see the left hand axis, figure 1-2) and the influence coefficient varies around one for γ (right hand axis, figure 1-2).

From this model one can see that the instrumentation needs vary with the turbine test parameters, and that unless one is careful, it would be possible to design instrumentation appropriate to obtain the desired efficiency accuracy for one turbine, but not for another.

1.5 The Purpose and Outline of the Paper

This paper has several goals. Primarily it is to document the methods and techniques which will be used in the uncertainty analysis at the ATARR facility, and thus, ultimately the

turbine stage efficiency accuracy. This paper can also be used as a basis for future work. One which uses the techniques suggested by Moffat[8], to derive uncertainty milestones which the different components of the facility will have to meet as they are installed, thus simplifying the shakedown process of the facility. The second would be to develop an error budget for the specific turbine being studied.

With these goals in mind the paper is divided into six main sections. The first section presents some of the analytical tools and definitions which are used in the analysis. The different roles of measurement errors, instrument calibration, statistical analysis, and error propagation. The second section derives the uncertainty in the efficiency analysis for two different ways of measuring the stage efficiency (either thermodynamically, or through work extraction) for cooled, partially cooled, and uncooled stage configurations as a function of measurement error.

The next three sections use the techniques of section 1 to flesh out the results of section 2. In the third section, the questions about the assumptions of the facility are answered. Concerns such as real gas effects and the definition of the gas properties are defined. The fourth section discusses the error introduced in the gas properties through the supply tank filling process. The fifth section deals with the problems of measuring the mass flow. The final section provides a quick overview of the facility instrumentation and discusses the future work which needs to be done in order to shake-down the facility.

References and Footnotes for the Introduction

Epstein, Alan, Gerald Guenette and Robert Norton "The Design of the MIT Blowdown Turbine Facility", GTL Report no 183, April 1985

[1] Guenette, G.R., A.H. Epstein and E. Ito "Turbine Aerodynamic Performance Measurements in Short Duration Facilities"; AIAA-89-2690, AIAA/ASME/SAE/ASEE 25th Joint Propulsion Conference, Monterey, CA July 10-12, 1989, p. 7

[2] Ibid

[3] Ibid, p. 5

[4] Ibid, equation 2, p. 6

[5] Ibid, equation 4, p. 6

[6] Ibid, equation 6, p. 6

[7] Ibid, p. 8

[8] Moffat, R. J. "Contributions to the Theory of Single-Sample Uncertainty Analysis"; Transactions of the ASME, Vol. 104, June 1982, pp. 250-260.

Section 1: Definitions and Analytical Concepts

Throughout this paper a variety of terms will be used in the evaluation of the efficiency uncertainty. Some of these are relatively basic, others are more subtle; some are highly context dependent, while others are quite general. There is always a trade-off between outlining all the "analytic tools" one will use at the beginning of a paper, and discussing them as they are needed in the course of the analysis. The former approach allows the development of the tools independently of the context creating a more concentrated approach to the real problems posed in the analysis without having to take repeated tangents to develop the analytic tools necessary. The latter approach provides both an appropriate context and a limit to how deeply the analytic tools need to be discussed. In the former approach there is always the possibility that topics which require volumes to do the appropriate detailed analysis will only be discussed lightly, resulting in a entirely unsatisfactory treatment of the subject.

In this paper, we have decided to break this category of "auxiliary analysis" into two different groups, those which are highly context dependent and those which are more general. This section will discuss the more general components such as the definition of measurement error and its relationship to instrument calibration, the uses of statistical analysis in this facility, and the different techniques which are used in error propagation. Other topics such as real gas effects, gas property standards and instrumentation practices are more context dependent and are dealt with either in later sections as they become important, or in separate appendices.

1.1 Measurement Error

Throughout the uncertainty analysis, a major concern will be how measurements of the fundamental properties in the facility: total temperature, total pressure and static pressure, influence some derived property, whether it be efficiency or other parameters such as the mass flow. To understand how the uncertainty in the measurements is translated into uncertainty in the derived quantity, one has to understand the basic definition of measurement uncertainty.

It is clear that the measurement uncertainty depends directly on the instrument calibration, but it also depends on the physical phenomenon being measured and the assumptions made about that phenomenon. If one was trying to measure a flow property (temperature for instance) at one specific location (radial, circumferential and axial), then the measurement error would depend only on the calibration error of the instrument. If the measurement at this one location was intended to represent the total flow field at this axial location, then the measurement error depends not only on the instrument calibration, but also on the homogeneity of the flow field at that location.

Since it is generally impractical to measure the entire flow field, assumptions are made about the conditions of the flow field. These assumptions are generally verified during shake-

9

down testing of the facility. Examining equation I-16 one can see that if the influence coefficient for the temperature ratio and the desired accuracy of the efficiency are known then the total accuracy of the temperature ratio measurement can be determined (as shown in figure I-1). But contained within this number is both an instrument accuracy and the accuracy of the assumptions of flow uniformity. The importance of this latter term depends on where one is in the test facility. Upstream of the rotor, the flow should be relatively uniform. But it is well known that downstream of the rotor the flow will be non-uniform because of the rotor wake structure. One could imagine a situation where the flow non-uniformity was in fact the leading source of error and much larger than the instrument calibrations. There are of course several avenues available to solve this problem, but the primary idea here is to realize that instrument calibration is not the only source of uncertainty in a measurement of a flow property and the relative importance of the instrumentation calibration depends on the flow field in which the measurement is taken.

1.2 Instrumentation Calibration

While it is clear that our definition of measurement error depends on the instrument calibration and our assumptions about the flow field, only the latter is clearly outlined. Instrument calibration can quickly become a nebulous topic, especially when one starts to predict what the actual calibration will look like before the instruments are even built! Despite this problem, we must analyze the different components of the instrument calibration before construction begins.

The definition in table I-1 is helpful because it defines the confidence level to which all instrumentation calibrations must be done (95%). Abernethy[1] has stated that all error in an instrument can be expressed as a function of bias and precision components. Bias components are those which are fixed during a set of calibration runs and are known to be constant. Precision terms are the random components that vary over the calibration tests. As one increases the number of controlled variables in the calibration, the number of bias errors are increased and the number of precision errors reduced to the point where the only precision error which remains is the resolution of the instrument. However, as the number of controlled variables increases and the number of bias errors become known, they can in fact be calibrated out of the instrument through a variety of techniques. Thus the actual influence of the bias errors drop to zero. This fact gives rise to another perspective on instrument calibration championed by Moffat[2], who claims that most instrument calibrations only have precision error, which represents all the unknown variables, or the known variables which could not be controlled during the calibration. If they could be controlled, then they would have been calibrated out.

The ultimate difference in these philosophies boils down to describing the overall uncertainty in an instrument. Abernethy has suggested that the best way to describe the overall

10

accuracy of an instrument is through precision and bias components. These can be combined in some fashion to provide a total uncertainty in the instrument, but it would be best to leave them as separate terms allowing the bias components to be propagated through from different instruments to obtain a bias component of the desired quantity. A similar procedure could be done with the precision component, and thus the total uncertainty of the final variable could be expressed as the combination of these two components.

Moffat's suggestion that in practice there really are only precision errors makes the process simpler since the precision error is the total uncertainty of the instrument. This paper has adopted the position taken by Moffat for the simple reason that any calibrations on instruments performed for this facility will have any known terms calibrated out. Thus, how to combine the different components becomes a non-problem, but reducing instrument accuracy with the required confidence level from the calibration data remains.

Suppose the instrument under consideration is a pressure sensor which utilizes a strain gauge mounted on a diaphragm. We know from both experience and theory that the output of this type of device has some dependency on temperature. Also these devices have a tendency to drift with time even at constant temperature. The pressure measured by the sensor (P_m) is really composed of several parts

$$P_m = P + E_t + E_T + R \qquad (1-1)$$

where P is the true value, E_t is the error due to drift, E_T is the error due to temperature changes, and R is a random variable which includes other variables which have yet to be identified. The object of the calibration is to obtain a continuous voltage versus pressure curve, with a corresponding uncertainty. In reality one has discrete data points as shown in figure 1-1
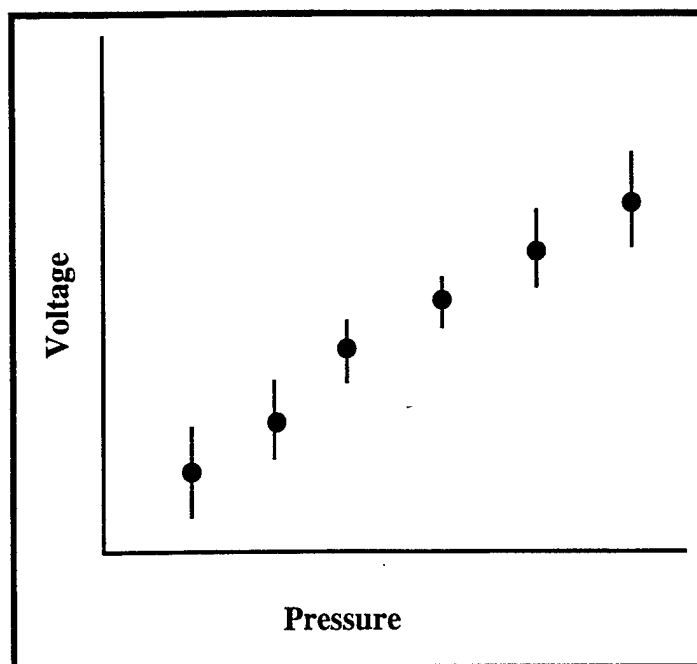
Figure 1-1   Components of Instrument Calibration

where the dots represent the mean value and the the bars represent the range over which the different voltage measurements fell for a given calibration pressure. These variations are due to the variations in temperature, time and the random variable. If the calibrations have been done enough times over the temperature ranges that are expected in the test, then these bars should represent the total range of measurements, and the frequency of measurements should be normally distributed around the mean. If this is the case then the total range is equivalent (for all real purposes to 6Ó, where Ó is the standard deviation of the curve). From the definition in table I-1 we need to specify the accuracy of the instruments to 95% confidence level which is a range of 4Ó (6Ó is 99.7% confidence limit). If the distribution is normal, to obtain the desired confidence level at any calibration point the actual range can be multiplied by 2/3 to obtain the range for the 95% confidence limit. Once this has been done for all the discrete data points then curves can be fit through the mean points to obtain a continuous distribution, and through the outer edges of the 95% confidence limit to obtain the continuous uncertainty distribution.

This is of course not the only way to proceed, nor may it be possible to claim that the variations around the mean point are normally distributed. Another alternate way to derive the continuous uncertainty band is to draw two parallel lines which bound all the data points. In this fashion the uncertainty does not have to be symmetric, but there are probably areas where the actual data points lie far closer to the mean then at other calibration points. These points are where the instrument is most accurate, and is where one would want to take the primary measurements. Unfortunately, using this technique the uncertainty at these points would be over specified. It would be possible to use the first procedure, but not to have a symmetric

12

uncertainty. One would have to decide whether it was easier to overestimate the error on one side to retain symmetry or whether it would be necessary to propagate the different limits separately. None of these questions can be answered before the form of the calibration curves has been observed. These are problems which can only be answered after their impact on the rest of the analysis has been determined.

1.3 Statistical Analysis

Some time needs to be spent discussing the various implications and uses of statistical analysis in this research program. We have already hinted at some of the uses with regard to the instrument calibrations, but there could be some confusion because within this type of experiment there are generally two types of data which require different statistical treatment. When time resolved data are being taken (for instance in a total pressure rake) then each data point must be considered a single sample. No averaging (before the data reduction) takes place and thus the uncertainty associated with the measurements (which is a combination of the instrument calibrations and flow assumptions) becomes the overall uncertainty of that data point. There are other places in the experiment (during the supply-tank fill process) where many different measurements will be averaged together, either over time or space to obtain some final measurement. In this case statistical analysis can be used to reduce the uncertainty in the final measurement below the individual measurement errors. One question will always be how low can one reduce the total uncertainty.

Ideally for these cases one could reduce the precision error to zero, through repeated sampling. If the uncertainty in the individual measurements is given by σ then the total uncertainty in the average value (assuming that all the individual uncertainties are equal) is

$$\sigma_m = \frac{\sigma}{\sqrt{N}}$$

(1-2)

where N is the number of measurements. There is a practical question of how the A-D discretation increments effect the level of uncertainty which can be reached. For single-sample data it is clear that one could never get better then 1/2 the A-D resolution and in fact the A-D resolution could be thought of as a bias error. But as the number of samples increase, the influence of the A-D diminishes which is equivalent of saying that it becomes more of a precision error. Where one is on the spectrum between single-sample and a statistically infinite number of measurements being used to create one final quantity, depends on the actual situation. This experiment covers the entire range. It is clear that if one sample was being used to create the measurement error, it would be greatly different from when 10 samples were averaged, which would be different from 50 samples being averaged for the final measurement.

1.4 Error Propagation

There are two basic forms of error propagation which could be used in this experiment. In most cases, the total measurement uncertainty will be a random variable. When different variables are independent and random then the actual propagation of errors from the measured quantities to efficiency is given by

$$\frac{\Delta\eta}{\eta} = \left[\sum_{i=1}^{n} \left(\frac{\partial f}{\partial u_i}\frac{u_i}{\eta}\right)^2 \left(\frac{\Delta u_i}{u_i}\right)^2\right]^{\frac{1}{2}}$$

(1-3)

if efficiency is expressed as $\eta = f(u_1, u_2, ...)$

The term in the first set of ( )

$$C_i = \frac{\partial f}{\partial u_i}\frac{u_i}{\eta}$$

can be labeled as the influence coefficient since it determines what contribution to the overall error a particular measurement makes. Equation 1-3 can be rewritten in terms of the influence coefficients as:

$$\frac{\Delta\eta}{\eta} = \left[\sum_{i=1}^{n} \left(C_i \frac{\Delta u_i}{u_i}\right)^2\right]^{\frac{1}{2}}$$

(1-4)

which is how the equations were written in section I. In these equations the uncertainty in the measurements and the final value are expressed as relative uncertainties or the uncertainty over the mean value. If one were to have separate bias and precision uncertainties, then they should be propagated separately (as explained by Abernethy) using these formulas.

However, there is another situation which requires a different form of error propagation. If the errors are not independent and are not random, but rather have a known sign, then if $X = f(u_1, u_2, ...)$ the relative error in X becomes:

$$\frac{\Delta X}{X} = \sum_{i=1}^{n} \left[\frac{\partial f}{\partial u_i}\frac{u_i}{X}\frac{\Delta u_i}{u_i}\right]$$

(1-5)

A good example of this would be the ideal gas law $PV=nRT$. In any given tank with a set mass, if one knew that the temperature was reading low, then one would know that the pressure would be reading low also. If one new the exact amount that the temperature was low by, then one would also know the exact amount the pressure was low by. The difference between equation 1-4 and 1-5 is that in previous situation, the errors are random and have an equal chance of being positive or negative, thus the requirement that they all be positive and added. In the latter situation, it is distinctly possible to get errors which cancel. Which situation is used depends upon the form of the uncertainty of the measure; but in most cases in this experiment, equation 1-4 will be used.

1.5 Conclusions

The topics noted above are just some of the different analytical techniques and issues which confront the designers of the ATARR facility. This section was not meant as a complete theoretical discussion on each of these points, nor was it meant to outline all the possible ways these techniques will be used in the ATARR facility. The former task would require several books, and the latter would be torture for the reader who would have to wade through several variations on a single theme for different specific cases, which had yet to be discussed! The goals were much more limited; trying only to expose the reader to the different techniques which will be used so that during the course of the paper minimum time will be devoted to developing the basic technique or issue and more attention can be devoted to the application of the technique to the specific situation at hand.

Having taken the time to outline this strategy, we are going to ignore it for the next section (to some degree) and develop the efficiency uncertainty analysis for different turbine configurations: uncooled, partially cooled, and fully cooled as a function of measurement uncertainty. Once that has been done, using the information in this section, we will begin to estimate the various sources of uncertainty for the variables derived in section 2.

Footnotes and References for Section 1

Which is taken to include errors in electronics and data processing.

[1] Abernethy, R. B. "ASME Measurement Uncertainty", Journal of Fluids Engineering, Vol 107, June 1985, p 161-164 and "Handbook on Uncertainty in Gas Turbine Measurements", USAF AEDC-TR-73-5, AD 755356, p 1-16.

[2] Moffat, R. J. "Contributions to the Theory of Single-Sample Uncertainty Analysis", Transactions of ASME, Vol 104, June 1982, p 250-260 and "Using Uncertainty analysis in the Planning of an Experiment", Journal of Fluids Engineering, Vol 107, June 1985, p 173-178.

15

Section 2 Efficiency Uncertainty Analysis

2.1 Methods of Measuring Efficiency

One of the primary requirements of the ATARR facility is to measure turbine stage efficiency over a variety of test parameters and stage configurations. For a short duration facility such as ATARR there are two primary ways of measuring efficiency; either thermodynamically, or through work extraction. A thermodynamic measurement is:

$$\eta = \frac{\text{actual change in thermodynamic state of the gas across the stage}}{\text{ideal change in thermodynamic state of the gas across the stage}} \quad (2\text{-}1)$$

or written in terms of thermodynamic properties:

$$\eta = \frac{\sum_{i=1}^{n} \dot{m}_i h_{ti} - \dot{m}_0 h_{t0} - L}{\sum_{i=1}^{n} \dot{m}_i (h_{ti} - h_{ti, ideal})} \quad (2\text{-}2)$$

where the numerator represents the summation of the total energy of all the inlet flows (the total enthalpies multiplied by their mass flows) minus the outlet energy of the flow minus any losses (L) due to either heat conduction or lost test gas through seals. The denominator represent the summation of the ideal change in thermodynamic properties across the stage. This is generally thought of as being unmixed and isentropically expanded from the pressure in the flow upstream of the turbine to the total average pressure downstream. A second approach would be to replace the numerator with the measured work extracted from the turbine. This is defined as the mechanical case and the efficiency is:

$$\eta = \frac{T_q \dot{\theta}}{\sum_{i=1}^{n} \dot{m}_i (h_{ti} - h_{ti, ideal})} \quad (2\text{-}3)$$

where T_q and $\dot{\theta}$ are the torque and the angular speed of the shaft.

Both representations of the efficiency would require an accurate knowledge of the heat lost to the walls and the test gas lost through the seals in order to estimate the "adiabatic efficiency" of the turbine stage (as shown in the introduction). This section of the paper compares these two methods by analyzing how uncertainties in measured values contribute to the uncertainty in the calculated efficiency of the stage for three different configurations of the facility: uncooled rotor and nozzle guide vanes, cooled rotor and vanes, and either cooled vanes or a cooled rotor.

16

2.2 The Ideal Process

The difference between the two methods of calculating the efficiency seem clear; one uses the actual change in the thermodynamic states of the gas, the other the mechanical power extraction. But in both cases the value of $h_{ti, \text{ideal}}$ must be evaluated. One way to determine the actual ideal enthalpy would be to use the entropy function and relative pressure data. For each gas entering the turbine stage (whether it is the core, or the coolant gases) the total temperature is known. This corresponds to a unique measure of the relative pressure. If this mapping is called G, then $P_{r1} = G(T)$ and since one knows the total pressure drop across the turbine $P_{r2} = P_{r1}*(P_1/P_2)$ which also has a unique temperature (this map is labeled J). Since the process being modeled is isentropic, the temperature which corresponds to J (P_{r2}) is the total temperature the gas would reach if it were isentropically expanded from P_1 to P_2. Thus the overall mapping in terms of the measured quantities is $J((P_1/P_2)*G(T_1))$ (this procedure is discussed in more detail in a latter section). This procedure has specific advantages. First it does not require an accurate knowledge of the ratio of specific heats, nor does it assume that it remains constant. Secondly, the information which it uses has already been obtained, so no new measurements are needed.

2.3 Stage Configurations

Since the ATARR facility will have the capability to run with a cooled rotor and cooled nozzle guide vanes, it is important to be specific about the different notation used in evaluating the different definitions of efficiency.

The quantities T, P, h are total temperature, pressure and enthalpy respectively (since only total qualities are used the subscript is dropped) and $\dot{m}$ is a mass flow rate. The subscripts $1, 2, n, r$ correspond to the upstream, downstream flows and the nozzle, and rotor coolant flows, respectively. Using this nomenclature $\dot{m}_1 \, h_1$ represents the total mass flow multiplied by the specific total enthalpy of the flow upstream of the stage. The subscript $_i$ refers to the ideal thermodynamic condition of the gas. The temperature which corresponds to this ideal condition is labeled J, and L represents the losses that occur in the engine either via heat transfer to the skin or through bleeds. The term C_p is the specific heat of the gas, $\overline{C}_p$ is the mean value of a gas between two different axial locations, and $C_{p, \text{avg}}$ is the mass-averaged specific heat of all the gas streams mixed together, and evaluated downstream of the rotor at axial location 2 (described below).

$$\overline{C}_p = \frac{C_{px}T_x - C_{py}T_y}{T_x - T_y}$$

$$C_{p,avg} = \frac{\sum_{i=1}^{n} C_{pi}m_i}{\sum_{i=1}^{n} m_i}$$

(2-4)

2.3.1 Uncertainty in Efficiency for Uncooled Configuration

For the uncooled configuration there are no coolant streams, thus $\dot{m}_1 = \dot{m}_2$ and the thermodynamic equation can be rewritten in terms of measurable quantities.

$$\eta = \frac{\dot{m}C_{p1}T_1 - \dot{m}C_{p2}T_2 - L}{\dot{m}\overline{C}_p (T_1 - J_1)}$$

(2-5)

which reduces to:

$$\eta = \frac{C_{p1}T_1 - C_{p2}T_2 - L^*}{\overline{C}_p (T_1 - J_1)} \quad , \quad L^* = \frac{L}{\dot{m}}$$

(2-6)

Assuming that the gas properties are known, then the uncertainty in the efficiency can be recombined as shown in the introduction to provide:

$$\frac{\Delta\eta}{\eta} = \left[\left\{ \left(\frac{-T_1}{T_1-J_1}\right) + \left(\frac{C_{p1}T_1}{C_{p1}T_1-C_{p2}T_2-L}\right) \right\}^2 \left\{\frac{\Delta T_1}{T_1}\right\}^2 + \left\{\frac{J_1}{T_1-J_1}\right\}^2 \left\{\frac{\Delta J_1}{J_1}\right\}^2 + \left\{\frac{-C_{p2}T_2}{C_{p1}T_1-C_{p2}T_2-L^*}\right\}^2 \left\{\frac{\Delta T_2}{T_2}\right\}^2 + \right.$$
$$\left. \left\{\frac{-L^*}{C_{p1}T_1-C_{p2}T_2-L^*}\right\}^2 \left\{\frac{\Delta L^*}{L^*}\right\}^2 \right]^{\frac{1}{2}}$$

(2-7)

The mechanical method (equation 2-2) can be written for the uncooled case as:

$$\eta = \frac{T_q\dot{\theta}}{\dot{m}_1\overline{C}_{p1} (T_1 - J_1)}$$

(2-8)

which has an uncertainty of:

$$\frac{\Delta\eta}{\eta} = \left[\left\{\frac{\Delta T_q}{T_q}\right\}^2 + \left\{\frac{\Delta\dot{\theta}}{\dot{\theta}}\right\}^2 + \left\{\frac{-\Delta\dot{m}}{\dot{m}}\right\}^2 + \left\{\frac{-T_1}{T_1-J_1}\right\}^2 \left\{\frac{\Delta T_1}{T_1}\right\}^2 + \left\{\frac{J_1}{T_1-J_1}\right\}^2 \left\{\frac{\Delta J_1}{J_1}\right\}^2 \right]^{\frac{1}{2}}$$

(2-9)

2.3.2 Uncertainty in Efficiency for Cooled Configuration

For a cooled stage (both rotor and stator) the equations become much more complicated. Equation 2-2 becomes:

$$\eta = \frac{\dot{m}_1C_{p1}T_1 + \dot{m}_nC_{pn}T_n + \dot{m}_rC_{pr}T_r - \dot{m}_2C_{p,avg}T_2 - L}{\dot{m}_1\overline{C}_{p1} (T_1-J_1) + \dot{m}_n\overline{C}_{pn} (T_n-J_n) + \dot{m}_r\overline{C}_{pr} (T_r-J_r)} = \frac{N}{D}$$

(2-10)

18

(where N represents the numerator and D the denominator). When the specific heats are known quantities there are 12 variables and the uncertainty in efficiency can be written as (in terms of N and D):

$$\frac{\Delta\eta}{\eta} = \Bigg[\quad \Big\{\frac{T_1\dot{m}_1\overline{C}_{p1}}{D}\Big\}^2\Big[\Big\{\frac{\Delta T_1}{T_1}\Big\}^2 + \Big\{\frac{\Delta\dot{m}_1}{\dot{m}_1}\Big\}^2 + \Big\{\frac{\overline{C}_{pn}T_n\dot{m}_n}{\overline{C}_{p1}T_1\dot{m}_1}\Big\}^2\Big\{\frac{\Delta T_n}{T_n}+\frac{\Delta\dot{m}_n}{\dot{m}_n}\Big\}^2 + \Big\{\frac{\overline{C}_{pr}T_r\dot{m}_r}{\overline{C}_{p1}T_1\dot{m}_1}\Big\}^2\Big\{\frac{\Delta T_r}{T_r}+\frac{\Delta\dot{m}_r}{\dot{m}_r}\Big\}^2 +$$

$$\Big\{\frac{J_1}{T_1}\Big\}^2\Big\{\frac{\Delta J_1}{J_1}\Big\}^2 + \Big\{\frac{\overline{C}_{pn}J_n\dot{m}_n}{\overline{C}_{p1}T_1\dot{m}_1}\Big\}^2\Big\{\frac{\Delta J_n}{J_n}\Big\}^2 + \Big\{\frac{\overline{C}_{pr}J_r\dot{m}_r}{\overline{C}_{p1}T_1\dot{m}_1}\Big\}^2\Big\{\frac{\Delta J_r}{J_r}\Big\}^2\Big] +$$

$$\Big\{\frac{T_1\dot{m}_1\overline{C}_{p1}}{N}\Big\}^2\Big[\Big\{1-\frac{2N\overline{C}_{p1}}{D\overline{C}_{p1}}\Big\}\Big(\Big\{\frac{\Delta T_1}{T_1}\Big\}^2+\Big\{\frac{\Delta\dot{m}_1}{\dot{m}_1}\Big\}^2\Big) + \Big\{\frac{C_{pn}T_n\dot{m}_n}{\overline{C}_{p1}T_1\dot{m}_1}\Big\}^2\Big\{1-\frac{2N\overline{C}_{pn}}{DC_{pn}}\Big\}\Big(\Big\{\frac{\Delta T_n}{T_n}\Big\}^2+\Big\{\frac{\Delta\dot{m}_n}{\dot{m}_n}\Big\}^2\Big) +$$

$$\Big\{\frac{C_{pr}T_r\dot{m}_n}{\overline{C}_{p1}T_1\dot{m}_1}\Big\}^2\Big\{1-\frac{2N\overline{C}_{pr}}{DC_{pr}}\Big\}\Big(\Big\{\frac{\Delta T_r}{T_r}\Big\}^2+\Big\{\frac{\Delta\dot{m}_r}{\dot{m}_r}\Big\}^2\Big)+\Big\{\frac{C_{p,avg}T_2\dot{m}_2}{\overline{C}_{p1}T_1\dot{m}_1}\Big\}^2\Big(\Big\{\frac{\Delta T_2}{T_2}\Big\}^2+\Big\{\frac{\Delta\dot{m}_2}{\dot{m}_2}\Big\}^2\Big)\Big] + \Big\{\frac{-L}{N}\frac{\Delta L}{L}\Big\}^2\Bigg]^{\frac{1}{2}}$$

(2-11)

The reason for writing the efficiency in this form becomes apparent when looking at the efficiency equation using mechanical power in the cooled operation mode.

$$\eta = \frac{T_q\theta}{\dot{m}_1\overline{C}_{p1}(T_1-J_1) + \dot{m}_n\overline{C}_{pn}(T_n-J_n) +\dot{m}_r\overline{C}_{pr}(T_r-J_r)} = \frac{T_q\theta}{D}$$

(2-12)

Where D is the denominator and is the same as the previous case and has an uncertainty expressed by:

$$\frac{\Delta\eta}{\eta} = \Bigg[\Big\{\frac{\Delta T_q}{T_q}\Big\}^2 + \Big\{\frac{\Delta\dot{\theta}_1}{\dot{\theta}_1}\Big\}^2 + \Big\{\frac{T_1\dot{m}_1\overline{C}_{p1}}{D}\Big\}^2\Big[\Big\{\frac{\Delta T_1}{T_1}\Big\}^2 + \Big\{\frac{\Delta\dot{m}_1}{\dot{m}_1}\Big\}^2 + \Big\{\frac{\overline{C}_{pn}T_n\dot{m}_n}{\overline{C}_{p1}T_1\dot{m}_1}\Big\}^2\Big\{\frac{\Delta T_n}{T_n}+\frac{\Delta\dot{m}_n}{\dot{m}_n}\Big\}^2 +$$

$$\Big\{\frac{\overline{C}_{pr}T_r\dot{m}_r}{\overline{C}_{p1}T_1\dot{m}_1}\Big\}^2\Big\{\frac{\Delta T_r}{T_r}+\frac{\Delta\dot{m}_r}{\dot{m}_r}\Big\}^2+\Big\{\frac{J_1}{T_1}\Big\}^2\Big\{\frac{\Delta J_1}{J_1}\Big\}^2 + \Big\{\frac{\overline{C}_{pn}J_n\dot{m}_n}{\overline{C}_{p1}T_1\dot{m}_1}\Big\}^2\Big\{\frac{\Delta J_n}{J_n}\Big\}^2 + \Big\{\frac{\overline{C}_{pr}J_r\dot{m}_r}{\overline{C}_{p1}T_1\dot{m}_1}\Big\}^2\Big\{\frac{\Delta J_r}{J_r}\Big\}^2\Big]\Bigg]^{\frac{1}{2}}$$

(2-13)

2.3.3 Uncertainty in Efficiency for Cooled NGV's

The third case which needs to be examined is the case where only the nozzle-guide vanes are cooled. The analysis would be the same if the rotor was the only part that was cooled, but because the first engine to be used in the ATARR facility has cooled NGV's we will look at this case in that context. This is a limiting case of the previous section where one of the two cooling flows goes to zero. Thus the thermodynamic definition of efficiency becomes:

$$\eta = \frac{\dot{m}_1C_{p1}T_1 + \dot{m}_nC_{pn}T_n - \dot{m}_2C_{p,avg}T_2 - L}{\dot{m}_1\overline{C}_{p1}(T_1-J_1) + \dot{m}_n\overline{C}_{pn}(T_n-J_n)} = \frac{N}{D}$$

(2-14)

and the accuracy in efficiency can be seen from equation 2-11.

$$\frac{\Delta\eta}{\eta} = \left[\quad \left\{\frac{T_1\dot{m}_1\overline{C}_{p1}}{D}\right\}^2\left[\left\{\frac{\Delta T_1}{T_1}\right\}^2 + \left\{\frac{\Delta\dot{m}_1}{\dot{m}_1}\right\}^2 + \left\{\frac{\overline{C}_{pn}T_n\dot{m}_n}{\overline{C}_{p1}T_1\dot{m}_1}\right\}^2\left\{\frac{\Delta T_n + \Delta\dot{m}_n}{T_n \quad \dot{m}_n}\right\}^2 + \right.\right.$$

$$\left.\left\{\frac{J_1}{T_1}\right\}^2\left\{\frac{\Delta J_1}{J_1}\right\}^2 + \left\{\frac{\overline{C}_{pn}J_n\dot{m}_n}{\overline{C}_{p1}T_1\dot{m}_1}\right\}^2\left\{\frac{\Delta J_n}{J_n}\right\}^2 + \left\{\frac{\overline{C}_{pr}J_r\dot{m}_r}{\overline{C}_{p1}T_1\dot{m}_1}\right\}^2\left\{\frac{\Delta J_r}{J_r}\right\}^2\right] +$$

$$\left\{\frac{T_1\dot{m}_1C_{p1}}{N}\right\}^2\left[\left\{1-\frac{2N\overline{C}_{p1}}{DC_{p1}}\right\}\left(\left\{\frac{\Delta T_1}{T_1}\right\}^2 + \left\{\frac{\Delta\dot{m}_1}{\dot{m}_1}\right\}^2\right) + \left\{\frac{C_{pn}T_n\dot{m}_n}{\overline{C}_{p1}T_1\dot{m}_1}\right\}^2\left\{1-\frac{2N\overline{C}_{pn}}{DC_{pn}}\right\}\left(\left\{\frac{\Delta T_n}{T_n}\right\}^2 + \left\{\frac{\Delta\dot{m}_n}{\dot{m}_n}\right\}^2\right) +$$

$$\left. + \left\{\frac{C_{p,avg}T_2\dot{m}_2}{\overline{C}_{p1}T_1\dot{m}_1}\right\}^2\left(\left\{\frac{\Delta T_2}{T_2}\right\}^2 + \left\{\frac{\Delta\dot{m}_2}{\dot{m}_2}\right\}^2\right)\right] + \left\{\frac{-L\,\Delta L}{N\,L}\right\}^2\right]^{\frac{1}{2}} \qquad (2\text{-}15)$$

The definition for efficiency using the mechanical method can be taken from equation 2-12.

$$\eta = \frac{T_q\dot{\theta}}{\dot{m}_1\overline{C}_{p1}(T_1-J_1) + \dot{m}_n\overline{C}_{pn}(T_n-J_n)} = \frac{T_q\dot{\theta}}{D} \qquad (2\text{-}16)$$

with accuracy:

$$\frac{\Delta\eta}{\eta} = \left[\left\{\frac{\Delta T_q}{T_q}\right\}^2 + \left\{\frac{\Delta\dot{\theta}_1}{\dot{\theta}_1}\right\}^2 + \left\{\frac{T_1\dot{m}_1\overline{C}_{p1}}{D}\right\}^2\left[\left\{\frac{\Delta T_1}{T_1}\right\}^2 + \left\{\frac{\Delta\dot{m}_1}{\dot{m}_1}\right\}^2 + \left\{\frac{\overline{C}_{pn}T_n\dot{m}_n}{\overline{C}_{p1}T_1\dot{m}_1}\right\}^2\left\{\frac{\Delta T_n + \Delta\dot{m}_n}{T_n \quad \dot{m}_n}\right\}^2 + \right.\right.$$

$$\left.\left. \left\{\frac{\overline{C}_{pr}T_r\dot{m}_r}{\overline{C}_{p1}T_1\dot{m}_1}\right\}^2\left\{\frac{\Delta T_r + \Delta\dot{m}_r}{T_r \quad \dot{m}_r}\right\}^2 + \left\{\frac{J_1}{T_1}\right\}^2\left\{\frac{\Delta J_1}{J_1}\right\}^2 + \left\{\frac{\overline{C}_{pn}J_n\dot{m}_n}{\overline{C}_{p1}T_1\dot{m}_1}\right\}^2\left\{\frac{\Delta J_n}{J_n}\right\}^2\right]\right]^{\frac{1}{2}} \qquad (2\text{-}17)$$

2.4 Evaluation of General Expressions

There are two question which need to be answered: 1) which method is better for measuring efficiency? and 2) what is the error in the efficiency measurement? Concentrating on the first question; the relationship between the two methods can be simplified by subtracting common terms from both sides of the equations. For the uncooled case the relationship between equations 2-7 and 2-9 is reduced to:

$$\left\{\left(\frac{-2T_1}{T_1-J_1}\right) + \frac{C_{p1}T_1}{C_{p1}T_1-C_{p2}T_2-L^*}\right\}\left\{\frac{C_{p1}T_1}{C_{p1}T_1-C_{p2}T_2-L^*}\right\}\left\{\frac{\Delta T_1}{T_1}\right\}^2 + \left\{\frac{-C_{p2}T_2}{C_{p1}T_1-C_{p2}T_2-L^*}\right\}^2\left\{\frac{\Delta T_2}{T_2}\right\}^2 +$$

$$\left\{\frac{-L^*}{C_{p1}T_1-C_{p2}T_2-L^*}\right\}^2\left\{\frac{\Delta L^*}{L^*}\right\}^2 \qquad \langle ? \rangle \qquad \left\{\frac{\Delta T_q}{T_q}\right\}^2 + \left\{\frac{\Delta\dot{\theta}}{\dot{\theta}}\right\}^2 + \left\{\frac{-\Delta\dot{m}}{\dot{m}}\right\}^2 \qquad (2\text{-}18)$$

On the left hand side (the thermodynamic technique) are three uncertainties and their influence coefficients. Two of them (T_1 and T_2) are measured quantities while the third (L^*) is a conglomerate term of all losses in the system and needs to be broken down into other measured parameters to be evaluated. On the right hand side (the mechanical method) there are also three variables, two of which are measured (the torque and the speed) with the third being the mass flow, which is not a directly measured quantity. (the $<?>$ indicates that the relationship between the two methods is yet to be determined). L^* can be reduced one step further by recognizing that:

$$\frac{\Delta L^*}{L^*} = \left[\left\{\frac{\Delta L}{L}\right\}^2 + \left\{\frac{-\Delta \dot{m}}{\dot{m}}\right\}^2\right]^{.5}$$

(2-19)

and equation 2-18 now takes the form:

$$\left\{\left(\frac{-2T_1}{T_1-J_1}\right) + \frac{C_{p1}T_1}{C_{p1}T_1-C_{p2}T_2-L^*}\right\}\left\{\frac{C_{p1}T_1}{C_{p1}T_1-C_{p2}T_2-L^*}\right\}\left\{\frac{\Delta T_1}{T_1}\right\}^2 + \left\{\frac{-C_{p2}T_2}{C_{p1}T_1-C_{p2}T_2-L^*}\right\}^2\left\{\frac{\Delta T_2}{T_2}\right\}^2 +$$

$$\left\{\frac{-L^*}{C_{p1}T_1-C_{p2}T_2-L^*}\right\}^2\left[\left\{\frac{\Delta L}{L}\right\}^2 + \left\{\frac{-\Delta \dot{m}}{\dot{m}}\right\}^2\right] \quad \langle ? \rangle \quad \left\{\frac{\Delta T_q}{T_q}\right\}^2 + \left\{\frac{\Delta \dot{\theta}}{\dot{\theta}}\right\}^2 + \left\{\frac{-\Delta \dot{m}}{\dot{m}}\right\}^2$$

(2-20)

A similar procedure can be used for the cooled equations:

$$\left\{\frac{T_1\dot{m}_1 C_{p1}}{N}\right\}^2\left[\left\{1-\frac{2N\overline{C}_{p1}}{DC_{p1}}\right\}\left(\left\{\frac{\Delta T_1}{T_1}\right\}^2 + \left\{\frac{\Delta \dot{m}_1}{\dot{m}_1}\right\}^2\right) + \left\{\frac{C_{pn}T_n\dot{m}_n}{C_{p1}T_1\dot{m}_1}\right\}^2\left\{1-\frac{2N\overline{C}_{pn}}{DC_{pn}}\right\}\left(\left\{\frac{\Delta T_n}{T_n}\right\}^2 + \left\{\frac{\Delta w\dot{m}_n}{\dot{m}_n}\right\}^2\right) +$$

$$\left\{\frac{C_{pr}T_r\dot{m}_n}{C_{p1}T_1\dot{m}_1}\right\}^2\left\{1-\frac{2N\overline{C}_{pr}}{DC_{pr}}\right\}\left(\left\{\frac{\Delta T_r}{T_r}\right\}^2 + \left\{\frac{\Delta \dot{m}_r}{\dot{m}_r}\right\}^2\right) + \left\{\frac{C_{p,avg}T_2\dot{m}_2}{C_{p1}T_1\dot{m}_1}\right\}^2\left(\left\{\frac{\Delta T_2}{T_2}\right\}^2 + \left\{\frac{\Delta \dot{m}_2}{\dot{m}_2}\right\}^2\right)\right] + \left\{\frac{-L}{N}\frac{\Delta L}{L}\right\}^2$$

$$\langle ? \rangle \quad \left\{\frac{\Delta T_q}{T_q}\right\}^2 + \left\{\frac{\Delta \dot{\theta}}{\dot{\theta}}\right\}^2$$

(2-21)

In equation 2-21, the first two lines correspond to the uncertainty in the efficiency as measured using the thermodynamic techniques and the last line to the mechanical method, when the common terms have been excluded. More simplification at this point may be counterproductive, since one does not know the particulars of the turbines that would fall into these cases. But for the turbine which will be studied initially in the ATARR facility, some greater simplification can be done since it will only have cooled vanes.

2.5 Evaluation of Efficiency Expressions for a Partially Cooled Stage
Thermodynamic Method:

For this particular stage configuration, equation 2-14 can be non-dimensionalized by the core flow. It might seem that we would gain little since the loss term and the idealized temperatures, J_1 and J_n would remain. But since the ultimate goal is to see how the mechanical method and the thermodynamic method of evaluating the efficiency compare some simplifying assumptions can be made. Assume that the loss terms are negligible[1] and that the idealized temperature downstream can be given by the isentropic expansion of the gas across the stage at constant γ.

$$J = T\left(\frac{P_2}{P_1}\right)^{\frac{\gamma-1}{\gamma}} \text{ or } J = Tr$$

(2-22)

then equation 2-14 can be written as:

---

[1] On would naturally expect these to be small, and thus this assumption may be valid for this type of analysis. But for the actual efficiency calculation, the loss term would have to be measured. It is clear that this case of assuming the loss term= 0 is the best answer that this method could provide.

21

$$\eta = \frac{\dot{m}_1 C_{p1} T_1 + \dot{m}_n C_{pn} T_n - (\dot{m}_1 + \dot{m}_n) C_{p,avg} T_2}{(\dot{m}_1 \overline{C_{p1}} T_1 + \dot{m}_n \overline{C_{pn}} T_n)(1-r)}$$

$$(2-23)$$

This can be normalized by the main core flow and if the following symbols are used:

$$\varepsilon = \frac{\dot{m}_n}{\dot{m}_1} \quad T_{2r} = \frac{T_2}{T_1} \quad T_{nr} = \frac{T_n}{T_1} \quad C_{pr} = \frac{C_{p,avg}}{C_{p1}}$$

$$(2-24)$$

converts equation 2-23 to:

$$\eta = \frac{1 + \varepsilon \dfrac{C_{pn}}{C_{p1}} T_{nr} - (1+\varepsilon) C_{pr} T_{2r}}{(\dfrac{\overline{C_{p1}}}{C_{p1}} + \varepsilon \dfrac{\overline{C_{pn}}}{C_{p1}} T_{nr})(1-r)}$$

$$(2-25)$$

This facility is designed to run with either pure N_2 or with a N_2-CO_2 mixture as the main gas flow and a pure N_2 cooling flow. For a standard test (see appendix A for description) the ideal gas specific heats would be 1.039 (J/g-K) for the cooling gas entering at 216°K and 1.036 for the core mixture at 520 °K (see figures A-2 and A-5, as well as Table A-1 in appendix A) Thus for this exercise the ratio of the specific heats can be ignored. However, the term C_{pr} will be retained for now because it represents a downstream measurement (which may be hard to acquire). Finally, equation 2-25 becomes:

$$\eta = \frac{1 + \varepsilon T_{nr} - (1+\varepsilon) C_{pr} T_{2r}}{(1 + \varepsilon T_{nr})(1-r)}$$

$$(2-26)$$

The uncertainty in the efficiency for the thermodynamic method is:
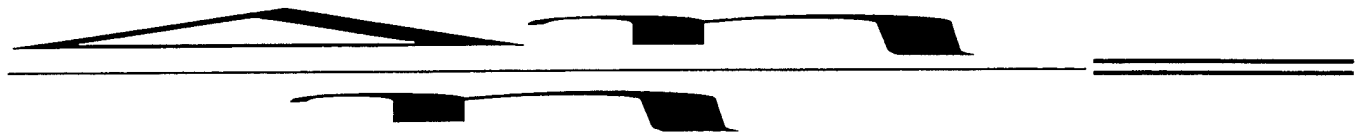
$$\frac{\Delta \eta}{\eta} = \left[\left(\frac{(\varepsilon+1) C_{pr} T_{2r}}{T_{nr}\varepsilon + 1 - (\varepsilon+1) C_{pr} T_{2r}} \right)^2 \left[\left(\frac{(T_{nr}-1)\varepsilon}{(\varepsilon+1)(T_{nr}\varepsilon+1)} \right)^2 (\frac{\Delta\varepsilon}{\varepsilon})^2 + \left(\frac{T_{nr}\varepsilon}{(T_{nr}\varepsilon+1)} \right)^2 (\frac{\Delta T_{nr}}{T_{nr}})^2 + \right. \right.$$

$$\left. \left. \left(\frac{(T_{nr}\varepsilon + 1 - (\varepsilon+1) C_{pr} T_{2r}) r}{(1-r)(\varepsilon+1) C_{pr} T_{2r}} \right)^2 (\frac{\Delta r}{r})^2 + (\frac{\Delta C_{pr}}{C_{pr}})^2 + (\frac{\Delta T_{2r}}{T_{2r}})^2 \right] \right]^{.5}$$

$$(2-27)$$

The Mechanical Method:

A similar methodology can be used for this method, resulting in a non-dimensional equation

$$\eta = \frac{\{T_q \theta\}}{\{\dot{m}_1 \overline{C_{p1}} T_1\}\{1-r\}\{1 + \varepsilon T_{nr}\}}$$

$$(2-28)$$

with an uncertainty of:

$$(2-29)$$

Comparing equations 2-27 and 2-29 can be done by using the adiabatic turbine equation to obtain an expression for T_{2r} in terms of the efficiency and the r factor.

$$\eta = \frac{1-T_{2r}}{1-r} \tag{2-30}$$

While one could solve for both the stage efficiency and r, to avoid unnecessary complication, a stage efficiency of 90% is assumed which reduces T_{2r} to:

$$T_{2r} = .1 + .9r \tag{2-31}$$

If we assume a cooling flow of 20% of the main core flow and a cooling gas temperature to core temperature ratio of .42 (212°K/520°K) and specific heat ratio $C_{pr} = 1$ (as stated above), then substitution into equations 2-327 and 2-29 show that the thermodynamic method reduces to:

$$\frac{\Delta\eta}{\eta} = \left[(\frac{r}{(1-r)})^2 (\frac{\Delta r}{r})^2 + (A)^2 \left[(\frac{\Delta C_{pr}}{C_{pr}})^2 + (\frac{\Delta T_{2r}}{T_{2r}})^2 \right] \right]^{.5}$$

$$A = \frac{.1 + .9r}{0.9033 - (.1 + .9r)} \tag{2-32}$$

Since all the other terms are much smaller. And the mechanical method reduces to

$$\frac{\Delta\eta}{\eta} = \left[(\frac{r}{(1-r)})^2 (\frac{\Delta r}{r})^2 + (\frac{\Delta \overline{C}_{p1}}{\overline{C}_{p1}})^2 + (\frac{\Delta T_1}{T_1})^2 + (\frac{\Delta T_q}{T_q})^2 + (\frac{\Delta \dot{m}_1}{\dot{m}_1})^2 + (\frac{\Delta\theta}{\theta})^2 \right]^{.5} \tag{2-33}$$

Both equations have the same contribution from the r factor, and thus it can be ignored. Equation 2-32 needs to be expanded so that it represents real measurements (since presently it is expressed in non-dimensional form).

$$\frac{\Delta\eta}{\eta} = \left[(\frac{r}{(1-r)})^2 (\frac{\Delta r}{r})^2 + (A)^2 \left[(\frac{\Delta C_{p2}}{C_{p2}})^2 + (\frac{\Delta C_{p1}}{C_{p1}})^2 + (\frac{\Delta T_2}{T_2})^2 + (\frac{\Delta T_1}{T_1})^2 \right] \right]^{.5}$$

$$A = \frac{.1 + .9r}{0.9033 - (.1 + .9r)} \tag{2-34}$$

To reduce this further we have to skip ahead to the next section of the paper which discusses how the gas properties are determined. As shown in appendix A, the uncertainty in the gas properties (the specific heat in this case) is ultimately a function of the uncertainty in the temperature and pressure measurements. and for any reasonable measurement accuracy, the uncertainty of the individual gas properties will be quite smaller then the levels of accuracy being investigated. As a result these variations can be neglected in this case (see appendix A for further details) and equation 2-34 becomes:

$$\frac{\Delta\eta}{\eta} = \left[(\frac{r}{(1-r)})^2 (\frac{\Delta r}{r})^2 + (A)^2 \left[(\frac{\Delta T_2}{T_2})^2 + (\frac{\Delta T_1}{T_1})^2 \right] \right]^{.5}$$

$$A = \frac{.1 + .9r}{0.9033 - (.1 + .9r)} \tag{2-35}$$

and equation 2-33 as:

$$\frac{\Delta\eta}{\eta}=\left[(\frac{r}{(1-r)})^2(\frac{\Delta r}{r})^2 +(\frac{\Delta T_1}{T_1})^2+(\frac{\Delta T_q}{T_q})^2+(\frac{\Delta \dot{m}_1}{\dot{m}_1})^2+(\frac{\Delta\theta}{\theta})^2\right]^{.5}$$

(2-36)

These equations can be compared by looking at how the influence coefficients behave. Shown in figure 2-1 are the values of r/(1-r) and A as a function of r.
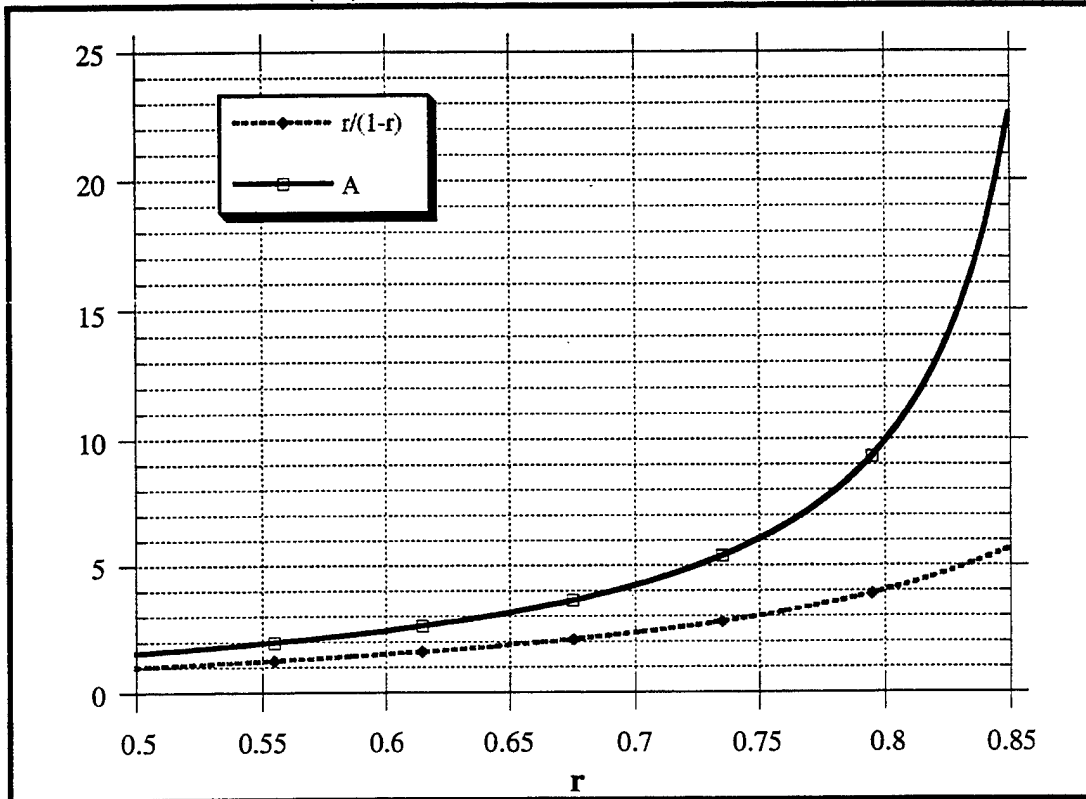
Figure 2-1 Plot of r/(1-r) and A as a Function of r

There are several points of interest. First when comparing the two different procedures, the dependance on the uncertainty in r is equivalent, leaving only those factors which have an influence coefficient of A in the thermodynamic case and those with an influence coefficient of 1 in the mechanical case contributing to the difference in the methods for measuring efficiency. To determine which method is better requires an evaluation of the different uncertainties. If the temperatures were the only important variable (which is equivalent to claiming that all the other variables can be neglected), then at an r of .75 (which is close to the operating condition of the facility) the thermodynamic procedure would require two measurements which when combined would have to be 6 times the accuracy of the mechanical method to achieve the same results. But realistically what one is trading off is the number and location of the measurements. For the thermodynamic procedure, one needs only two uncertainties, upstream and downstream temperature. While the upstream temperature uncertainty will probably be dominated by the instrument accuracy, the same cannot be said about the downstream measurement, because the flow is not expected to be uniform (since the overall accuracy of the measurement is a function

24

both of the instrument and how well the instrument location represents the entire flow field). In the mechanical method, there are no measurements needed downstream and both the torque and speed of the shaft are easily measured. However, one requires the mass flow through the turbine which might be hard to derive. At this point we need to begin to look at how these uncertainties will be defined.

Section 3: Errors in Assumptions About The Flow Field

3.1 Problem Definition:

Throughout the last section, the overall uncertainty in the efficiency of the stage configuration has been found in terms of relative measurement errors such as $\Delta T/T$, or $\Delta P/P$. And as pointed out in the introduction, these uncertainties really have two distinct components; those which are due to instrument inaccuracies, and those which are due to assumptions about the flow field. This section will discuss the latter group.

It is important to realize that inherent assumptions about the flow were made in section 2 when different terms were considered to be variables and constants. For instance all the gas properties have been assumed to be accurately known, and the problems inherent in determining the isentropic temperature of the gas downstream of the turbine have been ignored. This section will limit its discussion of this topic to the problems inherent in determining the values of the gas constants and the isentropic temperature downstream of the turbine for the simple reason that the other issues need an experimental answer. Ideally the flow should be uniform from the supply tank to the NGV inlet. If this was the case then only one pressure or temperature measurement would be needed at any axial location to determine the entire flow field condition at that axial location. To determine how close the facility is operating to this ideal condition will require many tests with instrumentation at different locations. All of this will have to be determined experimentally.

To create a proper system for addressing the gas properties problems requires answers to the following questions. What will the standards be for determining the gas constants? And how will errors in the independent property be transmitted through a table to the errors in the dependent property? As with the rest of the ATARR program, there is no "right" answer, only different ways of solving these problems.

3.2 The Question of Gas Property Standards and Gas Behavior

When air is at 517 °K what is the specific heat at constant pressure (C_p)? To answer this question one generally relies on tabular values of zero-pressure specific heats that may be given in 50°K increments. To obtain a reasonable answer, one might do a linear interpolation between the listed values at 500 °K and 550 °K. However the question becomes how good are these tabulated values, what happens if the gas is at 7 atm. instead of 1 atm.? Where did these tabulated values come from? Are they taken from experimental results, calculated from ideal gas equations, or an empirical curve fit through several different experiments? If one is just comparing different sets of experimental data all taken at one facility, then the answer might not

26

be that critical; but, when data are being compared among facilities it is important that the various research groups use consistent property data.

In addition to the questions revolving around the physical properties of the gas, there are also questions about the modeling of the gas behavior. For the relatively low temperatures and pressures at which the ATARR facility operates, the gases are generally assumed to exhibit ideal behavior. Thus empirical laws such as the law of partial pressures (which is used in the filling process of the supply tank which will be discussed in the next section) are expected to be valid. But looking at Table 3-1 which contains the compressibility factor for Air, N_2, and CO_2 one can see that for all the test gases, the real gas effects are the same order of magnitude as the total allowable error in efficiency. Thus using properties which are not based on real gas equations of state could lead to unacceptable errors.

Table 3-1: Compressibility Factor for Test Gases at 550 °K and 4 atm

	Temperature	Air	N_2	CO_2
Z	550	1.00148	1.00172	.99825
% Variation		.148%	.172%	.175%

The question of whether these real gas effects would influence the final results of any derived parameter will be dependent on that parameter. It is possible that there may be some properties which are not affected by the real gas effect, and others that are greatly affected. The main question becomes, "if the ideal gas model can not be used, then what type of model should be?" Before this question is answered, the easier problem of defining the actual gas properties should be dealt with.

This facility needs five pieces of data: C_p, C_v (the specific heats at constant pressure and volume, respectively), R (the gas constant), P_r (the relative pressure data), and some measure of real gas effects. Both C_p and C_v are related to each other through the ratio of specific heats γ, so only two of these three need to be known. It is clear from Table 1 that real gas effects are important at the level of accuracy that we are dealing with, thus the idealization of C_p, C_v and P_r being only functions of temperature can not be accepted. There are two readily available sources for tabulated data available.

Gas Tables: Thermodynamic Properties of Air, Products of Combustion, and Component Gases, Compressible Flow Functions, by Keenan, Chao, and Kaye[1]

This book contains detailed lists of the relative pressure tables and the specific heats as a function of temperature only (i.e they were calculated using the ideal gas law). Because real gas

---

[1] Keenan, Chao, and Kaye; Gas Tables: Thermodynamic Properties of Air, Products of Combustion, and Component Gases, Compressible Flow Functions, Second edition (SI units), John Wiley and Sons, 1983.

effects could be a source of problems for achieving the ATARR efficiency accuracy goals and a better source would be:

Tables of Thermodynamic and Transport Properties of Air, Argon, Carbon Dioxide, Carbon Monoxide, Hydrogen, Nitrogen, Oxygen, and Steam by Hilsenrath, Beckett, Benedict, Fano, Hoge, Masi, Nuttall, Touloukian, and Woolley[2]

This book does not contain the relative pressure data as a separate table, but the value of C_p/R is tabulated for different pressures. Relative pressures can be obtained from these data through the following transformation.

$$Ln(P_r)=\frac{\varnothing}{R}$$

$$\varnothing(T)=\int_{T_0}^{T}\frac{C_p}{T}dT$$

(3-1)

Once a reference point is selected (say 150°K) then the table of P_r could be derived from the table of C_p/R using the trapezoidal rule

$$Ln(P_r)=(\frac{\frac{C_p}{TR}\bigg|_{T_0+\Delta T}+\frac{C_p}{TR}\bigg|_{T_0}}{2})\Delta T$$

(3-2)

and each subsequent entry is devised by incrementing from the previous value. Since data for C_p/R are presented at different pressures, the relative pressure data can also be determined for those pressures.

It is important to realize that the properties listed in reference 2 are all based on the equation of state used to calculate z (shown in Appendix A) which is a third order viral equation. Thus all the properties are based on a mutually consistent database. To answer the question posed in the previous paragraph, of which model to use, we would have to have alternative gas models and some method for comparing them. Other possible equations of state are the van der Walls and Redlich-Kwong. If we had P-V-T data over the range of pressures and temperatures of interest, then it would be a simple matter to evaluate each of the models and see how different they were from the "true" value. Since such a reference point is not available, we can only evaluate each model at the test conditions and show the variance among them (this is done in Appendix B).

3.3 Accuracy of the Tables

---

[2]Hilsenrath, Beckett, Benedict, Fano, Hoge, Masi, Nuttall, Touloukian, and Woolley; Tables of Thermodynamic and Transport Properties of Air, Argon, Carbon Dioxide, Carbon Monoxide, Hydrogen, Nitrogen, Oxygen, and Steam; Pergamon Press 1960

A similar question is faced when defining the accuracy of the table properties. As stated above, these are all based on the virial equation of state. Reference 2 provides some indication of the accuracy of the tables (which is derived from matching to some experimental data, and uncertainties in physical constants), but the main problem reduces to what one wishes to believe, the model or the experiment. It is our contention that averaging the model together with the experimental data does not produce any real insight into what the "Truth" is, and that in fact, the "actual" gas properties are not critical. As long as one reduces the data in a consistent frame of reference, then there should be no problem. This may seem equivalent to assuming away our problems, and to some degree it is, but there is little to be gained by creating more uncertainty which basically arises from how well the gas models represent reality. Data can still be compared among facilities, as long as the different gas models and properties are stated. Any inaccuracies in the model will be endemic to all the facilities.

3.4 Interpolation in the Tables

The variables of interest will require interpolation both in pressure and temperature and the question of "how does one propagate uncertainty in the independent variables (mainly temperature and pressure) to the dependant variable?" remains. There are two distinct error propagation problems. The first deals only with one independent variable (either temperature or pressure); the second with two independent variables. In the first case the error in temperature or pressure will be given as

$$\frac{\Delta T}{T_m}$$

where T_m is the measured temperature (or pressure). Using the mean temperature and the definition of error we find that $\pm \Delta T$ is the 95% confidence range. Using interpolation on the tables we can find not only the dependent variable X_m but also $X_{m+} = F(T_m + \Delta T)$ and $X_{m-} = F(T_m - \Delta T)$. In most cases $X_{m+} - X_m = X_m - X_{m-}$ but it will not always be so. In this case the question becomes whether to leave the error for the dependent variable as a non-symmetric bias, re-offset X_m so that it remains symmetric, or take the larger of the two differences and make that the range. Since we will ultimately be interested in the relative error

$$\frac{\Delta X}{X_m}$$

any differences between $X_{m+} - X_m$ and $X_m - X_{m-}$ should be small. To keep the error propagation as simple as possible it is recommended taking the larger value of $X_{m+} - X_m$ or $X_m - X_{m-}$ and making that the range. This should not overstate the error bounds in a manner which influences the final error in efficiency in an unreasonable manner. A similar method for two independent variables will leave a value of X_m with four outlining corners $(T_-,P_-; T_-,P_+; T_+,P_-; T_+,P_+)$. There will generally be no great increase in the error band if the largest value of $X - X_m$ (X is taken at any of the four corners) is taken as the ΔX.

29

Using these procedures we can now calculate the error propagation through the table or any temperature or pressure. And by considering that the data in reference 2 is the gas property standard for this facility, we can reduce the definitional error associated with the tables to zero, plus we have defined our basis, so that comparison with data obtained in other facilities will be easier to do. The gas properties and equations used are shown in appendix A. Figures A-10a and A-11a show the variation in mixture compressibility and γ from the initial conditions (as calculated in equation 3-2).

$$\%\Delta\gamma = \frac{(\gamma - \gamma_{T=520, P=7\ atm})100}{\gamma_{T=520, P=7\ atm}} \quad \text{similar expression for } z \qquad (3\text{-}2)$$

One can see that the variation is not large in an overall percentage range, but could be substantial when developing an overall accuracy of efficiency of 0.25%.

Section 4 Supply Tank Filling Procedure and Resulting Uncertainty in γ and Other Initial Conditions

4.1 Introduction

Analyzing the supply tank fill procedure and the resulting uncertainty in the initial conditions at the end of the fill is a critical, yet a subjective task. There are many ways to approach this type of analysis and the selection of the final procedure for filling the tank will be based on experiment as well as the analysis presented below. However, there are some theoretical issues which need to be addressed.

The procedure used to fill the supply tank is based on the law of partial pressures. This law, which is empirically based, has as a major assumption that the presence of each component does not influence the other. This is an idealization, and as demonstrated in the earlier section, the test gases exhibit real gas effects in the pressure and temperature ranges in which they are being used. In some operating regions the law of partial pressures can be modified by adding the individual compressibility of each component. The question then becomes, "how good is this approximation to the "truth"?". To determine this we would need either a definitive answer, upon which this model could be compared, or a variety of different models to determine the spread of results. At this point, there are no clear alternatives, so we will resort to the technique of section 3 and declare that for the ATARR facility, the rule of partial pressures is valid (after being modified for compressibility factors). As long as the facility data are reduced in a manner which is consistent with this assumption, then there should not be a problem with this process. When comparing data to other facilities, the error introduced in this process might need to be accounted for.

4.2 Tank Fill Procedure

There are two distinct operating modes for the ATARR facility: when a single test gas is used, and when a mixture of gases is used to match the appropriate test conditions. In the former case there is relatively little uncertainty introduced in the fill process. Since both the gas and its properties are known and exact, the only uncertainty in the initial conditions comes from the uncertainty in pressure and temperature propagated through the gas property tables (as described in section 3). When a mixture is used, the problem of determining the relative uncertainty in the initial properties becomes more complicated. This sub-section of the report describes the fill process and the resulting uncertainty for the two gas mixture case.

The tank is to be filled using partial pressures and as shown in section 3, the compressibility of the gas could cause some error in the measurements so the fill equations need to reflect these real gas effects. If γ and T of the test gas in the tank are to match the desired

31

operating conditions in the field then the three equations used to specify the loading pressures and temperatures are:

$$\gamma = \frac{C_{px} m_x + C_{py} m_y}{C_{vx} m_x + C_{vy} m_y}$$

(4-1)

$$m_x = \frac{P_1 V}{T_1 z_{x,1} R_x}$$

(4-2)

$$\left[z_x R_x m_x + z_y R_y m_y \right]\Big|_2 = \frac{P_2 V}{T_2}$$

(4-3)

where C_{px}, C_{vx} are the specific heats of gas x (similar notation for gas y);

m_x and m_y are the masses of each gas;

V is the volume of the tank;

R_x and R_y are the gas constants of each gas;

z_x, and z_y are the compressibility of the two gases

1 and 2 are subscripts refer to two different measurement points.

Nominally T_1, T_2, are equal and are the same as the desired test temperature T. Equations 4-3 follows from the law of partial pressures corrected for compressibility effects, evaluated at the measurement conditions. Equation 4-2 is used to determine the partial pressure level which the calculated mass of gas x would generate. The tank is filled to that level, where a reading is taken (after equilibrium is established) which is labeled 1. The second gas is added until the desired test pressure is reached, where another measurement is taken labeled 2. One can see that the ratio of the two masses is the important variable and equations 4-1 to 4-3 can be rewritten in terms of only a single variable m_y/m_x.

$$\gamma = \frac{C_{px} + C_{py} \dfrac{m_y}{m_x}}{C_{vx} + C_{vy} \dfrac{m_y}{m_x}}$$

(4-4)

$$m_x = \frac{P_1 V}{T_1 z_{x,1} R_x}$$

(4-5)

$$\left[z_x R_x m_x \left(1 + \frac{z_y R_y m_y}{z_x R_x m_x}\right) \right]\Big|_2 = \frac{P_2 V}{T_2}$$

(4-6)

Combining equations 4-5 and 4-6 and making the following substitutions:

$$Zr_2 = \frac{z_{y,2}}{z_{x,2}} \qquad \frac{z_{x,1}}{z_{x,2}} = Zx_{12} \qquad \frac{z_{x,1}}{z_{y,2}} \frac{z_{x,2}}{z_{x,2}} = \frac{Zx_{12}}{Zr_2}$$

we obtain:

$$\frac{m_y}{m_x} = \frac{R_x}{R_y} \left(\frac{P_2 T_1}{P_1 T_2} \frac{Zx_{12}}{Zr_2} - \frac{1}{Zr_2} \right)$$

(4-7)

For any desired test gamma, a unique ratio of masses can be determined, and this ratio can be found from the two different measurements outlined earlier. Rewriting equation 4-4 in slightly different terms creates:

$$\gamma = \gamma_x \frac{1 + \frac{C_{py}}{C_{px}} Mr}{1 + \frac{C_{vy}}{C_{vx}} M}$$

(4-8)

where Mr is the mass ratio m_y/m_x. The relative uncertainty in gamma written in these terms becomes:

$$\frac{\Delta\gamma}{\gamma} = \left[\frac{(\frac{\Delta C_{p_x}}{C_{p_x}})^2 + (\frac{\Delta C_{p_x}}{C_{p_x}})^2}{\left[\frac{C_{p_x}}{C_{p_y}Mr} + 1\right]^2} + \frac{(\frac{\Delta C_{v_y}}{C_{v_y}})^2 + (\frac{\Delta C_{v_x}}{C_{v_x}})^2}{\left[\frac{C_{v_x}}{C_{v_y}Mr} + 1\right]^2} + (\frac{\Delta\gamma_x}{\gamma_x})^2 + \left[\frac{\frac{\gamma_y}{\gamma_x} - 1}{(\frac{C_{v_x}}{C_{v_y}} + Mr\frac{\gamma_y}{\gamma_x})(\frac{C_{v_y}}{C_{v_x}} + \frac{1}{Mr})} \right]^2 (\frac{\Delta Mr}{Mr})^2 \right]^{\frac{1}{2}}$$

(4-9)

The uncertainty in Mr ($=m_y/m_x$) can be developed as:

$$\frac{\Delta(\frac{m_y}{m_x})}{\frac{m_y}{m_x}} = \left[\left(\frac{1}{1 - \frac{T_2 P_1}{P_2 T_1 Zx_{12}}} \right)^2 \left((\frac{\Delta P_2}{P_2})^2 + (\frac{\Delta P_1}{P_1})^2 + (\frac{\Delta T_2}{T_2})^2 + (\frac{\Delta T_1}{T_1})^2 + (\frac{\Delta Zx_{12}}{Zx_{12}})^2 \right) + (\frac{\Delta Zr_2}{Zr_2})^2 \right]^{\frac{1}{2}}$$

(4-10)

During the actual filling process, the value of the test gas gamma can be determined by using equation 4-7 to determine m_y/m_x and then using equation 4-4. Its uncertainty can be calculated to the confidence level used in the calibration procedures through equation 4-8 and 4-9.

The uncertainty in the test gas constant can be derived from the original equation:

$$R = \frac{R_x + R_y\frac{m_y}{m_x}}{1 + \frac{m_y}{m_x}}$$

(4-11)

as:

$$\frac{\Delta R}{R} = \left[\frac{\left\{1 - \frac{R_x}{R_y}\right\}^2}{\left\{\frac{R_x m_x}{R_y m_y} + 1\right\}^2 \left\{1 + \frac{m_y}{m_x}\right\}^2} \left\{\frac{\Delta\frac{m_y}{m_x}}{\frac{m_y}{m_x}}\right\}^2 \right]^{.5}$$

(4-12)

Since there are no errors in the gas constants.

33

4.2 Influence of Real Gas Effects on Fill Conditions and Uncertainties

At this point it is worthwhile to examine the influence of the gas compressibility on the fill conditions. To determine the influence of assuming ideal gas behavior on the values of m_y/m_x and $\Delta m_y/m_x$, equations 4-7 and 4-9 can be evaluated in the following form.

$$\text{Influence of Real gas} = \frac{V\big|_{real} - V\big|_{ideal}}{V\big|_{ideal}} \tag{4-13}$$

Where V is the variable of interest which for equation 4-7 becomes:

$$= [\frac{X}{X-1}]\frac{Zx_{12}}{Zr_2} - [\frac{1}{X-1}]\frac{1}{Zr_2} - 1$$

$$\text{where } X = \frac{P_2 T_1}{P_1 T_2} \tag{4-14}$$

and for equation 4-10:

$$= [1-\frac{1}{X}]\left[\frac{(\frac{\Delta Zr_2}{Zr_2})^2}{\Delta^2} + \frac{\frac{(\frac{\Delta Zx_{12}}{Zx_{12}})^2}{Zx_{12}} }{\Delta^2} + 1}{[1 - \frac{1}{XZx_{12}}]^2} \right]^{\frac{1}{2}} - 1$$

$$\text{where } \Delta^2 = (\frac{\Delta P_1}{P_1})^2 + (\frac{\Delta P_2}{P_2})^2 + (\frac{\Delta T_1}{T_1})^2 + (\frac{\Delta T_2}{T_2})^2 \tag{4-15}$$

where X is the same as in equation 4-14. If the uncertainty in the compressibility is small compared to the total uncertainty (which it is from appendix A) then the variables

$$\frac{(\frac{\Delta Zr_2}{Zr_2})^2}{\Delta^2} \to 0 \quad \text{and} \quad \frac{(\frac{\Delta Zx_{12}}{Zx_{12}})^2}{\Delta^2} \to 0$$

which would result in an overall difference between the real and the ideal measurement of:

$$= \frac{1 - Zx_{12}}{Zx_{12}X-1} \tag{4-16}$$

It is clear in both equations 4-14 and 4-15 that how close the compressibility factors are to one is critical in determining whether real gas effects are important. Assuming that the two temperature measurements during the filling process (numbers one and two) are the same (which they should be), then the different compressibility ratios Zr_2 ($=z_{y2}/z_{x2}$) and Zx_{12} ($= z_{x1}/z_{x2}$) can be evaluated as a function of test temperature and fill pressure ratio.

Zx_{12} is shown in figure 4-1 as a function of different fill pressure ratios (P_1/P_2) and test temperatures (based on a final test pressure of 105 psi (7 atm)) for nitrogen. A similar plot is shown in figure 4-2 for carbon dioxide. Figure 4-3 is a plot of how Zr_2 varies for different final test conditions
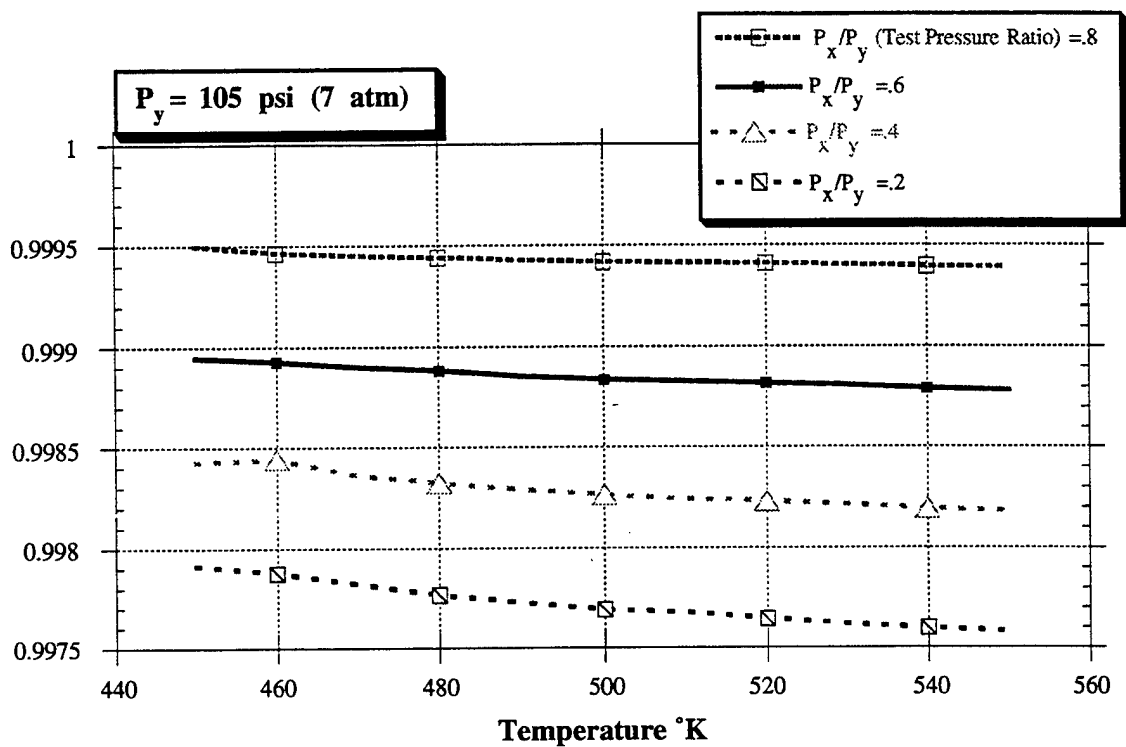
Figure 4-1 Zx_{12} as a Function of Test Temperature and Fill Pressure Ratio for Nitrogen
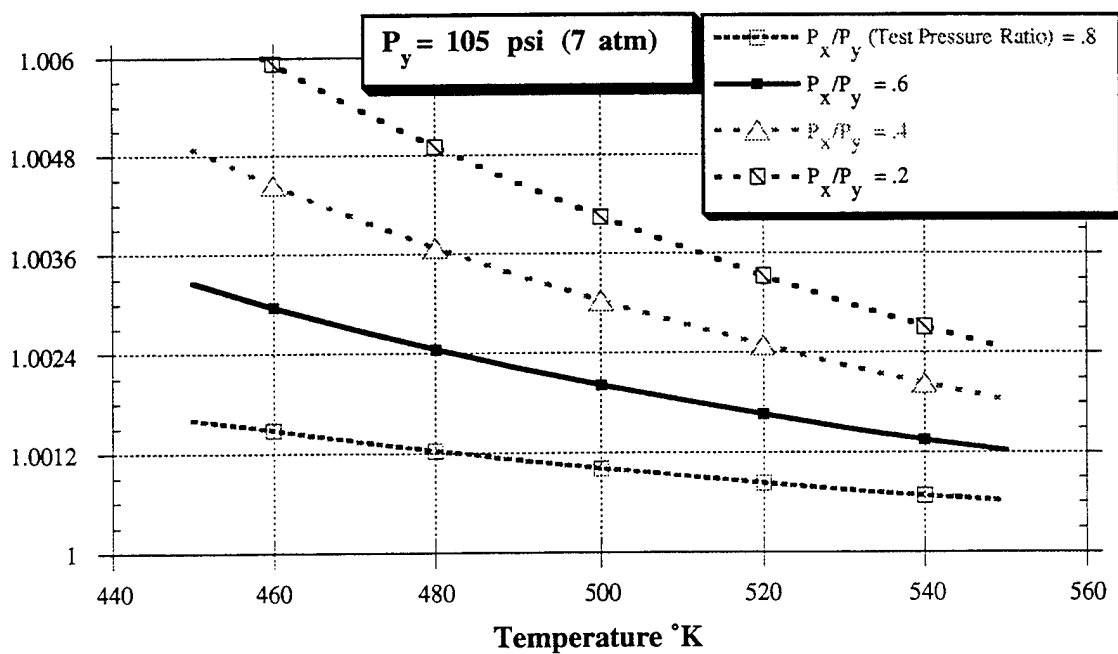
Figure 4-2 Zx_{12} as a Function of Test Temperature and Fill Pressure Ratio for Carbon Dioxide

35
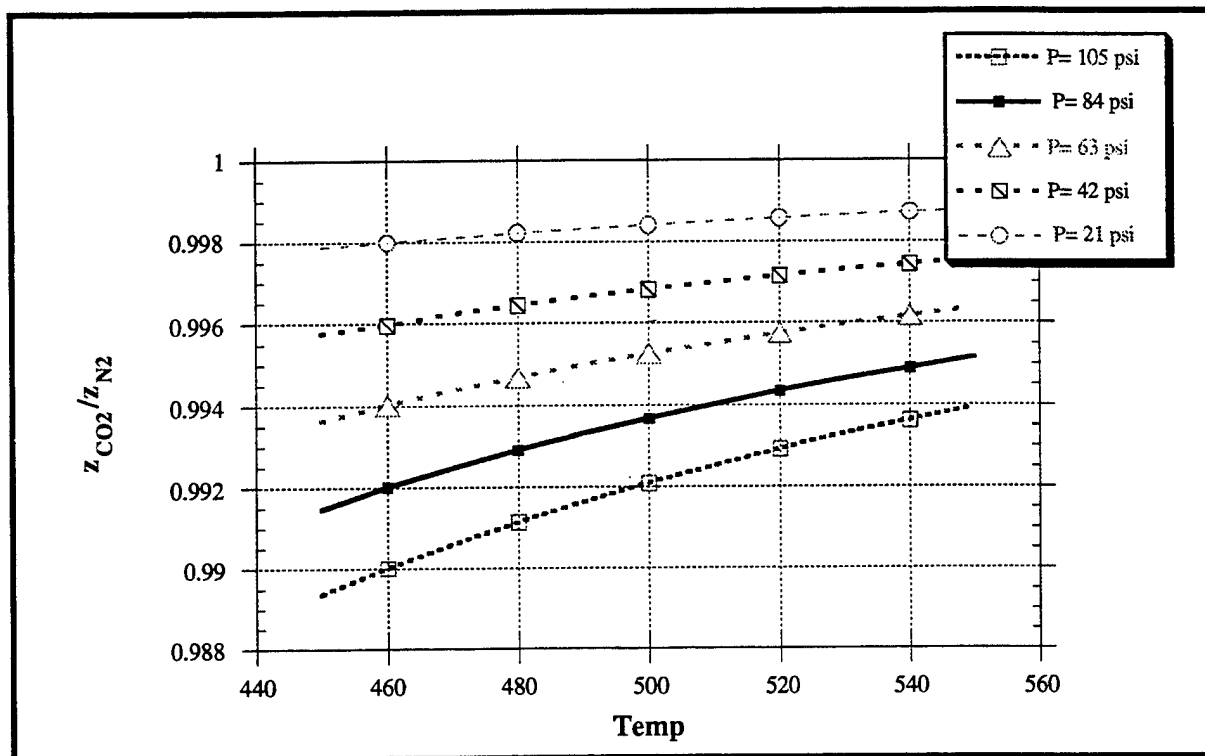
Figure 4-3 Z_{r2} ($=z_{CO2}/z_{N2}$) as a Function of Test Temperature and Final Pressure Level

For a standard fill, the pressure ratio P_2/P_1 will be 3.054 (creating a γ of 1.268, see appendix A). To show how the ideal gas approximation effects the final results as a function of temperature, we can assume that the temperature of the fill process remains constant (at the final test temperature). Form figure A-9 in Appendix A, which show the variation of Z_{x12} and Z_{r2} as a function of the test temperature, the results of equation 4-14 and 4-16 can be plotted as a function of test temperature as shown in figure 4-4.
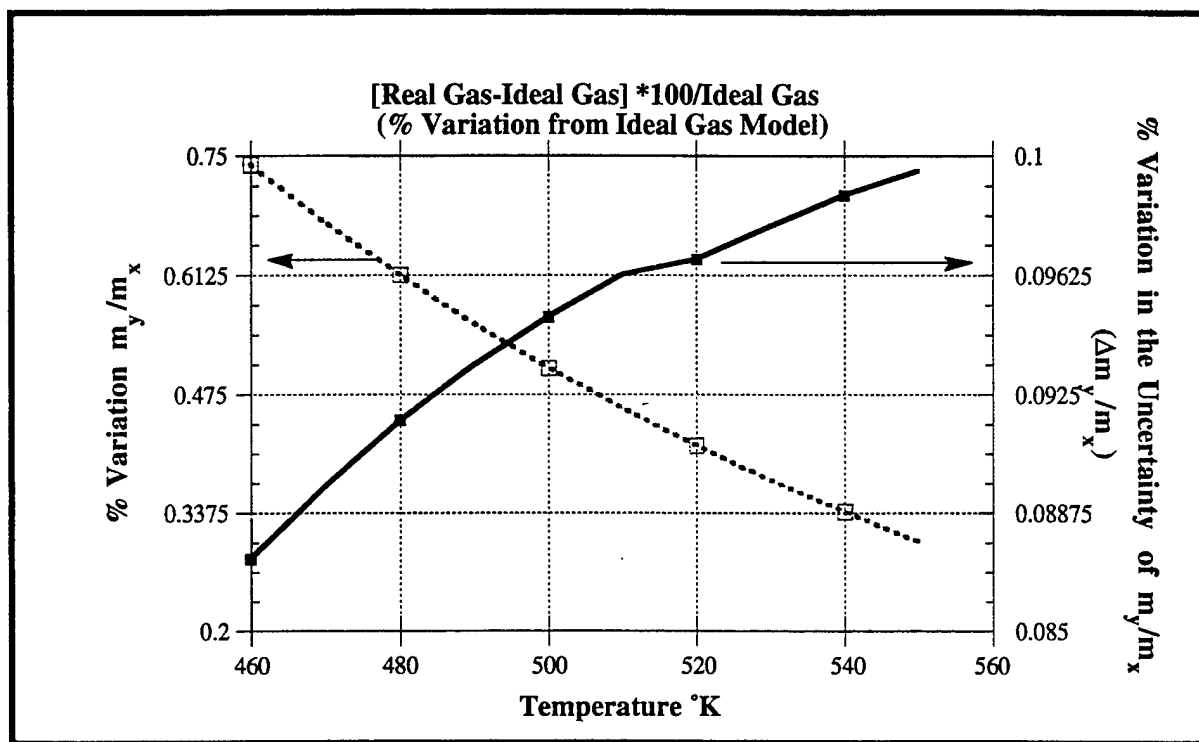
Figure 4-4 Relative Error in Ideal Gas Model

It is clear from figure 4-4 that the difference between the ideal gas model and the real gas model can be significant, even when the individual compressibility factors are close to one. An interesting point is that the difference between the real gas model and the ideal gas model is an order of magnitude bigger for the mass ratios than it is in the for the uncertainty in the mass ratio.

4.3 Subsequent Fills

Subsequent fills add a third measurement since the final condition of the test tank has to be known before it can be resupplied. There was no need for this measurement during the first fill because the tank was initially evacuated. After the first run the tank is considered to hold the same ratio of gas masses as existed before the test, with the same uncertainty. The second fill is denoted by the subscript $_b$, the first fill conditions by subscript $_a$, and the new ideal testing pressure, temperature and gamma are given by P_b, T_b, and γ_b. If after the first test the supply tank is brought to the second test temperature a third measurement is taken (denoted by $_3$) which corresponds to the final state of the tank at the new test temperature. The total amount of either gas can be calculated knowing P_3 and the ratio of masses in the tank, $m_2/m_1 \vert_a$. At this point the total masses needed for the next test can be estimated. There are three possibilities:

Case 1) **The total amount of both gases has to be reduced.**

The tank is bled until it reaches the pressure which corresponds to the least amount of gas needed in the tank. If this happens the third measurement taken is discarded and a new one is

37

taken at this point and this becomes measurement 3. Once here, this case progresses the same as case 2.

Case 2) **One of the masses is correct but the other has to be increased.**

The partial pressure which would result from an increase in the mass of that gas is calculated using equation 4-2 where m is taken as the mass increment and the gas is bled in until the new pressure (which is the old pressure plus the just calculated increment) is reached (labeled as measurement 4).

Case 3 **Both masses need to be incremented.**

This case is essentially the same as case 2 except it is repeated for the second gas yielding yet another measurement called 5.

The problem is similar to the earlier one, estimating the error in gamma, and equation 4-8 is still valid. The question is, "How does the new ratio of $m_y/m_x \,|_b$ depend on the measurements just taken and on the initial mixture in the tank?"

The fill conditions are complicated by the introduction of the compressibility factor. Examining the fill process discussed in case 3 (since it requires three new measurements) the equations which describe the different measurements are:

$$m_1\Big|_a = \frac{P_3 V}{T_3 R_1 z_1\Big|_3 (1 + \frac{R_2 z_2}{R_1 z_1}\Big|_3 \frac{m_2}{m_1}\Big|_a)} \tag{4-16}$$

$$m_1\Big|_b = (\frac{P_4 V}{T_4} - R_2 z_2\Big|_4 m_2\Big|_3)(\frac{1}{R_1 z_1\Big|_4}) \tag{4-17}$$

$$\frac{m_2}{m_1}\Big|_b = (\frac{P_5 V}{T_5 R_1 z_1\Big|_5 m_1\Big|_b} - 1)(\frac{R_1}{R_2} \frac{z_1\Big|_5}{z_2\Big|_5}) \tag{4-18}$$

$$m_2\Big|_a = \frac{m_2}{m_1}\Big|_a m_a\Big|_a \tag{4-19}$$

These can be recombined to give just one equation in terms of the measured pressures and temperatures and the initial gas mixture:

$$\frac{m_2}{m_1}\Big|_b = \left[\frac{\frac{P_5 T_4}{P_4 T_5}\frac{z_1\Big|_4}{z_1\Big|_5}\{\frac{R_1}{R_2} + \frac{z_2}{z_1}\Big|_3 \frac{m_2}{m_1}\Big|_a\}}{\frac{m_2}{m_1}\Big|_a\{\frac{z_2}{z_1}\Big|_3 - \frac{P_3 T_4}{P_4 T_3}\frac{z_1\Big|_4}{z_1\Big|_3}\} + \frac{R_1}{R_2}} - 1\right]\frac{R_1 z_1}{R_2 z_2}\Big|_5 \tag{4-20}$$

Equation 4-20 shows that the value of the mass ratios in the second fill is dependent on the pressure and temperature measurements taken between the last run and the present run, as

well as the initial mixture. In the worst case (which is outlined above) the error in any fill subsequent to the first will depend on seven measurement variables (rather than the four described in equation 4-7: (three temperature measurements, three pressure measurements, and the error in the fill from the run before) in addition to the vast array of compressibility factors. The uncertainty in the mass ratios for subsequent fills (equation 4-20) can be found in a similar method to that of equation 4-9 (although the mathematics can become quite complicated).

Before we proceed with this task we can simplify equation 4-20 by creating some new variables which are ratios of other variables.

$$\frac{1}{Rr} = \frac{R_x}{R_y} \qquad \frac{1}{Zr_5} = \frac{z_x}{z_y}\Big|_5 \qquad Zx_{45} = \frac{z_x\big|_4}{z_x\big|_5} \qquad Zy_{43} = \frac{z_y\big|_4}{z_y\big|_3} \qquad \frac{1}{Zr_3} = \frac{z_x}{z_y}\Big|_3$$

$$Mr_a = \frac{M_y}{M_x}\Big|_a$$

which reduces equation 4-20 to:

$$\frac{m_y}{m_x}\Big|_b = \left[\frac{\frac{P_5 T_4}{P_4 T_5} Zx_{45} \left\{ \frac{1}{Rr\,Zr_3} + Mr_a \right\}}{Mr_a \left\{ 1 - \frac{P_3 T_4}{P_4 T_3} Zy_{43} \right\} + \frac{1}{Rr\,Zr_3}} - 1 \right] \frac{1}{Rr\,Zr_5}$$

(4-21)

The uncertainty in the mass ratios for the second fill is given by:

$$\frac{\Delta \frac{m_y}{m_x}\Big|_b}{\frac{m_y}{m_x}\Big|_b} = \left[\left(\frac{\Delta Zr_5}{Zr_5}\right)^2 + F_a^2 \left\{ \left(\frac{\Delta P_4}{P_4}\right)^2 + \left(\frac{\Delta T_4}{T_4}\right)^2 \right\} + F_b^2 \left\{ \left(\frac{\Delta P_3}{P_3}\right)^2 + \left(\frac{\Delta T_3}{T_3}\right)^2 + \left(\frac{\Delta Zy_{43}}{Zy_{43}}\right)^2 \right\} \right.$$

$$\left. + F_c^2 \left\{ \left(\frac{\Delta P_5}{P_5}\right)^2 + \left(\frac{\Delta T_5}{T_5}\right)^2 + \left(\frac{\Delta Zx_{45}}{Zx_{45}}\right)^2 \right\} + F_d^2 \left\{ \frac{\Delta Mr_a}{Mr_a} + \left(\frac{\Delta Zr_3}{Zr_3}\right)^2 \right\} \right]^{.5}$$

(4-22)

where

$$F_a = \frac{1}{\left(1 - \frac{P_4}{P_5} + \frac{P_3}{P_5} \frac{Rr\,Mr_a}{Rr\,Mr_a + 1}\right)\left(1 - \frac{P_3}{P_4} \frac{Rr\,Mr_a}{Rr\,Mr_a + 1}\right)}$$

$$F_b = \frac{\frac{P_5}{P_3} \frac{Rr\,Mr_a}{Rr\,Mr_a + 1}}{\left(\frac{P_4}{P_3} + \frac{P_5}{P_3} + \frac{Rr\,Mr_a}{Rr\,Mr_a + 1}\right)\left(\frac{P_4}{P_3} + \frac{Rr\,Mr_a}{Rr\,Mr_a + 1}\right)}$$

$$F_c = \frac{1}{\left(1 - \frac{P_4}{P_5} + \frac{P_3}{P_5} \frac{Rr\,Mr_a}{Rr\,Mr_a + 1}\right)}$$

39

$$F_d = \cfrac{\cfrac{Rr\,Mr_a}{Rr\,Mr_a+1}}{\left(\cfrac{P_4}{P_3} - \cfrac{Rr\,Mr_a}{Rr\,Mr_a+1}\right)\left(1 - \cfrac{P_4}{P_5} + \cfrac{P_3}{P_5}\cfrac{Rr\,Mr_a}{Rr\,Mr_a+1}\right)\left(\cfrac{Rr\,Mr_a}{Rr\,Mr_a+1}+1\right)}$$

<div align="right">(4-23)</div>

While equations 4-22 and 4-23 allow the calculation of the uncertainty from known components, in its present form it is not very insightful, because of its complexity. By looking at the specific case of repeated fills the behavior of equation 4-22 can be better understood.

The following three graphs show two cycles in the filling procedure.
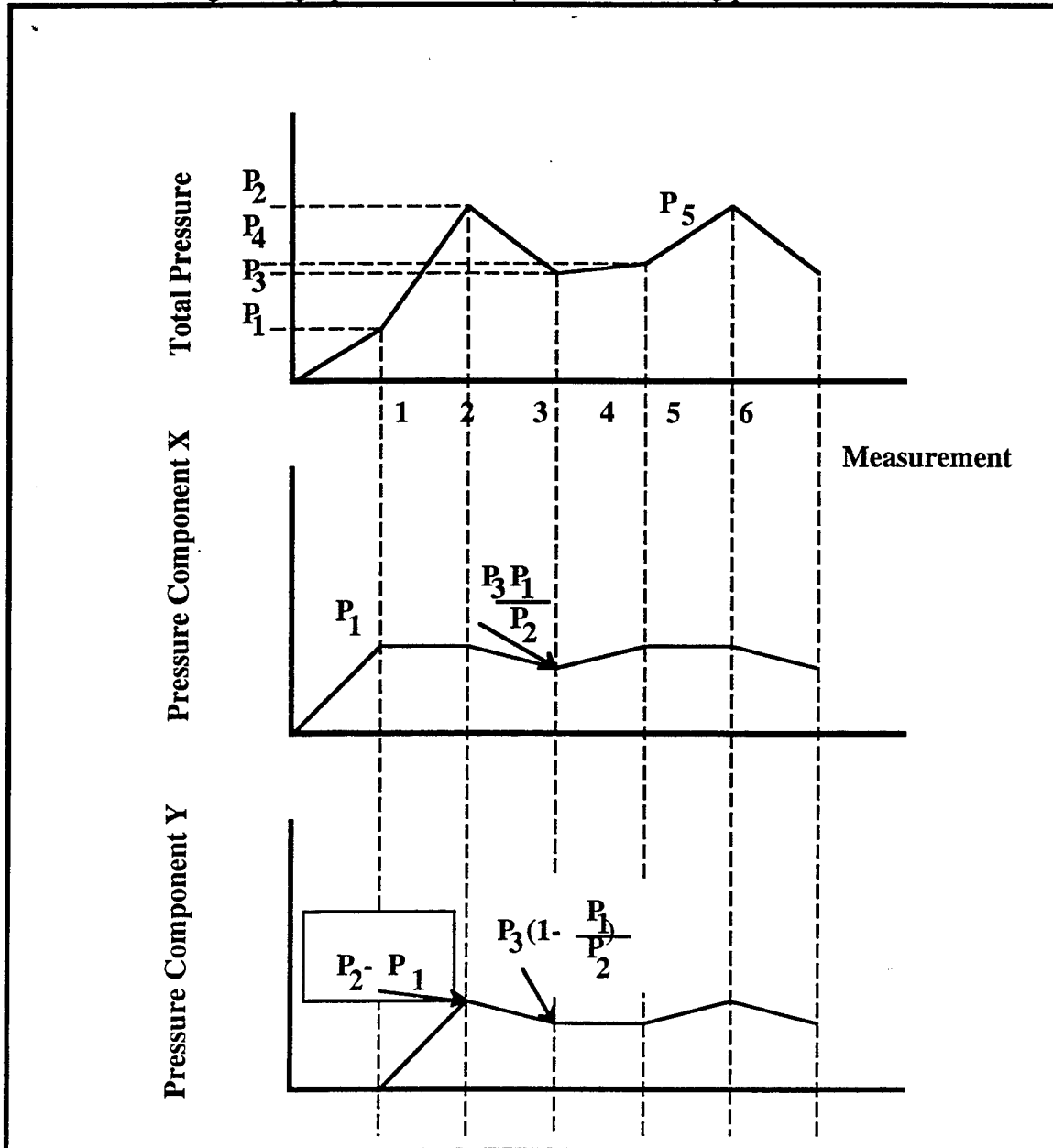
Figure 4-5 Repeated Fills to Same Conditions

Figure 4-5 shows the path of the different components during the fill process. Since each test is assumed to have the same initial conditions it is not surprising that $P_2 = P_5$. However the intermediate pressure P_4 depends on how much gas was lost during the first test (i.e. the pressure drop P_2-P_3). If the fill and testing temperatures all remain the same (which is the theoretical goal) and the mass ratio from the first test is assumed to remain constant, then the partial pressure of component X after the first test will be given by:

$$P_x = \frac{P_3 P_1}{P_2}$$

(4-24)

since the pressure ratio P_1/P_2 remains constant. To regain the proper amount of component X to achieve the final test pressure ($P_2=P_5$) component X has to be added until its pressure reaches P_1 again. Thus the pressure increments translates into a P_4 of:

$$P_4 = P_3 + P_1 - \frac{P_3 P_1}{P_2}$$

(4-25)

If the tank is assumed to always blow-down a specific fraction of its test pressure, such that

$$P_3 = FP_2$$

(4-26)

and the test mass ratio is given by the test pressure ratio:

$$\frac{P_1}{P_2} = G$$

(4-27)

and the compressibility factors are all assumed to be very close to one (so that they can be neglected for this order of magnitude analysis) then the constants in equation 4-23 can be simplified greatly. After setting the temperatures equal, and the compressibility factors to one, the constants in equation 4-23 become:

$$F_a = \frac{G + F(1-G)}{G(1-G)} \quad F_b = \frac{F}{G} \quad F_c = \frac{1}{(1-G)} \quad F_d = F$$

(4-28)

From their definitions, both F and G will range in value from 0 to 1 which points to some interesting behavior in equation 4-22. First, all the uncertainties in the compressibility factors can be translated into uncertainties in the measured pressure and temperature of the gas, since by definition any inaccuracy in the compressibility arises from inaccuracies in the temperatures and pressures. Secondly, F_d (which is the influence coefficient for the uncertainty of the mass ratio in the previous fill, $\Delta Mr_a/Mr_a$) will always be less then 1. Since the tank is expected to loose about 40% of its initial pressure in an average test, this makes the original mass ratio uncertainty a weak factor in the overall contribution to the uncertainty in the mass ratio of a subsequent fill. One can rearrange F_a to show that it will always be greater then one when:

$$F(\frac{1}{G} -1) > -G$$

(4-29)

41

which is always true since both F and G are less then one and are positive numbers. Thus only F_b has the possibility of being less then one. To obtain a lower bound on the overall uncertainty in the mass ratio, we can assume that the uncertainty in the compressibilities are very small compared to the uncertainties in the pressure and temperatures, and that the uncertainty in the temperatures and pressures are equal for all measurements. Thus equation 4-22 becomes:

$$\frac{\Delta \frac{m_y}{m_x}\Big|_b}{\frac{m_y}{m_x}\Big|_b} = \left[\left\{ F_a^2 + F_b^2 + F_c^2 \right\} \left\{ (\frac{\Delta P}{P})^2 + (\frac{\Delta T}{T})^2 \right\} + F_d^2 (\frac{\Delta Mr_a}{Mr_a})^2 \right]^{.5}$$

(4-30)

where the overall influence coefficient would become:

$$F_{Overall}^2 = \left\{ F_a^2 + F_b^2 + F_c^2 \right\} = \frac{2}{(1-G)^2} \{ (\frac{F}{G})^2 (G-1)^2 + \frac{F}{G}(1-G) + 1 \}$$

(4-31)

Making the substitution A=F/G and taking the square root of equation 4-31, we can plot this value as a function of A and G
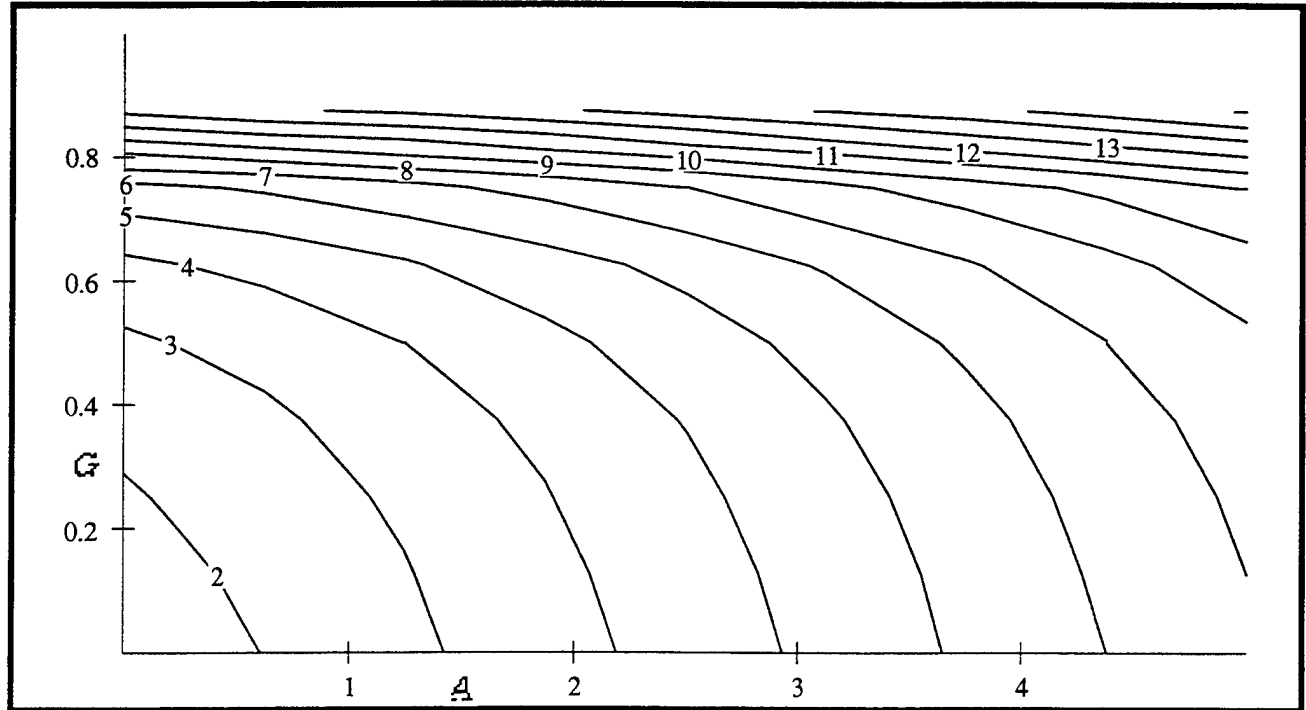
Figure 4-6

Contour Plot of Overall Influence Coefficient ($F_{Overall}$) as a Function of A and G

To see how the error propagates to subsequent fills, equation 4-30 and 4-9 can be written in terms of the error in the initial mass ratio and the error in the pressure and temperature measurements. Using the same assumptions listed above on equation 4-9 the uncertainty in the original mass ratio becomes:

42

$$\frac{\Delta(\frac{m_2}{m_1})}{\frac{m_2}{m_1}} = \left[\left(\frac{1}{1-G}\right)^2 \left((\frac{\Delta P}{P})^2 + (\frac{\Delta T}{T})^2\right)\right]^{\frac{1}{2}}$$

(4-32)

and equation 4-30 becomes:

$$\frac{\Delta\frac{m_y}{m_x}\big|_b}{\frac{m_y}{m_x}\big|_b} = \left[\left\{F^2_{Overall}\right\}\left\{(\frac{\Delta P}{P})^2 + (\frac{\Delta T}{T})^2\right\} + F^2(\frac{\Delta Mr_a}{Mr_a})^2\right]^{.5}$$

$$= \left[\left\{F^2_{Overall} + F^2 2\left(\frac{1}{1-G}\right)^2\right\}\left\{(\frac{\Delta P}{P})^2 + (\frac{\Delta T}{T})^2\right\}\right]^{.5}$$

(4-33)

Expanding this process to other fills one finds that

$$\frac{\Delta\frac{m_y}{m_x}\big|_n}{\frac{m_y}{m_x}\big|_n} = \left[\left\{F^2_{Overall} \left(\sum_{i=1}^{n-1} F^{2(i-1)}\right) + F^{2(n-1)} 2\left(\frac{1}{1-G}\right)^2\right\}\left\{(\frac{\Delta P}{P})^2 + (\frac{\Delta T}{T})^2\right\}\right]^{.5}$$

(4-34)

which expands to:

$$\frac{\Delta\frac{m_y}{m_x}\big|_n}{\frac{m_y}{m_x}\big|_n} = \left[\left\{F^2_{Overall} \left(1 + F^2 + \ldots F^{2(n-2)}\right) + F^{2(n-1)} 2\left(\frac{1}{1-G}\right)^2\right\}\left\{(\frac{\Delta P}{P})^2 + (\frac{\Delta T}{T})^2\right\}\right]^{.5}$$

(4-35)

where n goes from 2 to infinity (b to infinity). Since F<1 the influence of the original error in the mass ratio quickly becomes unimportant. But the overall uncertainty in the mass ratio will increase greatly until it reaches the limit where:

$$F^{2(n-2)}F^2_{Overall} \ll 1$$

(4-36)

since all the terms added after this point rapidly approach zero. Equation 4-35 can be rewritten as:

$$\frac{\Delta\frac{m_y}{m_x}\big|_n}{\frac{m_y}{m_x}\big|_n} = \left[\left\{F^2_{Overall} (K) + F^{2(n-1)} 2\left(\frac{1}{1-G}\right)^2\right\}\left\{(\frac{\Delta P}{P})^2 + (\frac{\Delta T}{T})^2\right\}\right]^{.5}$$

where $K = (1 + F^2 + \ldots F^{2(n-2)})$

(4-37)

and ultimately as:

$$\frac{\Delta\frac{m_y}{m_x}\Big|_n}{\frac{m_y}{m_x}\Big|_n} = \left[C^2\left\{(\frac{\Delta P}{P})^2 + (\frac{\Delta T}{T})^2\right\}\right]^{.5}$$

where $C^2 = F^2_{Overall}$ (K)

Th factor {K} can be plotted as a function of the number of fills (n) and the blowdown fraction (F).
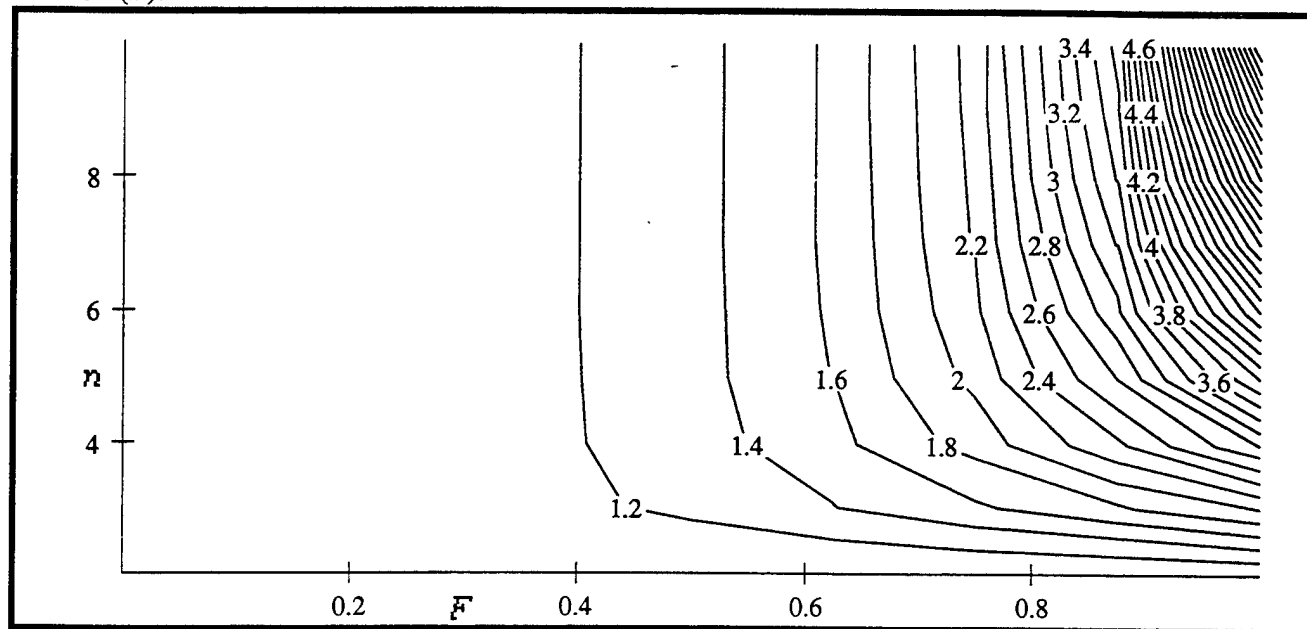
Figure 4-7 K as a Function of Number of Fills (n) and Blowdown Fraction (F)

Using figure 4-7 as a base, we can estimate the overall influence coefficient C as shown in figure 4-8.
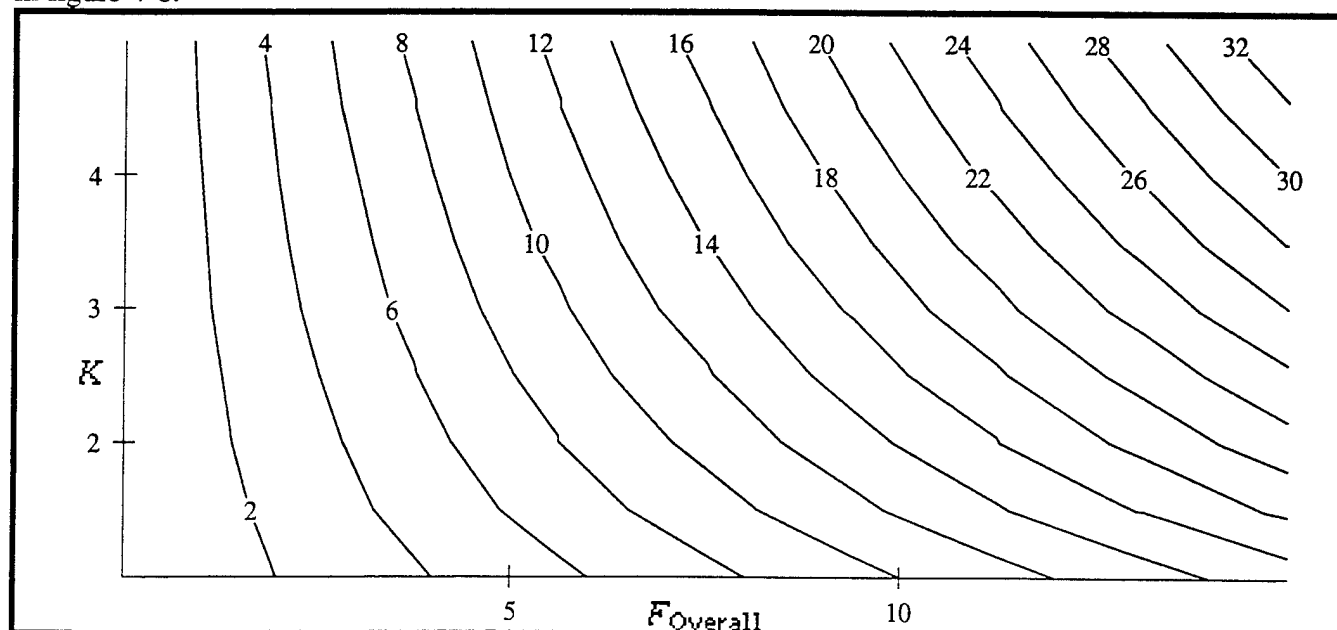
Figure 4-8
Limit in Mass Ratio Uncertainty as a Function of $F_{Overall}$ and K

4.4 Conclusions

This section of the paper has outlined the gas supply filling procedure for the ATARR facility in addition to showing how the uncertainties in the filling process are translated into uncertainties in the test gas properties. In addition, the differences between the real gas model and the ideal gas model have been shown to be significant in some cases. As discussed in the following section, most of the information contained in this section is important in deriving the uncertainty of the mass flow through the turbine stage. Which, in turn, is important in determining the overall efficiency accuracy when using the mechanical method of measurement (equations 2-9, 2-15, and 2-20). Until we have examined how the individual properties listed in this section contribute to the overall accuracy of the mass flow measurement, we will not know how important the real gas assumptions are.

Section 5 Estimation of Mass Flow

Sections 2.4 and 2.5 have shown that the main difference between measuring the turbine stage efficiency using a thermodynamic technique and a mechanical method is the information required. The thermodynamic technique requires an accurate knowledge of the downstream temperature while the mechanical method requires knowledge of the mass flow through the stage. This section of the report will address the problem of determining the mass flow through the stage and its relative uncertainty. There are several possible ways of measuring the core mass flow. The two main ways are to measure the corrected mass flow, or to measure the blowdown time-constant and the change in density of the supply tank over the test time. In section 5.1 these two methods will be quickly outlined for ideal gases. Section 5.2 will examine the complications which arise from real gas effects.

5.1 Potential Methods of Measuring Mass Flow Through the Turbine Stage for an Ideal Gas

Figure 5-1 shows the mass flow diagram and the choke points in the main facility.
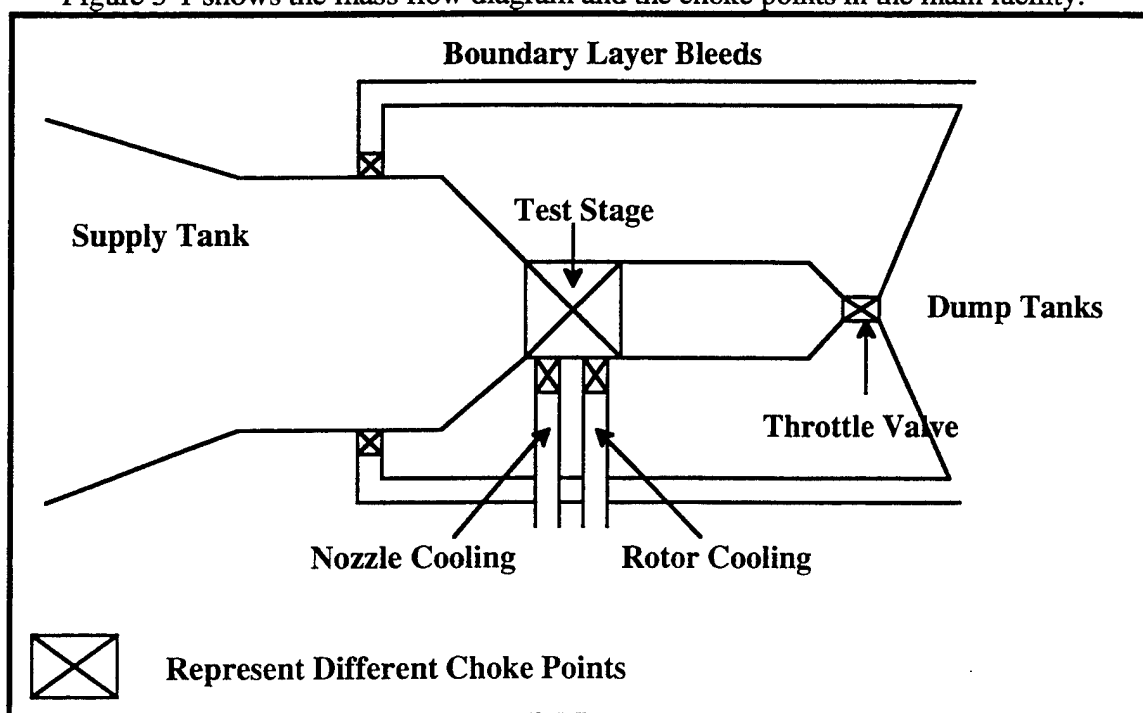
Figure 5-1 Mass Flow Diagram for ATARR

It is important to realize that the mass flow through the stage is not the same as the mass flow out of the supply tank. Some mass from the supply tank will exit the system through the boundary layer bleeds, and mass will be added from the cooling lines. In the present configuration the mass

46

flow from the cooling lines will be metered, thus their value and uncertainty as a function of time will be known from direct measurements.

5.1.1 Measurement of Mass Flow Based on Corrected Mass Flow

If the flow expands adiabatically as it leaves the supply tank (which it does everywhere except in the thermal boundary layers) then the total enthalpy of the flow will be constant and the relationship between the enthalpy in the supply tank and the enthalpy of the flow at the choked NGV's is given by equation 5-1.
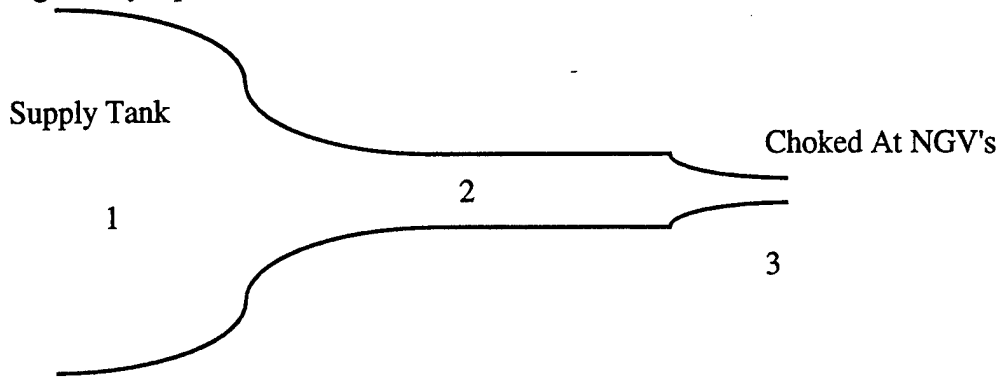
Figure 5-2   Notation Used in Mass Flow Calculations

$$h_1 = h_3 + \frac{V_3^2}{2}$$

(5-1)

If constant specific heats are assumed and the relationship

$$C_p = \frac{\gamma R}{\gamma - 1}$$

(5-2)

is used then equation 5-1 can be solved for the velocity and written as:

$$V_3^2 = \frac{2\gamma R}{\gamma - 1} T_1 (1 - \frac{T_3}{T_1})$$

(5-3)

The mass flow at the choke point is

$$\dot{m}_3 = \rho_3 V_3 A_3$$

(5-4)

which if the perfect gas law is used converts to:

$$\dot{m}_3 = \frac{V_3 A_3 P_1}{R T_1} (\frac{p_3 T_1}{p_1 T_3})$$

(5-5)

Since the gas is being isentropically expanded, the temperature ratio can be expressed as a function of the pressure ratio:

$$\frac{T_3}{T_1} = (\frac{p_3}{p_1})^{\frac{\gamma - 1}{\gamma}}$$

(5-6)

Combining equations 5-3, 5-4, and 5-6 the mass flow can be written as:

$$\dot{m}_3 = \frac{A_3 P_1}{\sqrt{T_1}} \sqrt{\frac{2\gamma}{R(\gamma - 1)}} (\frac{p_3}{p_1})^{\frac{1}{\gamma}} \sqrt{1 - (\frac{p_3}{p_1})^{\frac{\gamma - 1}{\gamma}}}$$

(5-7)

Since the flow is choked, the pressure ratio is fixed at:

$$\frac{p_3}{p_1} = \left(\frac{2}{\gamma+1}\right)^{\frac{\gamma}{\gamma-1}}$$

(5-8)

The corrected mass flow can be defined as:

$$m_{corr} = \frac{\dot{m}_3 \sqrt{\gamma R T_1}}{A_3 P_1}$$

(5-9)

and as shown in equation 5-7, this value remains constant as long as the flow is choked (and the gas properties remain constant). Equation 5-7 can be rewritten using the value of the pressure ratio which corresponds to choke conditions to yield a relationship between m_{corr} and γ.

$$m_{corr} = \gamma \left(\frac{2}{\gamma+1}\right)^{\frac{\gamma+1}{2(\gamma-1)}}$$

(5-10)

This shows that the mass flow at any point in time can be calculated from equation 5-9 if the instantaneous pressure and temperature in the supply tank as well as γ are known. However, this would only work if the flow were inviscid since A_3 would be the geometric choked area. But since the flow is viscous, there is a discharge coefficient associated with the inlet which reduces A_3. Thus requiring a separate method for determining the effective choked area.

5.1.2 Measurement of Mass Flow Based on Blowdown Time-Constant and the Change in Supply Tank Gas Density

Epstein, et al[1] developed the time dependent equations for the blowdown facility based on isentropic ideal gas assumptions as:

$$P_1(t) = P_1(0) \left[1+\frac{t}{\tau}\right]^{-\frac{2\gamma}{\gamma-1}}$$

$$T_1(t) = T_1(0) \left[1+\frac{t}{\tau}\right]^{-2}$$

$$\rho_1(t) = \rho_1(0) \left[1+\frac{t}{\tau}\right]^{-\frac{2}{\gamma-1}}$$

(5-11a,b,c)

were τ is the blowdown time constant and is given in this case as:

$$\frac{1}{\tau} = \frac{(\gamma-1)(1+\alpha)A_3\sqrt{\gamma R T_1(0)}}{\gamma} \frac{m_{corr}}{2V}$$

(5-12)

where V is the tank volume, A_3 is the choke area, and α is the fraction of the main flow exhausted through the bleeds. In theory one could measure the blowdown time constant by taking repeated pressure (or temperature) measurements and fitting the resulting pressure decay in the supply tank to the above curve, which would yield τ. This would provide the ratio of A_3 to V, but neither independently. If the supply tank volume were known from some other method, then A_3 could be determined using this method.

---

[1] Epstein, Alan, Gerald Guenette, and Robert Norton "The Design of the MIT Blowdown Turbine Facility", GTL Report no 183 April 1985, p. 123

In its most basic form, the mass flow out of the supply tank is given as:

$$\dot{m} = -V\frac{\partial \rho}{\partial t}$$

(5-13)

Using the time dependent functions of pressure and temperature given by equations 5-11(a-c), one can rewrite equation 5-13 in the form:

$$\dot{m} = V\frac{P_1(0)}{\tau R T_1(0)}(\frac{2}{\gamma-1})[1+\frac{t}{\tau}]^{\frac{-1-\gamma}{\gamma-1}}$$

(5-14)

Equation 5-14 shows that the mass flow can be directly measured using the supply tank initial conditions if the volume and the supply tank time constant are known and the gas properties remain the same.

5.1.3 Uncertainty in Mass Flow and the Uncertainty in the Measurement of Tau for an Ideal Gas

Using equation 5-14 we can examine how the mass flow uncertainty varies over the course of a test. Equation 5-14 provides the uncertainty in the mass flow out of the supply tank which must be combined with the uncertainty in the flow through the boundary layer bleeds to obtain the uncertainty in the mass flow entering the test section. The mass flow through the test section is given by

$$\dot{m}_3 = \frac{\dot{m}_1}{\alpha+1}$$

(5-15)

with a resulting uncertainty of

$$\frac{\Delta \dot{m}_3}{\dot{m}_3} = \left[\left[\frac{\alpha}{\alpha+1}\right]^2\left[\frac{\Delta\alpha}{\alpha}\right]^2 + \left[\frac{\Delta \dot{m}_1}{\dot{m}_1}\right]^2 \right]^{.5}$$

(5-16)

the uncertainty in the mass flow out of the supply tank is taken from equation 5-14:

$$\frac{\Delta \dot{m}_1}{\dot{m}_1} = \left[\left[\frac{\Delta\tau}{\tau}\right]^2\left[\frac{2\frac{t}{\tau}-\gamma+1}{(1+\frac{t}{\tau})(\gamma-1)}\right]^2 + \left[\frac{\Delta\gamma}{\gamma}\right]^2\left[\frac{\gamma}{1-\gamma}+\frac{2\ln(1+\frac{t}{\tau})}{(\gamma-1)^2}\right]^2 + \left[\frac{\Delta P_0}{P_0}\right]^2 + \left[\frac{\Delta T_0}{T_0}\right]^2 + \left[\frac{\Delta R}{R}\right]^2 + \left[\frac{\Delta V}{V}\right]^2 \right]^{.5}$$

(5-17)

or

$$\frac{\Delta \dot{m}_1}{\dot{m}_1} = \left[\left[\frac{\Delta\tau}{\tau}\right]^2 C_\tau^2 + \left[\frac{\Delta\gamma}{\gamma}\right]^2 C_\gamma^2 + \left[\frac{\Delta P_0}{P_0}\right]^2 + \left[\frac{\Delta T_0}{T_0}\right]^2 + \left[\frac{\Delta R}{R}\right]^2 + \left[\frac{\Delta V}{V}\right]^2 \right]^{.5}$$

(5-18)

In the situation under consideration, the uncertainty in the volume is a fixed number, independent of the test. The uncertainty in γ and R are only functions of the mixing process. The uncertainty in R can be expressed as a function of the uncertainty in the initial temperature and pressure measurements (this assumes that the total uncertainty in the measurements taken during the fill

49

process are the same as the uncertainty in the measurements at the beginning of the test). From equations 4-11 and 4-9:

$$\left[\frac{\Delta R}{R}\right]^2 = [.2]^2 \left[\left[\frac{\Delta P_0}{P_0}\right]^2 + \left[\frac{\Delta T_0}{T_0}\right]^2\right]$$

(5-19)

The uncertainty in γ can be found using the ideal gas pressure ratios for a standard fill (equation A-13 in appendix A), coupled with equations A-28 and A-10. Since the dependency of the individual components on the measurement error is quite small these terms can be ignored (as shown in appendix A) resulting in a γ uncertainty of:

$$\left[\frac{\Delta \gamma}{\gamma}\right]^2 = \left[\frac{1}{17.7}\right]^2 \left[\left[\frac{\Delta P_0}{P_0}\right]^2 + \left[\frac{\Delta T_0}{T_0}\right]^2\right]$$

(5-20)

which for a γ of 1.268 reduces equation 5-17 to:

$$\frac{\Delta \dot{m}_1}{\dot{m}_1} = \left[\left[\frac{\Delta \tau}{\tau}\right]^2 \left[\frac{7.46\frac{t}{\tau} - 1}{(1+\frac{t}{\tau})}\right]^2 + \left[\left[\frac{1}{3.75} + 1.57 \ln(1+\frac{t}{\tau})\right]^2 + 1.04\right] \left[\left[\frac{\Delta P_0}{P_0}\right]^2 + \left[\frac{\Delta T_0}{T_0}\right]^2\right] + \left[\frac{\Delta V}{V}\right]^2\right]^{.5}$$

(5-21)

or

$$\frac{\Delta \dot{m}_1}{\dot{m}_1} = \left[\left[\frac{\Delta \tau}{\tau}\right]^2 \left[C_\tau^2\right] + \left[C_{initial}^2\right] \left[\left[\frac{\Delta P_0}{P_0}\right]^2 + \left[\frac{\Delta T_0}{T_0}\right]^2\right] + \left[\frac{\Delta V}{V}\right]^2\right]^{.5}$$

(5-22)

Figure 5-3 is a plot of $C_{initial}$ as a function of test time.
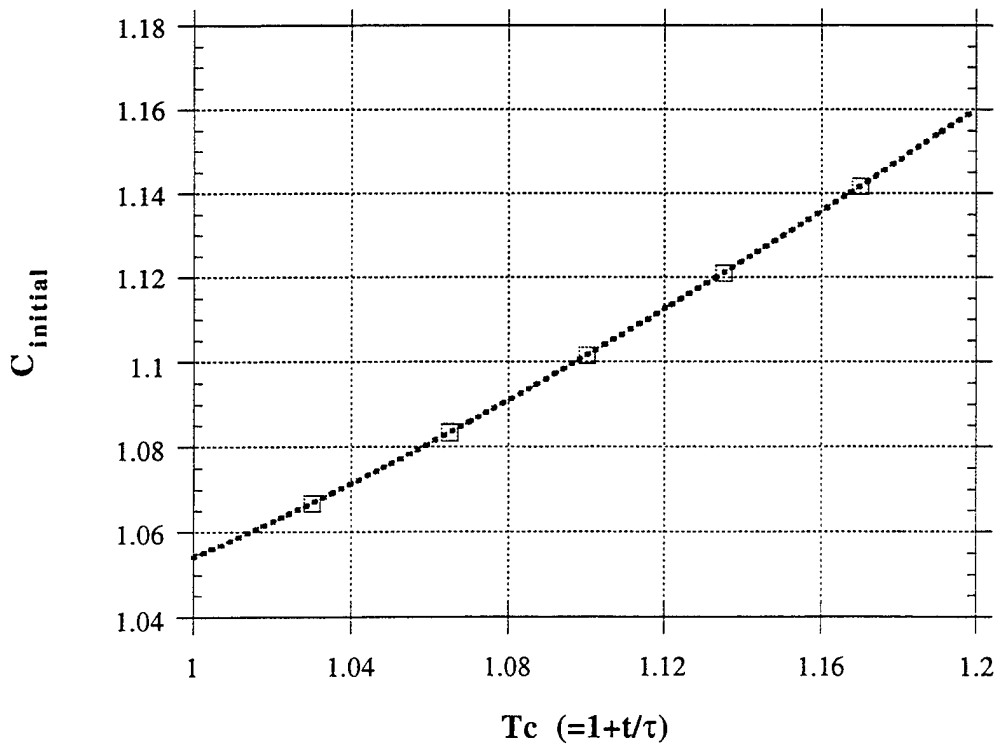
Figure 5-3 $C_{initial}$ as a Function of Time

50

In a similar fashion C_τ can also be plotted as a function of test time.
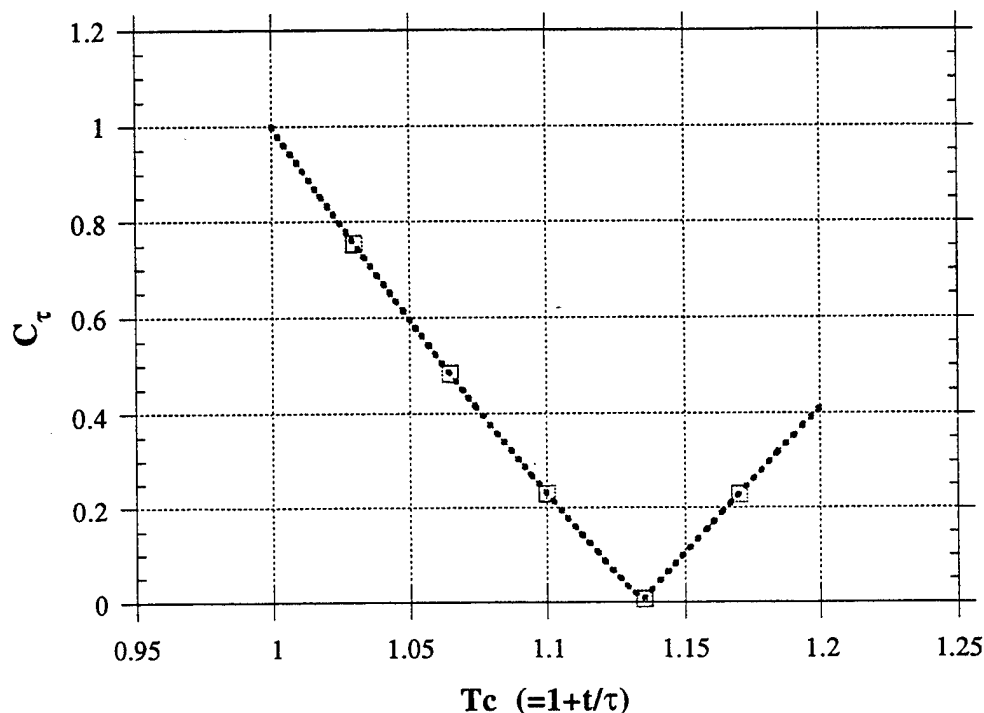
Figure 5-4 C_τ as a Function of Test Time

One of the interesting things to note in figure 5-4 is that the influence of τ drops to zero at a specific point in the test, where

$$\frac{t}{\tau} + 1 = \frac{\gamma+1}{2}$$

(5-23)

As a result, one would like to make efficiency measurements using the mechanical method as close to this time as possible.

A value for τ is needed to find the value of the mass flow. Equation 5-11 provides two direct ways of measuring τ which do not require any knowledge about the choke area using either temperature measurements:

$$\tau = \frac{t}{\left(\left[\frac{T_t}{T_0}\right]^{-.5} - 1\right)}$$

(5-24)

or pressure measurements:

$$\tau = \frac{t}{\left[\left[\frac{P_t}{P_0}\right]^{\frac{\gamma-1}{-2\gamma}} - 1\right]}$$

(5-25)

The uncertainty in τ using pressure measurements can be calculated and is given by:

51

$$\frac{\Delta\tau_i}{\tau_i} = \left[\left[\frac{1}{2\gamma}\frac{\gamma-1}{1-\left[\frac{P_i}{P_0}\right]^{\frac{\gamma-1}{2\gamma}}}\right]^2\left[(\frac{\Delta P_i}{P_i})^2+(\frac{\Delta P_0}{P_0})^2+(\frac{Ln(\frac{P_i}{P_0})}{\gamma-1})^2(\frac{\Delta\gamma}{\gamma})^2\right]\right]^{0.5}$$

(5-26)

and for temperature

$$\frac{\Delta\tau_i}{\tau_i} = \left[\left\{\frac{1}{2}\frac{1}{1-(\frac{T_i}{T_0})^{.5}}\right\}^2\left\{(\frac{\Delta T_i}{T_i})^2+(\frac{\Delta T_0}{T_0})^2\right\}\right]^{.5}$$

(5-27)

Which method is better for measuring τ depends not only on the influence coefficients, but also on the relative accuracy of the pressure and temperature measurements. In the supply tank during the test it will probably be much easier to obtain accurate pressure measurements than it will be to obtain accurate temperature measurements. Assuming that the relative accuracies in pressure and temperature are about the same (for the moment), then to see which method is better, the influence coefficient for γ in the pressure measurement technique,

$$C_\gamma = \frac{Ln(\frac{P_i}{P_0})}{\gamma-1}$$

(5-28)

needs to be examined first. From equation A-35 (for the ideal gas case), the total contribution of γ to the uncertainty in τ is

$$\left[C_\gamma\frac{\Delta\gamma}{\gamma}\right]^2 = \left[.21\,Ln(\frac{P_i}{P_0})\right]^2\left[(\frac{\Delta T_0}{T_0})^2+(\frac{\Delta P_0}{P_0})^2\right]$$

(5-29)

For pressure ratios larger than .37 (which should always be the case during most tests, see appendix A) the log of the pressure ratio will be less then one implying that the total contribution in uncertainty due to γ will be small compared to the other pressure terms so it can be ignored in this analysis . Comparing the influence coefficients in equations 5-26 and 5-27 we find that the ratio

$$Cr = \frac{C_p}{C_T}$$

(5-30)

where

$$C_P^2 = \left[\frac{1}{2\gamma}\frac{\gamma-1}{1-\left[\frac{P_i}{P_0}\right]^{\frac{\gamma-1}{2\gamma}}}\right]^2$$

(5-31)

$$C_T^2 = \left\{\frac{1}{2}\frac{1}{1-(\frac{T_i}{T_0})^{.5}}\right\}^2$$

(5-32)

52

is equal to

$$Cr = \frac{\gamma-1}{\gamma}$$

(5-33)

which has a behavior as outlined in figure 5-5
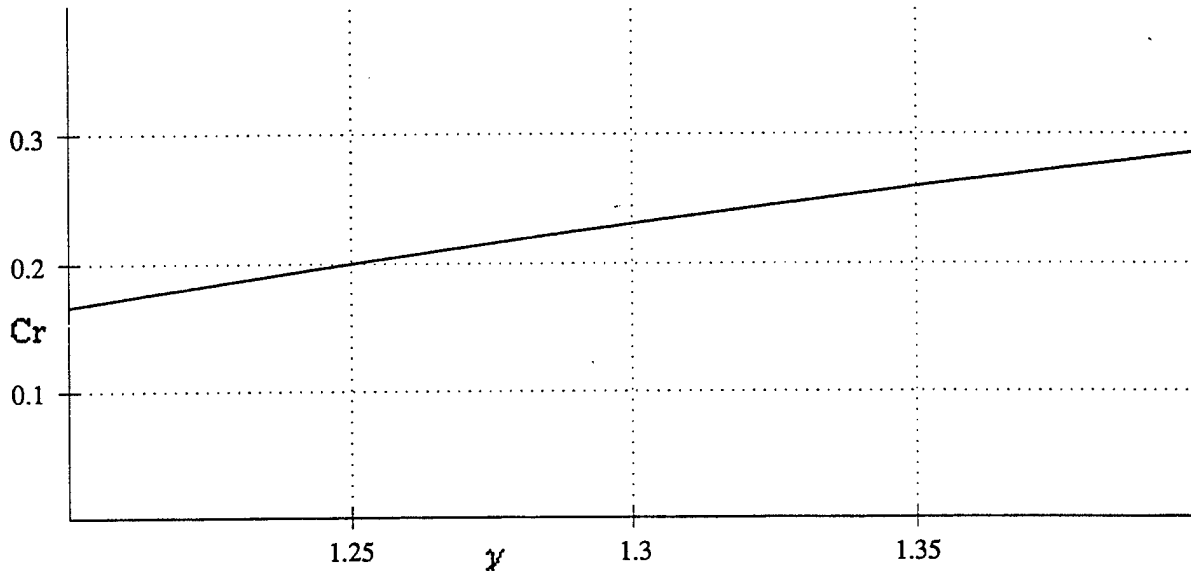
Figure 5-5 Plot of Cr versus γ

In this scenario the pressure measurement system would be better. To avoid repetition, the rest of this section will assume that the pressure technique to measure τ is used. If it happens that the temperature measurements are much better than the pressure measurements, then the results of this section can be scaled by 1/Cr to obtain the proper equations for the temperature measurement technique.

It is clear from equation 5-31 and 5-32 that the closer one is to the initial condition, the worse is the uncertainty in τ. To see how the influence coefficient for the pressure measurements behaves over the test time, we can substitute the definition of the pressure ratio from equation 5-11, labeling the term

$$Tc = 1 + \frac{t}{\tau}$$

(5-34)

(which will be examined in more depth latter) reducing equation 5-31 to:

$$C_P^2 = \{\frac{\gamma-1}{2\gamma(1-\frac{1}{Tc})}\}^2$$

(5-35)
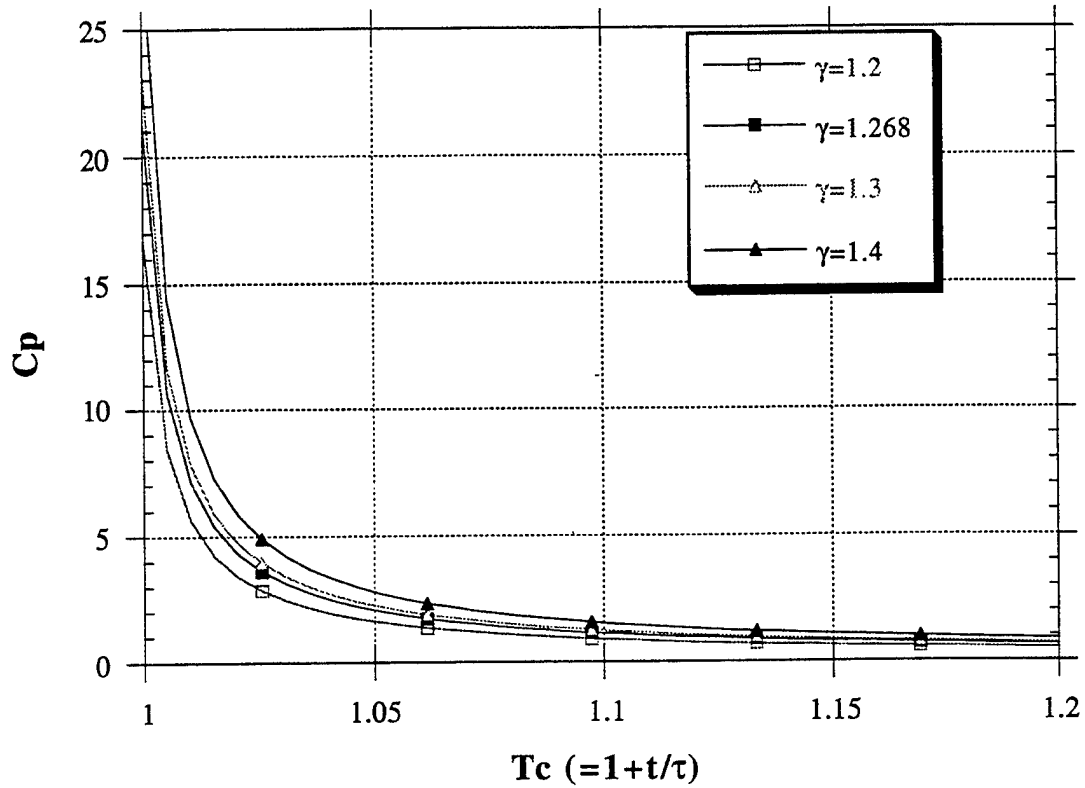
Figure 5-6 C_p for τ Using Pressure Measurements

Since τ is a constant in the ideal gas case we can use repeated measurements to reduce the overall uncertainty in τ. The uncertainties vary over the test time requiring the use of a weighted averaging system which would provide a prediction of τ to be:

$$\bar{\tau} = \frac{\displaystyle\sum_{i=1}^{n} \frac{\tau_i}{\left[\dfrac{\Delta\tau_i}{\tau_i}\right]^2}}{\displaystyle\sum_{i=1}^{n} \frac{1}{\left[\dfrac{\Delta\tau_i}{\tau_i}\right]^2}}$$

(5-36)

with an overall uncertainty of

$$\left[\frac{\Delta\tau_i}{\tau_i}\right]^2 = \frac{1}{\displaystyle\sum_{i=1}^{n} \frac{1}{\left[\dfrac{\Delta\tau_i}{\tau_i}\right]^2}}$$

(5-37)

Substituting equation 5-26 into 5-37 creates a total uncertainty in τ over the entire test of:

54

$$\left[\frac{\Delta\tau_i}{\tau_i}\right]^2 = \frac{(\frac{\Delta P_i}{P_i})^2+(\frac{\Delta P_0}{P_0})^2}{\displaystyle\sum_{i=1}^{n}\left[\frac{2\gamma(1-\frac{1}{Tc})}{\gamma-1}\right]^2}$$

(5-38)

Equation 5-38 is a function both of the sample rate and on the time period being evaluated. To see how this behaves we can take the limit as this approaches a continuous problem, converting the summation to an integral resulting in

$$\left[\frac{\Delta\tau_i}{\tau_i}\right]^2 = \frac{(\frac{\Delta P_i}{P_i})^2+(\frac{\Delta P_0}{P_0})^2}{\left[\frac{2\gamma}{\gamma-1}\right]^2(Tc-\frac{1}{Tc}-2\ln(Tc))}$$

(5-39)

which can be plotted as a function of final test time (for a γ of 1.268, integration goes from 1 to final test time)
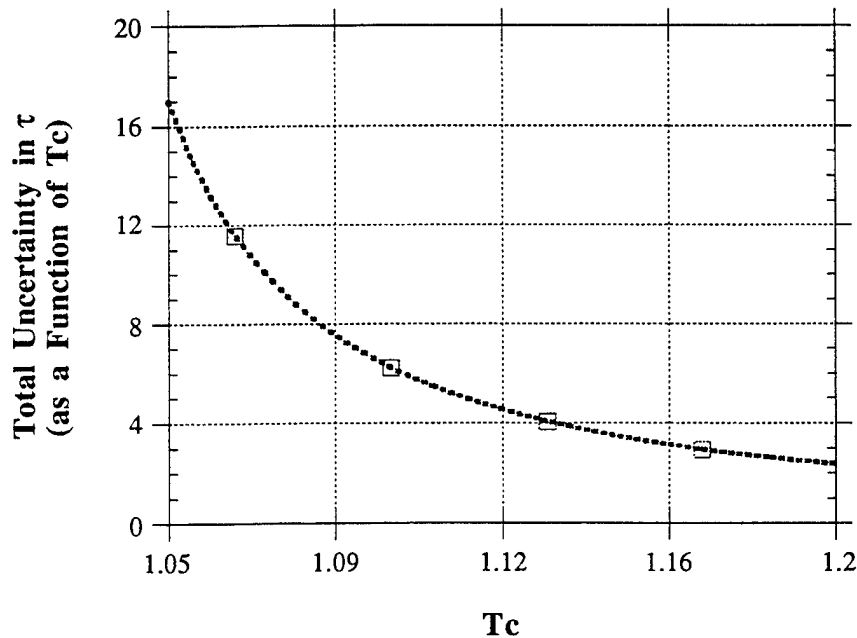
Figure 5-7 $\Delta\tau/\tau$ as a Function of final Test Time

Equation 5-38 can be combined with equation 5-22 to obtain:

$$\frac{\Delta \dot{m}_1}{\dot{m}_1} = \left[\left[C_\tau^2 C_{p'}^2 + C_{initial}^2 \right] \left[\frac{\Delta P_0}{P_0} \right]^2 + C_{initial}^2 \left[\frac{\Delta T_0}{T_0} \right]^2 + \left[C_\tau^2 C_{p'}^2 \right] \left[\frac{\Delta P_i}{P_i} \right]^2 + \left[\frac{\Delta V}{V} \right]^2 \right]^{.5}$$

$$\text{where } C_{p'}^2 = \frac{1}{\left[\frac{2\gamma}{\gamma\text{-}1} \right]^2 (Tc - \frac{1}{Tc} - 2\ln(Tc))}$$

(5-40)

The function $C_\tau C_{p'}$ is shown below in figure 5-8
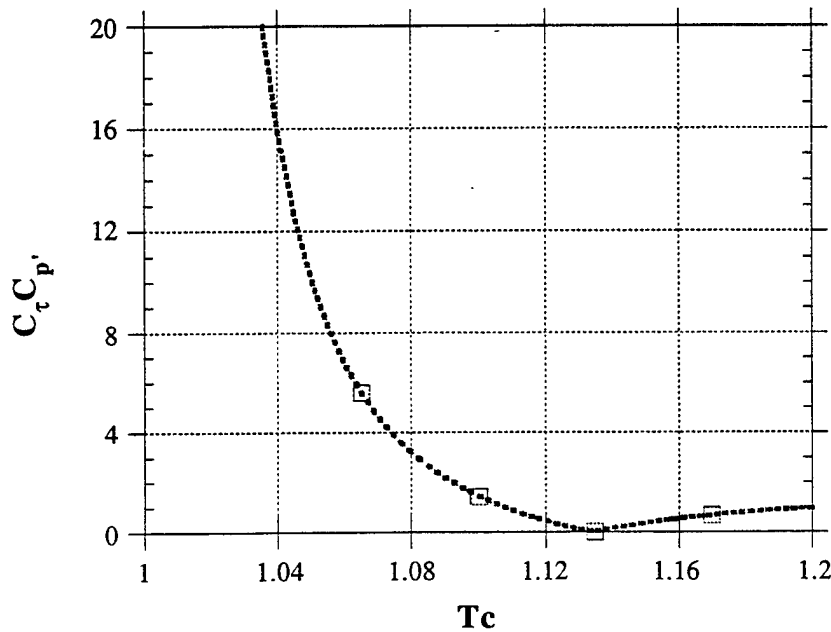
Figure 5-8 $C_\tau C_{p'}$ as a Function of Final Test Time

These last two graphs describe quite well the problem with using the mechanical method. One would like to measure the mass flow at the time where C_t approaches zero, which is when equation 5-23 is satisfied. How close we need to be to this time is determined by how accurately the mass flow has to be known. If all the other variables in section two were ignored, then to achieve an uncertainty in the efficiency of 0.25% one would need the mass flow to be accurate to 0.25%. If one assumes that the uncertainty in the volume of the tank is small enough to be ignored, and that the uncertainty in the initial test measurements can be reduced far below the instrument accuracies because of repeated sampling and the uniform flow conditions, then the only single sample data is taken at P_i which if assumed to have an uncertainty of .1% (.1 psi/105 psi range), would require that $C_\tau C_{p'}$ be about 2.5 (a testing time of about 1.07).

Clearly there are a lot of assumptions listed here and thus the accuracy estimated on the mass flow and ultimately on the measurement P_i is probably underestimated. Even with these

56

assumptions there is still the need to estimate the percentage of flow through the boundary layer bleeds and its accuracy (equation 5-16). There are several ways of doing this. One would be to drain the boundary layer bleeds into a separate tank of known volume and record its density change by using pressure measurements as suggest above. A second way to proceed is to run two tests, one with the boundary layer bleeds on, the other with them off, and measure τ. From equation 5-12, the ratio of these two measurements will be:

$$\frac{\tau_{no\ Bleeds}}{\tau_{Bleeds}} = 1+\alpha \tag{5-41}$$

and the uncertainty in the measurements will be the root sum square of the uncertainties in the individual time constants. Since the influence coefficient for the bleed ratio will always be less then 1 (generally about .23) a larger variance in the uncertainty of the bleed ratio can be tolerated. But it is clear that where one is in the testing time is important for the overall determination of the mass flow and thus we should spend a little more time examining the definition of the variable Tc and what influences it.

5.1.4   The Definition of the ATARR Non-Dimensional Time

The variable Tc (defined in equation 5-34) is probably the most important parameter in differentiating the performance of the facility from the test article. As shown in the introduction, the overall instrumentation requirements on an uncooled adiabatic turbine vary with the turbine being studied. Since that analysis used the thermodynamic method of measuring efficiency it is not surprising that the variation was dependent on the pressure ratio and the test γ (the r factor). But for the mechanical method it depends on the uncertainty in the mass flow which is a function of the supply tank time constant.

The name implies that this is a function of the supply tank alone, but a quick examination of equation 5-12 shows that to be erroneous. It is partially a function of the initial gas conditions, but far more importantly it is a function of the choke area and the percentage of flow passing through the boundary layer bleeds. In addition, where one is during the test (t) is also important. It is distinctly possible that in the ideal gas case one would measure t at a time much different from the efficiency, or measure the boundary layer bleed flow over a time which is much longer then an actual turbine test. Thus the combination of t and τ is labeled the ATARR non-dimensional time, and it is only a function of the testing configuration.

This is a particularly good parameter to characterize the blowdown because all turbine tests, no matter what their configuration of boundary layer bleeds and choke areas will always behave similarly for equivalent values of Tc. In addition it can help us to decipher how accurate the measurements in the mass flow rate can be made.

This can be done by writing a mass balance on the entire testing facility:

$$M_T - m_{S,t} = m_{D,t} \qquad (5\text{-}42)$$

where M_T is the initial starting mass in the supply tank, $m_{S,t}$ is the mass in the supply tank at time t, and $m_{D,t}$ is the mass in the dump tank at time t. Since the mass at any point in time is given by

$$M = \rho V$$

equation 5-42 can be written as:

$$V_S \rho_{S,t} \left(\frac{\rho_{S,0}}{\rho_{S,t}} - 1 \right) = \rho_{D,t} V_D \qquad (5\text{-}43)$$

Now the the change in density in the supply tank is given by equation 5-11(c) so rearranging terms one finds:

$$\left(\frac{1}{Tc^{\frac{-2}{\gamma-1}}} - 1 \right) = \frac{P_{D,t} V_D T_{S,t}}{V_S P_{S,t} T_{D,t}} \qquad (5\text{-}44)$$

Assuming that the temperature ratio of the gas can be approximated by the adiabatic uncooled turbine equation:

$$\eta = \frac{1-\tau}{1-r} \quad \text{(From equation I-14)}$$

where

$$\frac{1}{\tau} = \frac{T_S}{T_D} \bigg|_t \qquad (5\text{-}45)$$

Since most turbines operate at a r factor of about .75 with an efficiency of 90%, $1/\tau$ is about 1.3.

Defining a new variable

$$Vr = \frac{V_D}{V_S \tau} \qquad (5\text{-}46)$$

equation 5-44 reduces to:

$$\left(\frac{1}{Tc^{\frac{-2}{\gamma-1}}} - 1 \right) = \frac{P_D}{P_S} \bigg|_t Vr \qquad (5\text{-}47)$$

we can now ask the question, "At what value of Tc does the supply tank become unchoked?" Since the pressure ratio across the choked orifice is given by:

$$\frac{P_D}{P_S} \bigg|_t = \left[\frac{2}{\gamma+1} \right]^{\frac{\gamma}{\gamma-1}} \qquad (5\text{-}48)$$

The time at which the supply tank becomes unchoked is only a function of gamma and the ratio of the volume of the dump tank to the supply tank.

$$\left(\frac{1}{\left[\left[\frac{2}{\gamma+1} \right]^{\frac{\gamma}{\gamma-1}} Vr + 1 \right]^{\frac{\gamma-1}{-2}}} \right) = Tc \qquad (5\text{-}49)$$

The results are plotted below in figure 5-9.
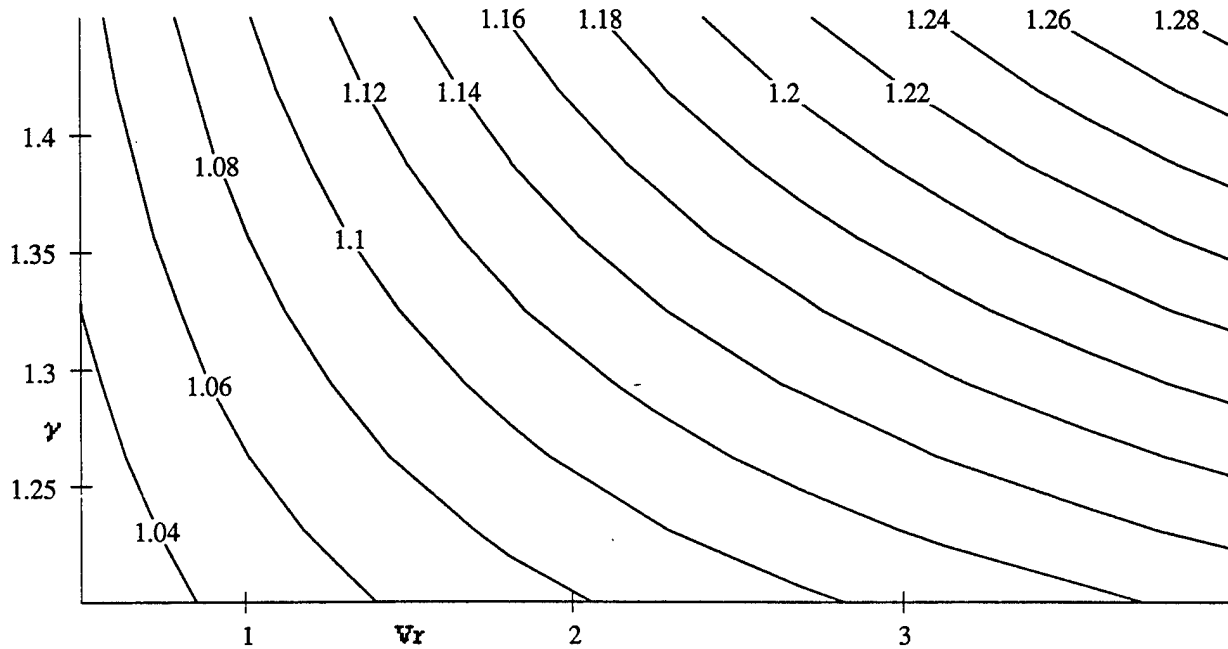
Figure 5-9 Contour Plot of Tc versus γ and Vr

For this configuration which has a value of $1/\tau =1.3$, γ of 1.268 and a tank volume ratio of about 2.1 (including the test section volume); the value for Vr is 2.73 resulting in a value of Tc=1.13. Therefore, any value of Tc greater then this will not be achievable since the facility will no longer remained choked. This information can be used to evaluate the best level accuracy to which the mass flow could be obtained. Assuming that the uncertainty in the initial pressures and temperatures can be reduced though statistical processes to very low values, and that the uncertainty in the volume of the supply tank is negligible, then equation 5-40 reduces to:

$$\frac{\Delta \dot{m}_1}{\dot{m}_1} = \left[\left[C_\tau^2 C_{p'}^2 \right] \left[\frac{\Delta P_i}{P_i} \right]^2 \right]^{.5}$$

(5-50)

For a Tc of 1.13 and γ of 1.268 the influence coefficient reduces to:

$$C_{p'}= 4.28, \quad C_\tau = .0267 \quad \text{and} \quad C_\tau C_{p'}=.1143$$

Thus to achieve an accuracy of the mass flow out of the supply tank of 0.25% the uncertainty in the pressure measurements taken during the tests have to be good to 2.18% (which is quite achievable). However measuring the mass flow out of the supply tank is only half the challenge since we also need the uncertainty in the boundary layer bleed to obtain the uncertainty in the mass flow through the test section. The uncertainty in the boundary layer bleeds is equal to

$$\frac{\Delta \alpha}{\alpha} = \left[2 \left[\frac{\Delta \tau_i}{\tau_i} \right]^2 \right]^{.5}$$

(5-51)

Making the same assumptions that the initial pressure measurements are negligible compared to the transient pressure measurements, then equation 5-16 becomes:

$$\frac{\Delta \dot{m}_3}{\dot{m}_3} = \left[\left[C_{p'}^2 \left(2 \left[\frac{\alpha}{\alpha+1} \right]^2 + C_{\tau'}^2 \right) \right] \left[\frac{\Delta P_i}{P_i} \right]^2 \right]^{.5}$$

(5-52)

For a 30% bleed, the overall influence coefficient is about 1, implying that the accuracy of the pressure measurement can be no worse then .25%.

It is clear from this analysis, and the many assumptions that have been made, that for an ideal gas the practicality of measuring the mass flow, and thus the efficiency to within 0.25% is an optimistic goal. But to further complicate matters, the results from the previous sections show that the gas properties do change, and that ideal gas behavior is not necessarily an appropriate model since compressibility effects have to be taken into accounted. To see whether or not a real gas model may alleviate some of the problems present here, the next section examines how the blowdown equations need to be modified to account for real gas effects.

5.2 Evaluating the Blowdown Equations for a Real Gas

As stated above, equations 5-11 and 5-12 may not be completely applicable to real gases unless some corrective action is taken. There are three primary concerns. The first is the real gas effects as exhibited by the compressibility of each gas, and its influence on the information derived from pressure and temperature measurements. The second is the change in the gas properties over the test time. It is clear that γ changes and that the change is both a function of temperature and pressure, but it is not yet clear how important this drift in γ really is. Finally, because the gas properties are changing, and they could be a component in the overall efficiency uncertainty, certain isentropic processes which assume constant gas properties need to be evaluated to see if they can still be used in this situation. To obtain a better insight into how varying gas properties effect the parameters being measured section 5.2.1 examines how the derived properties (such as mass flow and the supply tank time constant) are influenced by changes in the gas properties. Section 5.2.2 shows how the ratio of the specific heats varies during a test run. Finally in section 5.2.3 equation 5-11 will be redeveloped accounting for real gas effects.

5.2.1 Gas Property Variation Influences on Various Mass Flow Parameters

Much of the variation in the gas properties comes from the uncertainty in γ which is composed of two parts. One part arises from inaccuracies in the mixing process as described by equation 4-8. The other part comes from the natural variation in γ because the temperature and pressure of the gas change during a test. This latter part is really not an uncertainty in the typical sense, rather it is a type of drift. But it is obvious that both components will contribute to the overall change in any parameter which is dependent on γ. Since much of the ideal analysis is based on the assumption of constant gas properties throughout the testing time, it is appropriate to include both effects.

60

Examining the dependency of the corrected mass flow on γ one finds that it varies by about 0.85 of the variation in γ.

$$\frac{\Delta \dot{m}_{corr}}{\dot{m}_{corr}} = \left| \frac{1}{2} \frac{\gamma\text{-}2}{\gamma\text{-}1} - \frac{\gamma \ln(\frac{2}{\gamma+1})}{(\gamma\text{-}1)^2} \right| \frac{\Delta \gamma}{\gamma}$$

(5-53)

which is relatively indifferent to the value of γ (going from about 0.86 at $\gamma = 1.2$ to 0.845 at $\gamma = 1.4$). The uncertainty in the supply tank time constant (from equation 5-12) reduces to the following (after m_{corr} has been replaced by its equivalent expression for γ).

$$\frac{\Delta\frac{1}{\tau}}{\frac{1}{\tau}} = \frac{\Delta\tau}{\tau} = \left[\left[\frac{\alpha}{\alpha+1} \right]^2 \left[\frac{\Delta\alpha}{\alpha} \right]^2 + \left[\frac{\Delta V}{V} \right]^2 + \left[\frac{\Delta A_3}{A_3} \right]^2 + \frac{1}{4} \left[\left[\frac{\Delta R}{R} \right]^2 + \left[\frac{\Delta T_1(0)}{T_1(0)} \right]^2 \right] \right.$$

$$\left. + \left[\frac{\Delta\gamma}{\gamma} \right]^2 \left[\left[\frac{2(\ln(\frac{2}{\gamma+1})+1\text{-}\gamma)\gamma}{1\text{-}\gamma} + \gamma\text{-}1 \right] \left[\frac{1}{2(\gamma\text{-}1)} \right]^2 \right]^2 \right]^{.5}$$

(5-54)

The influence coefficient for the variation in γ is relatively large. Labeling this coefficient as K,

$$K = \sqrt{ \left[\frac{2(\ln(\frac{2}{\gamma+1})+1\text{-}\gamma)\gamma}{1\text{-}\gamma} + \gamma\text{-}1 \right]^2 \left[\frac{1}{2(\gamma\text{-}1)} \right]^2 }$$

(5-55)

it's level of influence can be plotted as a function of γ.
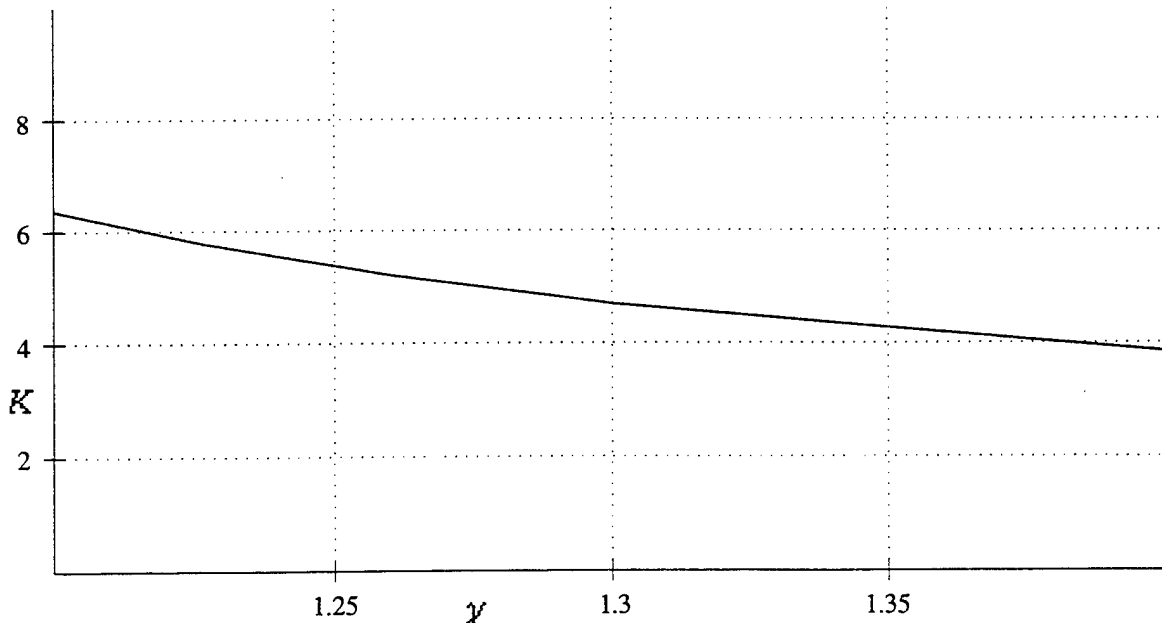
Figure 5-10   (K) Influence coefficient for γ on Supply Tank Time Constant

Examining how the various parameters influence the overall uncertainty in the mass flow out of the supply tank, we rewrite equation 5-17 in terms of the initial properties and Tc:

61

$$\frac{\Delta \dot{m}_1}{\dot{m}_1} = \left[\left[\frac{\Delta P_1(0)}{P_1(0)}\right]^2 + \left[\frac{\Delta R}{R}\right]^2 + \left[\frac{\Delta T_1(0)}{T_1(0)}\right]^2 + \left[\frac{\Delta V}{V}\right]^2 + \left[\frac{\Delta \gamma}{\gamma}\right]^2 \left[\frac{2\gamma\ln(Tc)}{(\gamma-1)^2} + \frac{\gamma}{(-\gamma+1)}\right]^2 \right.$$
$$\left. + \left[\frac{\Delta \tau}{\tau}\right]^2 \left[\frac{2Tc-1-\gamma}{(Tc)(\gamma-1)}\right]^2 \right]^{.5}$$

(5-56)

The influence coefficient for γ in equation 5-56 is:

$$[K_1]^2 = \left[\frac{2\gamma\ln(Tc)}{(\gamma-1)^2} + \frac{\gamma}{(-\gamma+1)}\right]^2$$

(5-57)
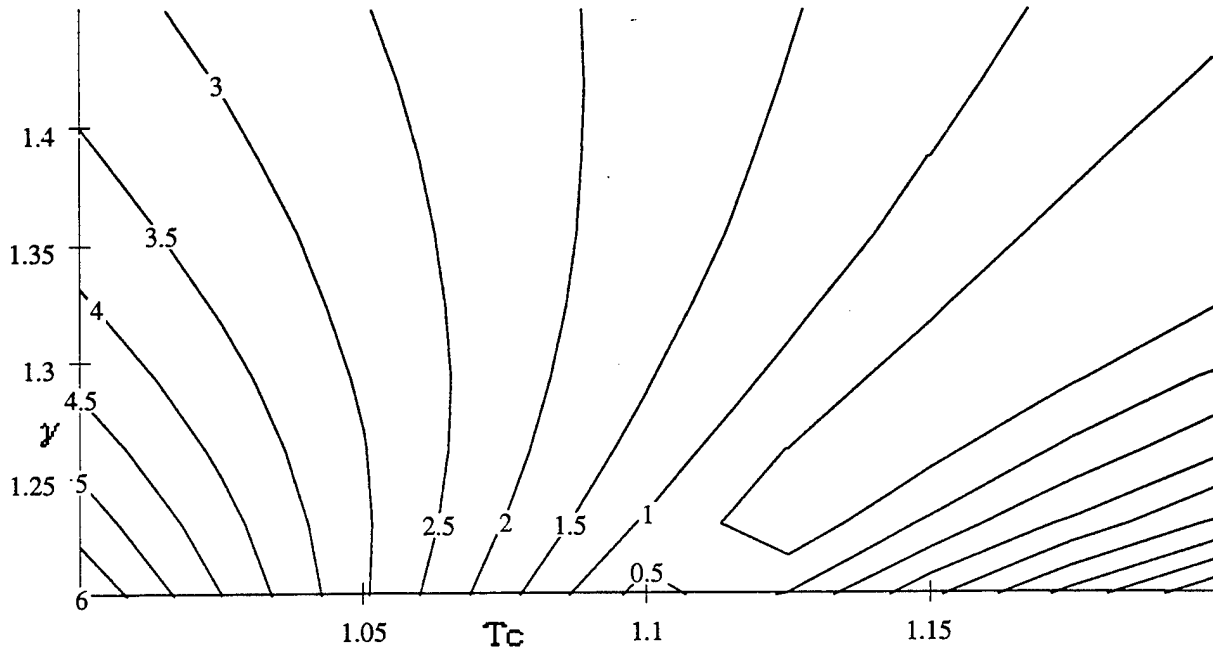
Figure 5-11 (K_1) Direct Influence of γ on Supply Tank Mass Flow Uncertainty

The influence coefficient for τ can be plotted in a similar manner.

$$[K_2]^2 = \left[\frac{2Tc-1-\gamma}{(Tc)(\gamma-1)}\right]^2$$

(5-58)
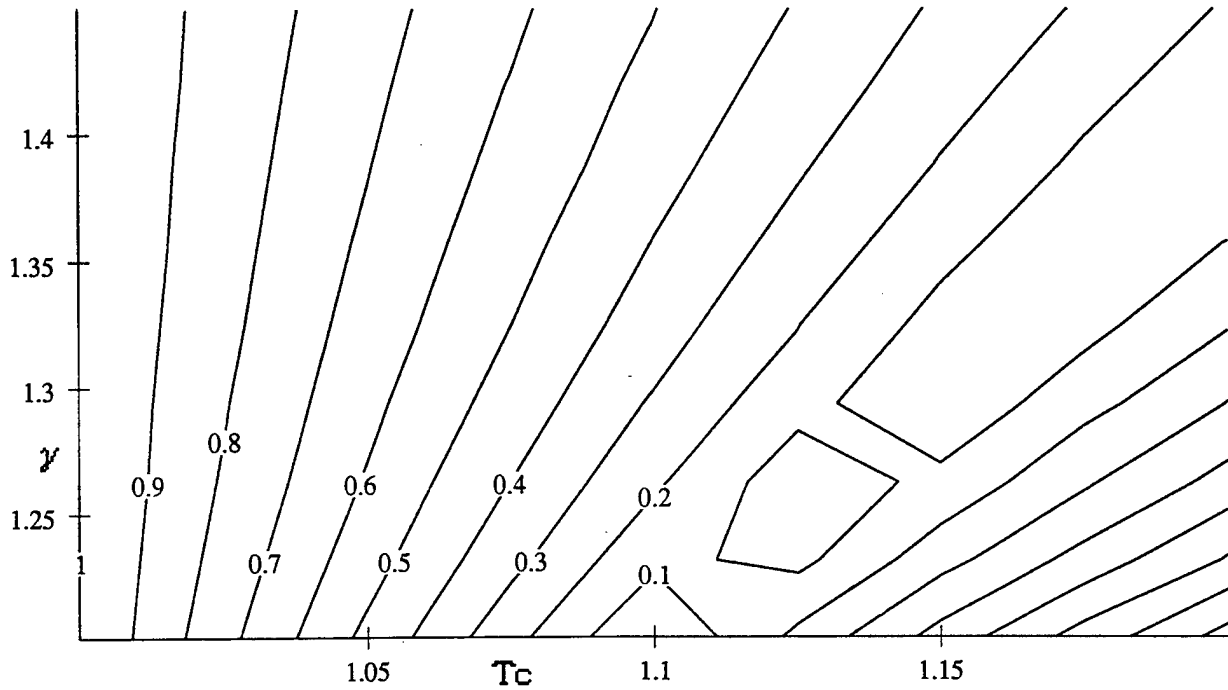
Figure 5-12 (K₂) Direct Influence of τ on Supply Tank Mass Flow Uncertainty

Rewriting equation 5-56 in terms of the influence coefficients listed above and using equation 5-54 and 5-55 one obtains:

$$\frac{\Delta \dot{m}_1}{\dot{m}_1} = \left[\left[\left[\frac{\Delta P_1(0)}{P_1(0)} \right]^2 + \left[\frac{\Delta R}{R} \right]^2 + \left[\frac{\Delta T_1(0)}{T_1(0)} \right]^2 \right] \left[1 + \frac{K_2^2}{4} \right] + \left[\frac{\Delta V}{V} \right]^2 \left[1 + K_2^2 \right] \right.$$

$$\left. + K_2^2 \left[\left[\frac{\Delta A_3}{A_3} \right]^2 + \left[\frac{\alpha}{\alpha+1} \right]^2 \left[\frac{\Delta \alpha}{\alpha} \right]^2 \right] + \left[K_2^2 K^2 + K_1^2 \right] \left[\frac{\Delta \gamma}{\gamma} \right]^2 \right]^{.5}$$

(5-59)

The overall influence coefficient for γ

$$K_{overall} = \sqrt{ \left[K_2^2 K^2 + K_1^2 \right] \left[\frac{\Delta \gamma}{\gamma} \right]^2 }$$

(5-60)

while not readily reducible can be plotted as a function of γ and Tc.
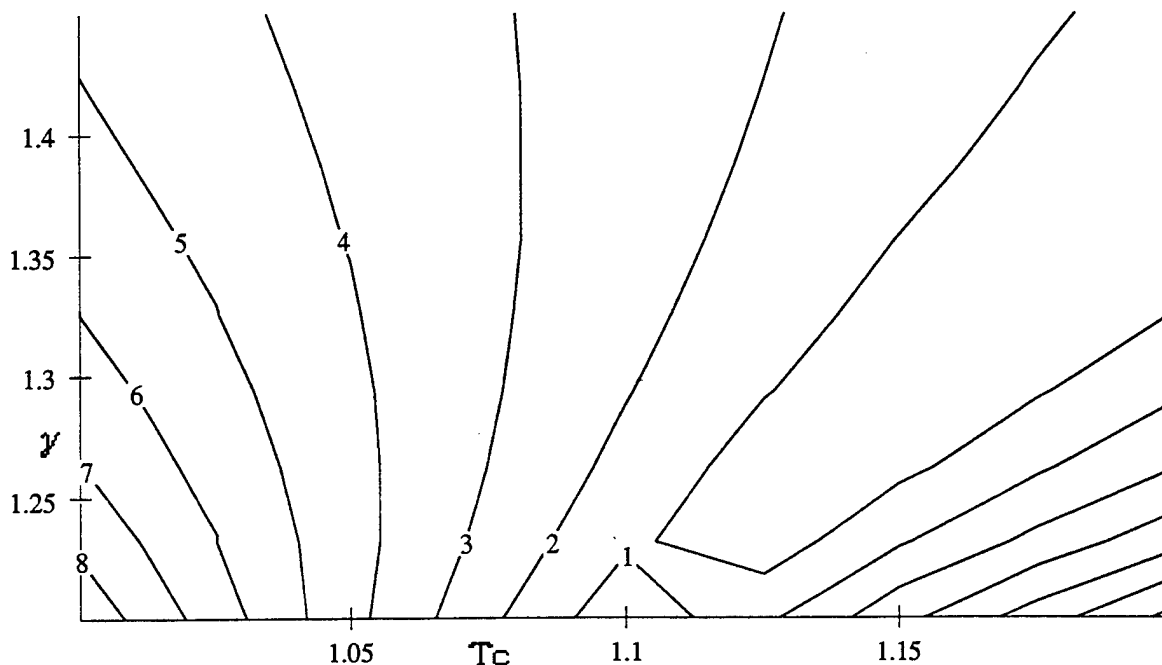
Figure 5-13 (K$_{overall}$) Overall Influence Coefficient for γ on Mass Flow

Equation 5-59 is not much use to the experimentalist since it contains terms which are not measurable (i.e the uncertainty in the choke area). But it can be used to show, theoretically, how the uncertainty in γ affects the uncertainty in the mass flow. Examining equations 2-9 and 2-40 (the uncertainty in efficiency using the mechanical method for the uncooled and cooled NGV stages), it is clear that the influence coefficient for the mass flow on the efficiency is one. If all the other terms in these equations were ignored, then to achieve a .25% accuracy in efficiency would require at least a .25% accuracy in the mass flow. If we use the same process on equation 5-59 and all the terms other then the change in γ were ignored, then the overall contribution of γ would need to be 0.25%. Figure 5-13 shows that the influence coefficient for γ ranges from about 7 (at the beginning of the test) to about 3 at the end (this will be developed in the next section), creating a need for a stability in γ of .035% to .08%. To see if this level of stability is realistic section 5.2.2 will examine how γ varies over the course of a test.

5.2.2 Variation in γ During a Test

There are two fundamentally different processes through which the properties of the test gas change; (1) when it is going through the isentropic expansion as gas leaves the supply tank and (2) as energy is extracted from it by the turbine. The change in gas properties during an isentropic expansion is well documented for an ideal gas. By examining the isentropic expansion process first, one can see if the variation in γ is important, and if it is, avoid delving into how the flow properties change as it passes through the turbine. Equations 5-11 show that one only needs to now the initial values of the property and the value of Tc to find the value of the property at any

64

point in time. Equation 5-12 can be used as an approximation to estimate τ for different types of gas mixtures.

The nominal dimensions of the ATARR facility are:

$V = 3100$ ft^3

$A_3 = 72$ in$^2 = .5$ ft^2

these can be used to estimate τ for two different cases; one with air at 520°K and one with a N_2-CO_2 mixture at 520°K.

Air:	$\gamma = 1.4$	N_2-CO_2:	$\gamma = 1.268$
	$R = 287$ J/[Kg-K]		$R = 214$ J/[Kg-K]
	$m_{corr} = .81$		$M_{corr} = .74$
	$\tau = 35.4$ sec		$\tau = 63$ sec

These values do not include the amount taken off through the boundary layer bleed which could be 30% or more of the flow. Incorporating a 30% bleed value reduces the supply tank time constants to 27 seconds for air and 48.5 seconds for N_2-CO_2. The design run time of the facility is 2 seconds thus for the air the value of Tc becomes 1.075 and for N_2-CO_2 1.04. As the turbines become smaller, the testing time could increase, and the percentage of the flow exhausted by the boundary layer bleeds could increase. Thus it makes sense to use the ATARR non-dimensional time (Tc) to characterize the uncertainty in the gas properties.

Equation 5-11b shows that the temperature decay is a direct function of the variable Tc and its generic plot is shown in figure A-22. A similar plot is shown in figure A-23 for equation 5-11a, but the pressure variation depends on γ, and in this graph the pressure drop is plotted as a function of both Tc and γ. Figure A-21a is a plot of the standard mixture γ as a function of pressure level and non-dimensional time (Tc) instead of temperature. One can see that even for small values of Tc, the change in γ from its initial conditions becomes larger then the upper bound placed on the variation in γ of 0.08% shown in the previous section. One last avenue of investigation is to note that as the non-dimensional time increases, the pressure drops dramatically (figure A-23) and one can see from figure A-21a that as the pressure drops the value of γ becomes more constant. An interative method is needed to calculate the change in γ only as a function of Tc since one has to find the pressure drop associated with that value of Tc, use the gas tables to interpolate a value of γ and then use that value to re-estimate the pressure drop (explained in more detail in appendix A). The results are shown in figure A-24 and one can see that the effects of the pressure decay do not keep γ varying past acceptable levels.

At this point there are several conclusions which can be drawn. First, using the present process the mechanical method cannot be used to measure efficiency to within 0.25% during a standard test because the variation in γ during the isentropic expansion (which is only part of the temperature and pressure drop which would occur during a test to the flow gas) greatly exceeds the

limits imposed on it by equation 5-59. How accurately one could measure the efficiency using this method is a direct function of Tc (as shown earlier). One positive note comes from examining equation 4-8 (shown in Appendix A and resulting in equation A-21) and finding that the uncertainty in γ which is due to the mixing process (the lowest value of the uncertainty in γ that one could achieve used a mixed test gas) is only a weak function of the temperature and pressure uncertainty (the influence coefficient is 1/22). To achieve an uncertainty in γ of 0.035%, the combined uncertainty in the temperature and pressure measurements during the filling process would only need to be 0.77%, which if the uncertainty in both measurements were equal, would require each measurement be accurate to 0.54%. Which are values much larger then the expected accuracies of these measurements and thus the mixing procedure is not necessarily doomed from the start.

Using the thermodynamic technique avoids the problem of making mass flow measurements, which negates this entire problem of changing gas properties. The problem with this process is that the nonuniformity downstream of the rotor could create measurement errors which far exceed the instrumentation uncertainty, thus also limiting the efficiency accuracy (in addition there still remains that slight problem of defining the losses in the system). As one moves the measurement location further downstream, the flow becomes more uniform, but the measured efficiency of the stage now includes the mixing losses that occurred downstream of the rotor, thus lowering the measured stage efficiency. To avoid the experimental problem of measuring the energy state of the fluid downstream of the rotor, the next section will look at the derivation of equation 5-11 accounting for real gas effects, to see if it is possible to account for the variation which occurs in γ.

5.2.3 Derivation of Blowdown Equations with Real Gas Effects

There are several ways to proceed. Since the mass flow out of the supply tank has to equal the mass flow through the boundary layer bleeds plus the mass flow into the test section inlet, this can be written as:

$$\dot{m}_1 = (1+\alpha)\dot{m}_3 \tag{5-61}$$

which can be multiplied by 1 (in various forms) to achieve:

$$\dot{m}_1 = (1+\alpha)\left[\frac{\dot{m}_3\sqrt{\gamma_c RT_{T3}}}{P_{T3}A_3}\right]\frac{P_{T3}}{P_{T1}}\left[\frac{T_{T1}}{T_{T3}}\right]^{\frac{1}{2}}\frac{P_{T1}A_3}{\sqrt{\gamma_c RT_{T1}}} \tag{5-62}$$

γ_c represents the instantaneous value of γ at any point in the test.

Outside of the boundary layer, the isentropic flow assumption is valid so that the total pressure and temperature do not change:

$$\dot{m}_1 = (1+\alpha)\left[\frac{\dot{m}_3\sqrt{\gamma_c RT_{T3}}}{P_{T3}A_3}\right]\frac{P_{T1}A_3}{\sqrt{\gamma_c RT_{T1}}} \tag{5-63}$$

and in the supply tank (station 1) the total quantities are the same as the static quantities creating:

$$\dot{m}_1 = (1+\alpha)\left[\frac{\dot{m}_3\sqrt{\gamma_c R T_{T3}}}{P_{T3}A_3}\right]\frac{P_1 A_3}{\sqrt{\gamma_c R T_1}} \tag{5-64}$$

Using the real gas law $P_1(t)$ can be substituted for

$$P_1(t) = z_1(t)\,\rho_1(t)\,R T_1(t) \tag{5-65}$$

and rearranging terms yields:

$$\dot{m}_1 = (1+\alpha)\left[\frac{\dot{m}_3\sqrt{\gamma_c R T_{T3}}}{P_{T3}A_3}\right]\frac{z_1(t)\rho_1(t)A_3\sqrt{\gamma_c R T_1(t)}}{\gamma_c} \tag{5-66}$$

combing with equation 5-13 produces:

$$\dot{m}_1 = -V\frac{\partial\rho}{\partial t} = (1+\alpha)\left[\frac{\dot{m}_3\sqrt{\gamma_c R T_{T3}}}{P_{T3}A_3}\right]\frac{z_1(t)\rho_1(t)A_3\sqrt{\gamma_c R T_1(t)}}{\gamma_c} \tag{5-67}$$

The expansion process is isentropic outside of the boundary layer and the next step would be to relate T(t) to the initial temperature and the density ratio. However, the real gas effects keep us from applying the standard isentropic relationship:

$$\frac{T_1(t)}{T_1(0)} = \left[\frac{\rho_1(t)}{\rho_1(0)}\right]^{\gamma-1} \tag{5-68}$$

Appendix C develops the isentropic relationships among pressure, temperature and density and discusses in depth the problems inherent in the integration of equation 5-67. The results of appendix C show that one has to consider that the ideal gas law holds, but that the variables γ-1 needs to be replaced with C1 and γ-1/γ has to be replaced with C2 (as defined in appendix C). In addition, the value of τ will no longer be considered a constant since both the corrected mass flow and the compressibility vary with time. Thus the final blowdown equations can be written as:

$$\frac{\rho(t)}{\rho(0)} = \left[\frac{t}{\tau}+1\right]^{-\frac{2}{C1}}$$

$$\frac{1}{\tau} = \frac{(\frac{C1}{2})(1+\alpha)z_1(t)\sqrt{\gamma_c R T_1(0)}A_3}{\gamma_c V}\left[\frac{\dot{m}_3\sqrt{\gamma_c R T_{T3}}}{P_{T3}A_3}\right] \tag{5-69}$$

$$\frac{T(t)}{T(0)} = \left[\frac{t}{\tau}+1\right]^{-2} \tag{5-70}$$

$$\frac{P(t)}{P(0)} = \left[1+\frac{t}{\tau}\right]^{-\frac{2}{C2}} \tag{5-71}$$

5.2.4 Uncertainty in Mass Flow and τ for a Real Gas

Much of the analysis which was done in section 5.1.3 is still valid. Equation 5-16 provides the uncertainty in the mass flow through the test section and equation 5-17 needs to be modified to use the variable C1 instead of γ.

$$\dot{m} = V\frac{P_1(0)}{\tau R T_1(0)}(\frac{2}{C1})\left[1+\frac{t}{\tau}\right]^{\frac{-2-C1}{c2}} \tag{5-72}$$

and becomes:

$$\frac{\Delta\dot{m}}{\dot{m}} = \left[\left[\frac{\Delta\tau}{\tau}\right]^2\left[-\frac{1}{Tc} + [1-\frac{1}{Tc}]\frac{2}{C1}\right]^2 + \left[\frac{\Delta C1}{C1}\right]^2\left[-1 + \frac{2\ln(Tc)}{C1}\right]^2 + \left[\frac{\Delta P_0}{P_0}\right]^2 + \left[\frac{\Delta T_0}{T_0}\right]^2 + \left[\frac{\Delta R}{R}\right]^2 + \left[\frac{\Delta V}{V}\right]^2\right]^{.5}$$

or

$$\frac{\Delta\dot{m}}{\dot{m}} = \left[\left[\frac{\Delta\tau}{\tau}\right]^2 Km_1^2 + \left[\frac{\Delta C1}{C1}\right]^2 Km_2^2 + \left[\frac{\Delta P_0}{P_0}\right]^2 + \left[\frac{\Delta T_0}{T_0}\right]^2 + \left[\frac{\Delta R}{R}\right]^2 + \left[\frac{\Delta V}{V}\right]^2\right]^{.5} \tag{5-73}$$

As was done in section 5.1.3 , R is only a function of the mixing process and equation 5-19 can be used here. The uncertainty in C1 and the uncertainty in τ is now (because of the way we are calculating both τ and C1 and performing the mass flow integrations) only a function of the individual measurement (i.e only the uncertainty in the individual pressure and temperature measurement).

To find the uncertainty in C1 the individual components of C1 (equation c-17) can be substituted to derive an expression for C1 in terms of the component gases

$$C1 = \frac{Mr(R_2 + R_1)Z'}{Cv_1 + Cv_2 Mr} \tag{5-74}$$

where

$$Mr = \frac{M_2}{M_1} \quad \text{and} \quad Z' = T\frac{\partial Z}{\partial T} + Z$$

as shown in appendix A, the individual gas properties vary little as a function of instrument temperature and pressure uncertainty (this assumes that the instruments are accurate at least to a few degrees Kelvin, or a few psi, since we are attempting calibration accuracies of 0.1 °K and .1 psi there should be no problem here). Thus they can be considered a constant. Then the uncertainty in the terms C1 reduces to uncertainties in the mass ratio and in Z' as shown below.

$$\frac{\Delta C1}{C1} = \sqrt{\left[\frac{\Delta Z'}{z'}\right]^2 + \left[\frac{\frac{Rr}{Cvr} - 1}{\left[\frac{1}{Mr} + Rr\right]\left[\frac{1}{Cvr} + Mr\right]}\right]^2 \left[\frac{\Delta Mr}{Mr}\right]^2} \tag{5-75}$$

where

$$Mr = \frac{m_2}{m_1}, \quad Cvr = \frac{Cv_2}{Cv_1}, \quad \text{and} \quad Rr = \frac{R_2}{R_1}$$

From the information in appendix A, the uncertainty in Z' is negligible as a function both of temperature and pressure in the instrumental uncertainty range, so it can be ignored. Thus the final form of the uncertainty in C1 is:

$$\frac{\Delta C1}{C1} = \sqrt{\left[\frac{\frac{Rr}{Cvr} - 1}{\left[\frac{1}{Mr} + Rr\right]\left[\frac{1}{Cvr} + Mr\right]}\right]^2 \left[\frac{\Delta Mr}{Mr}\right]^2} \tag{5-76}$$

68

These component ratios have all been evaluated in appendix A and using the values for a standard fill, equation 5-76 reduces to:

$$\frac{\Delta C1}{C1} = \left[\frac{1}{9.29}\right]\left[\frac{\Delta Mr}{Mr}\right]$$

(5-77)

The uncertainty in the mass ratio is defined for a standard fill by equation A-29, and combining these values with equation 5-77 reduces the uncertainty in C1 to its final form:

$$\frac{\Delta C1}{C1} = \left[\frac{1}{4.41}\right]\sqrt{\left[\frac{\Delta P(0)}{P(0)}\right]^2 + \left[\frac{\Delta T(0)}{T(0)}\right]^2}$$

(5-78)

The uncertainty in τ can be found in a manner similar to that used in section 5.1.3 (using pressure measurements).

$$\tau = \frac{t}{\left[\left[\frac{P_t}{P_0}\right]^{\frac{C2}{-2}}\right]-1}$$

(5-79)

The uncertainty in equation 5-79 is:

$$\frac{\Delta \tau_i}{\tau_i} = \left[\left[\frac{C2}{2\,(1-\left[\frac{P_i}{P_0}\right]^{\frac{C2}{2}})}\right]^2\left[\left[\frac{\Delta P_i}{P_i}\right]^2 + \left[\frac{\Delta P_0}{P_0}\right]^2 + \left[\ln\left[\frac{P_i}{P_0}\right]\right]^2\left[\frac{\Delta C2}{C2}\right]^2\right]\right]^{.5}$$

(5-80)

The uncertainty in C2 can be derived in a similar manner to the uncertainty in C1 and results in

$$\frac{\Delta C2}{C2} = \sqrt{\left[\frac{\frac{Rr}{Cpr}-1}{\left[\frac{1}{Mr}+Rr\right]\left[\frac{1}{Cpr}+Mr\right]}\right]^2\left[\frac{\Delta Mr}{Mr}\right]^2}$$

(5-81)

which when combined with equation A-29 produces:

$$\frac{\Delta C2}{C2} = \left[\frac{1}{5.6}\right]\sqrt{\left[\frac{\Delta P(0)}{P(0)}\right]^2 + \left[\frac{\Delta T(0)}{T(0)}\right]^2}$$

(5-82)

using equation 5-71 to substitute Tc for the pressure ratio, equation 5-80 becomes:

$$\frac{\Delta \tau_i}{\tau_i} = \left[\left[\frac{C2}{2\,(1-\left[\frac{1}{Tc}\right])}\right]^2\left[\left[\frac{\Delta P_i}{P_i}\right]^2 + \left[\frac{\Delta P_0}{P_0}\right]^2 + \left[\frac{-2}{C2}\ln[Tc]\right]^2\left[\frac{\Delta C2}{C2}\right]^2\right]\right]^{.5}$$

(5-83)

or in terms of influence coefficients (and combining with equation 5-82):

$$\frac{\Delta \tau_i}{\tau_i} = \left[[K_1]^2\left[\left[\frac{\Delta P_i}{P_i}\right]^2 + \left[\frac{\Delta P_0}{P_0}\right]^2\right] + [K_2]^2\left[\left[\frac{\Delta T_0}{T_0}\right]^2 + \left[\frac{\Delta P_0}{P_0}\right]^2\right]\right]^{.5}$$

(5-84)

Now since we are interested in specific property values at different times, it is not necessary to interpolate between pressure levels in C2 to obtain a history of C2 with respect to Tc only. Since at any point we will know the temperature and the pressure and can just interpolate in the tables to obtain the correct value of C2. However, to show that the difference is not significant in any case,

figure 5-14 show K_1 and K_2 evaluated using C2 at both 4 atm and 7 atm. Figure 5-15 show the differences in these values due to the variation in C2.
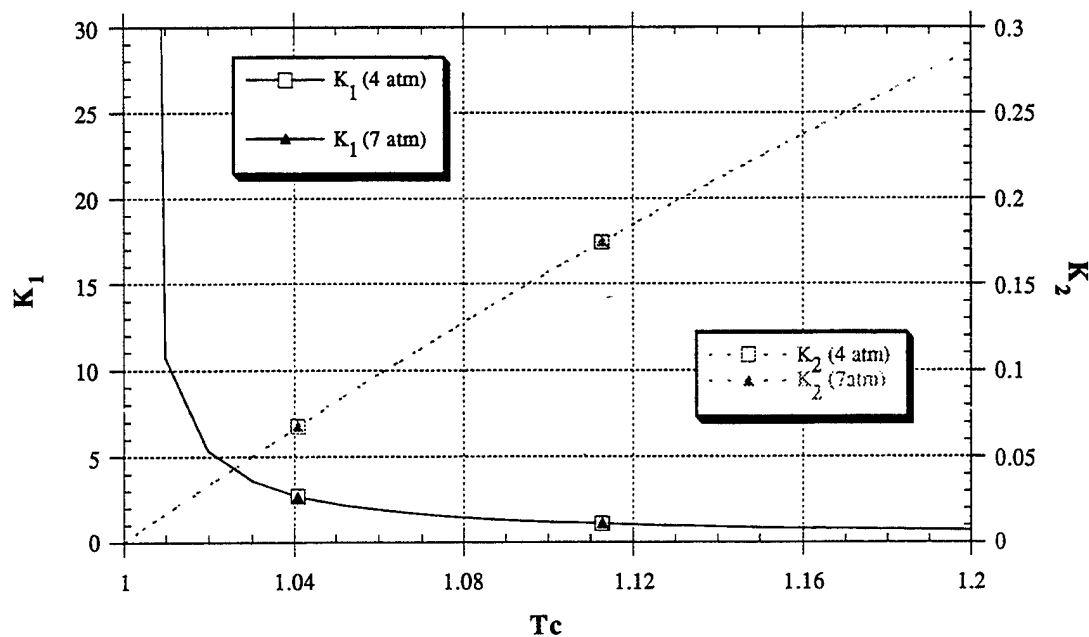
Figure 5-14 K_1 and K_2 as a Function of Tc and C2
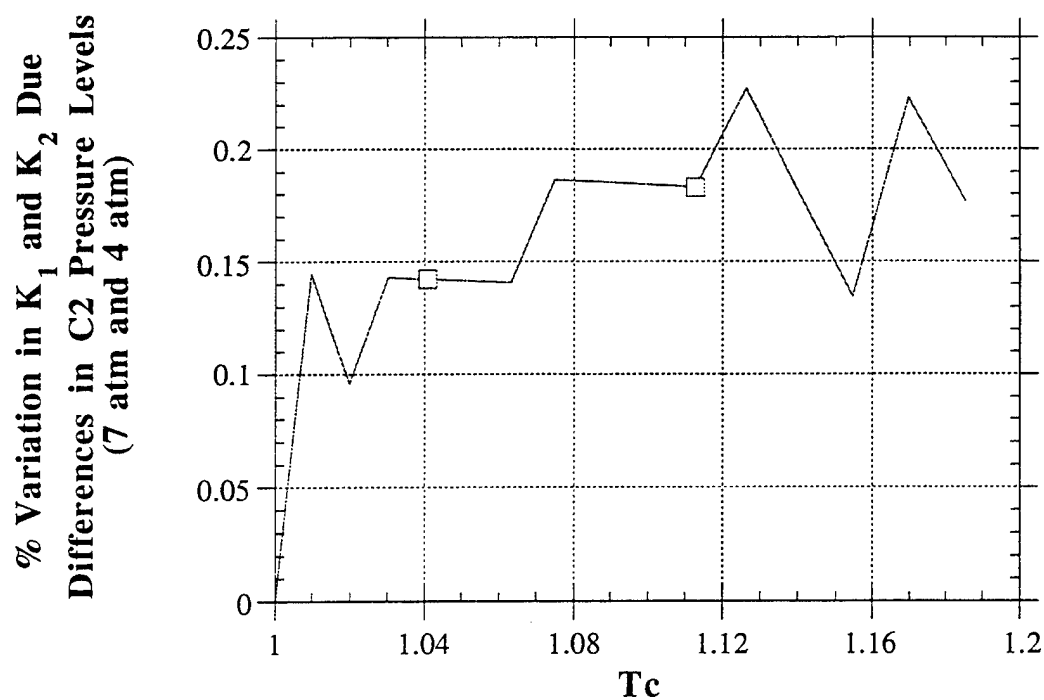
Figure 5-15 Variation in K_1 and K_2 Due to Differences in C2 as a Function of Tc

One of the interesting points to note from figure 5-15 is that the variation in C2 will actually get smaller as Tc approaches the value where the pressure becomes 1 atm and then it will grow again. And the functions K_1 and K_2 are such that there is no uncertainty at time Tc=1. Thus the actual uncertainty which arises from using C2 at 4 atm instead of the proper value of C2 calculated at every point in time will increase from zero at the beginning of a test, reach a peak at about Tc=1.03 and then decay back towards zero where the pressure level reaches 4 atm (at Tc =1.06). After this point it will increase once again. But whatever the behavior, figure 5-15 shows that the total variation is small.

Expanding equation 5-84 and setting $K_3 = K_1 K_2$ then

$$K_3 = K_1 K_2 = \frac{Tc \ln(Tc)}{(Tc-1)\, 5.6} \tag{5-85}$$

creating

$$\frac{\Delta \tau_i}{\tau_i} = \left[[K_1]^2 \left[\frac{\Delta P_i}{P_i}\right]^2 + \left[\frac{\Delta P_0}{P_0}\right]^2 \left[[K_1]^2 + [K_3]^2\right] + [K_3]^2 \left[\frac{\Delta T_0}{T_0}\right]^2 \right]^{.5} \tag{5-86}$$

Substituting equation 5-19, 5-78, and 5-86 into equation 5-73 develops the uncertainty in the mass flow out of the supply tank as a function only of the measured variables:

$$\frac{\Delta \dot{m}}{\dot{m}} = \left[K_{P0}^2 \left[\frac{\Delta P_0}{P_0}\right]^2 + K_{T0}^2 \left[\frac{\Delta T_0}{T_0}\right]^2 + K_{Pi}^2 \left[\frac{\Delta P_i}{P_i}\right]^2 + \left[\frac{\Delta V}{V}\right]^2 \right]^{.5} \tag{5-87}$$

where

$$K_{P0}^2 = Km_1^2 \, (K_1^2 + K_3^2) + \left[\frac{Km_2}{4.44}\right]^2 + 1.04$$

$$K_{T0}^2 = Km_1^2 K_3^2 + \left[\frac{Km_2}{4.44}\right]^2 + 1.04$$

$$K_{Pi}^2 = Km_1^2 \, K_1^2 \tag{5-88}$$

Figure 5-16 shows the traces of K_1 and $K3$ as a function of Tc

71
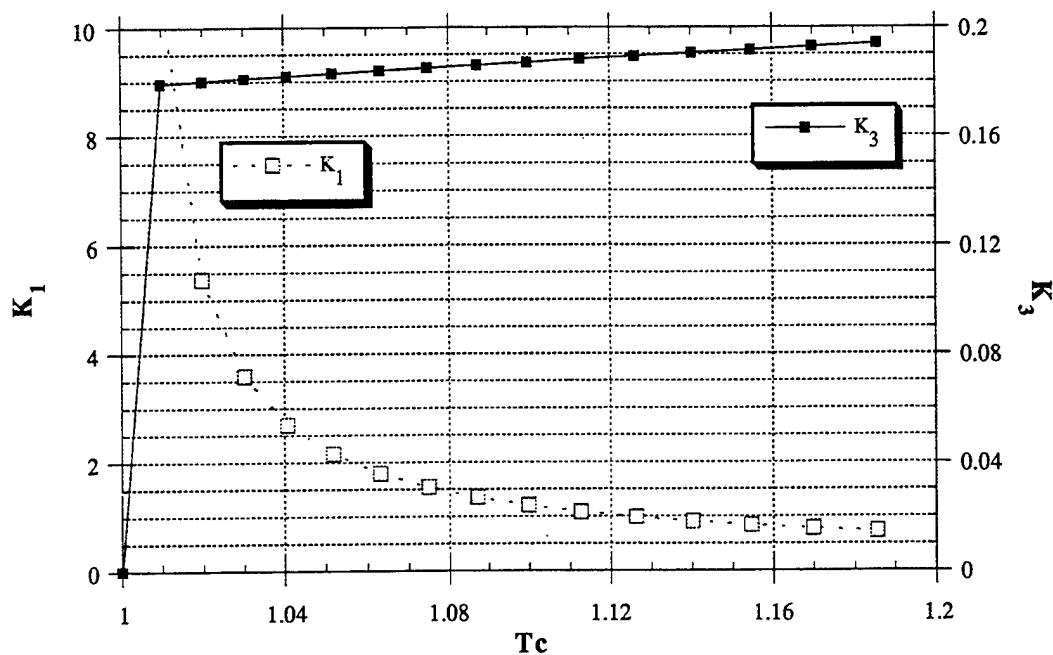
Figure 5-16 K_1 and K_3 as a Function of Tc

Figure 5-17 shows the values for K_{P0}, K_{T0}, and K_{Pi}.
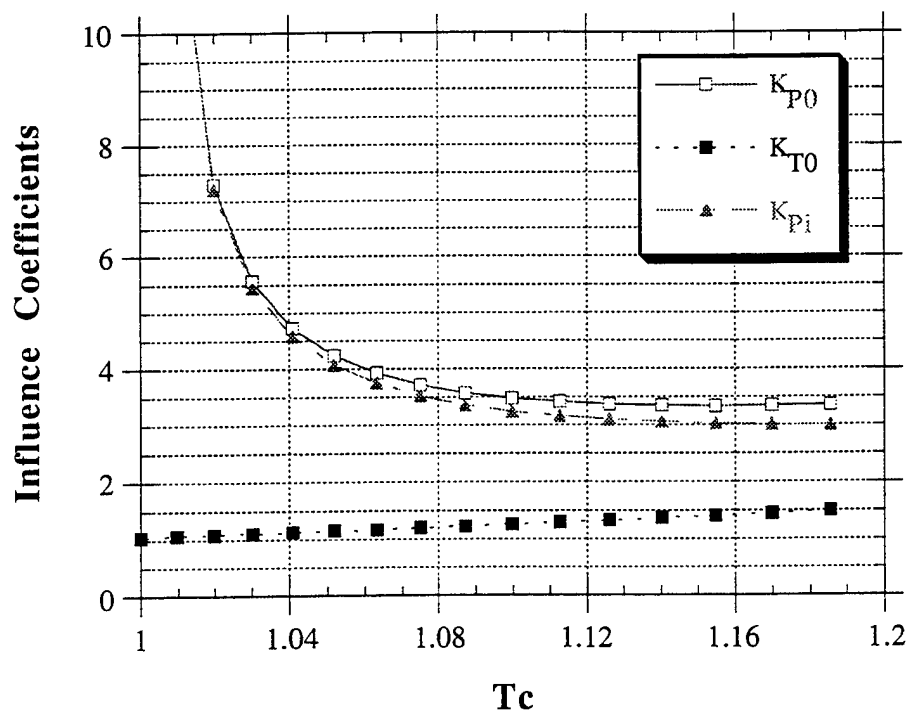
Figure 5-17 K_{P0}, K_{T0}, and K_{Pi} as a Function of Tc

As a final step, we need to determine the accuracy in the boundary layer bleed ratio in order to find the uncertainty in the mass flow through the test section. The information in section 5.1.3 as well as equation 5-41 is still valid and thus the uncertainty in the boundary layer bleed ratio will be the root sum square of the uncertainties in the two time constants

$$\frac{\Delta\dot{m}_3}{\dot{m}_3} = \left[\left[\frac{\Delta\dot{m}_1}{\dot{m}_1}\right]^2 + \left[\frac{\alpha}{1+\alpha}\right]^2 \left[\left[\frac{\Delta\tau_{Bleeds}}{\tau_{Bleeds}}\right]^2 + \left[\frac{\Delta\tau_{No\ Bleeds}}{\tau_{No\ Bleeds}}\right]^2\right]\right]^{.5}$$ (5-89)

If the uncertainties in the measurements are the same for both test then the overall uncertainty from the boundary layer bleeds are just a function of the influence coefficient in equation 5-86. For the standard fill conditions the dependency of the supply tank time constant on the boundary layer bleeds is shown in section 5.2.2. Without any boundary layer bleeds, the time constant is about 63 seconds, with a 30% bleed it is about 48.5 sec This corresponds to Tc values (at 1.5 seconds) of 1.023 and 1.03 respectively. Thus testing the facility with or without the boundary layer bleeds should develop the same influence coefficients, just offset on the Tc axis.

As an example assume that we wish to measure efficiency at 1.5 seconds, from figure 5-16, K_1 will be about 5.5 in one test and 3.5 in the other (K_2 remains constant at about .19). Thus equation 5-89 when combined with equation 5-86 (and assuming equal measurement uncertainties) produces:

$$\frac{\Delta\dot{m}_3}{\dot{m}_3} = \left[\left[\frac{\Delta\dot{m}_1}{\dot{m}_1}\right]^2 + \left[\frac{\alpha}{1+\alpha}\right]^2 \left[[6.52]^2\left[\frac{\Delta P_i}{P_i}\right]^2 + \left[\frac{\Delta P_0}{P_0}\right]^2 [6.54]^2 + [.27]^2\left[\frac{\Delta T_0}{T_0}\right]^2\right]\right]^{.5}$$ (5-90)

For a 30% bleed this reduces to:

$$\frac{\Delta\dot{m}_3}{\dot{m}_3} = \left[\left[\frac{\Delta\dot{m}_1}{\dot{m}_1}\right]^2 + [1.51]^2\left[\frac{\Delta P_i}{P_i}\right]^2 + \left[\frac{\Delta P_0}{P_0}\right]^2 [1.51]^2 + [0.06]^2\left[\frac{\Delta T_0}{T_0}\right]^2\right]^{.5}$$ (5-91)

From figure 5-17 at Tc=1.03 K_{Pi} = 1.1, and $K_{T0}=K_{P0}$ at about 5.25. Thus equation 5-91 becomes , for this example:

$$\frac{\Delta\dot{m}_3}{\dot{m}_3} = \left[\left[\frac{\Delta V}{V}\right]^2 + [1.87]^2\left[\frac{\Delta P_i}{P_i}\right]^2 + \left[\frac{\Delta P_0}{P_0}\right]^2 [5.46]^2 + [5.25]^2\left[\frac{\Delta T_0}{T_0}\right]^2\right]^{.5}$$ (5-92)

If the initial measurement uncertainty can be reduced through statistical analysis, and the uncertainty in the volume of the tank ignored then it is possible (but not highly probable that the transient pressure measurement will be accurate to 0.13% and thus the mass flow will be accurate to 0.25%.

5.3   Conclusions and the Mass Flow Uncertainty

There are several interesting connotations to equation 5-92. First, as one lengthens the test time Tc, the overall influence coefficients get much smaller, since they are primarily influenced by K_{P0} and K_{T0}. The uncertainty in the initial conditions can be driven using statistical processes to

73

levels where they are no longer important and thus the transient measurement will become the dominant error (which is the best one can do). As a side benefit, the influence of the supply tank time constant measurement is not that great in the determination of the boundary layer bleed ratio, which means that it can be measured at the same value of Tc for which the actual efficiency is being measured.

However, equation 5-92 has been developed at much cost. Appendix C has shown the importance of the real gas effects, both in the problems it causes in generating the isentropic relationships, and the effects it has on developing the constants C1 and C2. At the end of that appendix we were forced to assume that the ideal gas law is valid over small time increments. Figure C-14 showed that the difference between methods (all of which seemed legitimate) could be quite large. Thus the ultimate cost has come in the form of keeping track of the gas properties and the interpolation procedures used. Which, as stated earlier in the report, were arbitrarily selected.

Section 6 Results, Conclusions, and Future Work

The goal of this study has been to develop the relationships needed for measuring efficiency accurately; determining those variables which need to be controlled during the construction and operation of the ATARR facility, and determining how the uncertainty in the measurements impact the accuracy of the derived efficiency.. This has been done in Section 2, which outlines the equations for efficiency accuracy and in the other sections which relate these sub-components to measured properties.

There are two particular ways of measuring turbine efficiency. Using either a thermodynamic method, which evaluates the change in the energy of the test gas as it passes through the turbine stage; or a mechanical method which uses the actual work extracted by the turbine. One of the features of this study has been to see which method would provide a more accurate measurement, and for each method which parameters were important. As demonstrated in the introduction, for any set level of measurement accuracy, the calculated efficiency accuracy for an adiabatic uncooled turbine (simplest case) will depend on the turbine performance (the pressure ratio across the turbine, the test gas γ, and the stage efficiency). Section 1 reviewed the definition of measurement accuracy and demonstrated that instrument accuracy is only one component of the overall measurement uncertainty. The other, more nebulous part being the assumptions which are made about how well the flow at the point of measurement represented the flow field. The question of flow uniformity is especially critical for the downstream measurement of total temperature and total pressure when the thermodynamic technique of measuring efficiency is used. For both methods, Section 4 demonstrated that to measure efficiency accurately would require a detailed knowledge of the initial conditions and how real gas effects influence the initial properties. The influence of real gas effects on the test gas became clear as the work progressed and showed that great care needed to be exercised in the selection of gas properties. Section 3 discusses the choice of gas tables for use with this facility. Section 5 discusses the influence of real gas effects on the mass flow measurement, and appendices A and C show specific examples of how using real gas data varies from ideal gas behavior, even at these modest temperatures and pressures. It was known early in the program that to measure efficiency accurately requires that the supply tank volume be well known. As shown in equation 5-18 and 5-92, the uncertainty in the volume of the supply tank needs to be an order of magnitude better then 0.25% if the stage efficiency is to be measured to the desired accuracy.

The results of Section 5 illustrate that the mass flow through the test section can be measured. Since both the torque and speed of the shaft are directly measured, the opportunity exists to use the mechanical method to determine the efficiency of the turbine as well as using

75

the thermodynamic technique. A second important result has been the development of the ATARR non-dimensional time Tc (defined in equation 5-34) in the mechanical measurement technique. All different testing configurations can be collapsed to be function only of Tc. Likewise the gas properties can also be expresses solely as a function of Tc which allows experiments to be designed to yield optimal efficiency measuring points.

Thus, this study has developed the procedure by which efficiency measurements will be made on specific test turbines. The specific efficiency accuracy will be a function of measurement uncertainty, instrument uncertainty, the turbine configuration and which technique is ultimately used. In addition, this study has shown explicitly where assumptions are made in the effort to measure efficiency. It has been noted that key issues such as the differences between adiabatic and isothermal testing environments, how to measure the isothermal losses in this facility, or how other facilities measure how close they are to adiabatic, are critical in comparing data between facilities; but have been left out of this study because of the lack of data available on other facilities. Because of these problems it is suggested that the mechanical method be used for measuring efficiency since the problems of measuring the losses in this facility are irrelevant. But the trade-off includes several other assumptions, about the validity of the ideal gas law and the need to account for gas property variation during the test.

This study is only the first part of the work which will need to be done to bring the ATARR into operation. The need for extremely accurate temperature and pressure measurements both during the fill process and during the test, has been shown. Instrumentation and calibration procedures are being developed to provide this information. Secondly, this analysis is only the procedure for measuring efficiency, each test turbine must be evaluated using this procedure to determine how accurately efficiency may be measured. But before that can be done, the facility has to be up and running, with all of its instrumentation calibrated. In the attempt to make this process go smoother, the use of Moffat's[1] technique to estimate the acceptable level of uncertainty at different stages in the shake-down process of the ATARR facility is recommended.

With this, and the other work being performed, the ATARR facility should be capable of delivering state-of-the-art accuracies not only in efficiency, but also in types of data. The construction of the ATARR facility will allow detailed research and development of turbines, and in conjunction with other facilities should help to push the limits of understanding in turbine technology.

---

[1] Moffat, R. J. " Contributions to the Theory of Single-Sample Uncertainty Analysis"; Transactions of the ASME, Vol, 104, June 1982, pp. 250-260.

Appendix A
Test Gas Properties

The purpose of this section is threefold. The first is to list the tabulated values of the gas properties for nitrogen and carbon dioxide which will be used in the ATARR facility. The second is to show how different mixtures can be obtained and how the test gas properties depend on the individual gas properties. The third is to document the behavior of the test mixture during a standard test. Throughout this section particular focus will be directed to the propagation of uncertainty through the gas tables and the interpolation procedures and the differences which occur between using ideal gas properties and real gas properties.

Individual Gas Properties:

While the ATARR facility could use a wide range of test gas mixtures to simulate the turbine operating environment, the gases which are most likely to be used are a mixture of nitrogen and carbon dioxide for the main flow and a pure nitrogen cooling flow. The real gas properties of interest are the compressibility, specific heat at constant pressure and the ratio of specific heats. These properties are listed in tables A-1 and A-2 for both carbon dioxide and nitrogen for common pressures and temperatures. And as suggested in section 3, other pressures and temperatures can be found in reference 1[1]. Figures A-1 to A-8 are plots of the variation in these properties as a function of temperature and pressure. All the figures in this group have two axis. The left side is the nominal value of the parameter and the right side is the maximum variation of the parameter at a set temperature as a function of pressure (maximum variation is defined as the (maximum value-minimum value)100/minimum value). One can see that the variation between the ideal gas properties and the real tabulated properties can be significant and that even at the high temperatures, the variation in the properties could be of the same magnitude as the total uncertainty in the efficiency.

Standard Fill Conditions:

The next step is to examine how the individual gases combine in a standard fill and evaluate the behavior of the resulting mixture. As stated in section 5, the gas mixture is assumed to be a simple compressible mixture. Standard fill conditions will be assumed to include real gas effects and be a mixture of N_2-CO_2 supply tank gas at 105 psi (7 atm), 520°K with a desired γ of 1.268 and with N_2 as the cooling gas at 216 °K (-70 °F) and 73 psia. Equation 4-4 can be inverted to find the desired mass ratio as a function of the desired test γ and the gas properties

---

[1] Hilsenrath, Beckett, Benedict, Fano, Hoge, Masi, Nuttall, Touloukian, and Woolley; <u>Tables of Thermodynamic and Transport Properties of Air, Argon, Carbon Dioxide, Carbon Monoxide, Hydrogen, Nitrogen, Oxygen, and Steam,</u> Pergamon Press, New York, 1960

$$\frac{m_y}{m_x} = \frac{\gamma C_{vx} - C_{px}}{C_{py} - \gamma C_{vy}}$$

(A-1)

thus the desired pressure ratio can be found from equation 4-7

$$\frac{P_2 T_1}{P_1 T_2} = \frac{\dfrac{m_y R_y}{m_x R_x} Zr_2 + 1}{Zx_{12}}$$

(A-2)

and since the supply tank temperature is designed to be held constant this reduces to:

$$\frac{P_2}{P_1} = \frac{\dfrac{m_y R_y}{m_x R_x} Zr_2 + 1}{Zx_{12}}$$

(A-3)

(Zr_2 is the ratio Zy_2/Zx_2 and $Zx_{12} = Zx_1/Zx_2$)

It is important to note that together, equations A-3 and A-1 determine what the fill pressures should be; but to find out what the actual test conditions are, equation 4-7 and 4-4 will have to be used to account for variations in temperature and pressure from the design conditions. However the form of equation A-1 is troublesome since it represents the division of two small numbers. A-1 can be rewritten in terms of the individual component γ's.

$$\frac{m_y}{m_x} = \frac{C_{vx}(\gamma - \gamma_x)}{C_{vy}(\gamma_y - \gamma)}$$

(A-4)

Equation A-4 shows that the closer the individual component γ's are to the test γ the more unstable this ratio is. The uncertainty in the mass ratio can be given as:

$$\frac{\Delta \frac{m_y}{m_x}}{\frac{m_y}{m_x}} = \left[\frac{\left[\frac{\Delta C_{px}}{C_{px}}\right]^2 + \left[\frac{\gamma}{\gamma_x}\frac{\Delta C_{vx}}{C_{vx}}\right]^2}{\left[\frac{\gamma}{\gamma_x} - 1\right]^2} + \frac{\left[\frac{\Delta C_{py}}{C_{py}}\right]^2 + \left[\frac{\gamma}{\gamma_y}\frac{\Delta C_{vy}}{C_{vy}}\right]^2}{\left[1 - \frac{\gamma}{\gamma_y}\right]^2} + \left[\frac{\Delta\gamma}{\gamma}\right]^2 \left[\frac{\left[\frac{\gamma}{\gamma_x} - \frac{\gamma}{\gamma_y}\right]}{\left[1 - \frac{\gamma}{\gamma_y}\right]\left[\frac{\gamma}{\gamma_x} - 1\right]}\right]^2 \right]^{0.5}$$

(A-5)

Thus, small variations in the gas properties can have a large variation in the mass ratio. For the standard fill conditions listed above, from table A-1 {in KJ/[Kg-K]}

N_2: $C_p = 1.0623$ $C_v = .7626$ $\gamma = 1.393$ (Real): $C_p = 1.0594$ $C_v = .7626$ $\gamma = 1.389$ (ideal)

CO_2: $C_p = 1.0357$ $C_v = .8400$ $\gamma = 1.233$ (Real): $C_p = 1.0268$ $C_v = .8379$ $\gamma = 1.225$ (ideal)

The parameters

$$\left[\frac{\gamma}{\gamma_x} - 1\right]^2 = \left.\frac{1}{124}\right|_{real} \quad or \quad \left.\frac{1}{181}\right|_{Ideal}$$

$$\left[1 - \frac{\gamma}{\gamma_y}\right]^2 = \left.\frac{1}{1241}\right|_{real} \quad or \quad \left.\frac{1}{811}\right|_{Ideal}$$

So even though the variation in the gas properties is small at these conditions (<0.8%) the difference between the two mass ratios predicted is large. Using real gas parameters, equation A-4 reduces to:

$$\text{Mr} (=m_y/m_x)=3.24 \text{ (real) or } 2.59 \text{ (ideal) a 25\% variation!} \tag{A-6}$$

Fortunately, once we have measured the fill conditions, the actual testing value of γ is relatively insensitive to the mass ratio in the tank. Rewriting equation 4-4 in terms of the mass ratio and the component γ's

$$\gamma = \gamma_x \frac{1+\dfrac{C_{py}}{C_{px}}\text{Mr}}{1+\dfrac{C_{vy}}{C_{vx}}\text{Mr}} \tag{A-7}$$

with a resulting uncertainty of:

$$\frac{\Delta\gamma}{\gamma} = \left[\frac{\left[\dfrac{\Delta C_{px}}{C_{px}}\right]^2+\left[\dfrac{\Delta C_{py}}{C_{py}}\right]^2}{\left[\dfrac{C_{px}}{C_{py}\text{Mr}}+1\right]^2} + \frac{\left[\dfrac{\Delta C_{vx}}{C_{vx}}\right]^2+\left[\dfrac{\Delta C_{vy}}{C_{vy}}\right]^2}{\left[\dfrac{C_{vx}}{C_{vy}\text{Mr}}+1\right]^2} + \left[\frac{\Delta\gamma_x}{\gamma_x}\right]^2 + \left[\frac{\Delta\text{Mr}}{\text{Mr}}\right]^2 \left[\frac{\left[\dfrac{\gamma_y}{\gamma_x}-1\right]}{\left[\dfrac{C_{vx}}{C_{vy}}+\dfrac{\text{Mr}\gamma_y}{\gamma_x}\right]\left[\dfrac{1}{\text{Mr}}+\dfrac{C_{vy}}{C_{vx}}\right]}\right]^2 \right]^{\frac{1}{2}} \tag{A-8}$$

Disregarding the uncertainties in the individual gas properties (these will be analyzed latter, but it is clear that their influence coefficients can never be bigger then 1); the uncertainty in the test value of γ becomes a function of the uncertainty in the mass ratio. For real gas properties this reduces to

$$\frac{\Delta\gamma}{\gamma} = \left[\frac{\left[\dfrac{\Delta C_{px}}{C_{px}}\right]^2+\left[\dfrac{\Delta C_{py}}{C_{py}}\right]^2}{1.3166^2} + \frac{\left[\dfrac{\Delta C_{vx}}{C_{vx}}\right]^2+\left[\dfrac{\Delta C_{vy}}{C_{vy}}\right]^2}{1.2802^2} + \left[\frac{\Delta\gamma_x}{\gamma_x}\right]^2 + \left[\frac{\Delta\text{Mr}}{\text{Mr}}\right]^2\left[\frac{1}{-46.3478}\right]^2 \right]^{\frac{1}{2}} \tag{A-9}$$

and for ideal gas properties:

$$\frac{\Delta\gamma}{\gamma} = \left[\frac{\left[\dfrac{\Delta C_{px}}{C_{px}}\right]^2+\left[\dfrac{\Delta C_{py}}{C_{py}}\right]^2}{1.3984^2} + \frac{\left[\dfrac{\Delta C_{vx}}{C_{vx}}\right]^2+\left[\dfrac{\Delta C_{vy}}{C_{vy}}\right]^2}{1.3514^2} + \left[\frac{\Delta\gamma_x}{\gamma_x}\right]^2 + \left[\frac{\Delta\text{Mr}}{\text{Mr}}\right]^2\left[\frac{1}{-40.245}\right]^2 \right]^{\frac{1}{2}} \tag{A-10}$$

Using the difference in mass ratios between a real gas and an ideal gas (equation A-6), and the largest value for the influence coefficient, one finds that the difference in the test value of γ is approximately

$$\frac{\Delta\gamma}{\gamma} = \left[[0.25]^2\left[\frac{1}{1600}\right]\right]^{\frac{1}{2}} \rightarrow .63\% \text{ variation} \tag{A-11}$$

which is larger then the overall uncertainty in the efficiency desired, but a much more reasonable variation then the difference in the mass ratios.

At this point one might suspect that the calculation of the "fill targets" are quite susceptible to the differences between real gas properties and ideal gas properties, but that the actual testing properties which are obtained from pressure and temperature measurements are much less susceptible. This hypothesis can be checked by continuing through the fill process. Once the mass ratios are known, then the fill pressure ratios can be calculated from equation A-3. For both cases the ratio in gas constants

$$Rr = \frac{R_2}{R_1} = .6366$$

(A-12)

and for the situation using ideal gas values

$$\frac{P_2}{P_1} = 2.649$$

(A-13)

For the real gas values Zr_2 is found from table to be .99292. Finding the value Zx_{12} is clearly more difficult because we are not sure of the target state. From figure 4-1 we see that the variation in Z for nitrogen at 520 °K is about .05% between the values of P_x/P_y of 0.4 and 0.2. Therefore taking the mean produces a value of

$$\frac{P_2}{P_1} = 3.054$$

(A-14)

If we use the pressure ratio calculated in equation A-14 to interpolate in the tables, then we find that $Zx_{12} = .99802$ (a .003% error, which is good enough). A summary of the standard fill properties is listed below:

Table of Standard Gas Properties

Property		Real	Ideal
	$Mr = \dfrac{m_y}{m_x}$	3.24	2.59
	$Pr = \dfrac{P_y}{P_x}$	3.054	2.649
	$Rr = \dfrac{R_y}{R_x}$	.6366	.6366
	$Cpr = \dfrac{C_{py}}{C_{px}}$	.9692	.8819
	$Cvr = \dfrac{C_{vy}}{C_{vx}}$	1.1015	1.0987
Zr_2		.99292	NA
Zx_{12}		.99805	NA

The pressure ratios shown in equation A-13 (ideal gas) and A-14 (real gas) are vastly different, but these differences do not arise directly from the compressibility. In fact if one were to take the ideal mass ratio and use the compressibility ratios listed above one would obtain a pressure ratio difference of only about .25%. The rest of the difference is due to the difference in the mass ratios. Figure 4-4 shows the difference between the real gas model and the ideal gas model for these fill conditions. Figure A-9 shows a plot of the variation in Zr and Zx_{12} as a function of the test temperature.

At this point the behavior of the gas mixture can be defined. The first property of interest will be the compressibility of the mixture. Using the law of partial pressures

$$Z_m = Y_x Z_x + Y_y Z_y \Big|_{\text{at mixture T and P}}$$

$$Y = \text{mole ratio} \frac{N_i}{N_{total}} \tag{A-15}$$

The mole fraction can be related to the mass fraction through the molecular weights of the components

$$Y_i \frac{M_i}{M_{total}} = \frac{m_i}{m_{total}} \tag{A-16}$$

(M is the molecular weight)

Since the molecular weight is related to the gas constant by

$$R_i = \frac{\overline{R}}{M_i} \tag{A-17}$$

these relations can be used to reduce equation A-11 to

$$Z_m = \frac{Z_x(1 + \frac{m_y R_y Z_y}{m_x R_x Z_x})}{1 + \frac{m_y R_y}{m_x R_x}} \Bigg|_{\text{at mixture T and P}} \tag{A-18}$$

Since the mixture values of R, C_p, and C_v are all functions of the mass ratio, these properties are given by:

$$R_m = R_x \frac{(1 + \frac{R_x}{R_y} Mr)}{1 + Mr} = 214.36 \text{ (Real)} \tag{A-19}$$

$$C_{pm} = C_{px} \frac{(1 + \frac{C_{px}}{C_{py}} Mr)}{1 + Mr} \tag{A-20}$$

$$C_{vm} = C_{vx} \frac{(1 + \frac{C_{vx}}{C_{vy}} Mr)}{1 + Mr} \tag{A-21}$$

The values for C_{pm} and C_{vm} are tabulated for the standard mixture and for the ideal gas case in Table A-4. Also included in this table are the variations between the real gas mixture and the ideal gas mixture as a function of pressure, and the variation in the real gas mixture from 1 atm to 7 atm[2]. These variations are shown graphically in figures A-10 to A-13 (figures A-10a and A-11a show the variation from initial conditions). The left axis is the scale for the difference between the real gas mixture and the ideal gas mixture (in %) as a function of pressure level. The right-hand side is a plot of the % variation between the pressure levels (1 atm, 4 atm and 7 atm) for the real gas. It is apparent from the graphs that at low temperatures, the variations from ideal gas behavior (and between pressure levels becomes quite important (which is not surprising since one is approaching the freezing point of CO_2). At higher temperatures, the variation between the methods is small, but cannot to be eliminated as a factor.

Uncertainty in Gas Properties:

Throughout the paper the uncertainty in a derived quantity often depends on the uncertainty in the gas properties to some extent. We are now in a position to analyze this uncertainty. Since we are assuming that the values listed in the tables for the components are correct then the only uncertainty in the components comes from uncertainty in either the temperature or the pressure measurements used as a basis for interpolation in the tables. As stated earlier in the paper, this uncertainty is a combination of the instrument uncertainty and any uncertainty about the flow. The uncertainty in the derived parameters (equations A-12 to A-15) can be found in terms of uncertainty in the individual components.

For the mixture compressibility, the uncertainty in equation A-12 reduces to:

$$\frac{\Delta Z_m}{Z_m} = \left[\left[\frac{\Delta Z_y}{Z_y} \right]^2 \frac{1}{\left[\frac{1}{Mr\,Rr\,Zr} +1 \right]^2} + \left[\frac{\Delta Z_x}{Z_x} \right]^2 \frac{1}{[Mr\,Rr\,Zr +1]^2} + \left[\frac{\Delta Mr}{Mr} \right]^2 \left[\frac{[Zr - 1]}{[1 + Mr\,Rr]\,Zr + \frac{1}{Mr\,Rr} + 1} \right]^2 \right]^{\frac{1}{2}}$$

(A-22)

For the standard testing conditions A-22 reduces to:

---

2 Variation in this case has two meanings. For the differences between the real gas and the ideal gas mixture it is defined as:

$$\frac{(Real - Ideal)*100}{Ideal}$$

For the differences between pressure levels in the real gas it is defined as:

$$\frac{(Max - Min)*100}{Min}$$

$$\frac{\Delta Z_m}{Z_m} = \left[\left[\frac{\Delta Z_y}{Z_y}\right]^2 \frac{1}{1.488^2} + \left[\frac{\Delta Z_x}{Z_x}\right]^2 \frac{1}{3.0479^2} + \left[\frac{\Delta Mr}{Mr}\right]^2 \left[\frac{1}{-639.2^2}\right]\right]^{\frac{1}{2}} \qquad \text{(A-23)}$$

(this is not a parameter in an ideal gas case). One can see that the influence coefficients for the individual gas compressibilities are small and almost nonexistent for Mr. The uncertainty in the constant pressure specific heat is given by:

$$\frac{\Delta Cp_m}{Cp_m} = \left[\left[\frac{\Delta Cp_y}{Cp_y}\right]^2 \frac{1}{\left[\frac{1}{Mr\,Cp_r}+1\right]^2} + \left[\frac{\Delta Cp_x}{Cp_x}\right]^2 \frac{1}{[Mr\,Cp_r+1]^2} + \left[\frac{\Delta Mr}{Mr}\right]^2 \left[\frac{[Cp_r-1]}{[1+Mr]\left[\frac{1}{Mr}+Cp_r\right]}\right]^2\right]^{\frac{1}{2}} \qquad \text{(A-24)}$$

which reduces to:

$$\frac{\Delta Cp_m}{Cp_m} = \left[\left[\frac{\Delta Cp_y}{Cp_y}\right]^2 \frac{1}{1.3166^2} + \left[\frac{\Delta Cp_x}{Cp_x}\right]^2 \frac{1}{4.1589^2} + \left[\frac{\Delta Mr}{Mr}\right]^2 \left[\frac{1}{-217.35}\right]^2\right]^{\frac{1}{2}} \qquad \text{(A-25)}$$

when a real gas mixture is used and to:

$$\frac{\Delta Cp_m}{Cp_m} = \left[\left[\frac{\Delta Cp_y}{Cp_y}\right]^2 \frac{1}{1.3984^2} + \left[\frac{\Delta Cp_x}{Cp_x}\right]^2 \frac{1}{3.51039^2} + \left[\frac{\Delta Mr}{Mr}\right]^2 \left[\frac{1}{-158.12}\right]^2\right]^{\frac{1}{2}} \qquad \text{(A-26)}$$

when an ideal gas mixture is used. In both cases the influence coefficient for the component properties is less then 1, and that the influence coefficient for the mass ratio is very small. Finally, for the constant volume specific heat:

$$\frac{\Delta Cv_m}{Cv_m} = \left[\left[\frac{\Delta Cv_y}{Cv_y}\right]^2 \frac{1}{\left[\frac{1}{Mr\,Cv_r}+1\right]^2} + \left[\frac{\Delta Cv_x}{Cv_x}\right]^2 \frac{1}{[Mr\,Cv_r+1]^2} + \left[\frac{\Delta Mr}{Mr}\right]^2 \left[\frac{[Cv_r-1]}{[1+Mr]\left[\frac{1}{Mr}+Cv_r\right]}\right]^2\right]^{\frac{1}{2}} \qquad \text{(A-27)}$$

which for a real gas mixture is:

$$\frac{\Delta Cv_m}{Cv_m} = \left[\left[\frac{\Delta Cv_y}{Cv_y}\right]^2 \frac{1}{1.2802^2} + \left[\frac{\Delta Cv_x}{Cv_x}\right]^2 \frac{1}{4.5688^2} + \left[\frac{\Delta Mr}{Mr}\right]^2 \left[\frac{1}{58.91}\right]^2\right]^{\frac{1}{2}} \qquad \text{(A-28)}$$

and for an ideal mixture is:

$$\frac{\Delta Cv_m}{Cv_m} = \left[\left[\frac{\Delta Cv_y}{Cv_y}\right]^2 \frac{1}{1.3514^2} + \left[\frac{\Delta Cv_x}{Cv_x}\right]^2 \frac{1}{3.8457^2} + \left[\frac{\Delta Mr}{Mr}\right]^2 \left[\frac{1}{53.984}\right]^2\right]^{\frac{1}{2}} \qquad \text{(A-29)}$$

For all of these properties, the influence coefficient for the individual components are small (<1) Thus the only concern is how the individual properties vary with measurement uncertainty. These properties can be calculated from the data in tables A-1 and A-2 and are shown in tables A-5 and A-6, and graphically in figures A-14 to A-21. The tables include information about the variation in properties as a function of temperature (at any set pressure)

and the variation in properties due to pressure differences (at any given temperature). The formulas used are listed at the bottom of each table. It is important to note that these percentages are calculated as (maximum value-minimum value)/minimum value, thus the variation will always be positive and it will always be a maximum variation. In addition this variation has been normalized to either a unit psi difference, or a degree Kelvin difference (depending on the information). Now it is the desired goal of this project to make measurements which are far more accurate then 1 °K or 1 psi, thus once the uncertainties are known in the measurements a better approximation can be made to the total uncertainty in the gas properties.

Examining the graphical data in figures A-14 to A-21 it is clear that in the temperature range which the facility operates (400 to 520 °K) the property variations (note the different scales in the graphs) are an order of magnitude smaller then the variations of interest in the uncertainty analysis (even at this large scale of measurement uncertainty), and therefore can be considered independent of measurement accuracy in most cases. To determine if these property variations are important in the variation of the mixture parameters we need to use equation 4-9 (the uncertainty in the mass ratio as a function of measured properties, since equation A-5 is really an uncertainty in the prediction of the mass ratio, not the measured mass ratio). Equation 4-9 is:

$$\frac{\Delta Mr}{Mr} = \left[\left[\frac{1}{1-\frac{T_2 P_1}{P_2 T_1 Zx_{12}}} \right]^2 \left[\left[\frac{\Delta P_2}{P_2} \right]^2 + \left[\frac{\Delta P_1}{P_1} \right]^2 + \left[\frac{\Delta T_2}{T_2} \right]^2 + \left[\frac{\Delta T_1}{T_1} \right]^2 + \left[\frac{\Delta Zx_{12}}{Zx_{12}} \right]^2 \right] + \left[\frac{\Delta Zr_2}{Zr_2} \right]^2 \right]^{\frac{1}{2}} \quad \text{(A-30)}$$

The uncertainties in the compressibilities listed in equation A-30 are just the addition of the uncertainties of the individual components at each measurement. If one were able to achieve a measurement error of .1 psi and .1°K, (corresponding to a 0.1% pressure accuracy and a .03 % temperature,based on a 300 °K range, accuracy). It is clear from Figures A-20 and A-21 the uncertainties in the compressibilities would be much smaller then the measurement uncertainty, even at these optimistically accurate levels. As such the uncertainties in compressibility can be ignored and equation A-30 rewritten as:

$$\frac{\Delta Mr}{Mr} = \left[\left[\frac{1}{1-\frac{T_2 P_1}{P_2 T_1 Zx_{12}}} \right]^2 \left[\left[\frac{\Delta P_2}{P_2} \right]^2 + \left[\frac{\Delta P_1}{P_1} \right]^2 + \left[\frac{\Delta T_2}{T_2} \right]^2 + \left[\frac{\Delta T_1}{T_1} \right]^2 \right] \right]^{\frac{1}{2}} \quad \text{(A-31)}$$

Using the pressure ratio and compressibility of a real gas, assuming that the temperature during a fill is constant, and that the pressure and temperature uncertainty are the same at both measurement points, this equation reduces to

$$\frac{\Delta Mr}{Mr} = \left[[2.105]^2 \left[\left[\frac{\Delta P}{P} \right]^2 + \left[\frac{\Delta T}{T} \right]^2 \right] \right]^{\frac{1}{2}} \quad \text{(Real)} \quad \text{(A-32)}$$

$$\frac{\Delta Mr}{Mr} = \left[[2.272]^2 \left[\left[\frac{\Delta P}{P} \right]^2 + \left[\frac{\Delta T}{T} \right]^2 \right] \right]^{\frac{1}{2}} \text{ (Ideal)}$$

(A-33)

At this point it is hard to proceed since we do not know the actual uncertainty in the pressure and temperature measurements and these are critical in determining the overall uncertainty in the mixture properties. However since the individual gas component properties seem to be invariant to the temperature and pressure measurements errors, they can be eliminated from equation A-22 to A-29. This assumption will have to be checked after the facility is constructed, but it seems reasonable since as the measurement uncertainty decreases, both the uncertainty in the components and the mass ratio decreases. But as it drops below this level the entire term can be ignored. likewise, as the measurement uncertainty increases, the uncertainty in the components also increase, but we have estimated a maximum value for a very high uncertainty and this level is still at the point where it can be neglected, so in this case the mass ratio will dominate. As result we can combine equation A-32 with the previous results to find for a real gas that:

$$\frac{\Delta Z_m}{Z_m} = \left[\frac{1}{303.7^2} \left[\left[\frac{\Delta P}{P} \right]^2 + \left[\frac{\Delta T}{T} \right]^2 \right] \right]^{\frac{1}{2}}$$

(A-34)

$$\frac{\Delta Cp_m}{Cp_m} = \left[\left[\left[\frac{\Delta P}{P} \right]^2 + \left[\frac{\Delta T}{T} \right]^2 \right] \left[\frac{1}{-103.25} \right]^2 \right]^{\frac{1}{2}}$$

(A-35)

$$\frac{\Delta Cv_m}{Cv_m} = \left[\left[\left[\frac{\Delta P}{P} \right]^2 + \left[\frac{\Delta T}{T} \right]^2 \right] \left[\frac{1}{28} \right]^2 \right]^{\frac{1}{2}}$$

(A-36)

$$\frac{\Delta \gamma}{\gamma} = \left[\left[\left[\frac{\Delta P}{P} \right]^2 + \left[\frac{\Delta T}{T} \right]^2 \right] \left[\frac{1}{-22} \right]^2 \right]^{\frac{1}{2}}$$

(A-37)

Examples of Mixture Behavior During an Isentropic Blowdown:

As shown in section five, the ATARR non-dimensional time $(Tc=1+t/\tau)$ is the primary parameter that should be used to characterize the mixture behavior because the accuracy in efficiency depends directly on it. In actuality as shown in this section , the mixture properties depend on the temperature and pressure. Using equations 5-11 (repeated below) the temperature and pressure at any point in an isentropic process can be related to the variable Tc by:

$$\frac{T(t)}{T(0)} = [\, Tc]^{-2}$$

$$\frac{P(t)}{P(0)} = [\, Tc]^{-\frac{2}{C2}}$$

(A-38 a,b)

In the ideal case C2 becomes $(\gamma-1)/\gamma$ (see appendix C for more details). Figure A-22 shows the relationship between the temperature ratio and the variable Tc and figure A-23 shows the ideal

gas isentropic pressure decay as a function of γ and Tc. Using the data in table A-4 and the relationship between temperature and Tc in equation A-38(a), the the mixture γ can be plotted as a function of pressure level and Tc (Figure A-24). This figure also shows the variation from the initial starting value of γ on the right-hand axis (one can see that the variation is significant). An interesting observation of figure A-24 is that as Tc increases, γ also increases. But as the pressure level decreases, γ decreases at any given value of Tc. From figure A-23 we see that the pressure decay with Tc is dramatic, so their exists a possibility that if one could use equation A-38(b) to iteratively solve for the pressure decay as a function of Tc one could obtain the trace of the mixture γ as only a function of Tc.

This procedure was done in an iterative process for an ideal gas:

1) Select a value for the temperature ratio

2) Find the corresponding value in Tc from equation A-38(a)

3) From table A-4 find the corresponding γ at 7 atm

4) Use this value of γ to predict the pressure ratio for the selected value of Tc from equation A-38(b)

5) Use the resulting pressure ratio to interpolate between the various pressure levels in table A-4 (either 7 atm and 4 atm or 4 atm and 1 atm (depending on the situation) to determine a new value of γ.

6) Repeat steps four and five until there is no significant variation in the answer for γ. This is the value of γ at this value of Tc (and also the pressure ratio) and a new value of Tc can be selected using step 1 and repeating the entire process.

The results are shown in figure A-25 (data in table A-7). One can see that even taking into account the pressure decrease the variation in γ can be significant.

Table A-1
Nitrogen Gas Properties

Temperature °K	Real Gas Properties									Ideal Gas	
	Specific Heat Ratio			Cp (KJ/Kg K)			Cv (KJ/Kg K)			Cp (KJ/Kg K)	Cv
	1 atm	4 atm	7 atm	1 atm	4 atm	7 atm	1 atm	4 atm	7 atm		
150	1.409	1.437	1.468	1.0473	1.0744	1.1053	0.7433	0.7477	0.7530	Bolds are interpolation	
160	1.407	1.431	1.457	1.0460	1.0686	1.0934	0.7434	0.7468	0.7504	1.0390	0.7422
170	1.406	1.427	1.451	1.0450	1.0642	1.0847	0.7432	0.7457	0.7476	**1.0390**	**0.7422**
180	1.406	1.423	1.442	1.0442	1.0607	1.0781	0.7427	0.7454	0.7476	1.0390	0.7422
190	1.405	1.420	1.436	1.0436	1.0579	1.0729	0.7428	0.7450	0.7471	**1.0390**	**0.7422**
200	1.404	1.418	1.432	1.0430	1.0556	1.0687	0.7429	0.7444	0.7463	1.0390	0.7423
210	1.404	1.416	1.429	1.0426	1.0537	1.0652	0.7426	0.7442	0.7454	**1.0391**	**0.7423**
220	1.403	1.414	1.425	1.0423	1.0522	1.0624	0.7429	0.7441	0.7455	**1.0391**	**0.7423**
230	1.403	1.413	1.423	1.0419	1.0508	1.0599	0.7426	0.7437	0.7448	**1.0391**	**0.7423**
240	1.403	1.412	1.421	1.0417	1.0497	1.0579	0.7425	0.7434	0.7445	**1.0391**	**0.7424**
250	1.402	1.410	1.419	1.0415	1.0488	1.0562	0.7429	0.7438	0.7443	1.0391	0.7424
260	1.402	1.409	1.417	1.0414	1.0480	1.0547	0.7428	0.7438	0.7443	1.0393	**0.7425**
270	1.402	1.409	1.415	1.0412	1.0473	1.0534	0.7427	0.7433	0.7445	1.0394	0.7426
280	1.402	1.408	1.414	1.0412	1.0468	1.0524	0.7426	0.7434	0.7442	1.0395	**0.7427**
290	1.401	1.407	1.413	1.0411	1.0463	1.0515	0.7431	0.7436	0.7441	**1.0396**	**0.7428**
300	1.401	1.407	1.412	1.0412	1.0459	1.0507	0.7432	0.7434	0.7441	1.0397	0.7429
310	1.401	1.406	1.411	1.0412	1.0457	1.0500	0.7432	0.7437	0.7442	**1.0400**	0.7432
320	1.401	1.405	1.410	1.0414	1.0454	1.0495	0.7433	0.7441	0.7444	**1.0403**	0.7435
330	1.401	1.405	1.409	1.0416	1.0454	1.0492	0.7437	0.7443	0.7446	**1.0406**	0.7438
340	1.400	1.404	1.408	1.0418	1.0454	1.0489	0.7442	0.7446	0.7450	**1.0409**	**0.7440**
350	1.400	1.404	1.407	1.0421	1.0454	1.0488	0.7444	0.7449	0.7454	1.0411	0.7443
360	1.400	1.403	1.406	1.0425	1.0457	1.0488	0.7447	0.7453	0.7459	**1.0430**	**0.7449**
370	1.400	1.403	1.406	1.0430	1.0459	1.0488	0.7453	0.7458	0.7462	**1.0449**	**0.7455**
380	1.399	1.402	1.405	1.0435	1.0463	1.0490	0.7459	0.7463	0.7466	**1.0468**	**0.7461**
390	1.399	1.402	1.404	1.0441	1.0468	1.0493	0.7466	0.7469	0.7474	**1.0487**	**0.7467**
400	1.398	1.401	1.403	1.0449	1.0473	1.0497	0.7474	0.7475	0.7482	1.0505	0.7473
410	1.398	1.400	1.403	1.0456	1.0479	1.0502	0.7482	0.7485	0.7488	**1.0502**	**0.7483**
420	1.397	1.399	1.402	1.0465	1.0487	1.0508	0.7491	0.7496	0.7495	**1.0499**	**0.7493**
430	1.397	1.399	1.401	1.0474	1.0495	1.0516	0.7500	0.7505	0.7506	**1.0496**	**0.7503**
440	1.396	1.398	1.400	1.0484	1.0504	1.0524	0.7510	0.7514	0.7517	**1.0493**	**0.7512**
450	1.396	1.397	1.399	1.0495	1.0514	1.0533	0.7521	0.7526	0.7529	1.0490	0.7522
460	1.395	1.396	1.398	1.0508	1.0526	1.0543	0.7532	0.7540	0.7542	**1.0504**	**0.7536**
470	1.394	1.396	1.398	1.0520	1.0538	1.0554	0.7547	0.7551	0.7552	**1.0518**	**0.7550**
480	1.393	1.395	1.397	1.0534	1.0550	1.0566	0.7562	0.7563	0.7563	**1.0532**	**0.7564**
490	1.392	1.394	1.396	1.0548	1.0564	1.0579	0.7578	0.7578	0.7578	**1.0546**	**0.7578**
500	1.391	1.393	1.395	1.0564	1.0579	1.0593	0.7594	0.7594	0.7594	1.0560	0.7591
510	1.391	1.392	1.394	1.0579	1.0594	1.0608	0.7608	0.7610	0.7609	**1.0577**	**0.7609**
520	1.390	1.391	1.393	1.0596	1.0609	1.0623	0.7623	0.7627	0.7626	**1.0594**	**0.7626**
530	1.389	1.390	1.392	1.0613	1.0626	1.0639	0.7641	0.7645	0.7646	**1.0612**	**0.7644**
540	1.388	1.389	1.390	1.0631	1.0644	1.0656	0.7659	0.7663	0.7666	**1.0629**	**0.7661**
550	1.387	1.388	1.389	1.0649	1.0662	1.0673	0.7678	0.7681	0.7684	1.0647	0.7679
560	1.386	1.387	1.388	1.0669	1.0680	1.0692	0.7697	0.7700	0.7703	**1.0667**	**0.7699**
570	1.385	1.386	1.387	1.0688	1.0700	1.0710	0.7717	0.7720	0.7722	**1.0687**	**0.7720**
580	1.384	1.385	1.386	1.0709	1.0719	1.0730	0.7738	0.7740	0.7742	**1.0708**	**0.7740**
590	1.383	1.384	1.385	1.0730	1.0740	1.0750	0.7758	0.7760	0.7762	**1.0728**	**0.7760**
600	1.382	1.383	1.384	1.0751	1.0760	1.0771	0.7779	0.7781	0.7782	1.0748	0.7781

Table A-1(Con't)
Carbon Dioxide Gas Properties

Temperature °K	Real Gas Properties									Ideal Gas	
	Specific Heat Ratio			Cp (KJ/Kg K)			Cv (KJ/Kg K)			Cp	Cv
	1 atm	4 atm	7 atm	1 atm	4 atm	7 atm	1 atm	4 atm	7 atm	(KJ/Kg K)	
										Bolds are interpolation	
230	1.340	1.385	1.451	0.7889	0.9110	1.2695	0.5888	0.6577	0.8749	**0.7689**	**0.5800**
240	1.332	1.367	1.403	0.7967	0.8705	1.0421	0.5981	0.6368	0.7428	**0.7802**	**0.5913**
250	1.324	1.356	1.387	0.8052	0.8547	0.9395	0.6081	0.6303	0.6774	0.7914	0.6025
260	1.317	1.345	1.374	0.8144	0.8518	0.8998	0.6184	0.6333	0.6549	**0.8023**	**0.6133**
270	1.311	1.336	1.365	0.8239	0.8537	0.8836	0.6284	0.6390	0.6473	**0.8131**	**0.6242**
280	1.304	1.327	1.352	0.8333	0.8600	0.8868	0.6391	0.6481	0.6559	**0.8240**	**0.6350**
290	1.299	1.319	1.341	0.8430	0.8666	0.8908	0.6489	0.6570	0.6643	**0.8348**	**0.6459**
300	1.293	1.311	1.331	0.8526	0.8736	0.8953	0.6594	0.6663	0.6726	**0.8457**	0.6567
310	1.288	1.304	1.321	0.8620	0.8806	0.9002	0.6693	0.6753	0.6815	**0.8555**	**0.6666**
320	1.284	1.298	1.313	0.8715	0.8883	0.9055	0.6787	0.6844	0.6896	**0.8654**	**0.6765**
330	1.279	1.292	1.306	0.8807	0.8959	0.9112	0.6886	0.6934	0.6977	**0.8752**	**0.6863**
340	1.275	1.287	1.299	0.8900	0.9036	0.9174	0.6980	0.7021	0.7062	**0.8851**	0.6962
350	1.271	1.282	1.293	0.8989	0.9114	0.9240	0.7072	0.7109	0.7146	0.8949	0.7060
360	1.267	1.277	1.287	0.9078	0.9191	0.9306	0.7165	0.7197	0.7231	0.9038	**0.7148**
370	1.264	1.273	1.282	0.9165	0.9268	0.9374	0.7250	0.7281	0.7312	0.9126	**0.7237**
380	1.260	1.269	1.277	0.9250	0.9346	0.9442	0.7341	0.7365	0.7394	**0.9214**	**0.7325**
390	1.257	1.265	1.273	0.9335	0.9421	0.9510	0.7426	0.7448	0.7471	**0.9302**	**0.7413**
400	1.254	1.261	1.268	0.9416	0.9497	0.9578	0.7509	0.7531	0.7554	0.9390	0.7501
410	1.251	1.258	1.265	0.9497	0.9571	0.9648	0.7592	0.7608	0.7627	**0.9469**	**0.7580**
420	1.248	1.254	1.261	0.9575	0.9644	0.9714	0.7672	0.7691	0.7704	**0.9548**	**0.7659**
430	1.246	1.251	1.257	0.9652	0.9716	0.9782	0.7746	0.7767	0.7782	**0.9627**	**0.7738**
440	1.243	1.248	1.254	0.9728	0.9788	0.9850	0.7826	0.7843	0.7855	**0.9706**	**0.7817**
450	1.241	1.246	1.251	0.9803	0.9858	0.9916	0.7899	0.7912	0.7927	0.9785	0.7896
460	1.239	1.243	1.248	0.9875	0.9928	0.9981	0.7970	0.7987	0.7997	0.9856	**0.7966**
470	1.236	1.241	1.245	0.9947	0.9996	1.0045	0.8047	0.8055	0.8068	0.9927	**0.8037**
480	1.234	1.238	1.242	1.0017	1.0062	1.0109	0.8117	0.8128	0.8139	0.9998	**0.8108**
490	1.232	1.236	1.240	1.0085	1.0128	1.0173	0.8186	0.8194	0.8204	**1.0069**	**0.8179**
500	1.230	1.234	1.237	1.0153	1.0194	1.0236	0.8254	0.8261	0.8275	1.0140	0.8250
510	1.228	1.232	1.235	1.0219	1.0257	1.0296	0.8321	0.8325	0.8337	**1.0204**	**0.8315**
520	1.226	1.230	1.233	1.0283	1.0321	1.0357	0.8387	0.8391	0.8400	**1.0268**	**0.8379**
530	1.225	1.228	1.231	1.0347	1.0381	1.0417	0.8447	0.8454	0.8462	**1.0332**	**0.8443**
540	1.223	1.226	1.229	1.0410	1.0442	1.0476	0.8511	0.8517	0.8524	**1.0397**	0.8507
550	1.221	1.224	1.227	1.0470	1.0502	1.0532	0.8575	0.8580	0.8584	1.0461	0.8571
560	1.220	1.222	1.225	1.0530	1.0561	1.0591	0.8632	0.8642	0.8646	1.0519	0.8630
570	1.218	1.221	1.223	1.0589	1.0617	1.0646	0.8694	0.8696	0.8705	1.0577	0.8688
580	1.217	1.219	1.221	1.0648	1.0674	1.0700	0.8749	0.8756	0.8764	1.0636	0.8747
590	1.215	1.217	1.220	1.0704	1.0731	1.0755	0.8810	0.8817	0.8816	1.0694	0.8805
600	1.214	1.216	1.218	1.0761	1.0784	1.0808	0.8864	0.8868	0.8874	1.0752	0.8863

Table A-2
Compressibility Factors (Z) for
Nitrogen and Carbon Dioxide

Temperature °K	N2			CO2		
	1 atm	4 atm	7 atm	1 atm	4 atm	7 atm
230	0.99881	0.99525	0.99174	0.98790	0.94950	0.90320
240	0.99902	0.99613	0.99328	0.98950	0.95720	0.92190
250	0.99921	0.99688	0.99459	0.99085	0.96290	0.93370
260	0.99937	0.99751	0.99570	0.99197	0.96750	0.94230
270	0.99951	0.99807	0.99666	0.99291	0.97130	0.94920
280	0.99963	0.99854	0.99749	0.99372	0.97460	0.95500
290	0.99973	0.99895	0.99820	0.99441	0.97740	0.96000
300	0.99982	0.99930	0.99882	0.99501	0.97980	0.96440
310	0.99990	0.99961	0.99936	0.99553	0.98190	0.96810
320	0.99996	0.99988	0.99983	0.99598	0.98380	0.97140
330	1.00002	1.00012	1.00024	0.99638	0.98540	0.97430
340	1.00007	1.00032	1.00060	0.99673	0.98680	0.97680
350	1.00012	1.00050	1.00092	0.99705	0.98812	0.97900
360	1.00016	1.00066	1.00119	0.99732	0.98925	0.98100
370	1.00020	1.00081	1.00144	0.99757	0.99025	0.98280
380	1.00023	1.00093	1.00165	0.99779	0.99114	0.98440
390	1.00026	1.00104	1.00184	0.99799	0.99194	0.98580
400	1.00028	1.00113	1.00201	0.99817	0.99267	0.98714
410	1.00030	1.00122	1.00216	0.99833	0.99333	0.98830
420	1.00032	1.00130	1.00229	0.99848	0.99392	0.98934
430	1.00034	1.00136	1.00240	0.99861	0.99446	0.99029
440	1.00035	1.00142	1.00251	0.99873	0.99495	0.99115
450	1.00036	1.00147	1.00259	0.99885	0.99539	0.99193
460	1.00038	1.00151	1.00266	0.99895	0.99580	0.99265
470	1.00039	1.00155	1.00273	0.99904	0.99617	0.99330
480	1.00039	1.00159	1.00279	0.99912	0.99651	0.99390
490	1.00040	1.00161	1.00284	0.99920	0.99682	0.99445
500	1.00041	1.00164	1.00289	0.99927	0.99711	0.99496
510	1.00041	1.00167	1.00293	0.99934	0.99737	0.99542
520	1.00042	1.00168	1.00295	0.99940	0.99762	0.99585
530	1.00042	1.00170	1.00298	0.99946	0.99784	0.99625
540	1.00043	1.00171	1.00301	0.99951	0.99805	0.99661
550	1.00043	1.00172	1.00303	0.99956	0.99825	0.99695
560	1.00043	1.00173	1.00304	0.99960	0.99843	0.99727
570	1.00043	1.00174	1.00305	0.99964	0.99859	0.99756
580	1.00043	1.00174	1.00306	0.99968	0.99875	0.99783
590	1.00044	1.00174	1.00306	0.99972	0.99889	0.99808
600	1.00044	1.00174	1.00306	0.99975	0.99903	0.99832

Table A-3
Compressibility Factor (Z) for
Standard Nitrogen and Carbon Dioxide Mixture

	R2/R1 =	0.6366
	M2/M1 (real)=	3.24
	M2/M1 (Ideal)=	2.59

Temperature °K	Real			Ideal		
	1 atm	4 atm	7 atm	1 atm	4 atm	7 atm
230	0.99146	0.96444	0.93211	0.99202	0.96677	0.93663
240	0.99261	0.96991	0.94521	0.99309	0.97190	0.94885
250	0.99358	0.97400	0.95358	0.99401	0.97573	0.95669
260	0.99439	0.97730	0.95974	0.99476	0.97883	0.96246
270	0.99507	0.98004	0.96470	0.99540	0.98141	0.96712
280	0.99565	0.98242	0.96887	0.99595	0.98364	0.97104
290	0.99615	0.98444	0.97247	0.99642	0.98554	0.97442
300	0.99658	0.98617	0.97564	0.99683	0.98716	0.97739
310	0.99696	0.98768	0.97831	0.99718	0.98859	0.97990
320	0.99728	0.98905	0.98068	0.99748	0.98987	0.98213
330	0.99757	0.99021	0.98277	0.99775	0.99096	0.98409
340	0.99782	0.99121	0.98457	0.99799	0.99190	0.98579
350	0.99805	0.99216	0.98616	0.99821	0.99279	0.98728
360	0.99825	0.99298	0.98759	0.99839	0.99356	0.98862
370	0.99843	0.99370	0.98889	0.99856	0.99424	0.98984
380	0.99859	0.99434	0.99003	0.99871	0.99484	0.99091
390	0.99873	0.99491	0.99104	0.99885	0.99538	0.99186
400	0.99886	0.99543	0.99200	0.99897	0.99586	0.99275
410	0.99897	0.99591	0.99283	0.99907	0.99631	0.99353
420	0.99908	0.99633	0.99357	0.99917	0.99671	0.99423
430	0.99917	0.99671	0.99424	0.99926	0.99706	0.99486
440	0.99926	0.99706	0.99486	0.99934	0.99739	0.99544
450	0.99934	0.99738	0.99541	0.99942	0.99769	0.99595
460	0.99942	0.99766	0.99592	0.99949	0.99796	0.99643
470	0.99948	0.99793	0.99638	0.99955	0.99820	0.99686
480	0.99953	0.99817	0.99680	0.99960	0.99843	0.99726
490	0.99959	0.99838	0.99719	0.99965	0.99863	0.99762
500	0.99964	0.99859	0.99755	0.99970	0.99882	0.99795
510	0.99969	0.99877	0.99787	0.99974	0.99899	0.99826
520	0.99973	0.99895	0.99817	0.99979	0.99915	0.99853
530	0.99977	0.99910	0.99845	0.99982	0.99930	0.99879
540	0.99981	0.99925	0.99870	0.99986	0.99943	0.99903
550	0.99984	0.99938	0.99894	0.99989	0.99956	0.99925
560	0.99987	0.99951	0.99915	0.99991	0.99968	0.99945
570	0.99990	0.99962	0.99935	0.99994	0.99978	0.99963
580	0.99992	0.99973	0.99954	0.99996	0.99988	0.99980
590	0.99996	0.99982	0.99971	0.99999	0.99997	0.99996
600	0.99998	0.99991	0.99987	1.00001	1.00005	1.00011

Table A-3 (Con't)
Compressibility Factor (Z) Variation (in %)
Standard Nitrogen and Carbon Dioxide Mixture

Temperature °K	Between Real and Ideal			Due to Pressure
	1 atm	4 atm	7 atm	Real
230	0.05613	0.24197	0.48452	6.36750
240	0.04892	0.20474	0.38521	5.01492
250	0.04292	0.17796	0.32571	4.19448
260	0.03796	0.15663	0.28381	3.61037
270	0.03383	0.13933	0.25095	3.14797
280	0.03028	0.12430	0.22370	2.76360
290	0.02724	0.11166	0.20037	2.43441
300	0.02462	0.10086	0.17996	2.14646
310	0.02236	0.09146	0.16299	1.90634
320	0.02036	0.08293	0.14787	1.69235
330	0.01861	0.07583	0.13464	1.50580
340	0.01707	0.06957	0.12330	1.34570
350	0.01569	0.06365	0.11338	1.20620
360	0.01451	0.05861	0.10428	1.07887
370	0.01344	0.05421	0.09615	0.96496
380	0.01246	0.05022	0.08888	0.86403
390	0.01159	0.04666	0.08256	0.77634
400	0.01078	0.04335	0.07646	0.69190
410	0.01006	0.04041	0.07121	0.61921
420	0.00939	0.03778	0.06648	0.55480
430	0.00883	0.03531	0.06213	0.49592
440	0.00827	0.03310	0.05825	0.44224
450	0.00771	0.03109	0.05463	0.39505
460	0.00730	0.02919	0.05127	0.35128
470	0.00689	0.02750	0.04828	0.31130
480	0.00648	0.02596	0.04549	0.27407
490	0.00612	0.02447	0.04292	0.24091
500	0.00582	0.02314	0.04055	0.20981
510	0.00546	0.02196	0.03839	0.18211
520	0.00520	0.02073	0.03628	0.15676
530	0.00490	0.01971	0.03438	0.13280
540	0.00469	0.01868	0.03269	0.11121
550	0.00444	0.01771	0.03105	0.09098
560	0.00423	0.01684	0.02946	0.07176
570	0.00403	0.01607	0.02802	0.05457
580	0.00383	0.01526	0.02669	0.03874
590	0.00367	0.01454	0.02541	0.02491
600	0.00352	0.01382	0.02418	0.01076

Table A-4
Mixture Gas Properties

Temperature °K	Specific Heat Ratio			Cp (KJ/Kg K)			Cv (KJ/Kg K)			Ideal Gas M2/M1 = 2.59		
	Real Gas Properties M2/M1 = 3.24									Cp	Cv	γ
	1 atm	4 atm	7 atm	1 atm	4 atm	7 atm	1 atm	4 atm	7 atm	(KJ/Kg K)		
230	1.358	1.392	1.445	0.8486	0.9440	1.2201	0.6250	0.6780	0.8443	0.8442	0.6252	1.350
240	1.352	1.379	1.407	0.8545	0.9128	1.0458	0.6322	0.6620	0.7432	0.8523	0.6334	1.346
250	1.345	1.370	1.395	0.8609	0.9005	0.9670	0.6399	0.6571	0.6932	0.8604	0.6415	1.341
260	1.340	1.362	1.385	0.8680	0.8981	0.9364	0.6477	0.6594	0.6760	0.8683	0.6493	1.337
270	1.335	1.355	1.378	0.8751	0.8994	0.9236	0.6554	0.6636	0.6702	0.8761	0.6572	1.333
280	1.330	1.348	1.368	0.8823	0.9040	0.9258	0.6635	0.6705	0.6767	0.8840	0.6650	1.329
290	1.326	1.342	1.359	0.8897	0.9090	0.9287	0.6712	0.6774	0.6831	0.8919	0.6729	1.325
300	1.321	1.336	1.352	0.8971	0.9142	0.9319	0.6792	0.6845	0.6895	0.8997	0.6807	1.322
310	1.317	1.330	1.344	0.9043	0.9195	0.9355	0.6867	0.6914	0.6963	0.9069	0.6879	1.318
320	1.314	1.325	1.337	0.9116	0.9254	0.9395	0.6940	0.6985	0.7025	0.9141	0.6951	1.315
330	1.309	1.320	1.332	0.9187	0.9311	0.9437	0.7016	0.7054	0.7088	0.9213	0.7023	1.312
340	1.306	1.316	1.326	0.9258	0.9370	0.9484	0.7089	0.7121	0.7154	0.9285	0.7095	1.309
350	1.303	1.312	1.321	0.9327	0.9430	0.9534	0.7160	0.7189	0.7219	0.9357	0.7167	1.306
360	1.299	1.308	1.316	0.9396	0.9489	0.9585	0.7231	0.7258	0.7285	0.9425	0.7232	1.303
370	1.297	1.304	1.312	0.9463	0.9549	0.9637	0.7298	0.7322	0.7348	0.9494	0.7297	1.301
380	1.293	1.301	1.307	0.9529	0.9609	0.9689	0.7369	0.7388	0.7411	0.9563	0.7363	1.299
390	1.291	1.297	1.304	0.9596	0.9668	0.9742	0.7436	0.7453	0.7472	0.9632	0.7428	1.297
400	1.288	1.294	1.300	0.9659	0.9727	0.9795	0.7500	0.7518	0.7537	0.9701	0.7493	1.295
410	1.285	1.291	1.297	0.9723	0.9785	0.9850	0.7566	0.7579	0.7594	0.9757	0.7553	1.292
420	1.283	1.288	1.294	0.9784	0.9843	0.9902	0.7629	0.7645	0.7655	0.9813	0.7613	1.289
430	1.281	1.285	1.290	0.9846	0.9900	0.9955	0.7688	0.7705	0.7717	0.9869	0.7672	1.286
440	1.278	1.282	1.287	0.9906	0.9957	1.0009	0.7751	0.7765	0.7775	0.9925	0.7732	1.284
450	1.276	1.280	1.285	0.9966	1.0013	1.0062	0.7810	0.7821	0.7833	0.9981	0.7792	1.281
460	1.274	1.278	1.282	1.0024	1.0069	1.0113	0.7867	0.7882	0.7890	1.0036	0.7847	1.279
470	1.271	1.276	1.279	1.0082	1.0124	1.0165	0.7929	0.7936	0.7947	1.0091	0.7902	1.277
480	1.270	1.273	1.277	1.0139	1.0177	1.0217	0.7986	0.7994	0.8004	1.0146	0.7957	1.275
490	1.268	1.271	1.275	1.0194	1.0231	1.0269	0.8042	0.8049	0.8057	1.0201	0.8012	1.273
500	1.266	1.269	1.272	1.0250	1.0285	1.0320	0.8099	0.8104	0.8114	1.0257	0.8067	1.271
510	1.264	1.267	1.270	1.0304	1.0336	1.0370	0.8153	0.8157	0.8165	1.0308	0.8118	1.270
520	1.262	1.265	1.268	1.0357	1.0389	1.0419	0.8207	0.8211	0.8217	1.0359	0.8169	1.268
530	1.261	1.263	1.266	1.0410	1.0439	1.0469	0.8257	0.8263	0.8270	1.0410	0.8220	1.266
540	1.259	1.261	1.264	1.0462	1.0489	1.0518	0.8310	0.8315	0.8321	1.0461	0.8272	1.265
550	1.257	1.260	1.262	1.0512	1.0540	1.0566	0.8363	0.8368	0.8372	1.0513	0.8323	1.263
560	1.256	1.258	1.260	1.0563	1.0589	1.0615	0.8411	0.8420	0.8423	1.0560	0.8371	1.262
570	1.254	1.256	1.258	1.0612	1.0637	1.0661	0.8463	0.8465	0.8473	1.0608	0.8418	1.260
580	1.253	1.255	1.256	1.0662	1.0685	1.0707	0.8510	0.8517	0.8523	1.0656	0.8466	1.259
590	1.251	1.253	1.255	1.0710	1.0733	1.0754	0.8562	0.8568	0.8567	1.0704	0.8514	1.257
600	1.250	1.252	1.253	1.0759	1.0778	1.0799	0.8608	0.8612	0.8616	1.0751	0.8562	1.256

Table A-4 (con't)
Mixture Gas Property Variation

Temp. °K	% Variation Between Real Gas and Ideal Gas Properties									Variation Due to Pressure Real Gas		
	Specific Heat Ratio			Cp (KJ/Kg K)			Cv (KJ/Kg K)			γ	Cp	Cv
	1 atm	4 atm	7 atm	1 atm	4 atm	7 atm	1 atm	4 atm	7 atm			
230	0.5510	3.1128	7.0329	0.5216	11.8174	44.5284	-0.0292	8.4419	35.0317	6.4464	43.7785	35.0712
240	0.4415	2.4665	4.5720	0.2526	7.0978	22.7032	-0.1881	4.5198	17.3386	4.1123	22.3941	17.5597
250	0.2984	2.1668	4.0072	0.0557	4.6517	12.3868	-0.2420	2.4322	8.0567	3.6978	12.3241	8.3188
260	0.2065	1.8545	3.5850	-0.0388	3.4337	7.8390	-0.2448	1.5504	4.1067	3.3716	7.8809	4.3622
270	0.1590	1.6565	3.3677	-0.1153	2.6519	5.4207	-0.2739	0.9792	1.9860	3.2036	5.5423	2.2661
280	0.0453	1.4228	2.9199	-0.1872	2.2643	4.7329	-0.2324	0.8298	1.7616	2.8733	4.9293	1.9986
290	0.0158	1.2339	2.5706	-0.2416	1.9175	4.1268	-0.2573	0.6753	1.5172	2.5544	4.3790	1.7791
300	-0.0608	1.0526	2.2654	-0.2935	1.6120	3.5825	-0.2329	0.5535	1.2879	2.3276	3.8874	1.5243
310	-0.1114	0.8772	1.9249	-0.2865	1.3885	3.1582	-0.1753	0.5069	1.2101	2.0386	3.4546	1.3878
320	-0.1111	0.7504	1.6898	-0.2773	1.2332	2.7761	-0.1664	0.4792	1.0682	1.8029	3.0618	1.2366
330	-0.1841	0.6256	1.5042	-0.2823	1.0677	2.4350	-0.0985	0.4394	0.9170	1.6914	2.7250	1.0164
340	-0.2049	0.5520	1.3100	-0.2866	0.9226	2.1489	-0.0818	0.3686	0.8280	1.5181	2.4425	0.9106
350	-0.2221	0.4720	1.1668	-0.3201	0.7820	1.8995	-0.0983	0.3086	0.7243	1.3919	2.2268	0.8234
360	-0.3040	0.3263	0.9571	-0.3178	0.6791	1.6914	-0.0139	0.3517	0.7273	1.2649	2.0156	0.7413
370	-0.3386	0.2357	0.8103	-0.3300	0.5793	1.5030	0.0086	0.3428	0.6871	1.1529	1.8391	0.6784
380	-0.4365	0.1410	0.6590	-0.3549	0.4830	1.3210	0.0819	0.3415	0.6576	1.1003	1.6819	0.5752
390	-0.4779	0.0428	0.5552	-0.3773	0.3761	1.1437	0.1011	0.3331	0.5853	1.0380	1.5268	0.4838
400	-0.5218	-0.0592	0.3870	-0.4270	0.2721	0.9719	0.0953	0.3315	0.5826	0.9136	1.4049	0.4868
410	-0.5133	-0.0561	0.4007	-0.3452	0.2878	0.9504	0.1690	0.3441	0.5475	0.9187	1.3001	0.3779
420	-0.5075	-0.1175	0.3504	-0.2901	0.3070	0.9034	0.2185	0.4250	0.5510	0.8623	1.1970	0.3319
430	-0.4438	-0.1129	0.2874	-0.2350	0.3127	0.8736	0.2097	0.4261	0.5845	0.7344	1.1112	0.3740
440	-0.4443	-0.1118	0.2823	-0.1922	0.3205	0.8470	0.2533	0.4327	0.5632	0.7299	1.0412	0.3091
450	-0.3863	-0.0597	0.2742	-0.1485	0.3158	0.8077	0.2387	0.3758	0.5320	0.6630	0.9576	0.2926
460	-0.3782	-0.1208	0.2150	-0.1212	0.3241	0.7680	0.2580	0.4454	0.5518	0.5955	0.8903	0.2931
470	-0.4427	-0.1134	0.1614	-0.0928	0.3194	0.7302	0.3515	0.4333	0.5678	0.6068	0.8237	0.2156
480	-0.4466	-0.1705	0.1053	-0.0776	0.3018	0.6948	0.3707	0.4731	0.5888	0.5544	0.7730	0.2173
490	-0.4519	-0.1749	0.1018	-0.0739	0.2879	0.6626	0.3798	0.4636	0.5602	0.5562	0.7370	0.1798
500	-0.4591	-0.1812	0.0337	-0.0682	0.2755	0.6186	0.3927	0.4576	0.5847	0.4951	0.6873	0.1913
510	-0.4703	-0.1989	0.0167	-0.0385	0.2742	0.6002	0.4338	0.4740	0.5834	0.4892	0.6390	0.1490
520	-0.4827	-0.2187	-0.0020	-0.0217	0.2881	0.5833	0.4632	0.5079	0.5853	0.4830	0.6051	0.1216
530	-0.4409	-0.2392	-0.0301	-0.0024	0.2768	0.5692	0.4405	0.5172	0.5994	0.4127	0.5716	0.1583
540	-0.4638	-0.2613	-0.0593	0.0036	0.2663	0.5422	0.4696	0.5290	0.6018	0.4063	0.5385	0.1316
550	-0.4878	-0.2850	-0.0819	-0.0028	0.2579	0.5036	0.4874	0.5445	0.5860	0.4079	0.5065	0.0981
560	-0.4574	-0.3178	-0.1144	0.0257	0.2703	0.5142	0.4853	0.5900	0.6294	0.3445	0.4884	0.1433
570	-0.4918	-0.2875	-0.1476	0.0411	0.2703	0.4982	0.5355	0.5595	0.6467	0.3459	0.4569	0.1106
580	-0.4632	-0.3225	-0.1820	0.0583	0.2716	0.4843	0.5239	0.5961	0.6674	0.2825	0.4257	0.1428
590	-0.4997	-0.3589	-0.1533	0.0625	0.2735	0.4718	0.5649	0.6347	0.6261	0.3480	0.4090	0.0694
600	-0.4730	-0.3313	-0.1899	0.0673	0.2499	0.4466	0.5428	0.5831	0.6377	0.2844	0.3791	0.0944

Variation in Nitrogen Gas Properties

Temp. °K	Specific Heat Ratio				Cp (KJ/Kg K)				Cv (KJ/Kg K)			
	Variation in Temp. (%/°K)			Var. In Press. %/psi 1-7 atm	Variation in Temp. (%/°K)			Var. In Press. %/psi 1-7 atm	Variation in Temp. (%/°K)			Var. In Press. %/psi 1-7 atm
	1 atm	4 atm	7 atm		1 atm	4 atm	7 atm		1 atm	4 atm	7 atm	
Col 1	Col 2	Col 3	Col 4	Col 5	Col 6	Col 7	Col 8	Col 9	Col 10	Col 11	Col 12	Col 13
150	0.0142	0.0419	0.0755	0.0465	0.0122	0.0542	0.1091	0.0616	0.0020	0.0122	0.0334	0.0145
160	0.0071	0.0280	0.0414	0.0395	0.0094	0.0418	0.0802	0.0504	0.0023	0.0138	0.0387	0.0105
170	0.0000	0.0281	0.0624	0.0356	0.0077	0.0330	0.0614	0.0422	0.0077	0.0049	0.0010	0.0065
180	0.0071	0.0211	0.0418	0.0284	0.0060	0.0264	0.0484	0.0361	0.0011	0.0052	0.0066	0.0074
190	0.0071	0.0141	0.0279	0.0245	0.0051	0.0216	0.0397	0.0312	0.0020	0.0075	0.0117	0.0066
200	0.0000	0.0141	0.0210	0.0222	0.0040	0.0177	0.0323	0.0273	0.0040	0.0036	0.0113	0.0050
210	0.0071	0.0141	0.0281	0.0198	0.0034	0.0149	0.0268	0.0241	0.0037	0.0008	0.0012	0.0042
220	0.0000	0.0071	0.0141	0.0174	0.0034	0.0127	0.0232	0.0214	0.0034	0.0056	0.0092	0.0039
230	0.0000	0.0071	0.0141	0.0158	0.0020	0.0102	0.0188	0.0192	0.0020	0.0031	0.0047	0.0033
240	0.0071	0.0142	0.0141	0.0143	0.0020	0.0091	0.0166	0.0173	0.0051	0.0051	0.0025	0.0030
250	0.0000	0.0071	0.0141	0.0135	0.0014	0.0076	0.0138	0.0156	0.0014	0.0005	0.0003	0.0021
260	0.0000	0.0000	0.0141	0.0119	0.0014	0.0068	0.0121	0.0142	0.0014	0.0068	0.0020	0.0023
270	0.0000	0.0071	0.0071	0.0103	0.0003	0.0051	0.0102	0.0130	0.0003	0.0020	0.0031	0.0027
280	0.0071	0.0071	0.0071	0.0095	0.0003	0.0045	0.0085	0.0119	0.0069	0.0026	0.0014	0.0024
290	0.0000	0.0000	0.0071	0.0095	0.0003	0.0034	0.0073	0.0110	0.0003	0.0034	0.0003	0.0015
300	0.0000	0.0071	0.0071	0.0087	0.0006	0.0026	0.0062	0.0102	0.0006	0.0046	0.0009	0.0014
310	0.0000	0.0071	0.0071	0.0079	0.0014	0.0020	0.0048	0.0094	0.0014	0.0051	0.0023	0.0015
320	0.0036	0.0036	0.0071	0.0071	0.0020	0.0009	0.0034	0.0087	0.0056	0.0027	0.0037	0.0016
330	0.0036	0.0036	0.0071	0.0067	0.0023	0.0000	0.0023	0.0081	0.0059	0.0036	0.0048	0.0014
340	0.0000	0.0036	0.0071	0.0063	0.0028	0.0009	0.0017	0.0076	0.0028	0.0044	0.0054	0.0012
350	0.0000	0.0036	0.0071	0.0056	0.0040	0.0020	0.0000	0.0071	0.0040	0.0056	0.0071	0.0015
360	0.0036	0.0036	0.0036	0.0048	0.0043	0.0026	0.0006	0.0066	0.0078	0.0061	0.0041	0.0019
370	0.0036	0.0036	0.0036	0.0048	0.0051	0.0034	0.0020	0.0062	0.0087	0.0070	0.0055	0.0015
380	0.0036	0.0036	0.0071	0.0048	0.0060	0.0045	0.0028	0.0059	0.0095	0.0081	0.0100	0.0011
390	0.0036	0.0036	0.0071	0.0044	0.0068	0.0051	0.0040	0.0055	0.0104	0.0087	0.0111	0.0012
400	0.0036	0.0071	0.0036	0.0040	0.0071	0.0060	0.0045	0.0052	0.0107	0.0131	0.0081	0.0012
410	0.0036	0.0071	0.0036	0.0040	0.0085	0.0074	0.0059	0.0049	0.0121	0.0145	0.0095	0.0009
420	0.0036	0.0036	0.0071	0.0040	0.0088	0.0079	0.0068	0.0046	0.0124	0.0115	0.0139	0.0007
430	0.0036	0.0036	0.0071	0.0036	0.0099	0.0088	0.0079	0.0044	0.0135	0.0123	0.0151	0.0008
440	0.0036	0.0072	0.0071	0.0032	0.0105	0.0096	0.0085	0.0042	0.0141	0.0168	0.0156	0.0010
450	0.0036	0.0072	0.0072	0.0028	0.0116	0.0107	0.0099	0.0040	0.0152	0.0179	0.0170	0.0012
460	0.0072	0.0036	0.0036	0.0024	0.0121	0.0113	0.0104	0.0038	0.0193	0.0149	0.0140	0.0014
470	0.0072	0.0036	0.0036	0.0028	0.0127	0.0118	0.0112	0.0036	0.0199	0.0154	0.0148	0.0008
480	0.0072	0.0072	0.0072	0.0032	0.0138	0.0132	0.0124	0.0034	0.0210	0.0204	0.0195	0.0002
490	0.0072	0.0072	0.0072	0.0032	0.0146	0.0138	0.0132	0.0033	0.0218	0.0210	0.0204	0.0001
500	0.0036	0.0072	0.0072	0.0032	0.0149	0.0143	0.0137	0.0031	0.0185	0.0215	0.0209	0.0001
510	0.0036	0.0072	0.0072	0.0028	0.0154	0.0148	0.0143	0.0030	0.0190	0.0220	0.0215	0.0002
520	0.0072	0.0072	0.0108	0.0024	0.0165	0.0159	0.0154	0.0028	0.0237	0.0232	0.0262	0.0004
530	0.0072	0.0072	0.0108	0.0020	0.0168	0.0162	0.0156	0.0027	0.0240	0.0234	0.0264	0.0007
540	0.0072	0.0072	0.0072	0.0016	0.0173	0.0170	0.0164	0.0026	0.0245	0.0242	0.0236	0.0010
550	0.0072	0.0072	0.0072	0.0016	0.0181	0.0175	0.0172	0.0025	0.0253	0.0248	0.0245	0.0009
560	0.0072	0.0072	0.0072	0.0016	0.0184	0.0181	0.0175	0.0024	0.0256	0.0253	0.0247	0.0008
570	0.0072	0.0072	0.0072	0.0016	0.0192	0.0186	0.0183	0.0023	0.0264	0.0258	0.0255	0.0007
580	0.0072	0.0072	0.0072	0.0016	0.0194	0.0188	0.0188	0.0022	0.0266	0.0261	0.0260	0.0006
590	0.0072	0.0072	0.0072	0.0016	0.0196	0.0193	0.0190	0.0021	0.0269	0.0266	0.0263	0.0005
600				0.0016				0.0021				0.0004

Variation in Carbon Dioxide Gas Properties

Temp. °K	Specific Heat Ratio				Cp (KJ/Kg K)				Cv (KJ/Kg K)			
	Variation in Temp. (%/°K)			Var. In Press. %/psi 1-7 atm	Variation in Temp. (%/°K)			Var. In Press. %/psi 1-7 atm	Variation in Temp. (%/°K)			Var. In Press. %/psi 1-7 atm
	1 atm	4 atm	7 atm		1 atm	4 atm	7 atm		1 atm	4 atm	7 atm	
Col 1	Col 2	Col 3	Col 4	Col 5	Col 6	Col 7	Col 8	Col 9	Col 10	Col 11	Col 12	Col 13
230	0.0601	0.1317	0.3421	0.0920	0.0982	0.4644	2.1827	0.6769	0.1588	0.3284	1.7797	0.5401
240	0.0604	0.0811	0.1154	0.0592	0.1067	0.1857	1.0919	0.3423	0.1678	0.1037	0.9654	0.2687
250	0.0532	0.0818	0.0946	0.0529	0.1150	0.0333	0.4409	0.1854	0.1687	0.0484	0.3430	0.1265
260	0.0458	0.0674	0.0659	0.0481	0.1160	0.0222	0.1839	0.1165	0.1623	0.0897	0.1172	0.0656
270	0.0537	0.0678	0.0962	0.0458	0.1147	0.0730	0.0363	0.0805	0.1689	0.1413	0.1329	0.0334
280	0.0385	0.0607	0.0820	0.0409	0.1156	0.0769	0.0447	0.0713	0.1546	0.1380	0.1271	0.0293
290	0.0464	0.0610	0.0751	0.0359	0.1143	0.0807	0.0509	0.0630	0.1612	0.1422	0.1264	0.0262
300	0.0388	0.0537	0.0757	0.0327	0.1108	0.0800	0.0549	0.0556	0.1500	0.1341	0.1310	0.0223
310	0.0312	0.0462	0.0609	0.0285	0.1096	0.0880	0.0588	0.0492	0.1411	0.1346	0.1200	0.0202
320	0.0391	0.0464	0.0536	0.0251	0.1062	0.0851	0.0626	0.0434	0.1457	0.1319	0.1165	0.0179
330	0.0314	0.0389	0.0539	0.0235	0.1051	0.0865	0.0684	0.0384	0.1368	0.1256	0.1227	0.0146
340	0.0315	0.0390	0.0464	0.0209	0.0998	0.0857	0.0721	0.0342	0.1316	0.1251	0.1188	0.0130
350	0.0316	0.0392	0.0466	0.0192	0.0988	0.0850	0.0716	0.0311	0.1307	0.1245	0.1185	0.0116
360	0.0237	0.0314	0.0390	0.0175	0.0957	0.0843	0.0731	0.0280	0.1197	0.1160	0.1124	0.0103
370	0.0317	0.0315	0.0392	0.0158	0.0928	0.0836	0.0726	0.0254	0.1248	0.1154	0.1120	0.0095
380	0.0239	0.0316	0.0314	0.0150	0.0919	0.0809	0.0720	0.0231	0.1160	0.1127	0.1037	0.0080
390	0.0239	0.0317	0.0394	0.0141	0.0870	0.0802	0.0715	0.0209	0.1112	0.1122	0.1112	0.0067
400	0.0240	0.0238	0.0237	0.0124	0.0863	0.0776	0.0730	0.0192	0.1105	0.1016	0.0969	0.0067
410	0.0240	0.0319	0.0317	0.0124	0.0816	0.0770	0.0685	0.0177	0.1058	0.1091	0.1005	0.0052
420	0.0161	0.0240	0.0318	0.0116	0.0809	0.0744	0.0700	0.0162	0.0971	0.0986	0.1021	0.0046
430	0.0241	0.0240	0.0239	0.0098	0.0783	0.0739	0.0695	0.0150	0.1026	0.0981	0.0936	0.0052
440	0.0161	0.0161	0.0240	0.0098	0.0777	0.0714	0.0671	0.0140	0.0939	0.0876	0.0913	0.0042
450	0.0161	0.0241	0.0240	0.0090	0.0732	0.0709	0.0648	0.0128	0.0895	0.0952	0.0890	0.0039
460	0.0243	0.0161	0.0241	0.0081	0.0727	0.0685	0.0644	0.0119	0.0971	0.0847	0.0886	0.0038
470	0.0162	0.0242	0.0242	0.0081	0.0703	0.0662	0.0639	0.0110	0.0866	0.0905	0.0883	0.0029
480	0.0162	0.0162	0.0161	0.0072	0.0679	0.0657	0.0635	0.0103	0.0842	0.0820	0.0798	0.0030
490	0.0163	0.0162	0.0243	0.0072	0.0674	0.0653	0.0613	0.0098	0.0838	0.0816	0.0857	0.0026
500	0.0163	0.0162	0.0162	0.0063	0.0651	0.0612	0.0591	0.0091	0.0815	0.0775	0.0754	0.0028
510	0.0163	0.0163	0.0162	0.0063	0.0629	0.0626	0.0587	0.0084	0.0793	0.0790	0.0750	0.0021
520	0.0082	0.0163	0.0162	0.0063	0.0625	0.0586	0.0584	0.0080	0.0707	0.0750	0.0747	0.0016
530	0.0164	0.0163	0.0163	0.0054	0.0603	0.0582	0.0562	0.0075	0.0767	0.0746	0.0726	0.0021
540	0.0164	0.0163	0.0163	0.0055	0.0581	0.0579	0.0541	0.0071	0.0746	0.0743	0.0705	0.0016
550	0.0082	0.0164	0.0163	0.0055	0.0577	0.0558	0.0556	0.0066	0.0660	0.0722	0.0720	0.0012
560	0.0164	0.0082	0.0164	0.0046	0.0556	0.0537	0.0517	0.0064	0.0721	0.0619	0.0682	0.0018
570	0.0082	0.0164	0.0164	0.0046	0.0553	0.0534	0.0515	0.0059	0.0636	0.0699	0.0679	0.0014
580	0.0165	0.0164	0.0082	0.0037	0.0532	0.0531	0.0512	0.0055	0.0698	0.0696	0.0594	0.0019
590	0.0082	0.0082	0.0164	0.0046	0.0529	0.0493	0.0492	0.0053	0.0612	0.0576	0.0657	0.0007
600				0.0037				0.0049				0.0012

Notes:
Col 2,3,4,6,7,8,10,11,12 are = (Max{X(i+1),X(i)}-Min)*100/(Min*10)
　　Where X is the individual property in question and the 10 corresponds to the temperature difference
　　between measurements i+1 and i
Col 5, 9 ,and 13 are = High P-Low P)*100/(Low P *90)
　　The 90 converts the difference in atm (6) to psi

Table A-6
Variation in Component Compressibility

	CO2				N2			
	Variation in Temperature (%/kK)			Var. In Press. (%/psi)	Variation in Temperature (%/kK)			Var. In Press. (%/psi)
Temp.	1 atm	4 atm	7 atm	1-7 atm	1 atm	4 atm	7 atm	1-7 atm
°K	Col 1	Col 2	Col 3	Col 4	Col 5	Col 6	Col 7	Col 8
230	0.0162	0.0811	0.2070	0.1042	0.0021	0.0088	0.0155	0.0079
240	0.0136	0.0595	0.1280	0.0815	0.0019	0.0075	0.0132	0.0064
250	0.0113	0.0478	0.0921	0.0680	0.0016	0.0063	0.0112	0.0052
260	0.0095	0.0393	0.0732	0.0586	0.0014	0.0056	0.0096	0.0041
270	0.0082	0.0340	0.0611	0.0512	0.0012	0.0047	0.0083	0.0032
280	0.0069	0.0287	0.0524	0.0450	0.0010	0.0041	0.0071	0.0024
290	0.0060	0.0246	0.0458	0.0398	0.0009	0.0035	0.0062	0.0017
300	0.0052	0.0214	0.0384	0.0353	0.0008	0.0031	0.0054	0.0011
310	0.0045	0.0194	0.0341	0.0315	0.0006	0.0027	0.0047	0.0006
320	0.0040	0.0163	0.0299	0.0281	0.0006	0.0024	0.0041	0.0001
330	0.0035	0.0142	0.0257	0.0252	0.0005	0.0020	0.0036	0.0002
340	0.0032	0.0134	0.0225	0.0227	0.0005	0.0018	0.0032	0.0006
350	0.0027	0.0114	0.0204	0.0205	0.0004	0.0016	0.0027	0.0009
360	0.0025	0.0101	0.0183	0.0185	0.0004	0.0015	0.0025	0.0011
370	0.0022	0.0090	0.0163	0.0167	0.0003	0.0012	0.0021	0.0014
380	0.0020	0.0081	0.0142	0.0151	0.0003	0.0011	0.0019	0.0016
390	0.0018	0.0074	0.0136	0.0137	0.0002	0.0009	0.0017	0.0018
400	0.0016	0.0066	0.0118	0.0124	0.0002	0.0009	0.0015	0.0019
410	0.0015	0.0059	0.0105	0.0113	0.0002	0.0008	0.0013	0.0021
420	0.0013	0.0054	0.0096	0.0103	0.0002	0.0006	0.0011	0.0022
430	0.0012	0.0049	0.0087	0.0093	0.0001	0.0006	0.0011	0.0023
440	0.0012	0.0044	0.0079	0.0085	0.0001	0.0005	0.0008	0.0024
450	0.0010	0.0041	0.0073	0.0078	0.0002	0.0004	0.0007	0.0025
460	0.0009	0.0037	0.0065	0.0071	0.0001	0.0004	0.0007	0.0025
470	0.0008	0.0034	0.0060	0.0064	0.0000	0.0004	0.0006	0.0026
480	0.0008	0.0031	0.0055	0.0058	0.0001	0.0002	0.0005	0.0027
490	0.0007	0.0029	0.0051	0.0053	0.0001	0.0003	0.0005	0.0027
500	0.0007	0.0026	0.0046	0.0048	0.0000	0.0003	0.0004	0.0028
510	0.0006	0.0025	0.0043	0.0044	0.0001	0.0001	0.0002	0.0028
520	0.0006	0.0022	0.0040	0.0040	0.0000	0.0002	0.0003	0.0028
530	0.0005	0.0021	0.0036	0.0036	0.0001	0.0001	0.0003	0.0028
540	0.0005	0.0020	0.0034	0.0032	0.0000	0.0001	0.0002	0.0029
550	0.0004	0.0018	0.0032	0.0029	0.0000	0.0001	0.0001	0.0029
560	0.0004	0.0016	0.0029	0.0026	0.0000	0.0001	0.0001	0.0029
570	0.0004	0.0016	0.0027	0.0023	0.0000	0.0000	0.0001	0.0029
580	0.0004	0.0014	0.0025	0.0021	0.0001	0.0000	0.0000	0.0029
590	0.0003	0.0014	0.0024	0.0018	0.0000	0.0000	0.0000	0.0029
600				0.0016				0.0029

Notes:

Col 1, 2, 3, 5, 6, and 7 are =(Max(X{i+1},X{i})-Min)*100/(Min*10)

    Where X is the compressibility and the 10 corresponds to the temp. difference between locations i+1 and i

Col 4 and 8 are = (High P- Low P)*100/(Low P *90)

    Where the 90 coverts the difference in atm (6) to psi

Temp. °K	Tr =[T(t)/T(0)]	Tc	Pr = [P(t)/P(0)]	γ	% Var. from Initial Conditions
		Table A-7 γ **as a Function of Tc**			
520.00	1.0000	1.0000	1.0000	1.2680	0.0000
510.00	0.98077	1.0098	0.91260	1.2694	0.11041
500.00	0.96154	1.0198	0.83190	1.2708	0.22082
490.00	0.94231	1.0302	0.75780	1.2726	0.36278
480.00	0.92308	1.0408	0.68920	1.2740	0.47319
470.00	0.90385	1.0518	0.62680	1.2762	0.64669
460.00	0.88462	1.0632	0.56870	1.2775	0.74921
450.00	0.86538	1.0750	0.51610	1.2797	0.92272
440.00	0.84615	1.0871	0.46690	1.2810	1.0252
430.00	0.82692	1.0997	0.42260	1.2831	1.1909
420.00	0.80769	1.1127	0.38160	1.2848	1.3249
410.00	0.78846	1.1262	0.34550	1.2880	1.5773
400.00	0.76923	1.1402	0.31150	1.2903	1.7587

Figure A-1

γ as a Function of Temperature and Pressure for Nitrogen
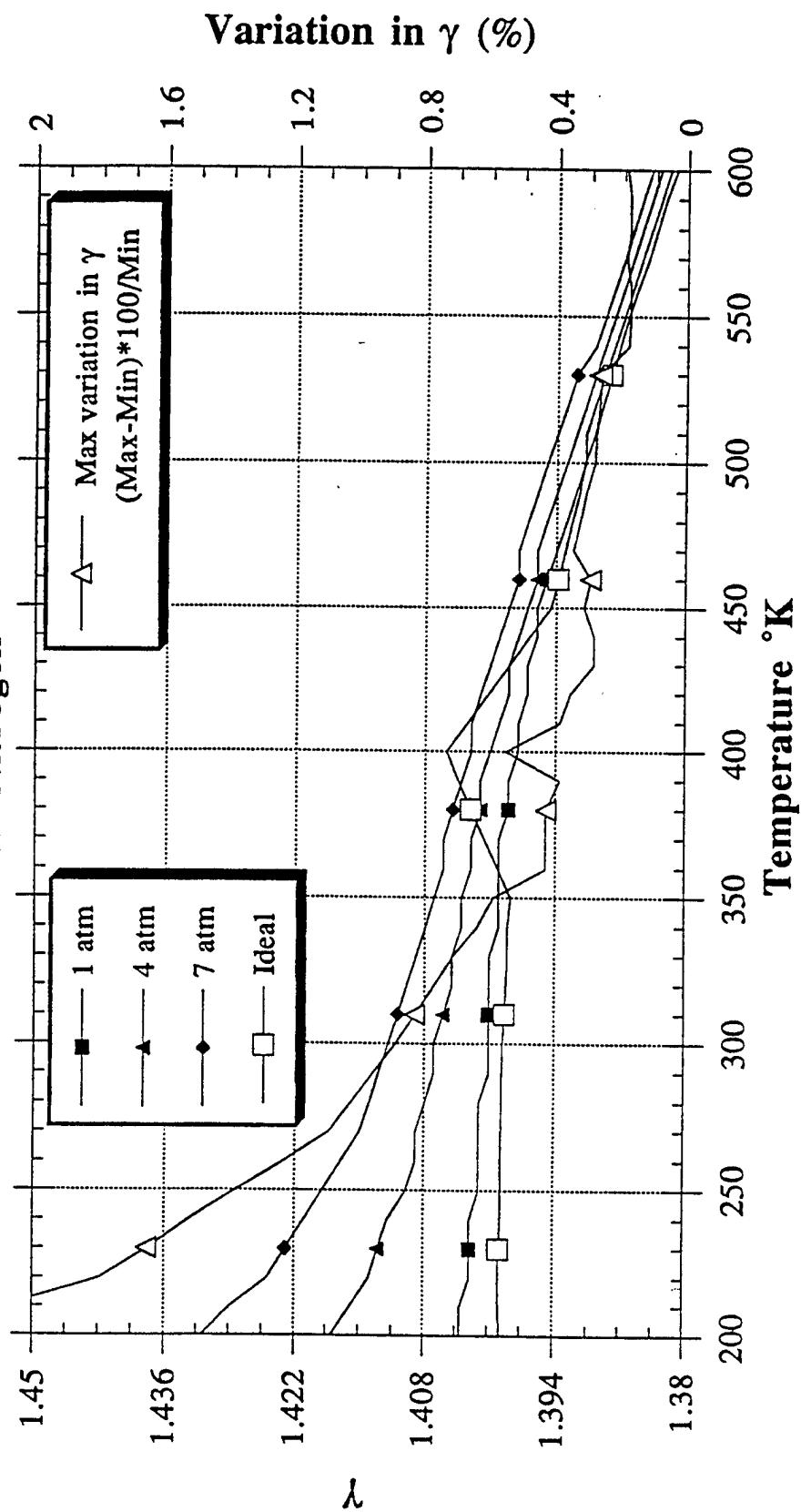
Figure A-2
C_p as a Function of Temperature and Pressure for Nitrogen
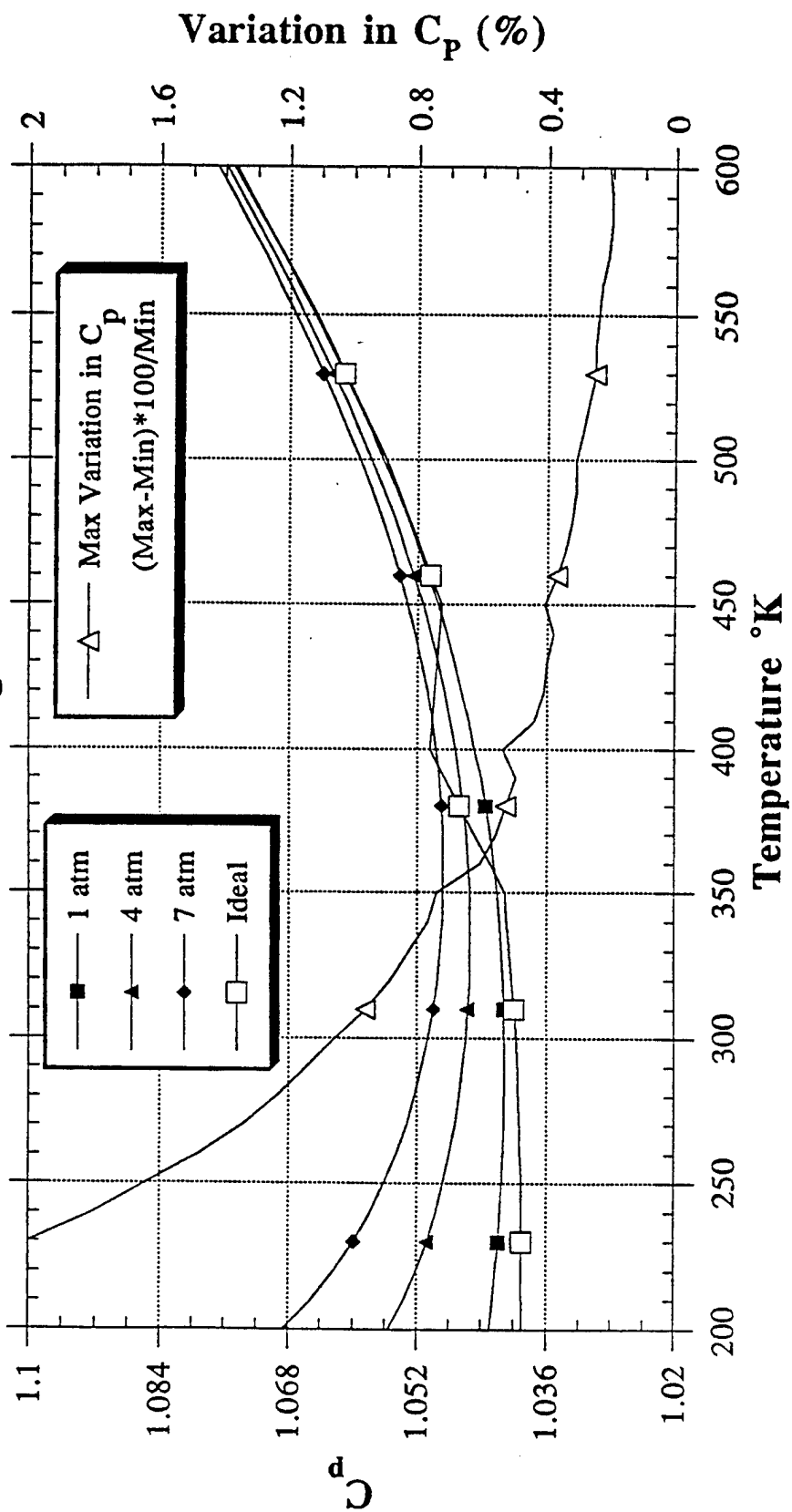
Figure A-3
C_v as a Function of Temperature and Pressure
for Nitrogen

100
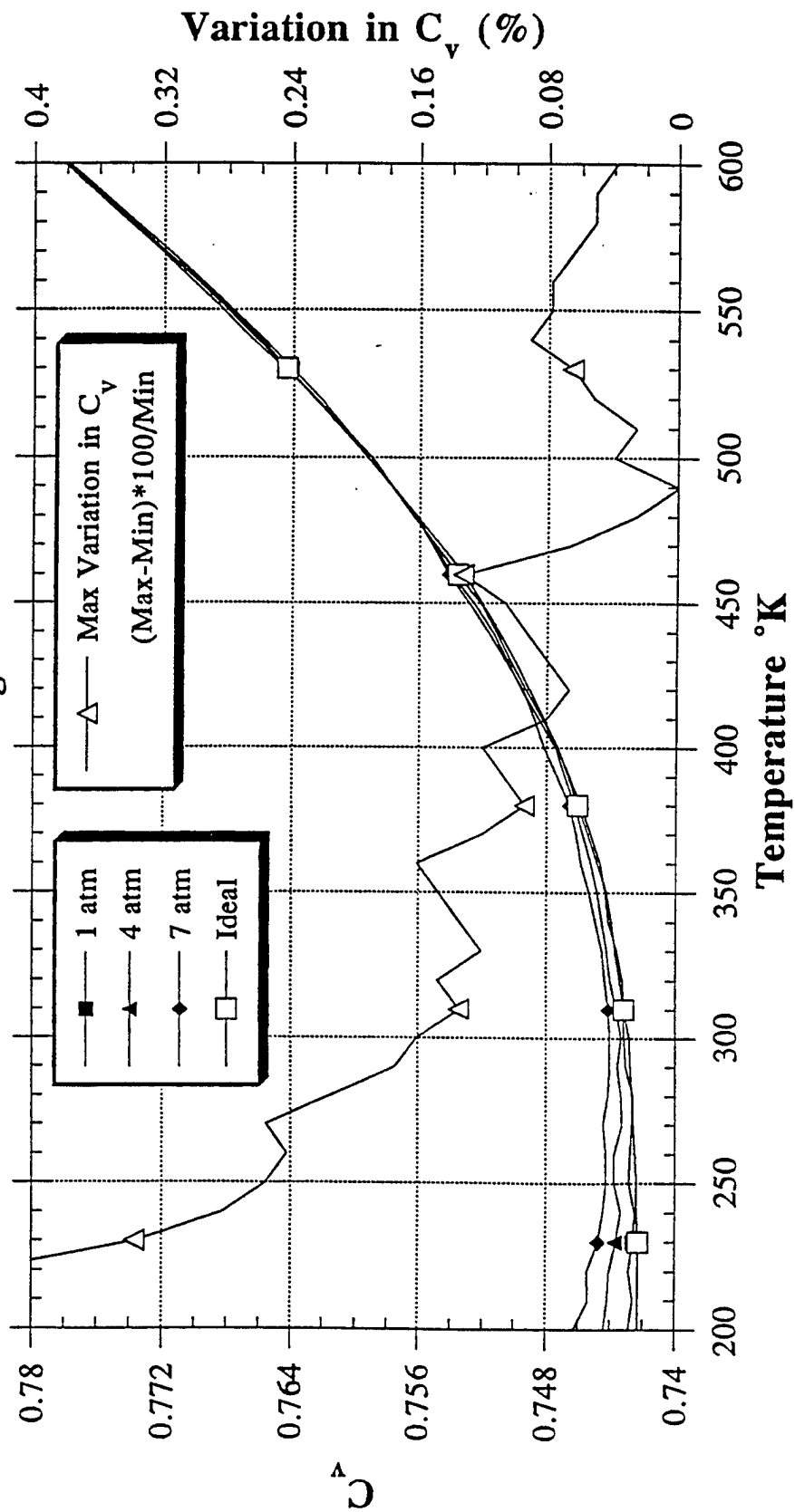
Figure A-4

γ as a Function of Temperature and Pressure
for Carbon Dioxide
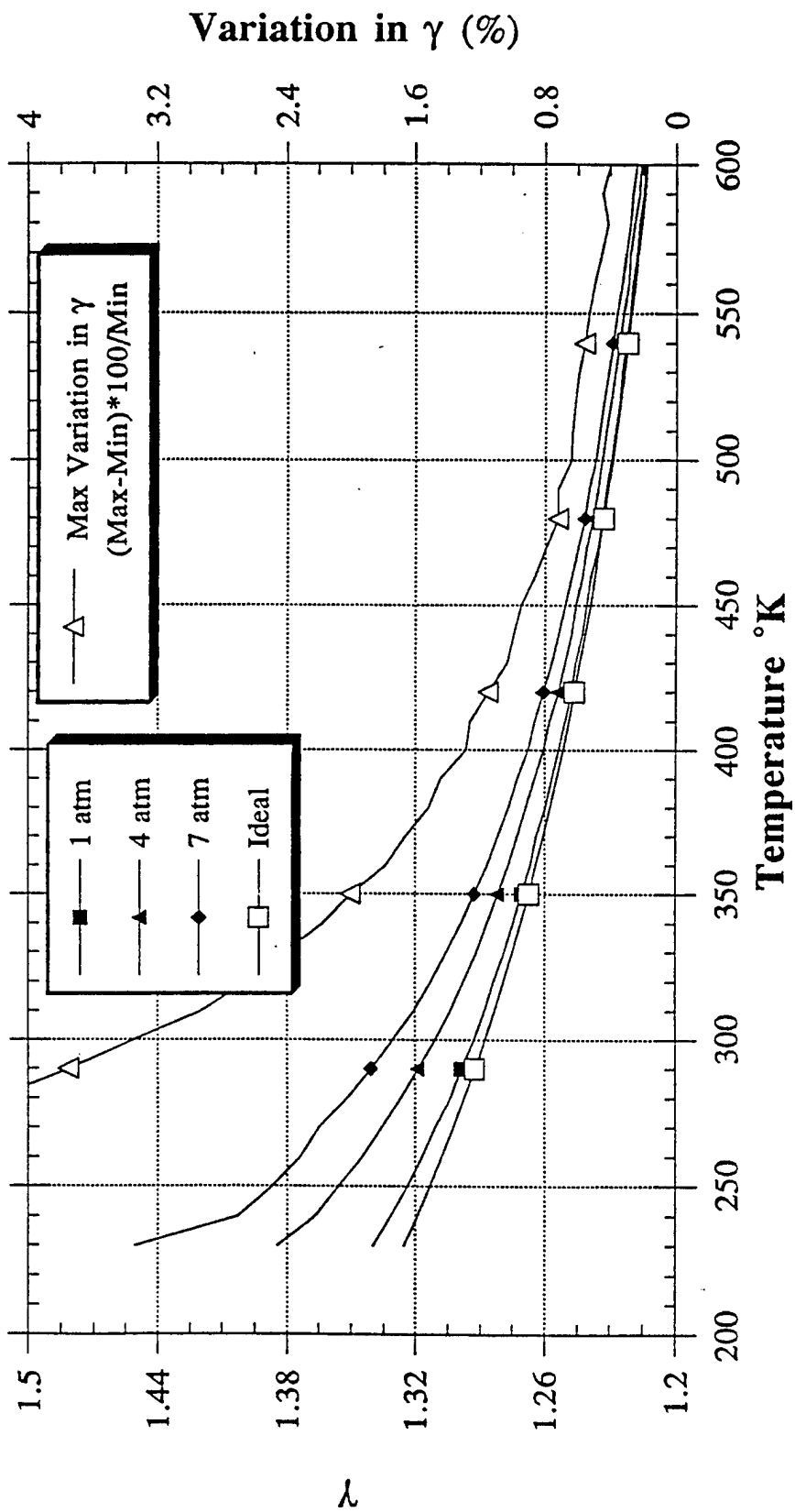
Figure A-5

C_p as a Function of Temperature and Pressure for Carbon Dioxide
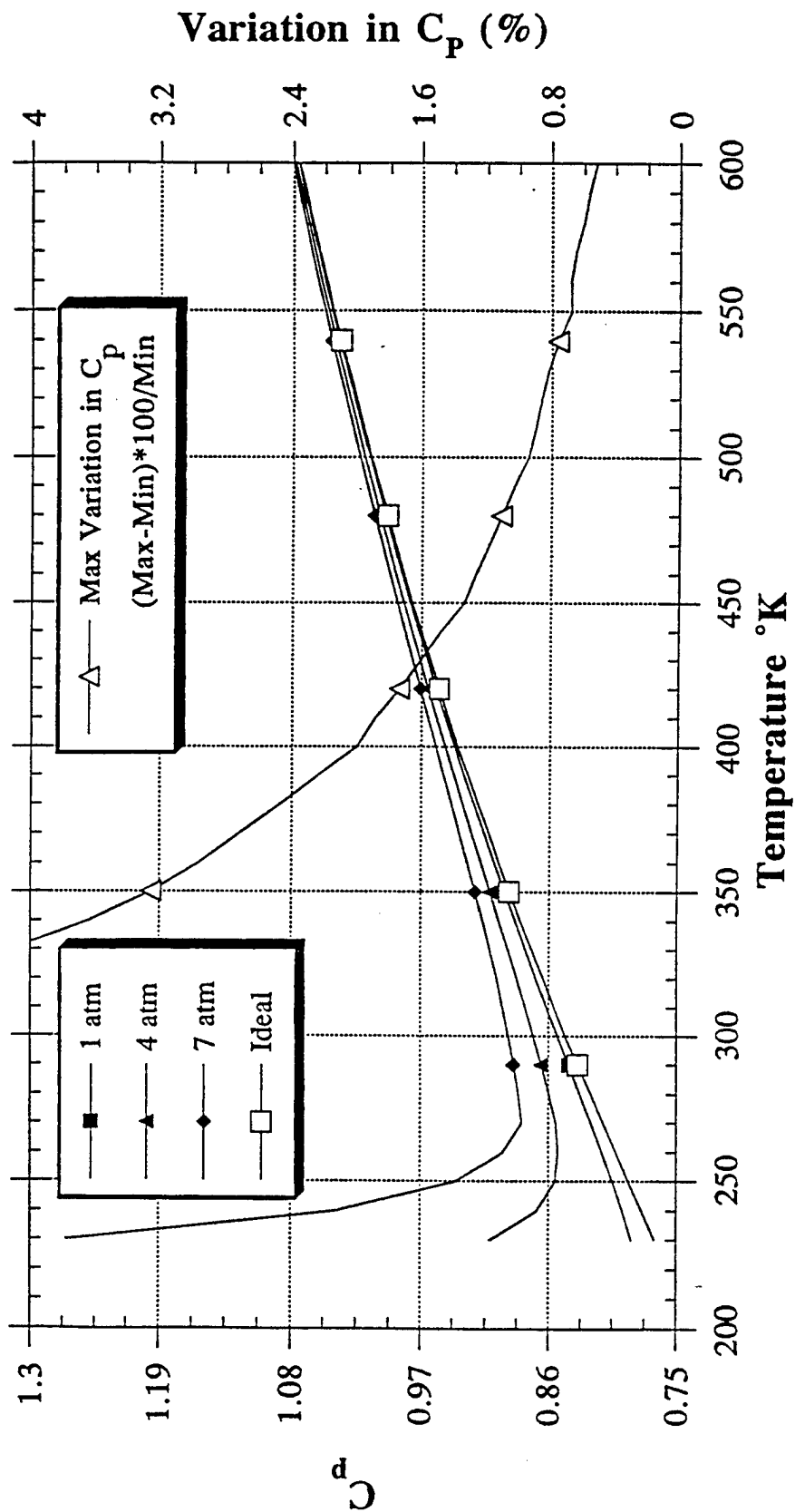
Figure A-6

C_v as a Function of Temperature and Pressure
for Carbon Dioxide
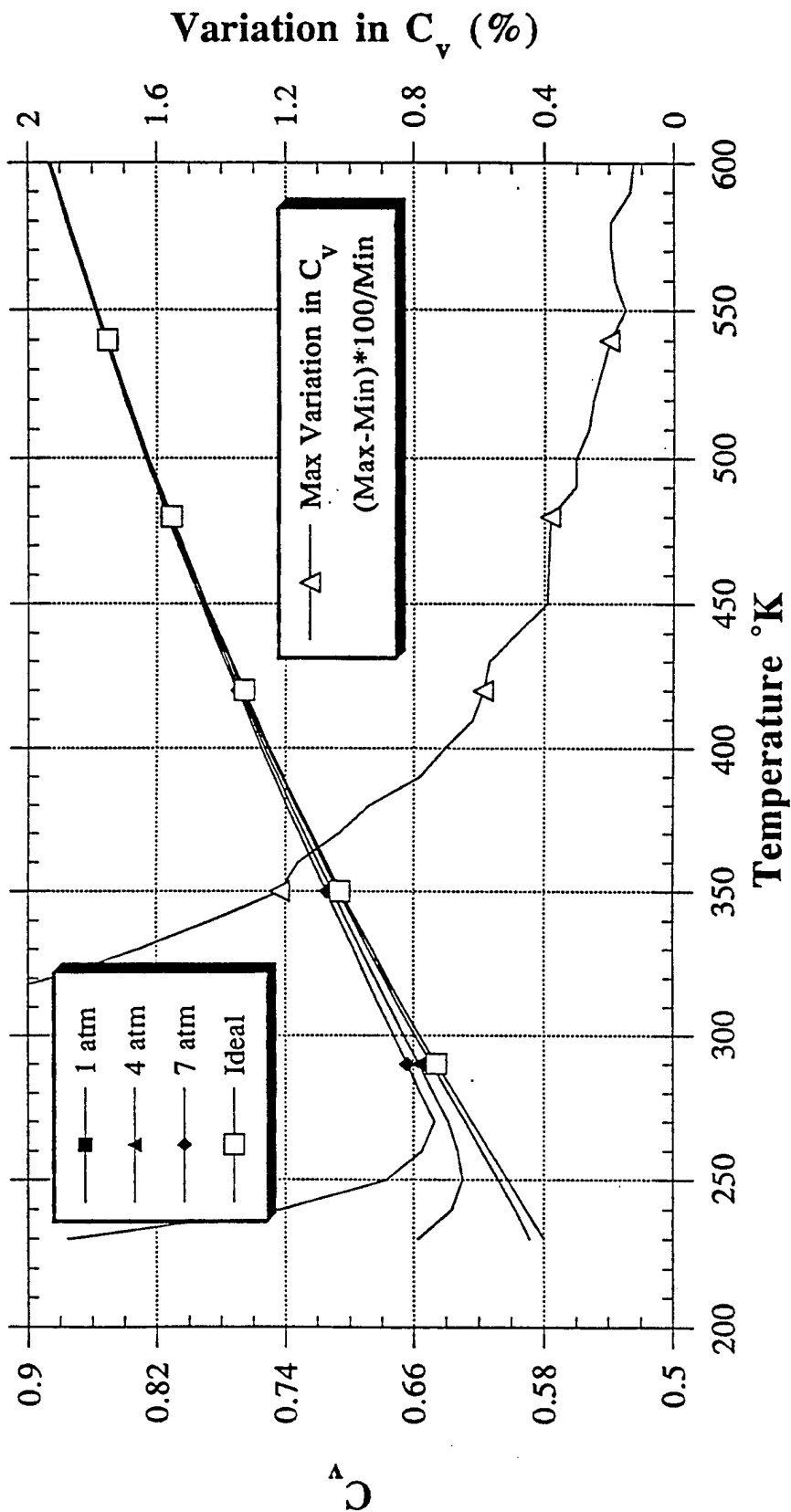
Figure A-7
Compressibility Factors
for Nitrogen

Figure A-8
Compressibility Factors
for Carbon Dioxide
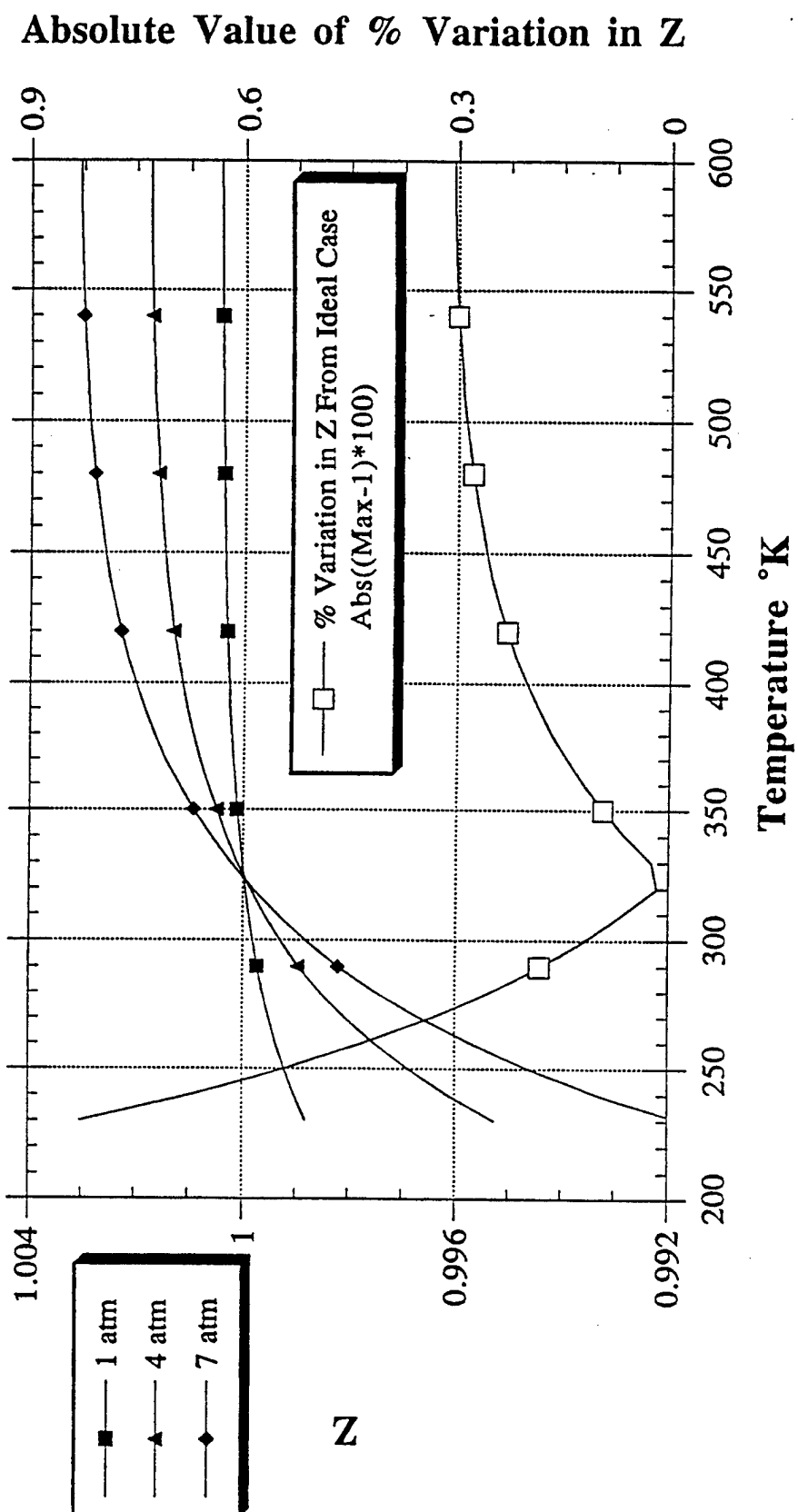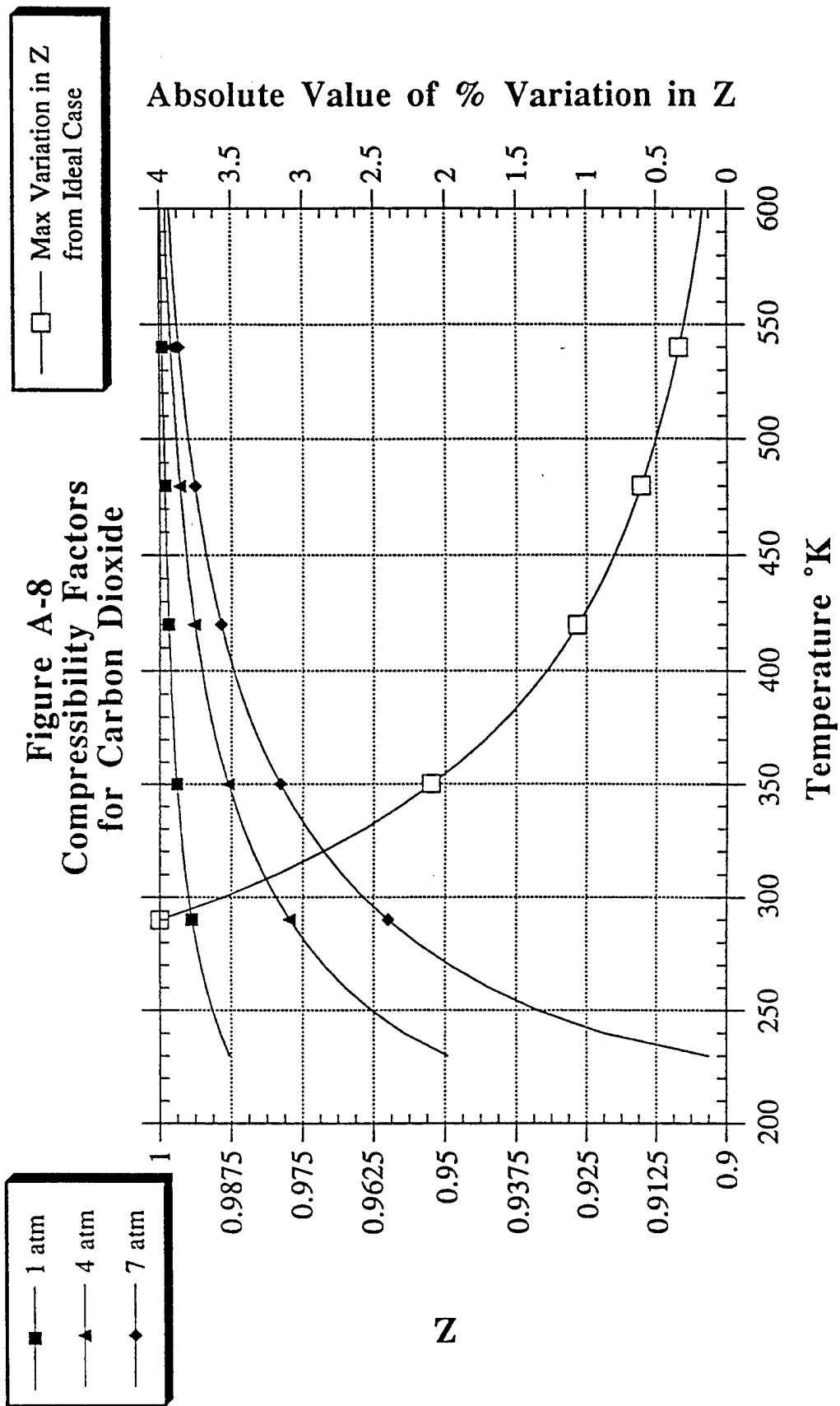
Figure A-9
Compressibility factors for Standard Gas Fill
$M_2/M_1 = 3.24$, $P_2/P_1 = 3.054$
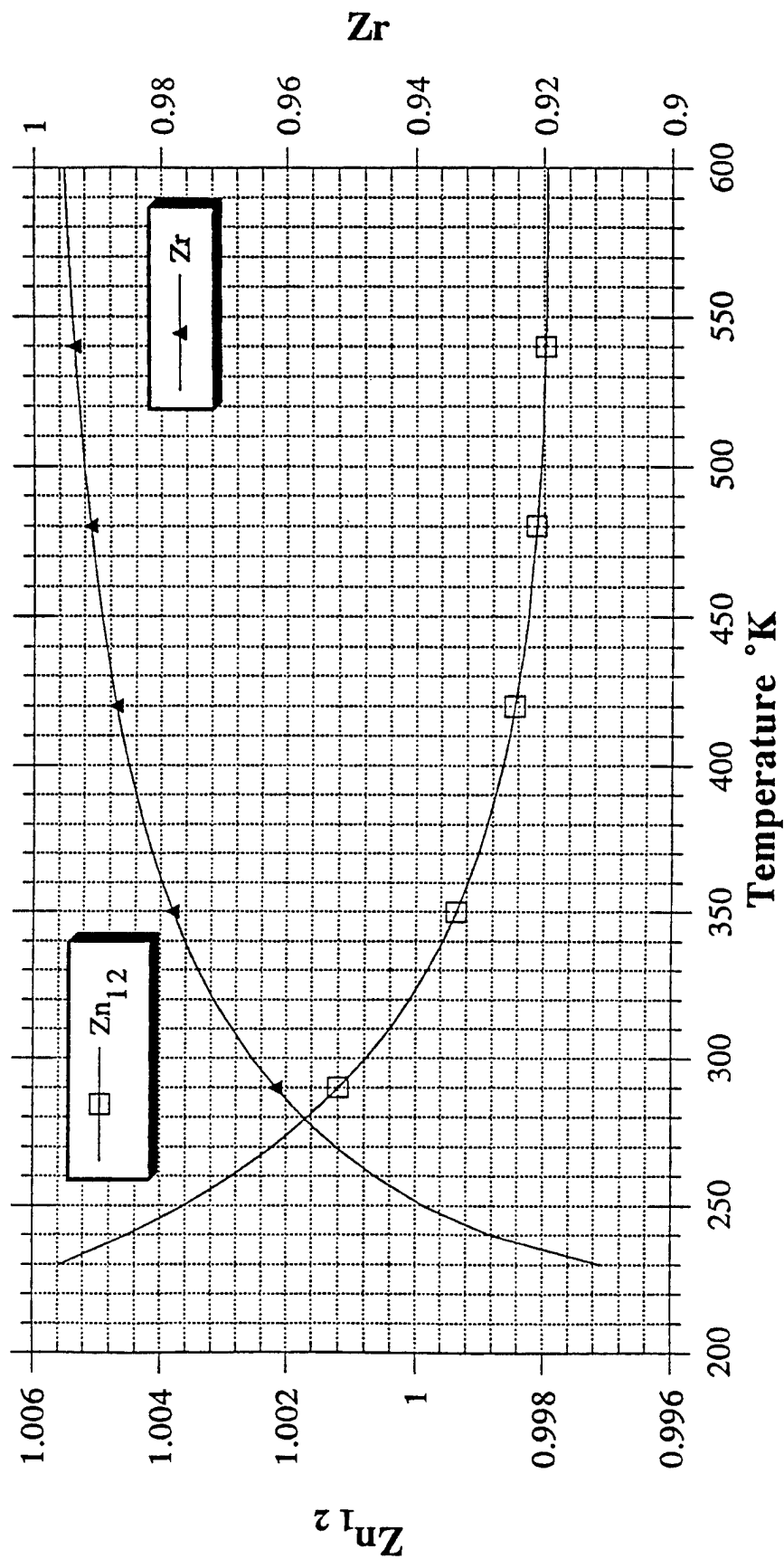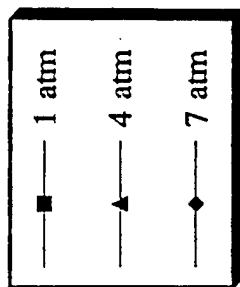
% Variation due to Pressure Differences

Figure A-10
Variation in Mixture Compressibility

% Variations Between Ideal and Real Gas Mixtures

Temperature °K

Real Gas Mixture
Variation between 1 atm and 7 atm

1 atm
4 atm
7 atm
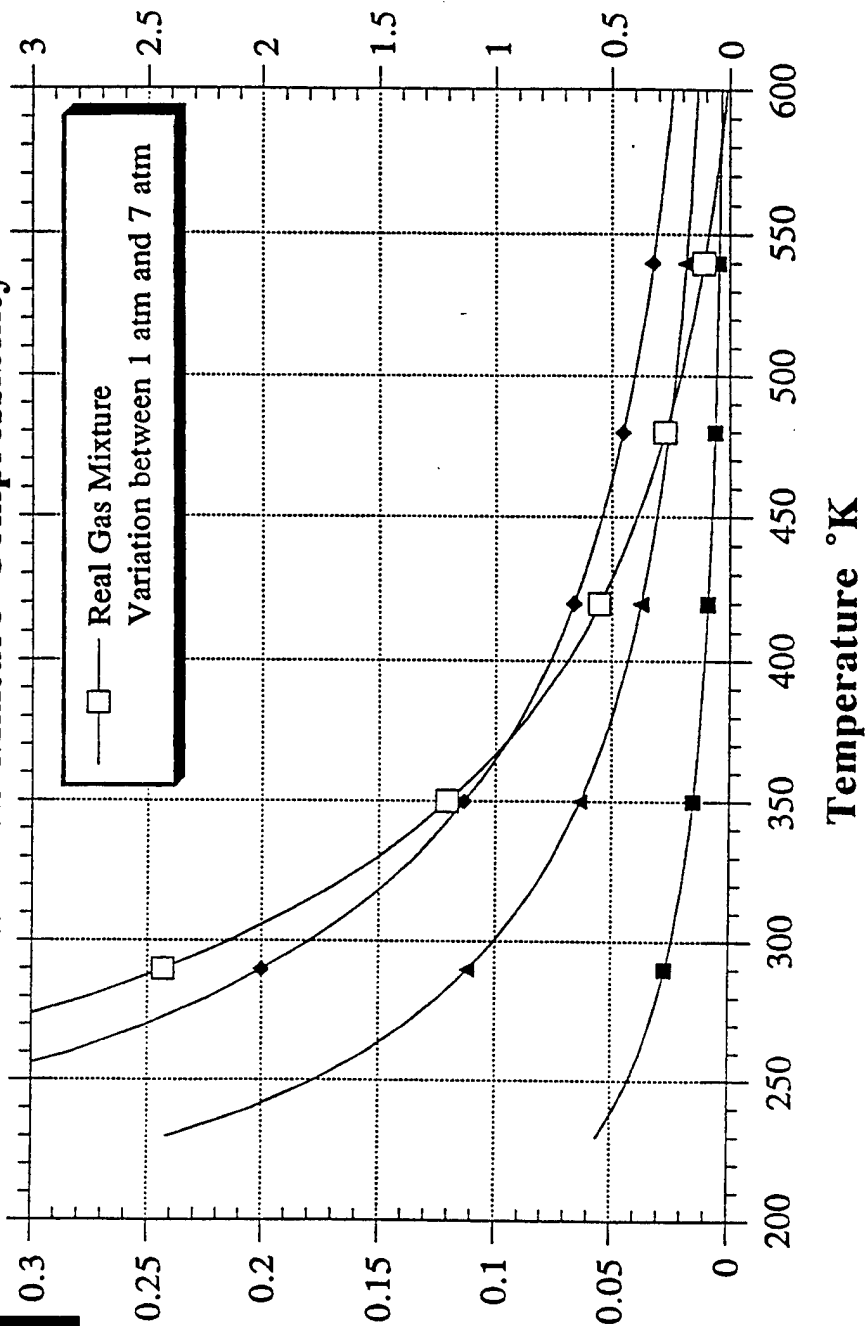
Figure A-10a
Variation in Mixture Z from Initial
Conditions at 520 °K and 7 atm

Figure A-11
Variation in Mixture γ

% Variation Due to Pressure Differences

Temperature °K

% Variations Between Ideal
and Real Gas Mixtures

Real Gas Mixture
%Δ Between 1 atm and 7 atm

1 atm
4 atm
7 atm
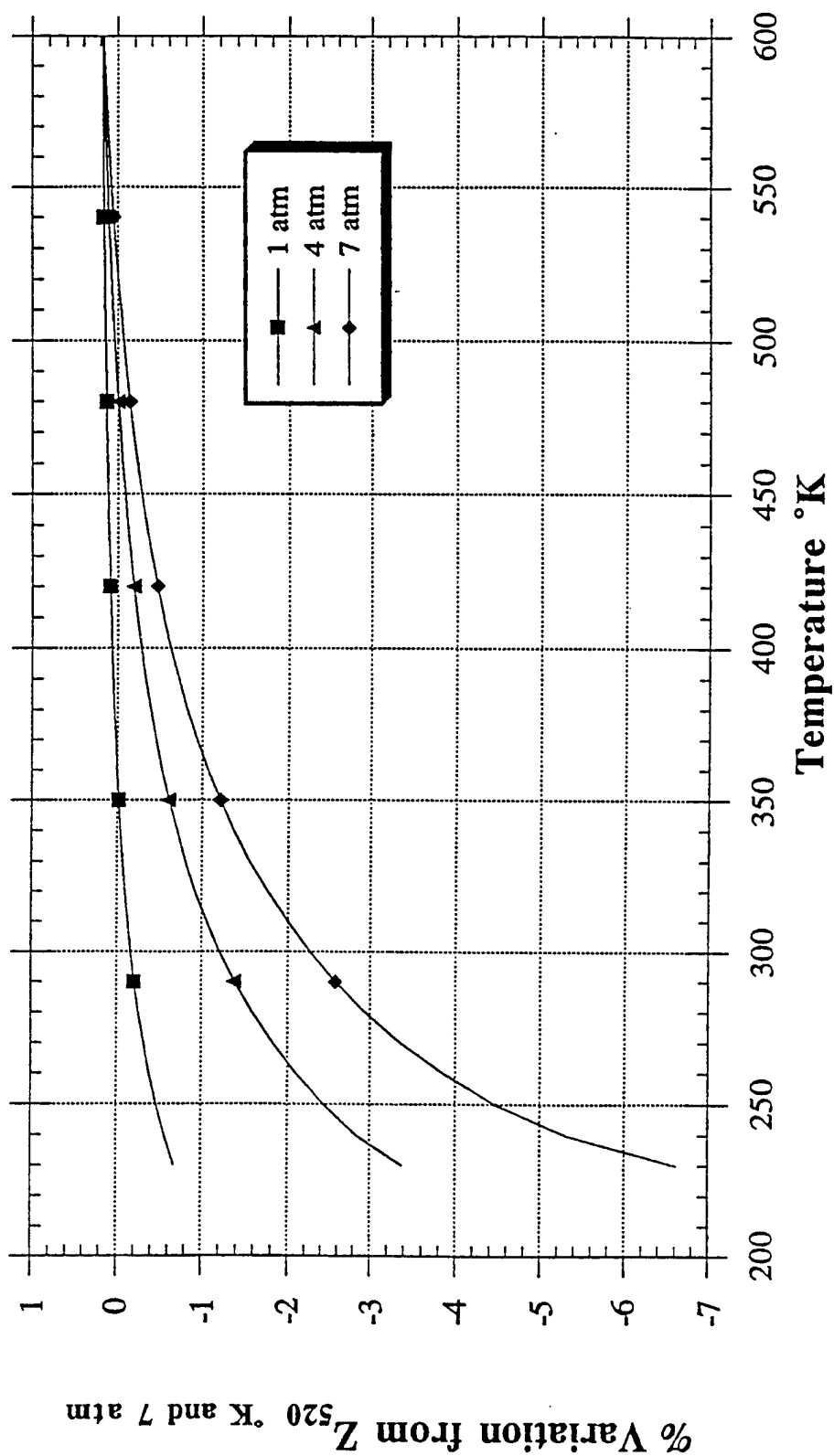
Figure A-11a

Variation in Mixture γ from Initial Conditions at 520 °K and 7 atm

% Variation Due to Pressure Differences

Figure A-12
Variation in Mixture C_p

% Variations Between Ideal and Real Gas Mixtures

Legend:
- Real Gas Mixture
- %Δ Between 1 atm and 7 atm

- 1 atm
- 4 atm
- 7 atm
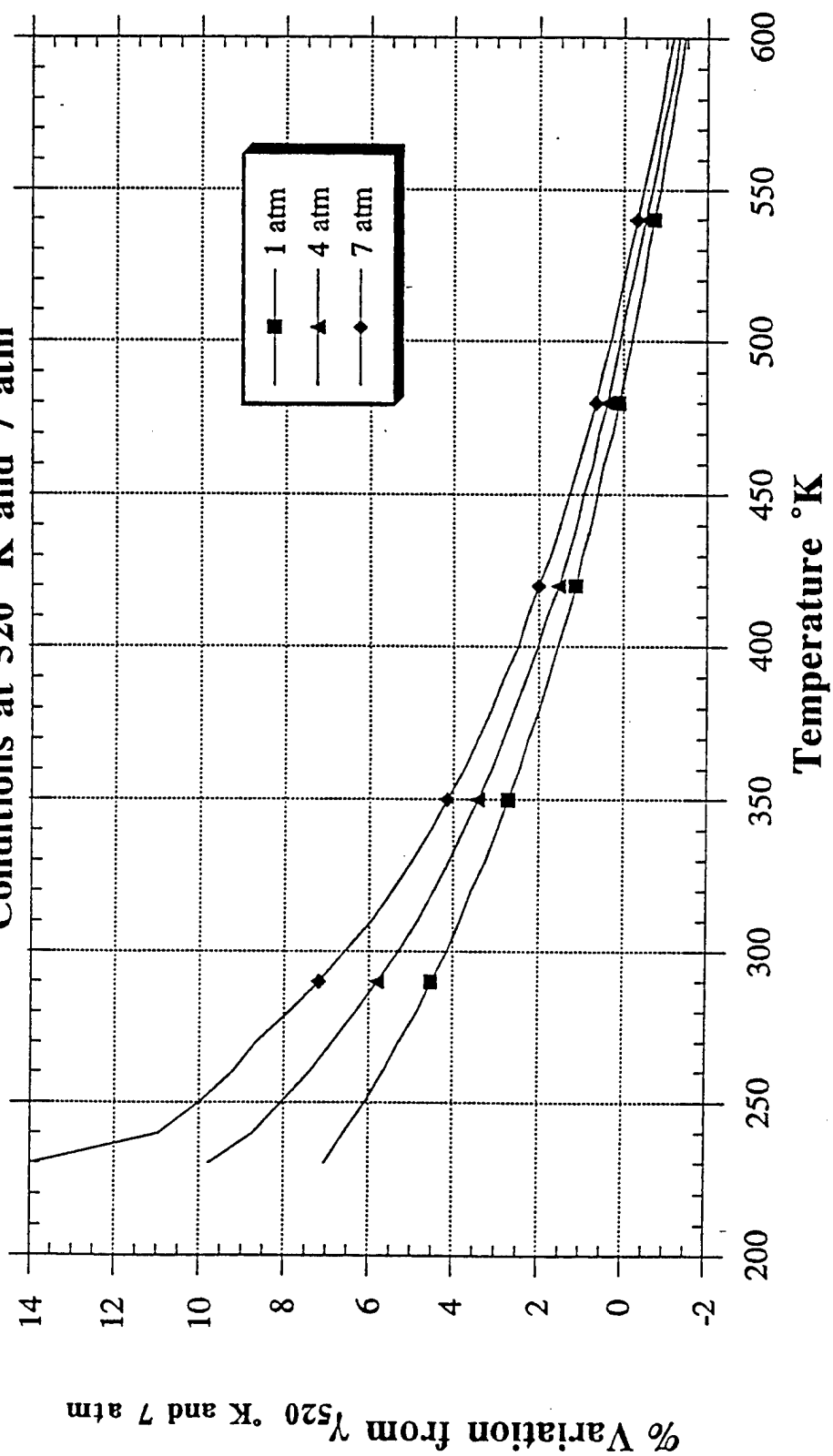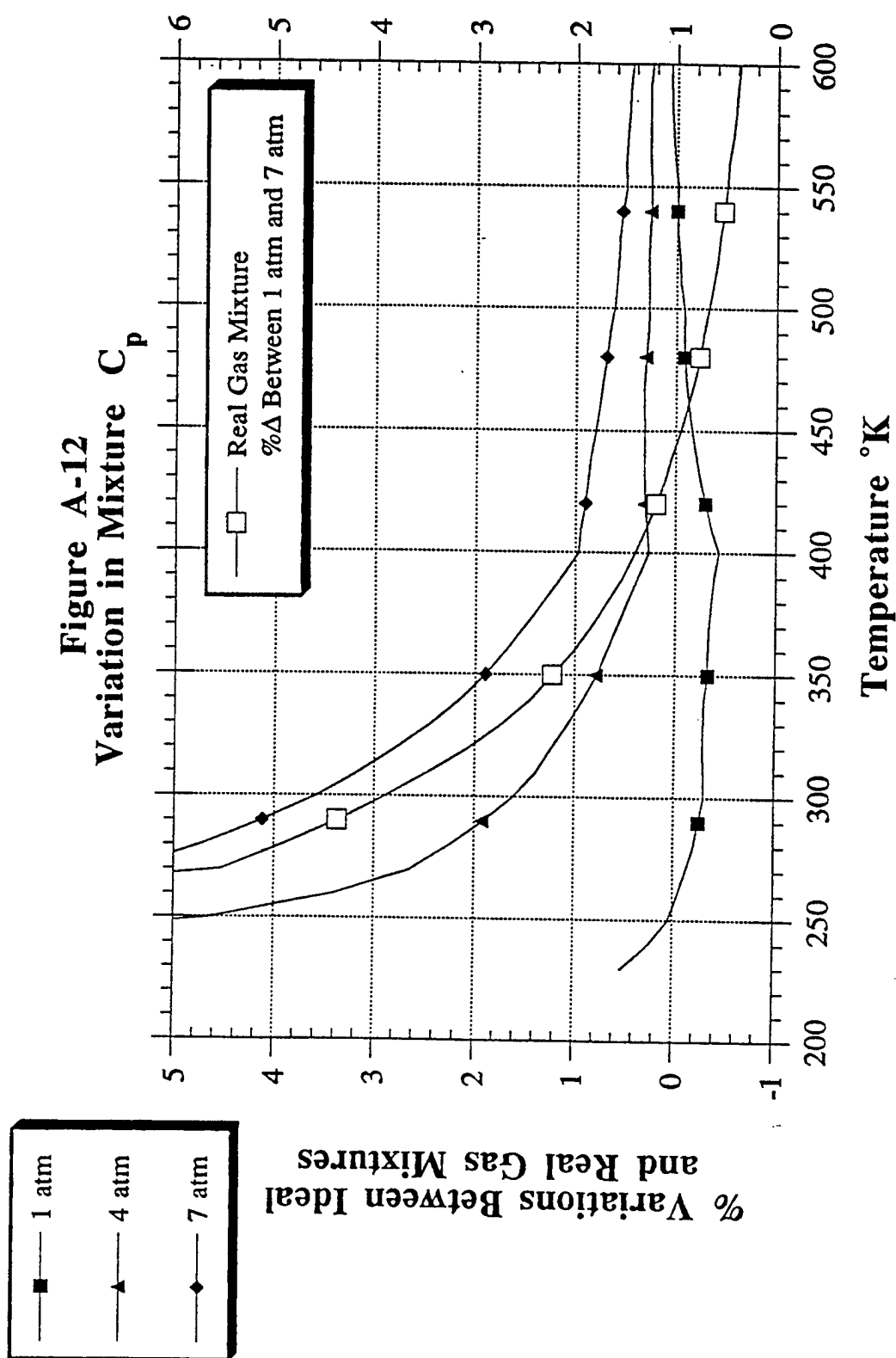
Temperature °K

% Variation Due to Pressure Differences

Figure A-13
Variation in Mixture C_v

112
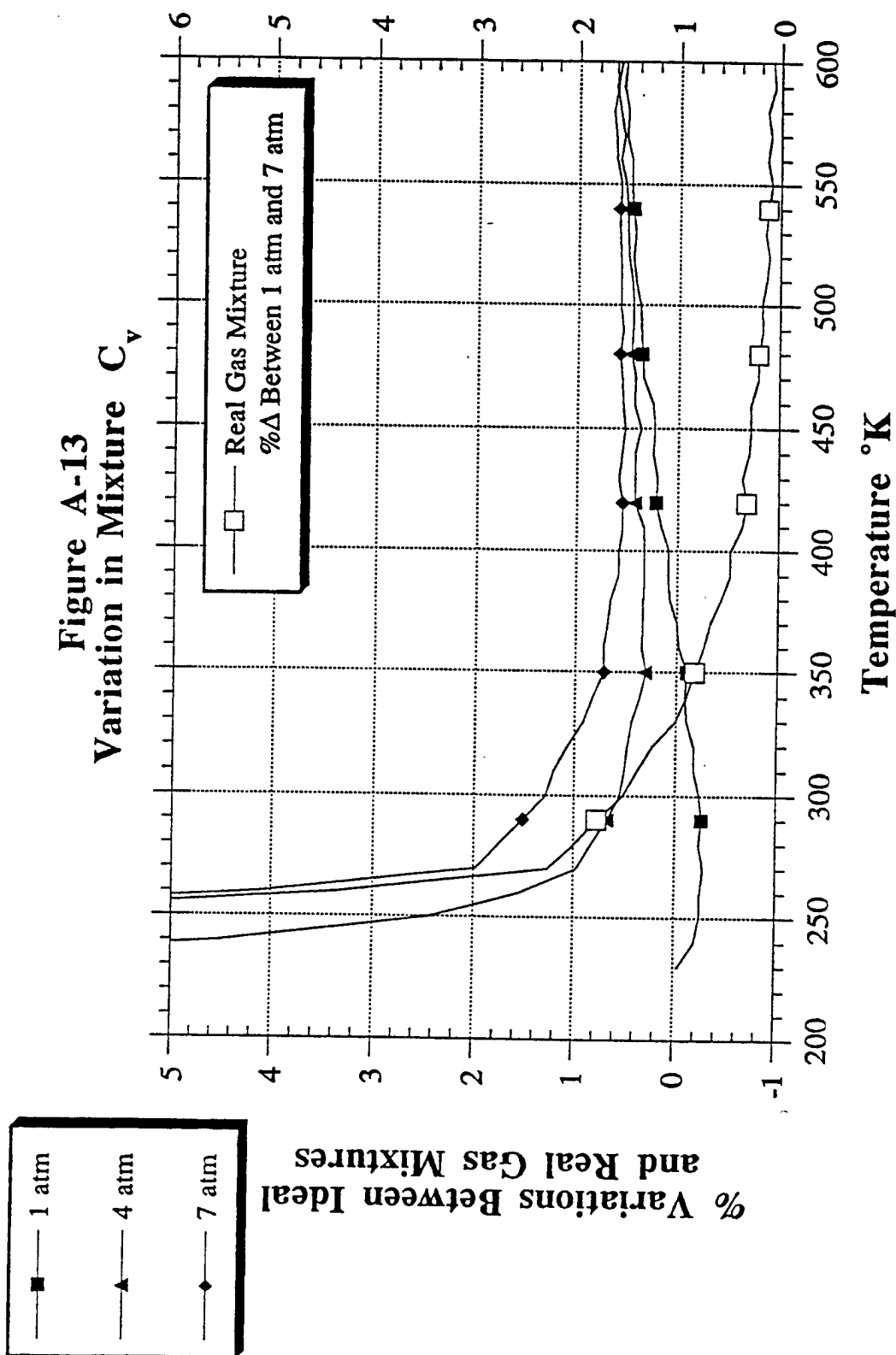
Figure A-14
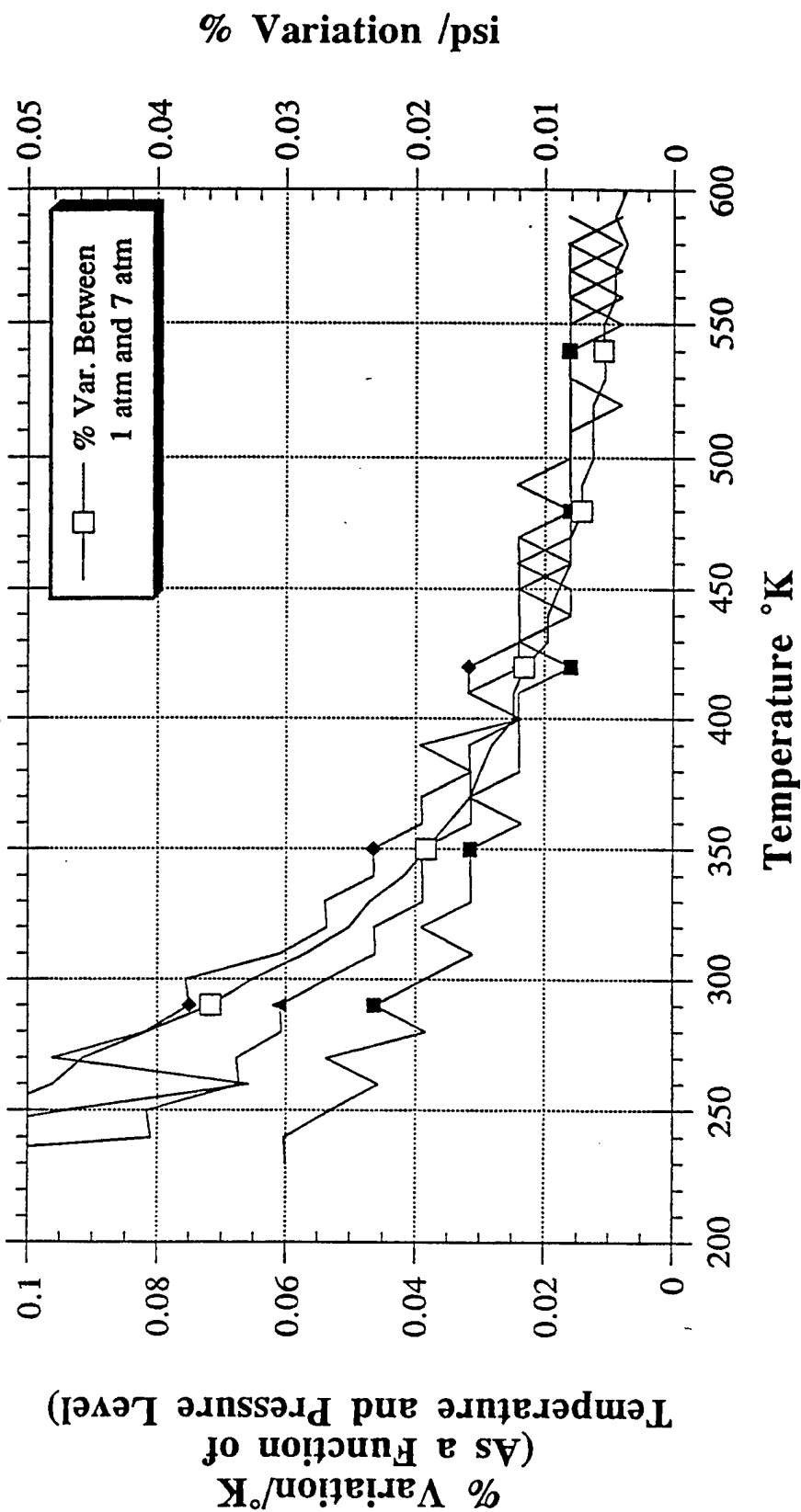Variation in Nitrogen γ
as a Function of Temperature and Pressure

113
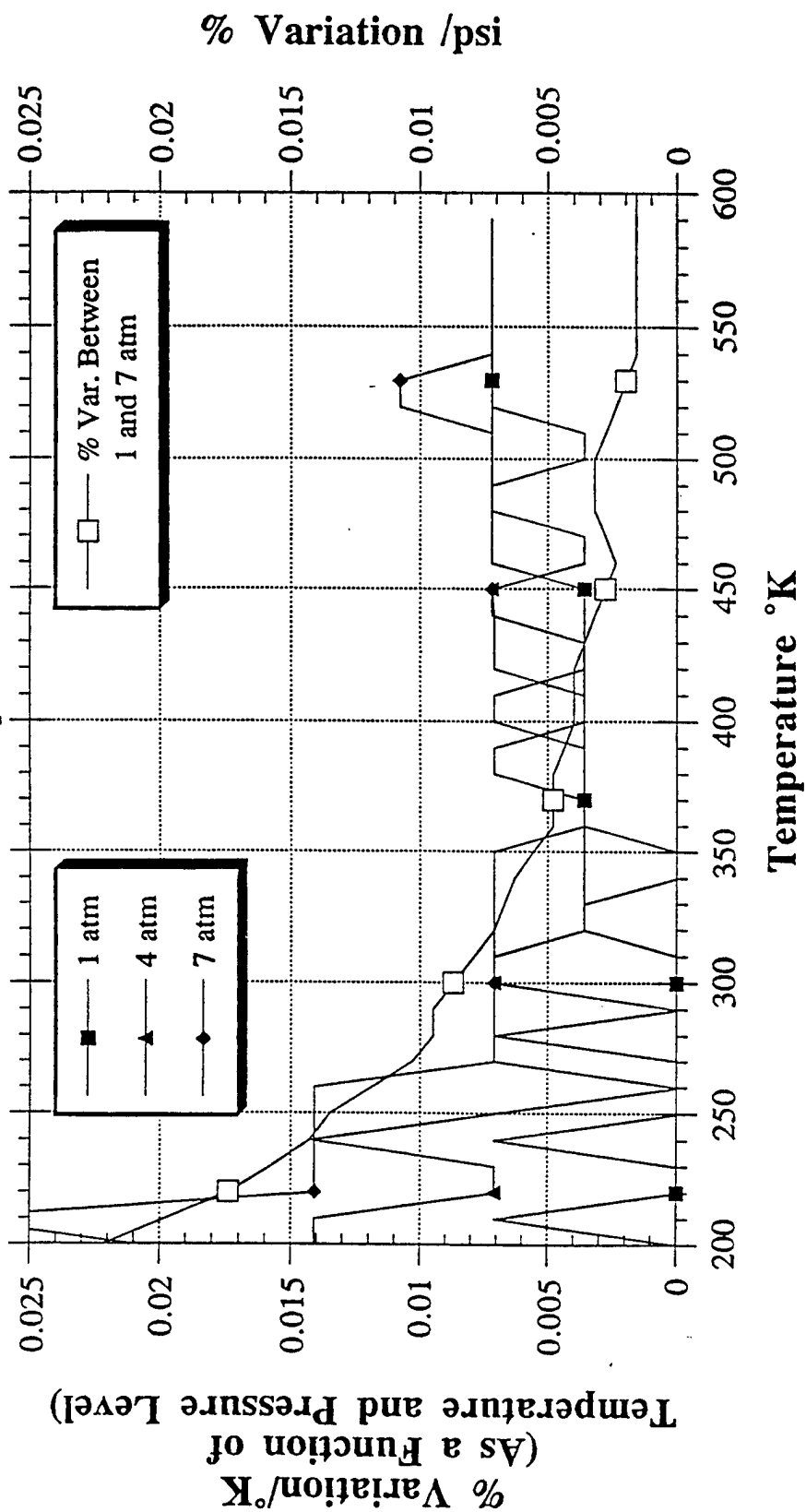
Figure A-15
Variation in Nitrogen C_p
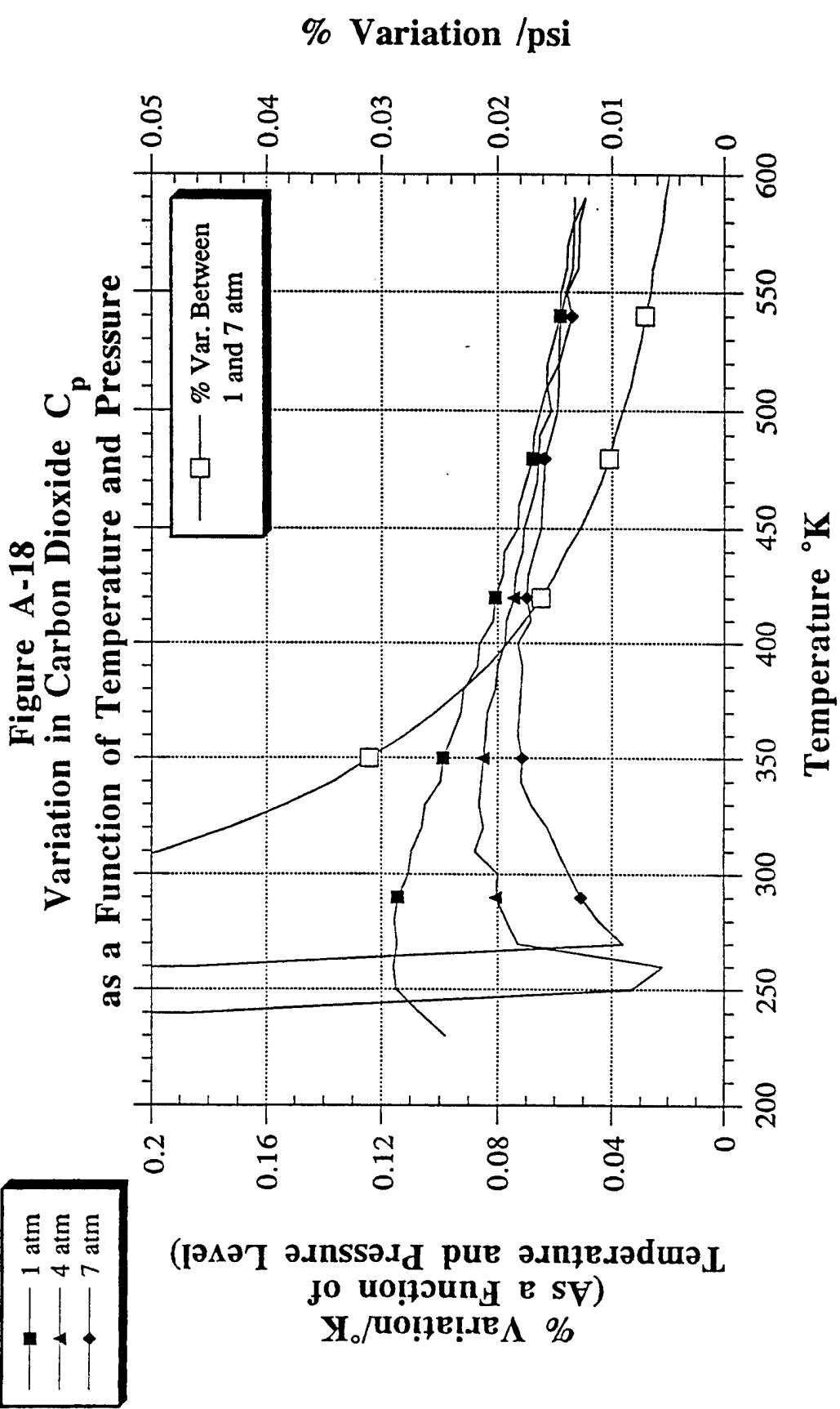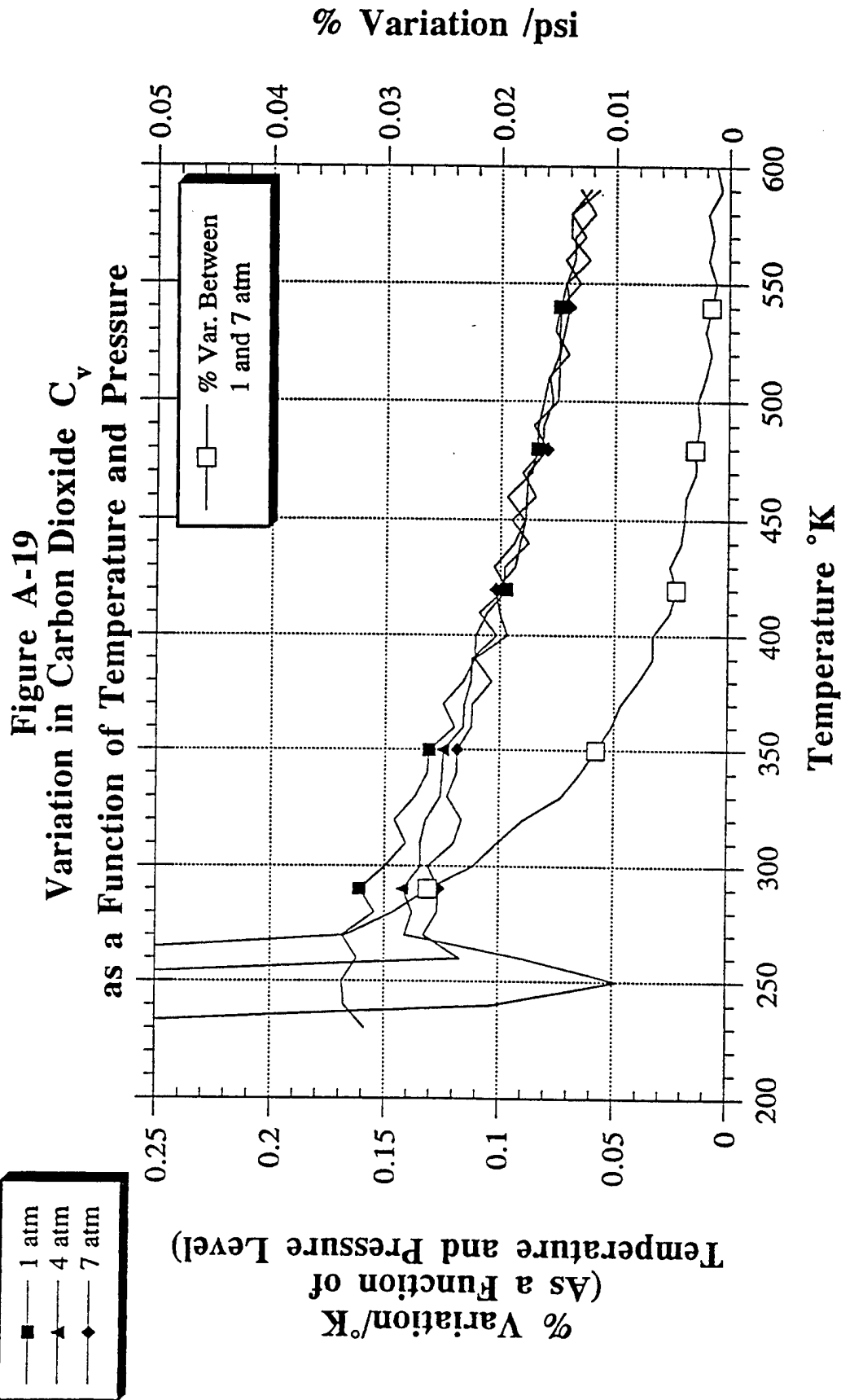as a Function of Temperature and Pressure

114

Figure A-16
Variation in Nitrogen C_v
as a Function of Temperature and Pressure

115
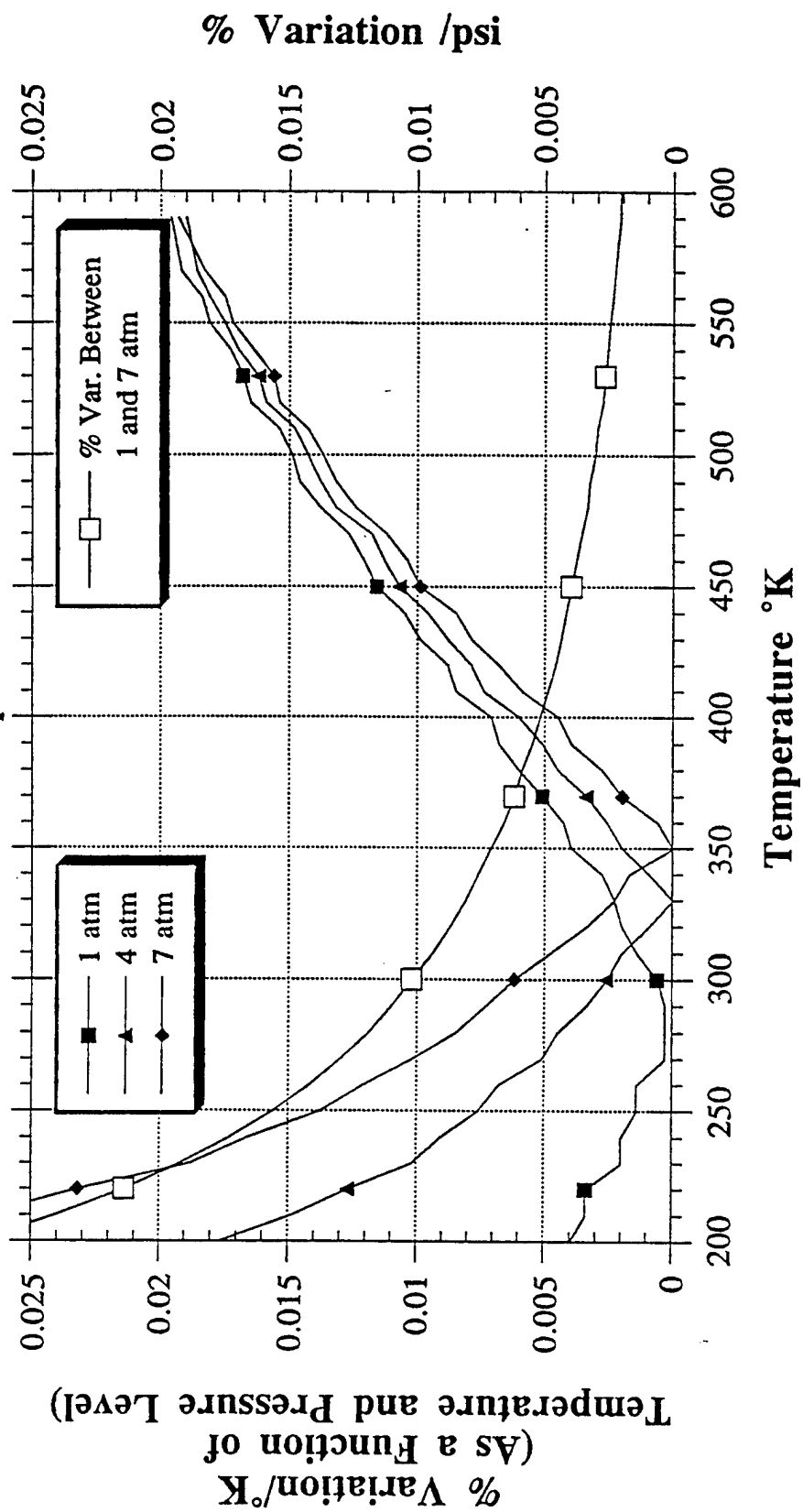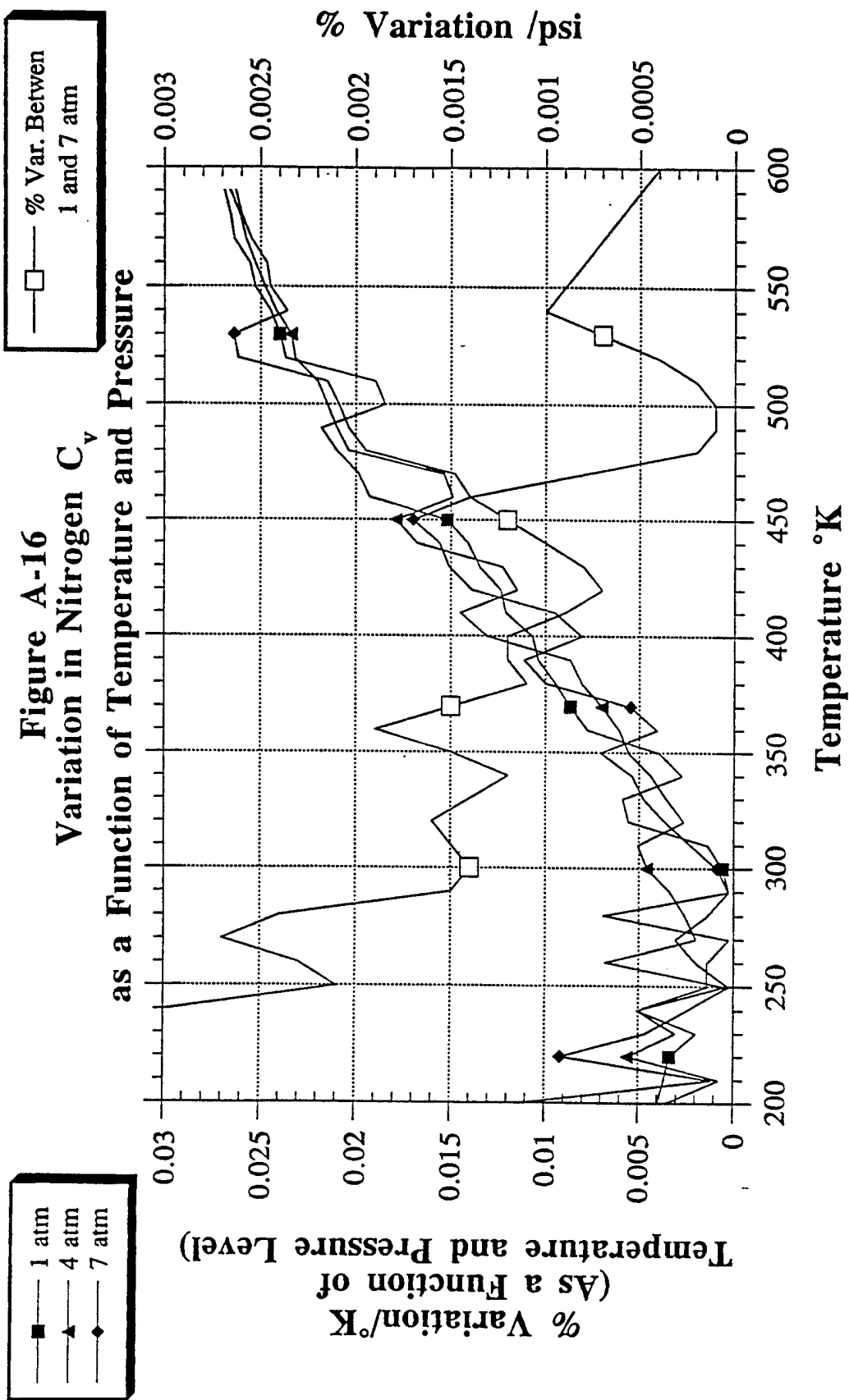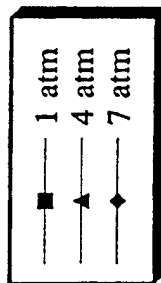
Figure A-17
Variation in Carbon Dioxide γ
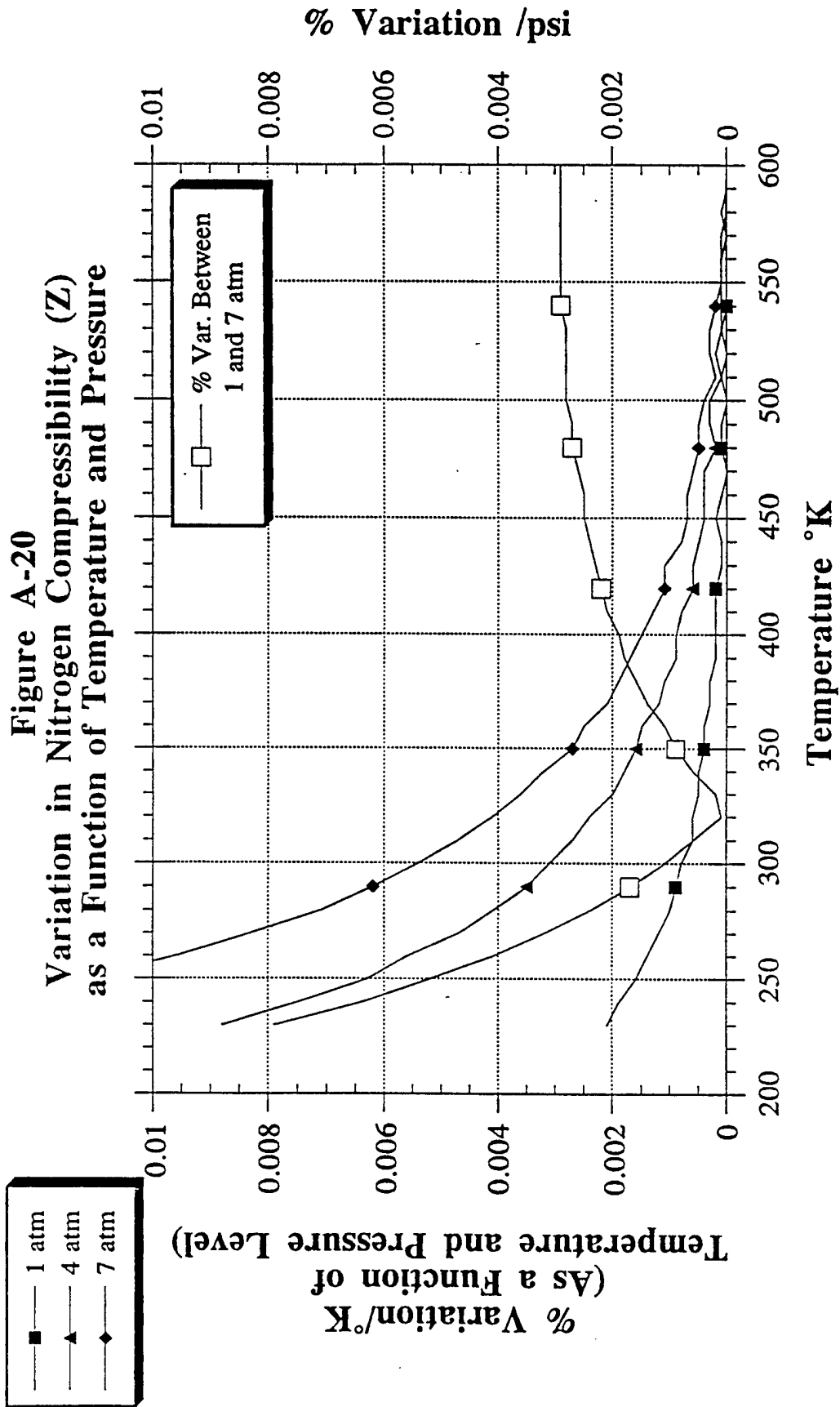as a Function of Temperature and Pressure

116

Figure A-18
Variation in Carbon Dioxide C_p
as a Function of Temperature and Pressure

Figure A-19
Variation in Carbon Dioxide C_v
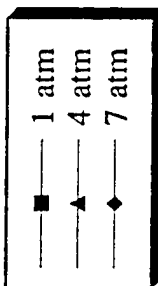as a Function of Temperature and Pressure

Figure A-20
Variation in Nitrogen Compressibility (Z)
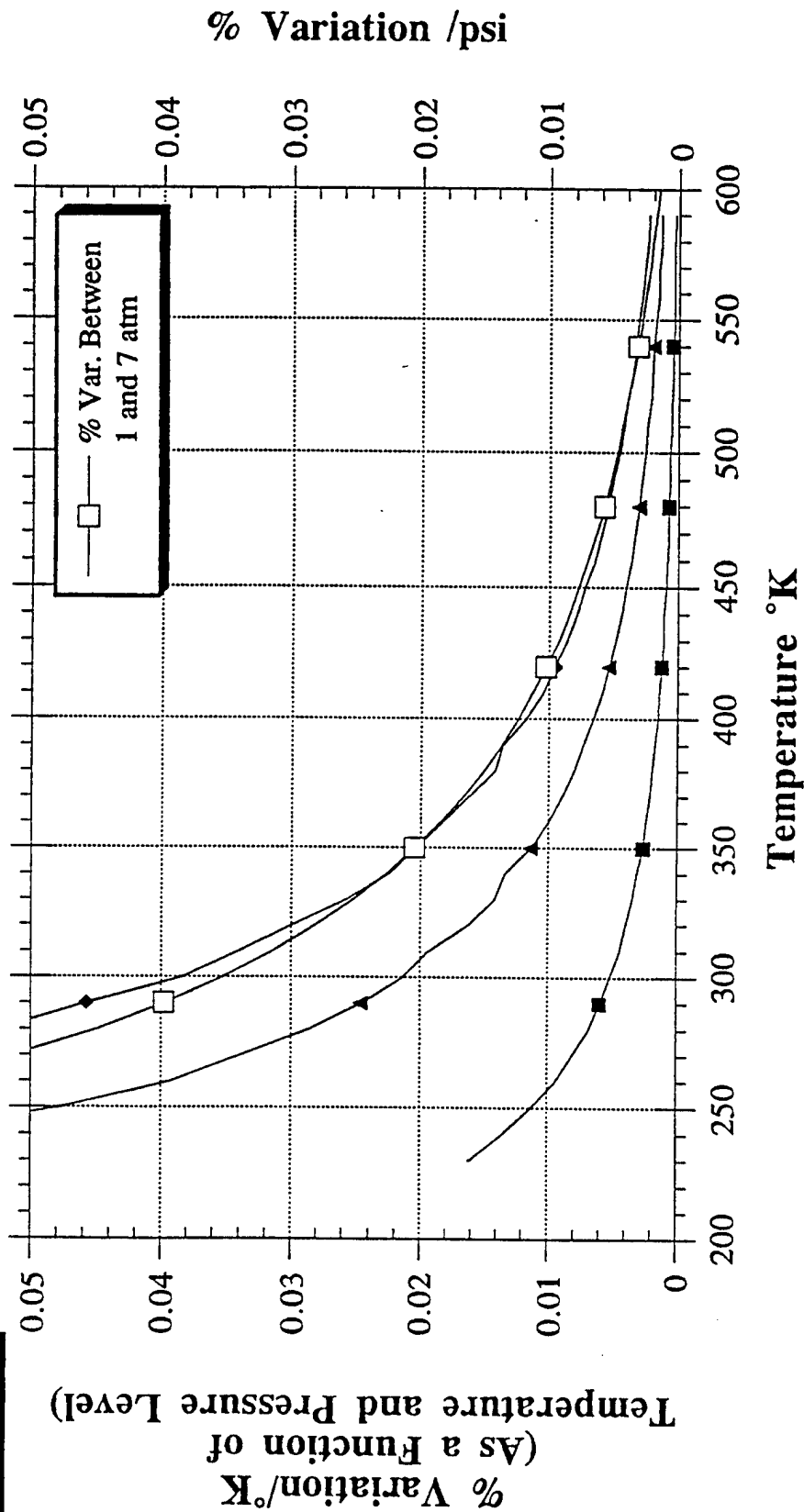as a Function of Temperature and Pressure

% Variation /psi

Temperature °K

% Variation/°K
(As a Function of
Temperature and Pressure Level)

% Var. Between
1 and 7 atm

1 atm
4 atm
7 atm

119

Figure A-21
Variation in Carbon Dioxide Compressibility (Z) as a Function of Temperature and Pressure

120

Figure A-22
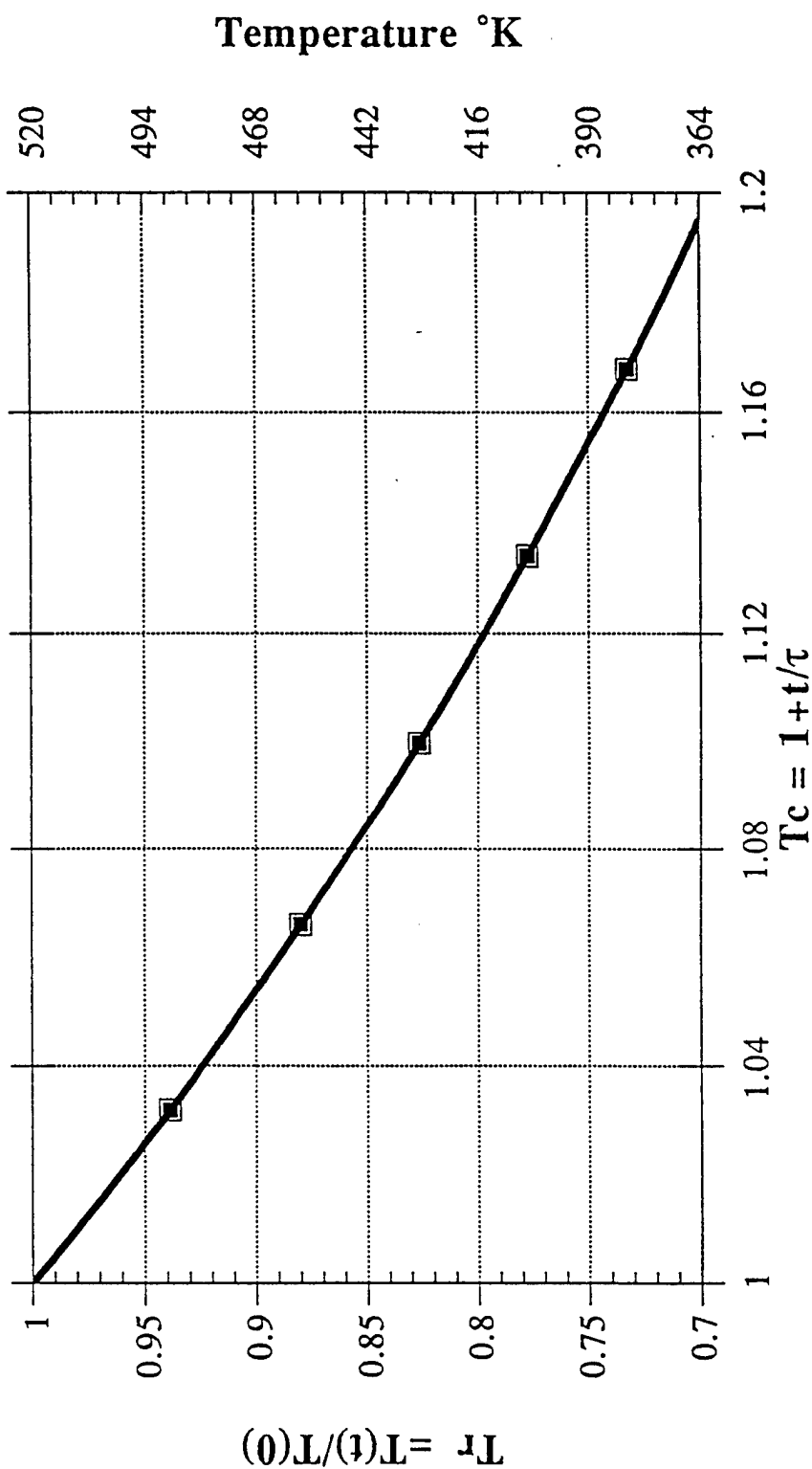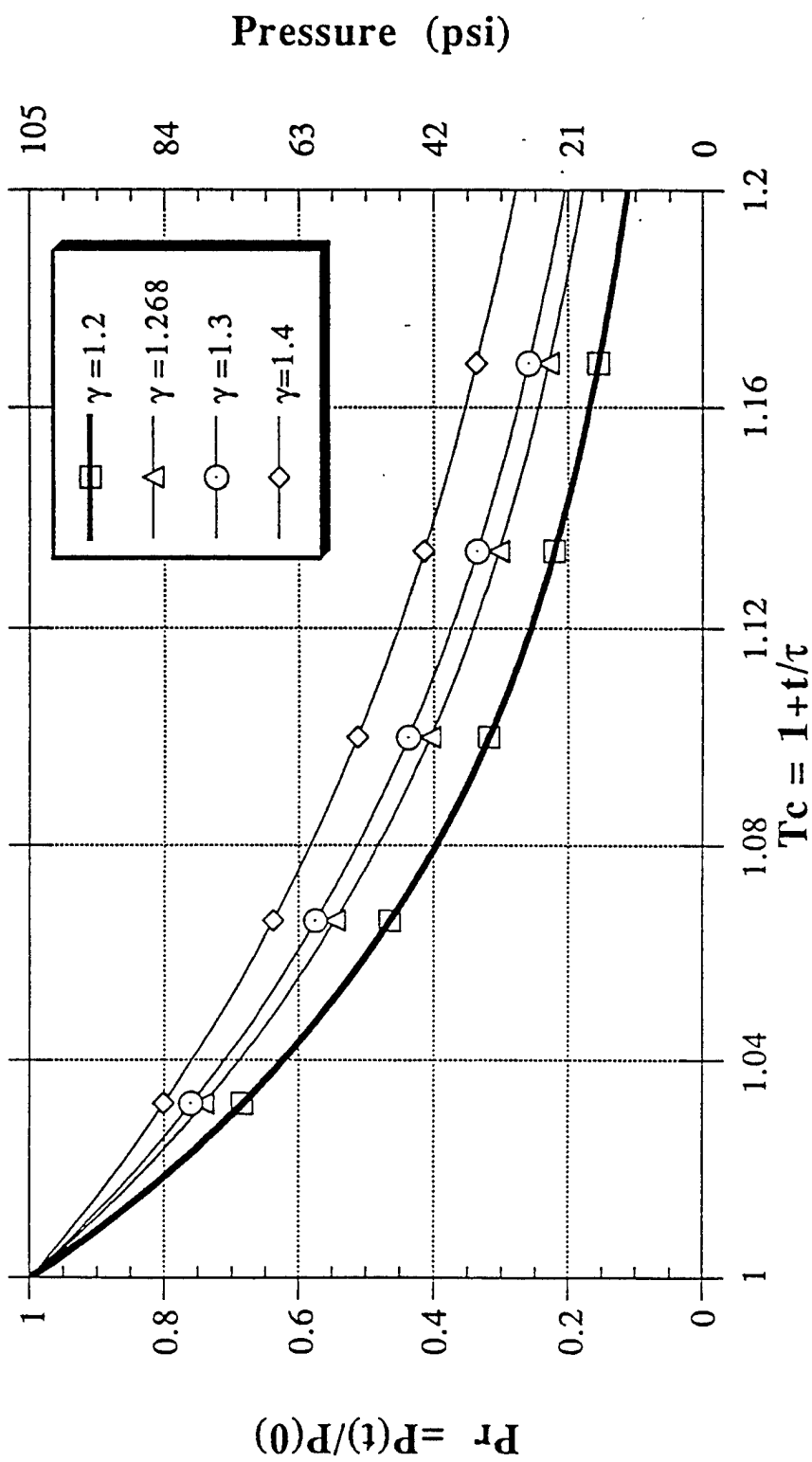Ideal Gas Temperature Drop as a Function
of Non-Dimensional Time (Tc)

Temperature °K

$T_r = T(t)/T(0)$

$Tc = 1 + t/\tau$

Figure A-23
Ideal Gas Pressure Drop as a Function of Non-Dimensional Time (Tc)

Figure A-24
γ vs. Tc
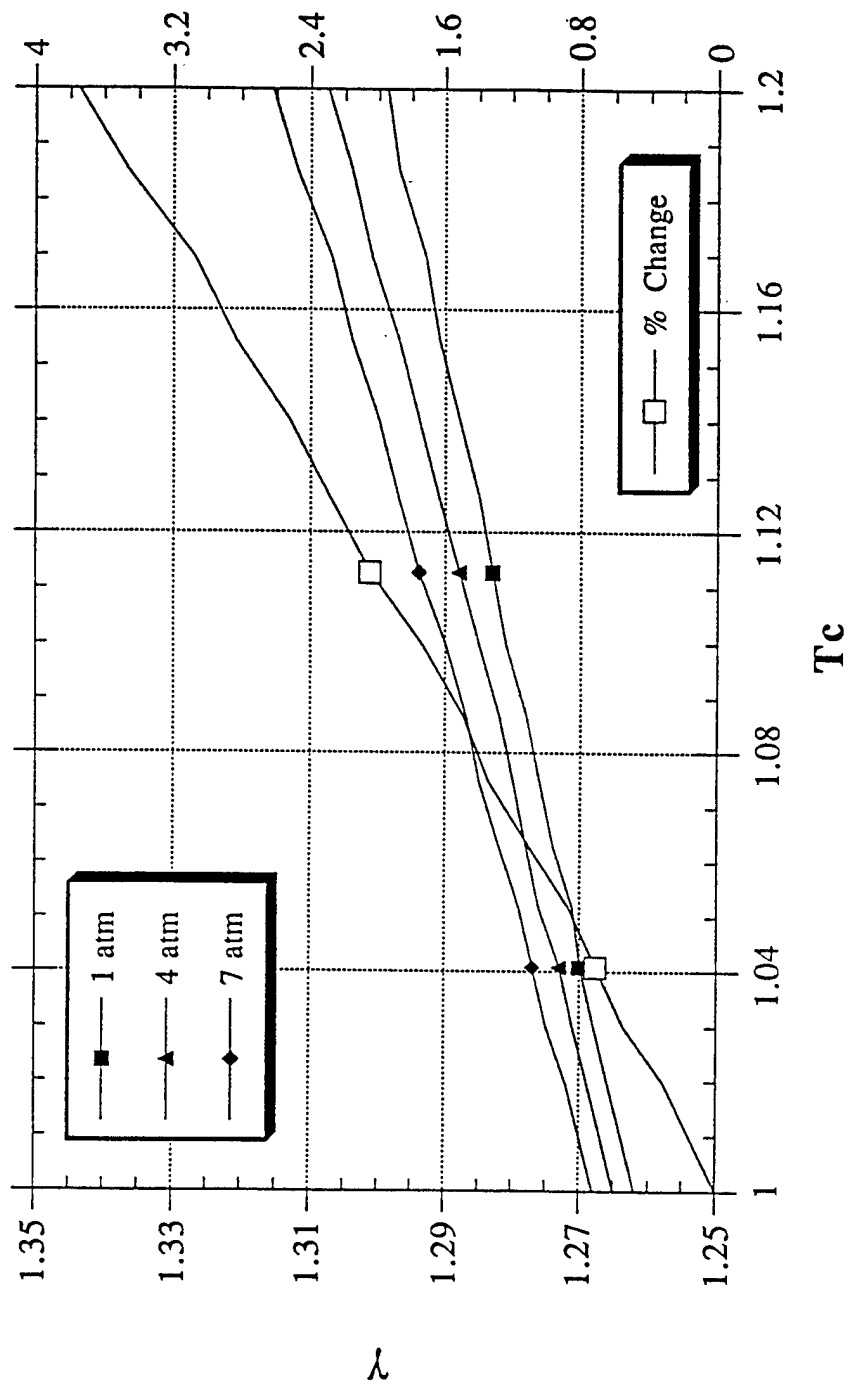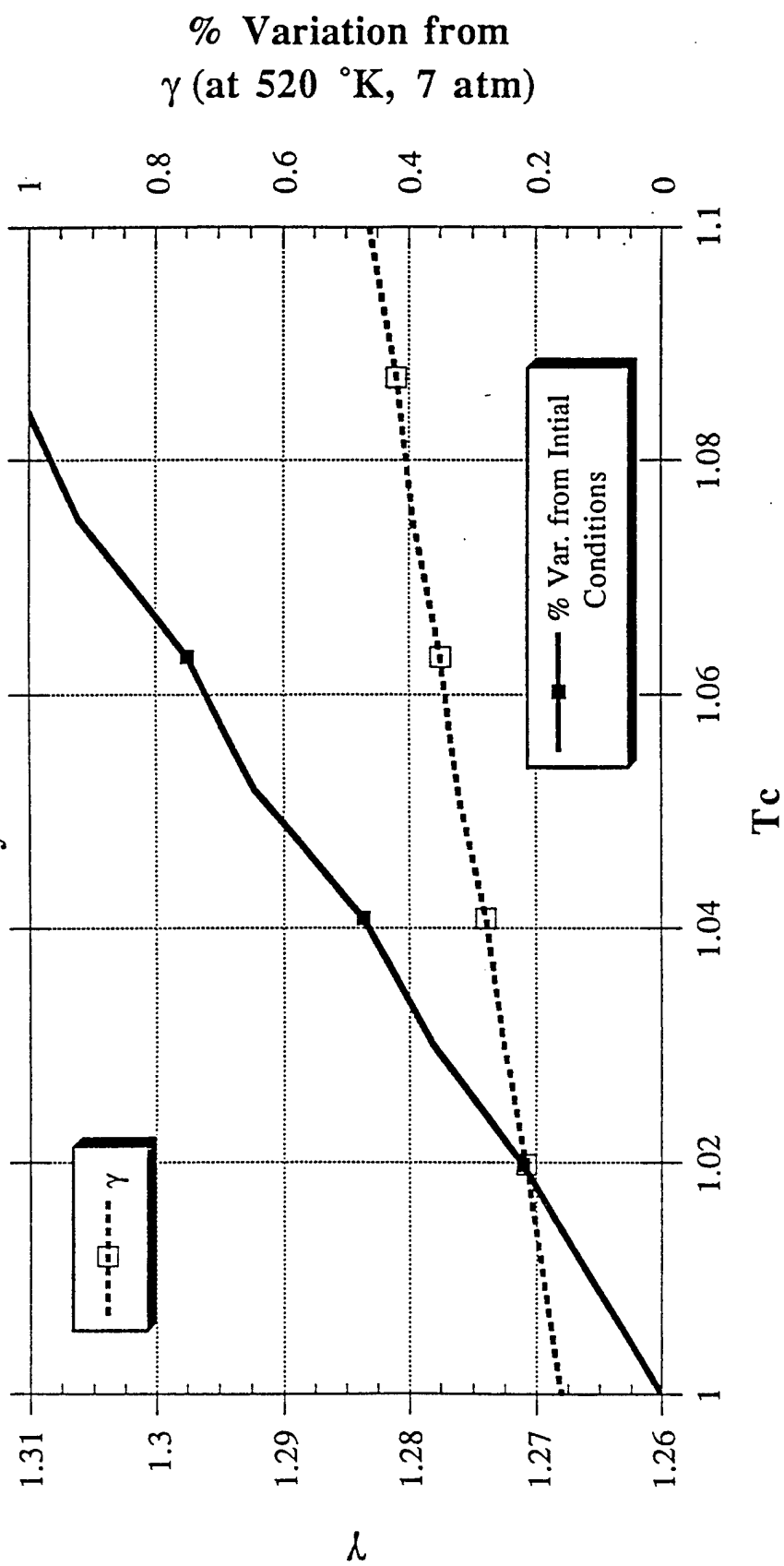
% Variation in γ (at 7 atm) from 1.268

Figure A-25
γ for Standard Mix as a Function
Only of Tc

Appendix B
Variation in Compressibility Based on Equation of State

As suggested in Section 3, the choice of reference data for determining the actual properties of the test mixture is critical if one wishes to compare data between facilities. The choice of reference data is not that critical for data being taken in only one facility, as long as all the data is from a mutually consistent data base. This means that the values for the specific heats need to be obtained from the same set of data that supplied the compressibility, the ratio of the specific heats, and the relative pressure data. However, when trying to measure efficiency to 0.25% it becomes critical when comparing data taken at different facilities that the source of the test gas data be documented.

Because all this information was readily available in one document we chose as the standard for the ATARR facility the Tables of Thermodynamic and Transport Properties[1]. However it is important to realize that the equations of state used to calculate the compressibility and other gas properties in this volume are not the only possible real gas models. Since we do not have any data by which to judge the validity of the models, it makes sense to compare the results found in this volume with other potential models.

Two which are easily used are the van der Waals model and the Redlich-Kwong model. These models are listed below

van der Waals:

$$(P + \frac{a}{v^2})\,(v - b) = RT \tag{B-1}$$

Redlich-Kwong:

$$P = \frac{RT}{(v - b)} - \frac{a}{v\,(v+b)\sqrt{T}} \tag{B-2}$$

The data obtained from the tables is described as

$$\frac{Pv}{RT} = z \tag{B-3}$$

It is an easy task to how these models compare. Solving equations B-1 and B-2 for RT and then dividing the result into Pv yields:

van der Waals:

$$\frac{Pv}{(P + \frac{a}{v^2})\,(v - b)} = z\ (vdW) \tag{B-4}$$

---

[1] Hilsenrath, Beckett, Benedict, Fano, Hoge, Masi, Nuttall, Touloukian, and Woolley; <u>Tables of Thermodynamic and Transport Properties of Air, Argon, Carbon Dioxide, Carbon Monoxide, Hydrogen, Nitrogen, Oxygen, and Steam</u>, Pergamon Press, New York, 1960

Redlich-Kwong:

$$\frac{Pv}{\left[P + \frac{a}{v\,(v+b)\sqrt{T}}\right](v - b)} = z \quad (RK)$$

(B-5)

Equations B-4 and B-5 yield effective compressibilities that can be compared with equation B-3. The constants used in the equations are[2]

van der Waals:	Nitrogen	Carbon Dioxide
a $[bar(M^3/(Kg\text{-}mol))^{\wedge}2]$	1.361	3.643
b $[M^3/(Kg\text{-}mol)]$	.0385	.0427
Redlich-Kwong:		
a $[bar\,K^{\cdot 5}(M^3/(Kg\text{-}mol))^{\wedge}2]$	15.59	64.64
b $[M^3/(Kg\text{-}mol)]$	.02681	.02969
Molec. Weight	28.008	44.01

The densities were taken from tabular values in reference 1. Using this information the equivalent compressibilities were calculated for carbon dioxide and nitrogen. Shown in figures B-1 to B-4 are these compressibilities for each gas at 1 atm and 7 atm. Also plotted in each graph is the variation between the two extremes, defined as:

$$\frac{[\text{Maximum} - \text{Minimum}]\,100}{\text{Average}}$$

(B-6)

For the temperature range of interest (between 400 °K and 550 °K) one can see in figure B-1 that for nitrogen at 1 atm there is less then a .04% difference between the methods, and none of the models is more then about .04% from ideal gas behavior. But when the pressure is increased to 7 atm (figure B-2), the variation among the models is about 0.25%. Both the Redlich-Kwong and the van der Waals models give compressibilities which are much closer to ideal then the tables (but are still off from ideal of by about 0.2%) The models agree much better for CO_2 at both pressures (figures B-3 and B-4). It is interesting to note that for nitrogen all the models were spaced more or less equally apart. With CO_2 however, the van der Waals model follows very closely the Redlich-Kwong model.

What can be derived from this information? Well it is apparent that which real gas model one chooses could have a significant effect on the overall results of the experiment. Appendix A demonstrated the influence that the compressibility had on the mixing process and from these figures it seems as though the compressibilities might be overstated. however there is no real way to determine the truth. The constants used in these equations were computed from critical data, not fitted to experimental data, so they could be in error. The important thing to remember is that any

---

[2] Wark, Kenneth; Thermodynamics, McGraw-Hill Book Company, New York, 1983; Tables A-2M (p. 781), A-3M (p. 782), and Table A-21M (p 815).

system chosen for the reference data has to be self-consistent. And when comparing measured efficiencies between facilities with 0.25% accuracy, it will be important to make sure that each facility is using the same reference data.
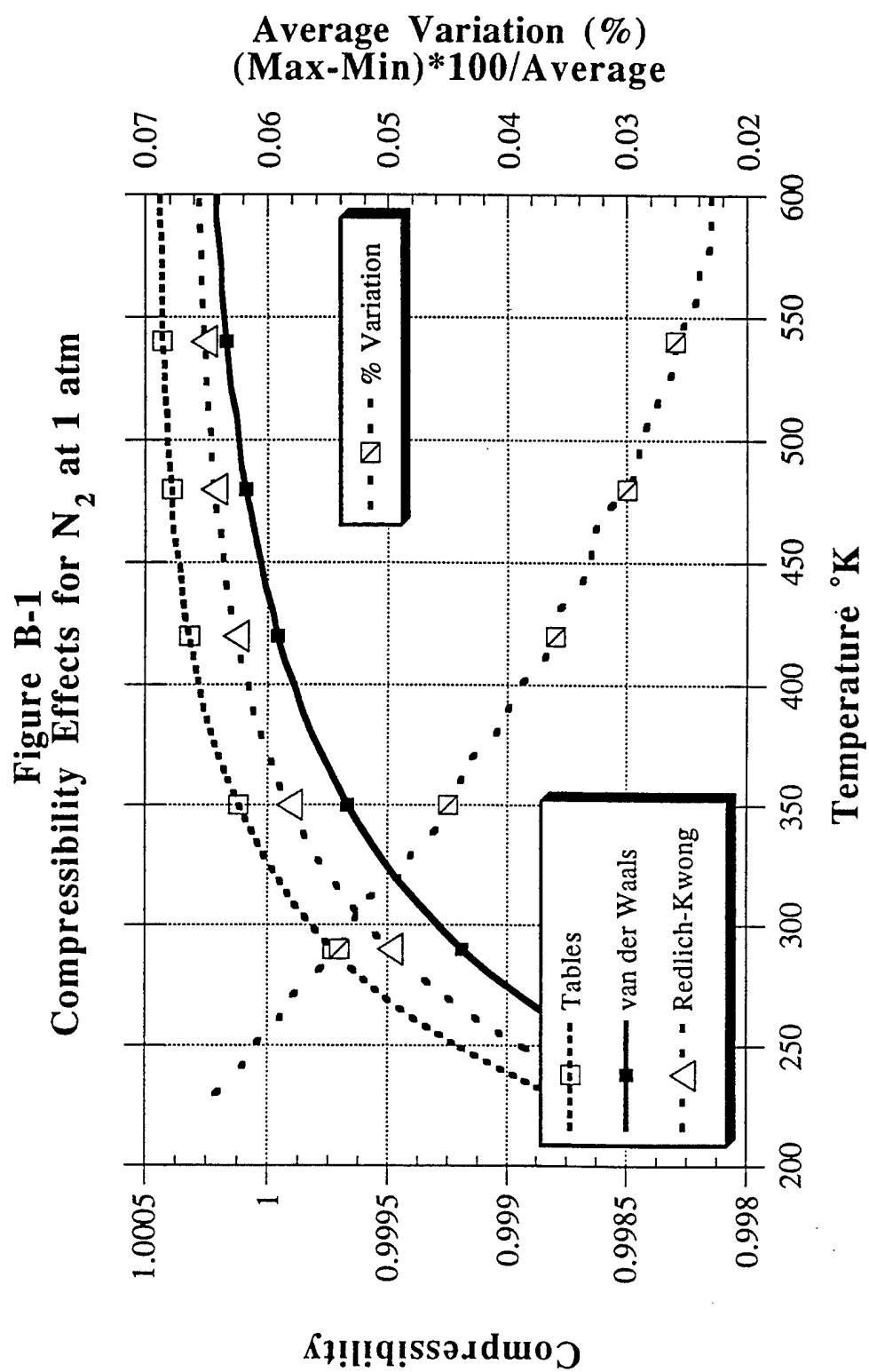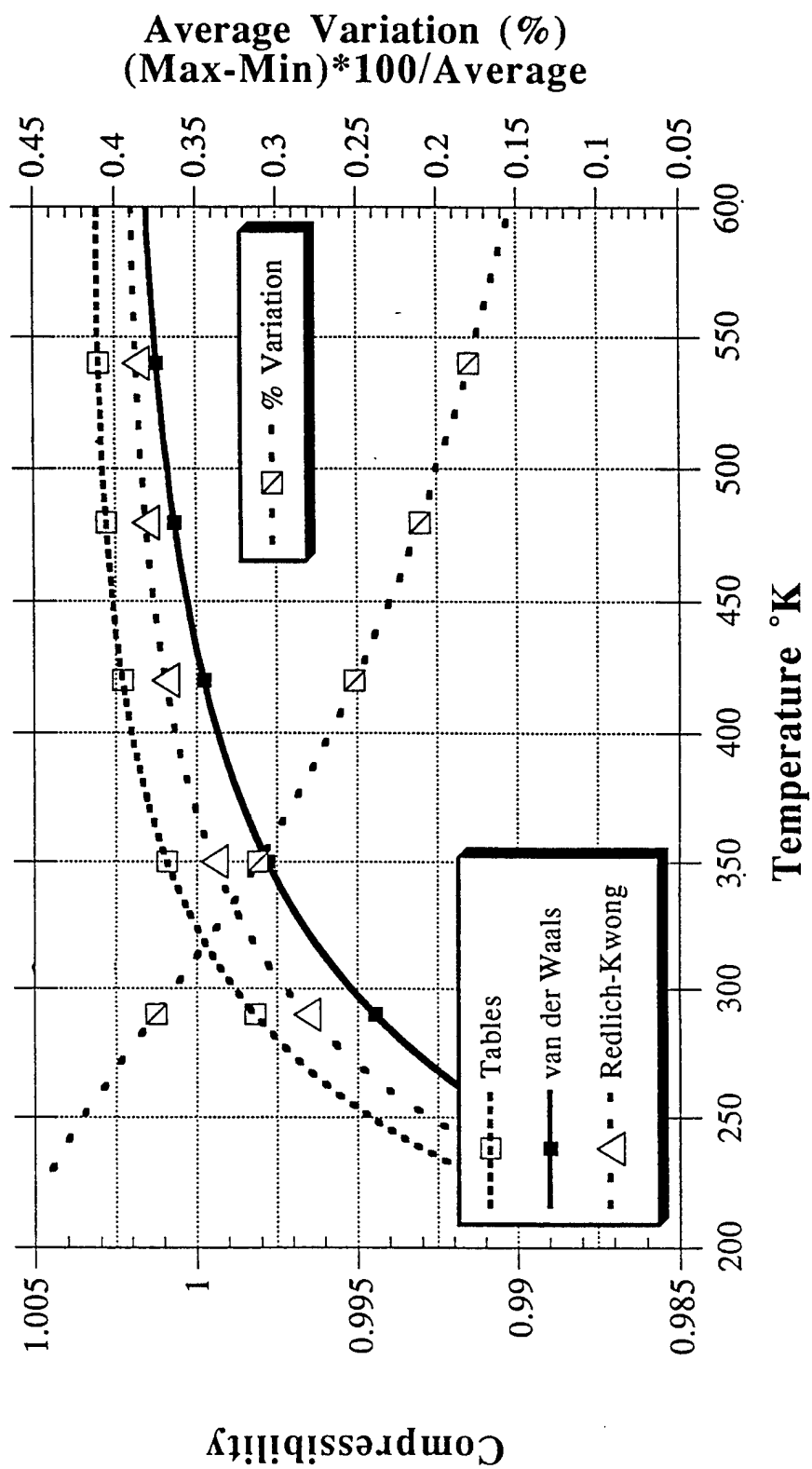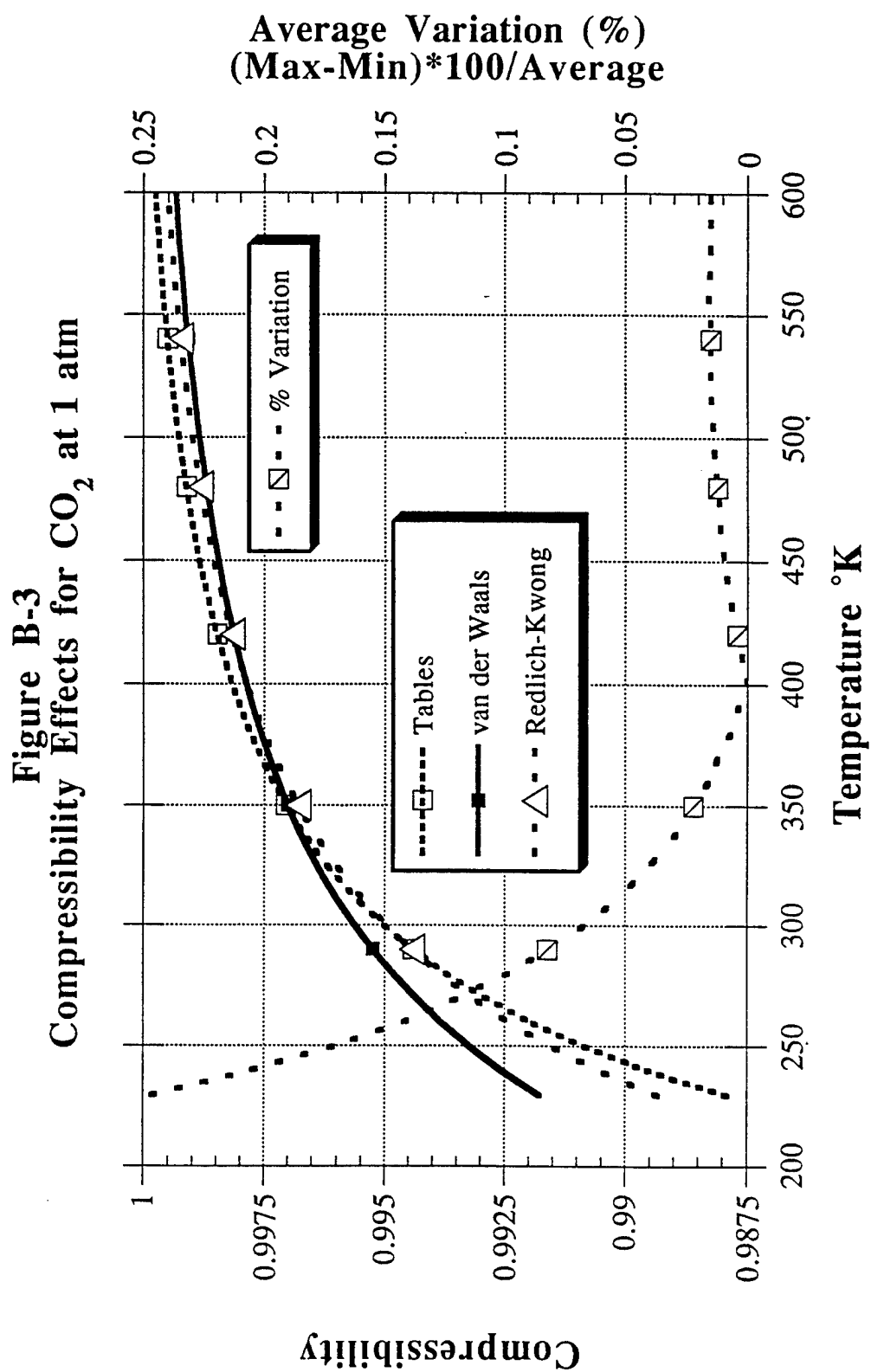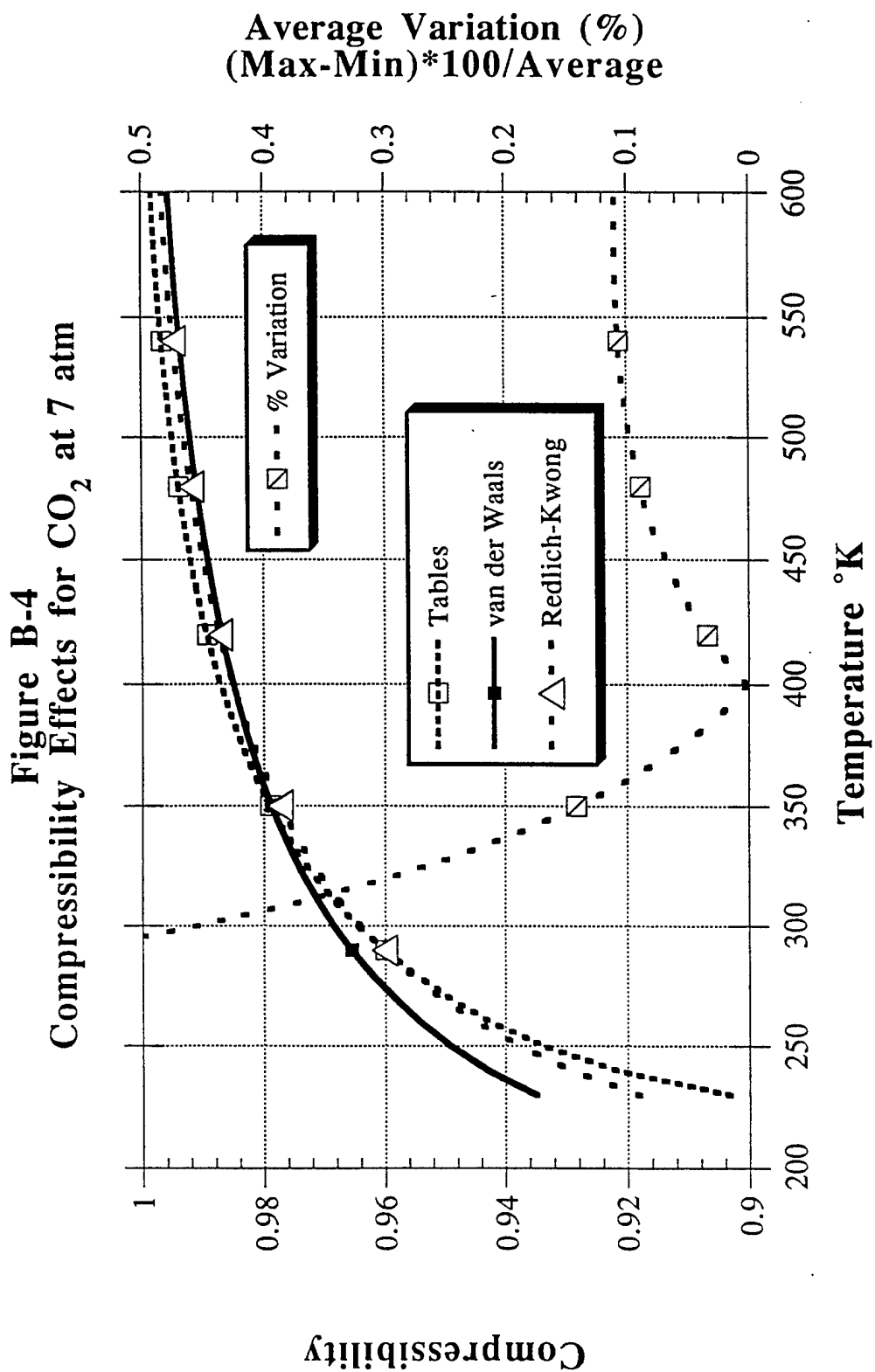
Figure B-1
Compressibility Effects for N_2 at 1 atm

128

Figure B-2
Compressibility Effects for N_2 at 7 atm

129

Figure B-3
Compressibility Effects for CO_2 at 1 atm

130

Figure B-4
Compressibility Effects for CO_2 at 7 atm

Appendix C
Derivation of Isentropic Relationships for a Simple Compressible Gas

For an isentropic process, the temperature, density and pressure between any two points can normally be related to each other through expressions which, for an ideal gas, involve only the ratio of specific heats .

$$\frac{T_2}{T_1} = \left[\frac{\rho_2}{\rho_1}\right]^{\gamma-1} \tag{C-1}$$

$$\frac{T_2}{T_1} = \left[\frac{P_2}{P_1}\right]^{\frac{\gamma-1}{\gamma}} \tag{C-2}$$

Consistent with the ideal gas assumption, the ratio of specific heats is assumed constant. In the case being discussed, real gas effects create a γ which varies during the testing process, thus keeping us from applying equations C-1 and C-2 directly. It is necessary to reexamine the derivations of these equations to determine the importance of the ideal gas assumptions to the engineering questions asked in the ATARR facility. Assuming that the gas mixture behaves as a simple compressible substance, then the entropy can be written as a function of two state variables,

$$s=s(T,v) \text{ and } s=s(T,P) \tag{C-3}$$

where $v=1/\rho$.

Taking the full derivative of both equations yields

$$T(ds)=T\left.\frac{\partial s}{\partial T}\right|_v (dT) +T\left.\frac{\partial s}{\partial v}\right|_T (dv) \tag{C-4}$$

$$T(ds)=T\left.\frac{\partial s}{\partial T}\right|_P (dT) +T\left.\frac{\partial s}{\partial P}\right|_T (dP) \tag{C-5}$$

From the definitions of C_v and C_p:

$$C_v = T\left.\frac{\partial s}{\partial T}\right|_v \tag{C-6}$$

$$C_P = T\left.\frac{\partial s}{\partial T}\right|_P \tag{C-7}$$

and the Maxwell Relationships

$$\left.\frac{\partial s}{\partial v}\right|_T = \left.\frac{\partial p}{\partial T}\right|_v \tag{C-8}$$

$$\left.\frac{\partial s}{\partial P}\right|_T = - \left.\frac{\partial v}{\partial T}\right|_P \tag{C-9}$$

and using the real gas law

$$P=\frac{zRT}{v} \tag{C-10}$$

132

equations C-4 and C-5 become:

$$T(ds) = C_v(dT) + T\frac{R}{v}(z + T\frac{\partial z}{\partial T})(dv)$$

(C-11)

$$T(ds) = C_p(dT) - T\frac{R}{C_p}(z + T\frac{\partial z}{\partial T})(\frac{dP}{P})$$

(C-12)

Since the process being examined is isentropic, these equations reduce to:

$$(\frac{dT}{T}) = -\frac{R}{C_v}(z + T\frac{\partial z}{\partial T})(\frac{dv}{v})$$

(C-13)

$$(\frac{dT}{T}) = \frac{R}{C_p}(z + T\frac{\partial z}{\partial T})(\frac{dP}{P})$$

(C-14)

For an ideal gas the term

$$\frac{R}{C_v}(z + T\frac{\partial z}{\partial T}) = 1-\gamma$$

(C-15)

and

$$\frac{R}{C_p}(z + T\frac{\partial z}{\partial T}) = \frac{1-\gamma}{\gamma}$$

(C-16)

Both of which are constant allowing equations C-13 and C-14 to be integrated, yielding equations C-1 and C-2. Unfortunately, for a real gas C_v, C_p and z depend both on pressure and temperature, and doing this integral and incorporating the result into the blowdown equations becomes quite difficult, if not impossible. Since the compressibility factors for a standard mix are available (see appendix A) and can be calculated for any mixture, we can numerically approximate the derivative of z with respect to T for various pressures. These values are labeled as:

$$\frac{R}{C_v}(z + T\frac{\partial z}{\partial T}) = C1$$

(C-17)

$$\frac{R}{C_p}(z + T\frac{\partial z}{\partial T}) = C2$$

(C-18)

and are listed in table C-1 for the standard fill conditions.

It is clear from both figures C-1 and C-2 that the variations in C1 and C2 from the ideal functions increases as the temperature decreases. And as shown in figure C-3 this variation can be significant (note the difference in values even at the beginning of the test). Since we are ultimately interested in seeing how these properties vary with non-dimensional time (Tc), we can use the ideal gas blowdown relationship between temperature ratio and Tc (equation 5-11) to obtain an approximate plot of C1 and C2 versus Tc (shown in figures C-4 and C-5, plotted only to values of Tc=1.2 since from figure 5-9 the facility will become unchoked for all configurations after this time).

Section 5.2.2 shows that for the standard test gas with a boundary layer bleed of 30%, the final value of Tc is 1.04; which corresponds to a temperature of 480 °K. However to obtain an

133

accurate measure of the mass flow requires a Tc measurement as close to the unchoking point as possible (about Tc=1.13, from equation 5-49) which translates into a temperature of 405°K. One can immediately see the problem. To measure mass flow accurately, one wants to run to as large a value of Tc as possible. To keep the property variations small, one needs to keep Tc as close to one as possible.

The problem that faces us has two distinct components. First we need to find a form for C1 and C2 such that the integrals

$$\int (\frac{dT}{T\ C1}) = \int - (\frac{dv}{v})$$

(C-19)

$$\int (\frac{dT}{T\ C2}) = \int (\frac{dP}{P})$$

(C-20)

can be performed. The natural tendency would be to eliminate the dependency on pressure, and thus C1 and C2 would become only functions of temperature allowing equations C-19 and C-20 to be integrated. However, even if an integration is possible one would then have to substitute the density ratio for the temperature dependance to allow the integration of equation C-21

$$\dot{m}_1 = - \rho_1(0)V\frac{\partial}{\partial t}\left[\frac{\rho(t)}{\rho_1(0)}\right] = (1+\alpha)\rho_1(t)\left[\frac{\dot{m}_3\sqrt{\gamma_c RT_{T3}}}{P_{T3}A_3}\right]\frac{z_1(t)\sqrt{\gamma_c RT_1(t)}A_3}{\gamma_c}$$

(C-21)

The integration of this equation poses two specific problems. One is that the temperature has to be found explicitly as a function of the initial temperature and the density ratio (in some form which would allow integration). Secondly both the corrected mass flow and z vary, not directly as a function of time, but rather as a function of temperature and pressure. Thus before equation C-21 can be integrated all of these parameters have to be put in terms of some common variable (probably temperature) and then integrated with respect to time. In order to do this assumptions have to be made about how important the pressure dependency is, or measurements have to be taken. All of which introduces more variables and uncertainty. The fall-back position is to claim that the ideal gas law hold over very small increments in time. In this fashion one uses the "correct" values for C1, z and m_{corr} at every point during the test to trace how the mass flow and the uncertainty in the mass flow vary over time. The catch to this process is that there is no way to verify how "accurate" the process is unless one can analytically solve equations C-19 and C-20 as a function of time.

With this problem in mind, we can try to evaluate C1 in such a a manner which allows both the integration of equation C-19, and equation C-21. At the end of this process we may have several different ways of calculating the isentropic relationship between temperature and density and we can see how the different procedures vary as a function either of time or temperature.

134

To begin with, both figures C-4 and C-5 show that the variation between pressure levels is small when compared to the change which occurs as the temperature drops. To integrate equations C-19 and C-20, C1 and C2 have to be made independent of pressure. There are several ways to proceed. One could solve for the pressure ratio for any value of Tc and γ, and then interpolate between the two known pressure levels to achieve a trace of either C1 or C2 as a function only of Tc. This however introduces a dependency on γ which might not be appreciated. A second procedure would be to to fit data to any one pressure level and then see how much variation occurs between pressure levels at any value of Tc. The resulting information would be an approximation to the uncertainty which would be introduced by assuming a constant pressure value for either C1 or C2, and in the proper circumstances, be considered small.

Since most measurements will occur at higher values of Tc, we can use the method described above with the 4 atm levels of C1 and C2 as a base line. To obtain an approximate ideal of how the error in this assumption varies with Tc, we can assume that γ remains constant at 1.268 and we can solve for Tc when the pressure level in the supply tank would approach 1 atm (this assumes that the supply tank is constantly dumping into a vacuum) which yields a Tc of 1.23. At the beginning of the run the pressure is 7 atm and the pressure level is 4 atm at Tc = 1.06. We can use these three points to see how the variation occurs which is shown in figures C-6 and C-7.

Using this information we can now claim that the 4 atm data represents the actual C1 and C2 to the level of accuracy listed in figures C-6 and C-7 (note that this number approaches zero at the values of Tc where efficiency measurement may occur). The approximation of pressure independence is quite good since for most of the test time variation is less then 0.1%. At this point both C1 and C2 can be approximated by several different types of functions. One possible type would be a second order polynomial as listed below

$$\frac{R}{C_v}(z +T\frac{\partial z}{\partial T}) =C1 =a_0 + a_1X + a_2X^2$$

(C-22)

With the choice of X being arbitrary. One could use the absolute temperature, but then the constant a_2 becomes small, and round-off errors could become significant. A better choice is the normalized temperature $Tr=T/T_0$ ($T_0 =520$ °K). However the integration becomes complicated and in fact takes the form:

$$\frac{T(t)}{T(0)} = \left[\frac{\rho(t)}{\rho(0)}\right]^{a_0} F_1$$

(C-23)

where

135

$$F_1 = \left[\frac{C1(T)}{C1(0)}\right]^{.5} \exp\left[\frac{a_1}{\sqrt{4a_2a_0 - a_1^2}}\tan^{-1}\left[\frac{\sqrt{4a_2a_0 - a_1^2}(1 - \frac{T(t)}{T(0)})}{2a_0 + a_1 + (2a_2 + a_1)\frac{T(t)}{T(0)}}\right]\right]$$

(C-24)

One cannot explicitly solve for the temperature ratio (since it not only appears in the exponent but also in the values for C1). Another function which has a little more promise is an inverse logarithm, or:

$$C1 = \frac{1}{a_0 + a_1 Ln(Tr)}$$

(C-25)

(similar function for C2). These functions fit the data quite well (variations less then 0.06%) as shown in figures C-8 to C-11. Putting this functional form into equations C-19 and C-20 results in the following expressions:

$$Tr^{a_0}\ exp[\frac{a_1}{2}\{ln(Tr)\}^2] = \frac{\rho_2}{\rho_1}$$

(C-26)

and

$$Tr^{b_0}\ exp[\frac{b_1}{2}\{ln(Tr)\}^2] = \frac{P_2}{P_1}$$

(C-27)

Equations C-26 and C-27 can not be used in equation C-21 as they stand (since one cannot not isolate the temperature ratios, nor if one could, would one be able to integrate the resulting mess). However these functions can be fit to another more manageable form. Labeling the function on the left side of equations C-26 and C-27 as D1 and D2 we can fit these to a power function.

$$D1 = a_0' Tr^{a_1}$$

(C-28)

(similar expression for D2, the primes denote new variables). With these functions in place, then the integration of equation C-21 can take place. The fit for D1 and D2 is shown in figure C-12. this is not as good as fit as before, and at this point we have compounded the uncertainty in this result through three different data fits! All of which have different dependencies on the temperature (and thus Tc).

Before we proceed it is worthwhile to see how these different methods predict the density ratio. Figure C-13 and C-13a (expanded view) show five different ways of calculating the density ratio based on the temperature ratio. The first assumes a constant value of γ set at the initial value 1.268. The second uses the relationship:

$$Tr^{C1^{-1}} = \frac{\rho_2}{\rho_1}$$

(C-29)

where C1 is allowed to vary with the temperature. The third case is the power fit or:

$$a_0' Tr^{a_1'} = \frac{\rho_2}{\rho_1}$$

(C-30)

The last two cases use the form:

$$Tr^{(\gamma-1)^{-1}} = \frac{\rho_2}{\rho_1}$$

(C-31)

where γ is either the value at 7 atm or 4 atm (varying with temperature).

The results are rather interesting and are best seen in figure C-13a. The density ratio calculated from the power fit and from $\gamma = 1.268$ lie close together at low values of Tr. The method which uses C1 is bounded on both sides, one by γ evaluated at 7 atm and the other at $\gamma=1.268$. Figure C-14 shows the difference in methods between using the power fit, γ at 7 atm, and γ at 1.268, and C1. As one can see the variations can become quite large as Tr drops off. One other interesting piece of information is that if one uses the γ calculated in Appendix A which is independent of pressure (it is only a function of temperature) in equation C-31 and plot this and values calculated using C1, one finds variations which are quite small (when compared to these other methods, figures C-15 and C-15a).

As predicted at the beginning we do not have nay real way to determine which method is providing the true answer. It is interesting to note that one would expect the density ratio evaluated with a γ at 7 atm to give a high value (since γ is increasing with decreasing temperature) and thus the density ratio calculated with $\gamma=1.268$ should give a low value, since this is the lowest value of γ during the entire test. And using either C1 (which is evaluated at 4 atm) or γ independent of pressure provide answers which are close to each other and are in between these two extremes. We are still caught in the quandary of which method to use. Since the variable C1 takes into account compressibility it is probably the better variable to use. And since we will be evaluating the isentropic relationship at every point in time and substituting in the correct values for C1 we can also do this in equation C-21 for γ and z allowing a full integration which implies that the blowdown equations are the same as equation 5-11 except the variable γ-1 is replaced by C1 and that τ takes into account compressibility factors.

$$\frac{\rho(t)}{\rho(0)} = \left[\frac{t}{\tau}+1\right]^{\frac{2}{-C1}}$$

$$\frac{1}{\tau} = \frac{(\frac{C1}{2})(1+\alpha)z_1(t)\sqrt{\gamma_c RT_1(0)}A_3}{\gamma_c V}\left[\frac{\dot{m}_3\sqrt{\gamma_c RT_{T3}}}{P_{T3}A_3}\right]$$

(C-32)

$$\frac{T(t)}{T(0)} = \left[\frac{t}{\tau}+1\right]^{-2}$$

(C-33)

$$\frac{P(t)}{P(0)} = \left[1+\frac{t}{\tau}\right]^{\frac{-2}{C2}}$$

(C-34)

137

Table C-1
Values For C1 and C2

Standard Fill Conditions: P2/P1=3.054   M2/M1= 3.24   R2/R1= .6366

Temperature °K	Z Mixture			T(dZ/dT) Mixture		
	Z (1 atm)	Z (4 atm)	Z (7 atm)	T(dZ/dT) (7 atm)	T(dZ/dT) (4 atm)	T(dZ/dT) (1 atm)
230	0.99146	0.96444	0.93211	0.30778	0.12862	0.02693
240	0.99261	0.96991	0.94521	0.19681	0.09597	0.02282
250	0.99358	0.97400	0.95358	0.14463	0.07764	0.01895
260	0.99439	0.97730	0.95974	0.11657	0.06444	0.01595
270	0.99507	0.98004	0.96470	0.09816	0.05583	0.01374
280	0.99565	0.98242	0.96887	0.08458	0.04746	0.01169
290	0.99615	0.98444	0.97247	0.07440	0.04067	0.01019
300	0.99658	0.98617	0.97564	0.06270	0.03561	0.00884
310	0.99696	0.98768	0.97831	0.05583	0.03214	0.00758
320	0.99728	0.98905	0.98068	0.04904	0.02716	0.00679
330	0.99757	0.99021	0.98277	0.04233	0.02369	0.00592
340	0.99782	0.99121	0.98457	0.03727	0.02227	0.00545
350	0.99805	0.99216	0.98616	0.03373	0.01911	0.00458
360	0.99825	0.99298	0.98759	0.03041	0.01698	0.00426
370	0.99843	0.99370	0.98889	0.02693	0.01501	0.00371
380	0.99859	0.99434	0.99003	0.02362	0.01351	0.00340
390	0.99873	0.99491	0.99104	0.02251	0.01224	0.00300
400	0.99886	0.99543	0.99200	0.01951	0.01114	0.00269
410	0.99897	0.99591	0.99283	0.01746	0.00995	0.00253
420	0.99908	0.99633	0.99357	0.01588	0.00901	0.00221
430	0.99917	0.99671	0.99424	0.01446	0.00822	0.00198
440	0.99926	0.99706	0.99486	0.01296	0.00735	0.00198
450	0.99934	0.99738	0.99541	0.01193	0.00680	0.00174
460	0.99942	0.99766	0.99592	0.01082	0.00616	0.00150
470	0.99948	0.99793	0.99638	0.00996	0.00569	0.00127
480	0.99953	0.99817	0.99680	0.00909	0.00506	0.00134
490	0.99959	0.99838	0.99719	0.00846	0.00482	0.00118
500	0.99964	0.99859	0.99755	0.00759	0.00435	0.00111
510	0.99969	0.99877	0.99787	0.00696	0.00403	0.00103
520	0.99973	0.99895	0.99817	0.00656	0.00364	0.00095
530	0.99977	0.99910	0.99845	0.00593	0.00340	0.00087
540	0.99981	0.99925	0.99870	0.00553	0.00324	0.00079
550	0.99984	0.99938	0.99894	0.00514	0.00293	0.00063
560	0.99987	0.99951	0.99915	0.00467	0.00261	0.00063
570	0.99990	0.99962	0.99935	0.00435	0.00253	0.00063
580	0.99992	0.99973	0.99954	0.00396	0.00222	0.00071
590	0.99996	0.99982	0.99971	0.00380	0.00222	0.00047
600	0.99998	0.99991	0.99987			

Table C-1 (con't)
Values For C1 and C2

Temp. °K	Cv (Mixture)			C1 (Mixture)			Specific Heat Ratio (Mixture)			C2 (Mixture)		
	1 atm	4 atm	7 atm	1 atm	4 atm	7 atm	1 atm	4 atm	7 atm	1 atm	4 atm	7 atm
230	0.6250	0.6780	0.8443	0.3493	0.3456	0.3148	1.358	1.392	1.445	0.2573	0.2482	0.2178
240	0.6322	0.6620	0.7432	0.3443	0.3452	0.3294	1.352	1.379	1.407	0.2547	0.2503	0.2341
250	0.6399	0.6571	0.6932	0.3392	0.3431	0.3396	1.345	1.370	1.395	0.2521	0.2503	0.2434
260	0.6477	0.6594	0.6760	0.3344	0.3387	0.3413	1.340	1.362	1.385	0.2495	0.2486	0.2464
270	0.6554	0.6636	0.6702	0.3300	0.3346	0.3399	1.335	1.355	1.378	0.2471	0.2469	0.2467
280	0.6635	0.6705	0.6767	0.3255	0.3292	0.3337	1.330	1.348	1.368	0.2447	0.2442	0.2439
290	0.6712	0.6774	0.6831	0.3214	0.3244	0.3285	1.326	1.342	1.359	0.2425	0.2418	0.2416
300	0.6792	0.6845	0.6895	0.3173	0.3200	0.3228	1.321	1.336	1.352	0.2403	0.2396	0.2388
310	0.6867	0.6914	0.6963	0.3136	0.3162	0.3184	1.317	1.330	1.344	0.2381	0.2378	0.2370
320	0.6940	0.6985	0.7025	0.3102	0.3119	0.3142	1.314	1.325	1.337	0.2361	0.2354	0.2350
330	0.7016	0.7054	0.7088	0.3066	0.3081	0.3100	1.309	1.320	1.332	0.2342	0.2334	0.2328
340	0.7089	0.7121	0.7154	0.3034	0.3051	0.3062	1.306	1.316	1.326	0.2323	0.2319	0.2310
350	0.7160	0.7189	0.7219	0.3002	0.3015	0.3029	1.303	1.312	1.321	0.2304	0.2299	0.2293
360	0.7231	0.7258	0.7285	0.2972	0.2983	0.2996	1.299	1.308	1.316	0.2287	0.2281	0.2277
370	0.7298	0.7322	0.7348	0.2944	0.2953	0.2964	1.297	1.304	1.312	0.2270	0.2264	0.2260
380	0.7369	0.7388	0.7411	0.2915	0.2924	0.2932	1.293	1.301	1.307	0.2254	0.2248	0.2243
390	0.7436	0.7453	0.7472	0.2888	0.2897	0.2908	1.291	1.297	1.304	0.2238	0.2233	0.2230
400	0.7500	0.7518	0.7537	0.2862	0.2870	0.2877	1.288	1.294	1.300	0.2223	0.2218	0.2214
410	0.7566	0.7579	0.7594	0.2838	0.2845	0.2852	1.285	1.291	1.297	0.2208	0.2204	0.2199
420	0.7629	0.7645	0.7655	0.2813	0.2819	0.2827	1.283	1.288	1.294	0.2194	0.2189	0.2185
430	0.7688	0.7705	0.7717	0.2791	0.2796	0.2802	1.281	1.285	1.290	0.2180	0.2176	0.2172
440	0.7751	0.7765	0.7775	0.2769	0.2773	0.2778	1.278	1.282	1.287	0.2167	0.2162	0.2158
450	0.7810	0.7821	0.7833	0.2748	0.2752	0.2757	1.276	1.280	1.285	0.2153	0.2150	0.2146
460	0.7867	0.7882	0.7890	0.2727	0.2730	0.2735	1.274	1.278	1.282	0.2140	0.2137	0.2134
470	0.7929	0.7936	0.7947	0.2705	0.2711	0.2715	1.271	1.276	1.279	0.2128	0.2125	0.2122
480	0.7986	0.7994	0.8004	0.2687	0.2690	0.2694	1.270	1.273	1.277	0.2116	0.2113	0.2110
490	0.8042	0.8049	0.8057	0.2668	0.2672	0.2676	1.268	1.271	1.275	0.2104	0.2102	0.2099
500	0.8099	0.8104	0.8114	0.2649	0.2653	0.2655	1.266	1.269	1.272	0.2093	0.2090	0.2088
510	0.8153	0.8157	0.8165	0.2631	0.2635	0.2638	1.264	1.267	1.270	0.2082	0.2080	0.2077
520	0.8207	0.8211	0.8217	0.2614	0.2617	0.2621	1.262	1.265	1.268	0.2071	0.2069	0.2067
530	0.8257	0.8263	0.8270	0.2598	0.2601	0.2603	1.261	1.263	1.266	0.2061	0.2059	0.2056
540	0.8310	0.8315	0.8321	0.2581	0.2584	0.2587	1.259	1.261	1.264	0.2050	0.2049	0.2047
550	0.8363	0.8368	0.8372	0.2564	0.2568	0.2571	1.257	1.260	1.262	0.2040	0.2039	0.2037
560	0.8411	0.8420	0.8423	0.2550	0.2551	0.2555	1.256	1.258	1.260	0.2030	0.2029	0.2027
570	0.8463	0.8465	0.8473	0.2534	0.2538	0.2539	1.254	1.256	1.258	0.2021	0.2020	0.2018
580	0.8510	0.8517	0.8523	0.2520	0.2522	0.2524	1.253	1.255	1.256	0.2012	0.2010	0.2009
590	0.8562	0.8568	0.8567	0.2505	0.2507	0.2511	1.251	1.253	1.255	0.2002	0.2001	0.2000
600	0.8608	0.8612	0.8616	0.2490	0.2489	0.2488	1.250	1.252	1.253	0.1992	0.1989	0.1985

Figure C-1

C1 and γ as a Function of Temperature and Pressure
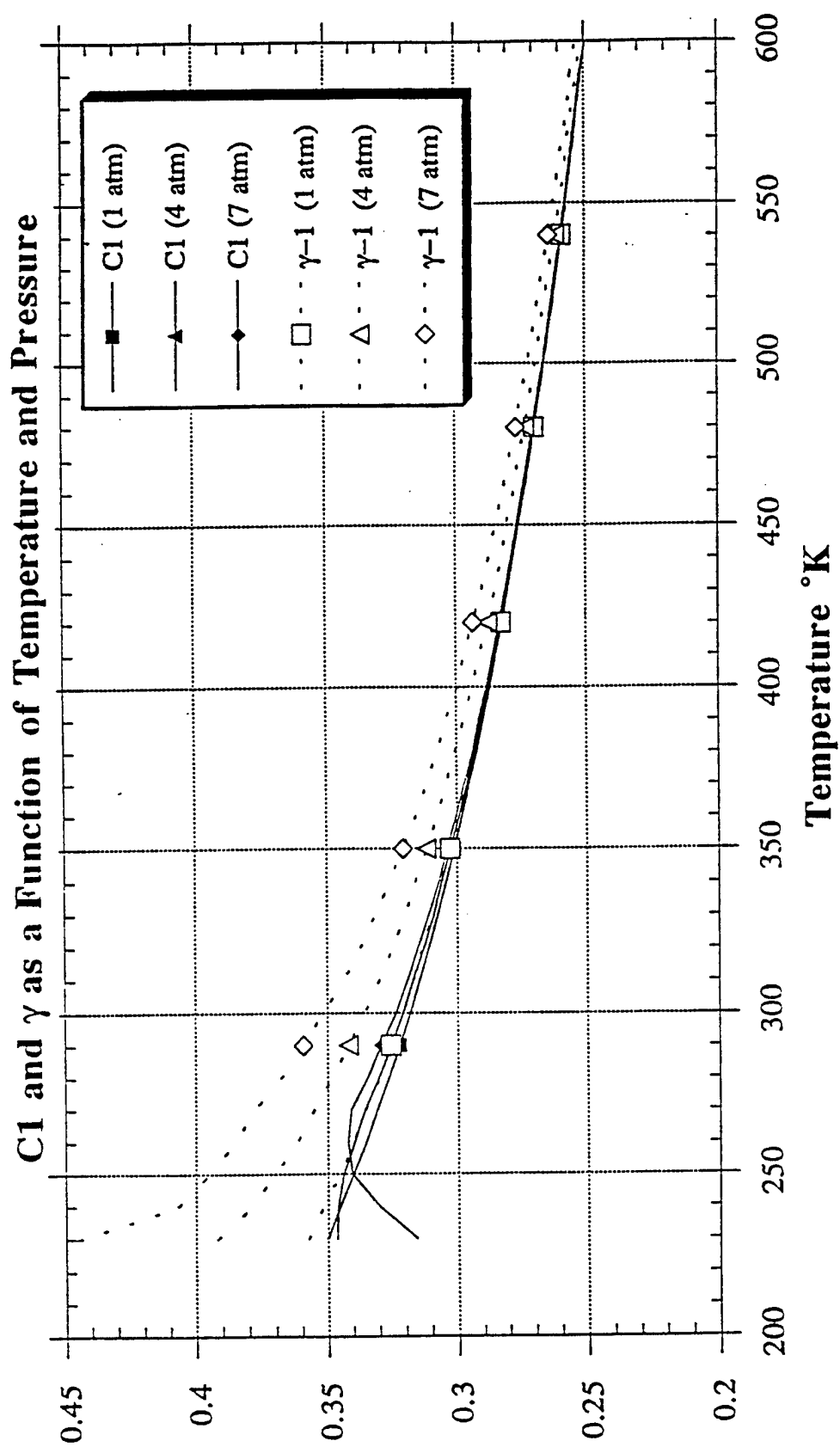
Figure C-2

C2 and $(\gamma-1)/\gamma$ as a Function of Temperature and Pressure

141

Figure C-3

Variation Between C1, C2 and F(γ) Over Test Temperature Range

Legend:
- ■ $((\gamma-1) - C1_{(7 \text{ atm}, 520 \text{ K})})/C1_{(7 \text{ atm}, 520 \text{ K})}$
- ▲ $((\gamma-1)/\gamma - C2_{(7 \text{ atm}, 520 \text{ K})})/C2_{(7 \text{ atm}, 520 \text{ K})}$

Temperature °K

% Variation

Figure C-4

C1 and γ as a Function of Pressure and
Non-Dimensional Time (Tc)

143
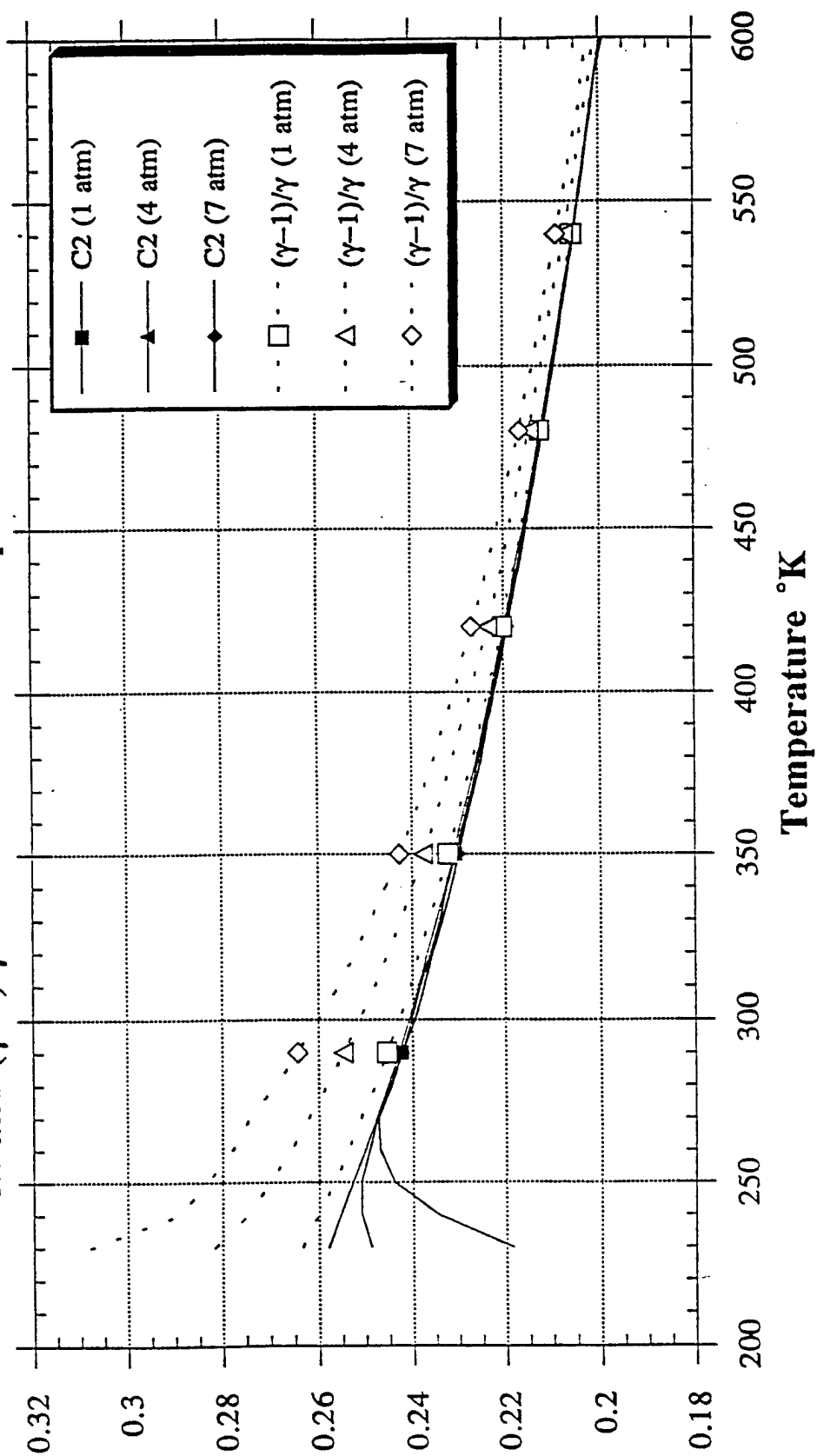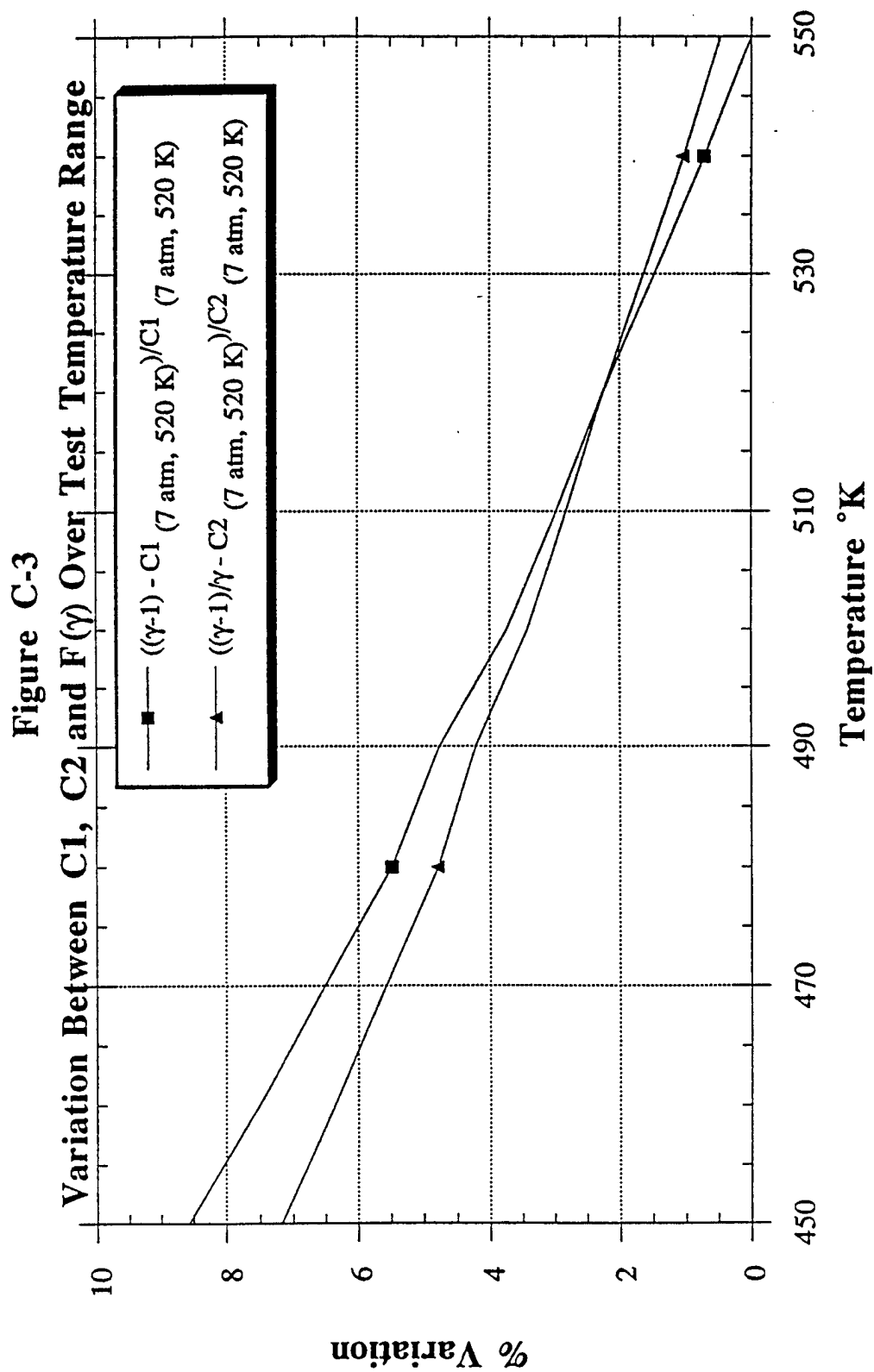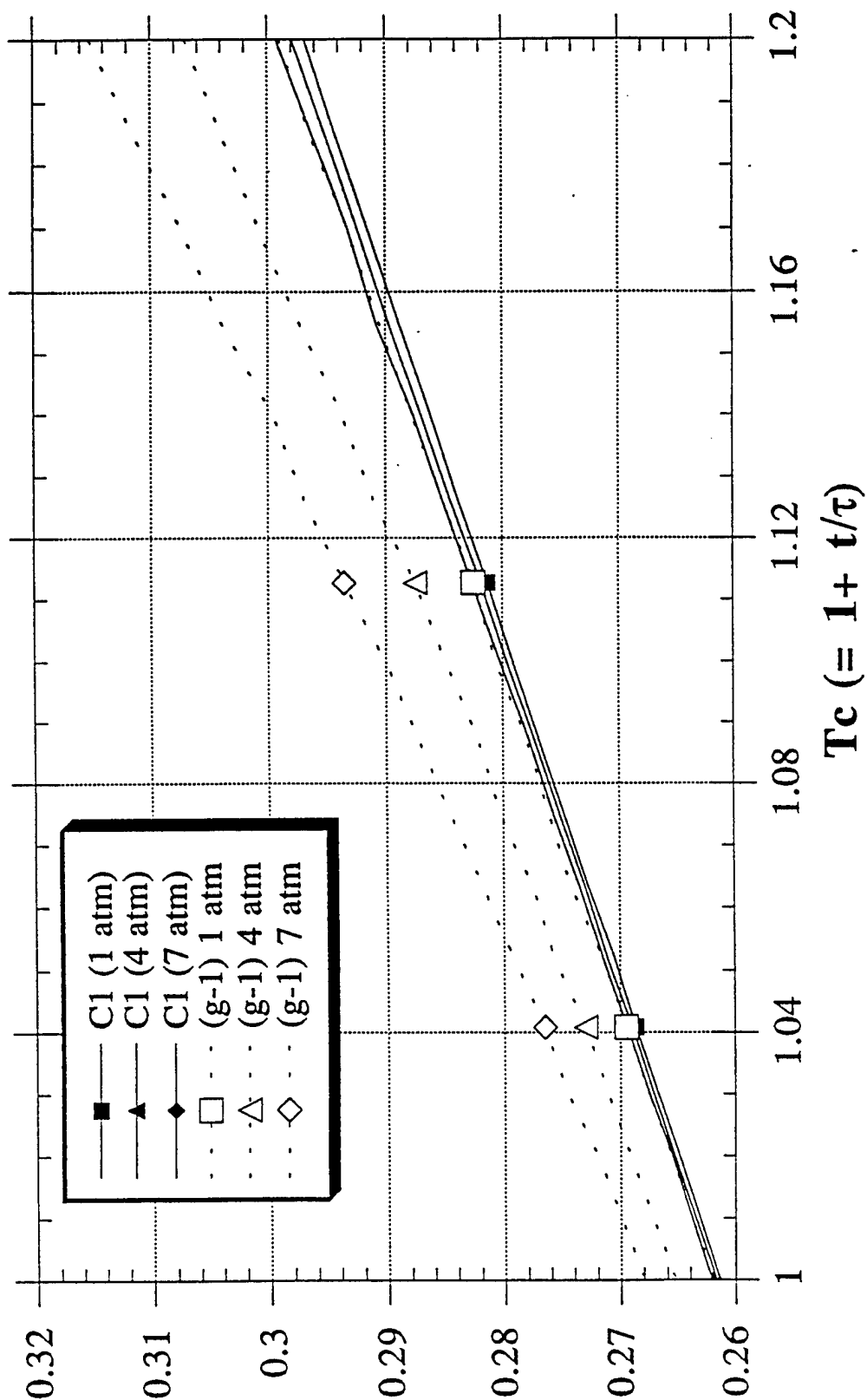
Figure C-5

C2 and γ as a Function of Pressure and Non-Dimensional Time (Tc)
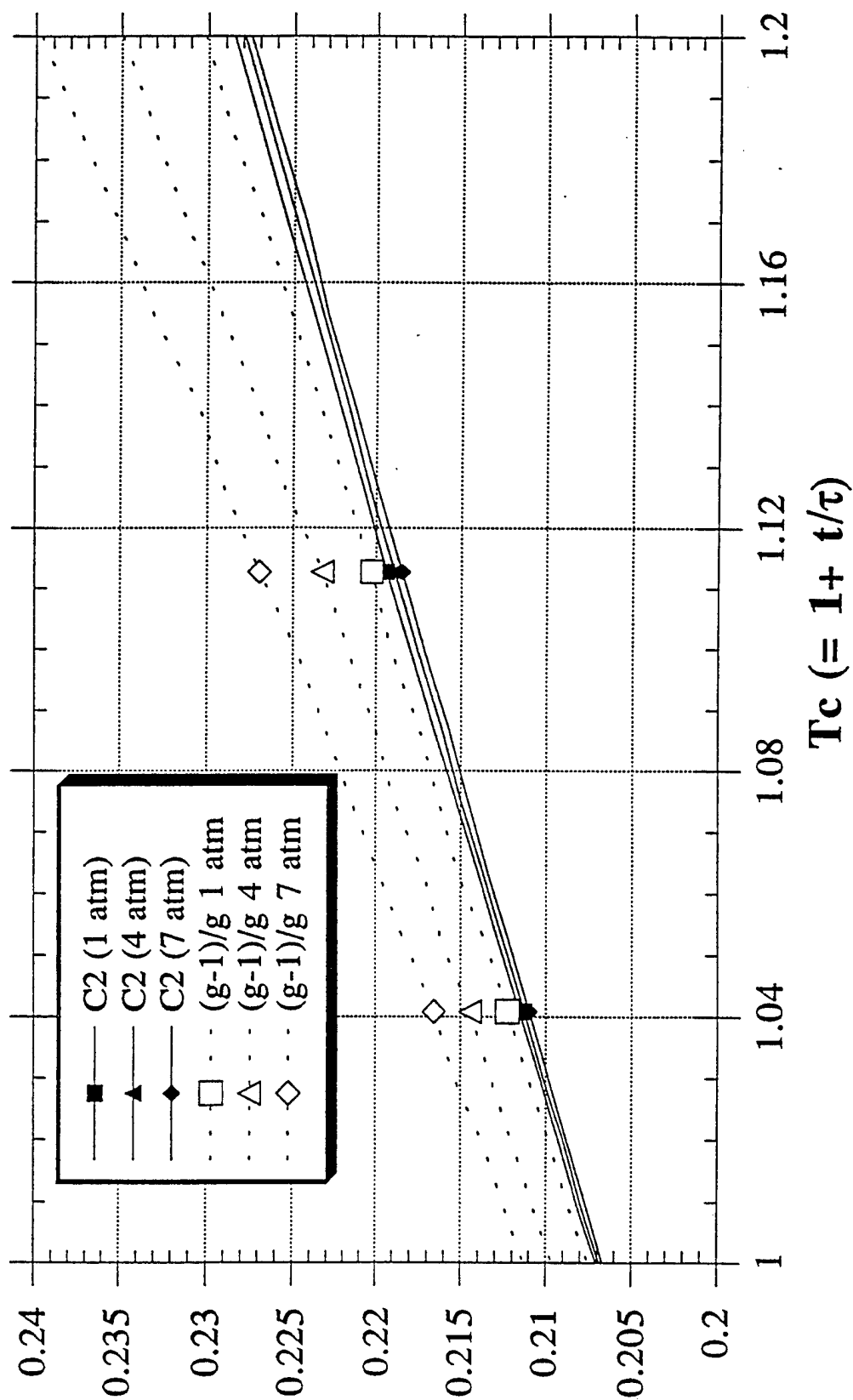
Figure C-6
% Variation in Actual C1 from C1 at 4 atm
(approximation)

145
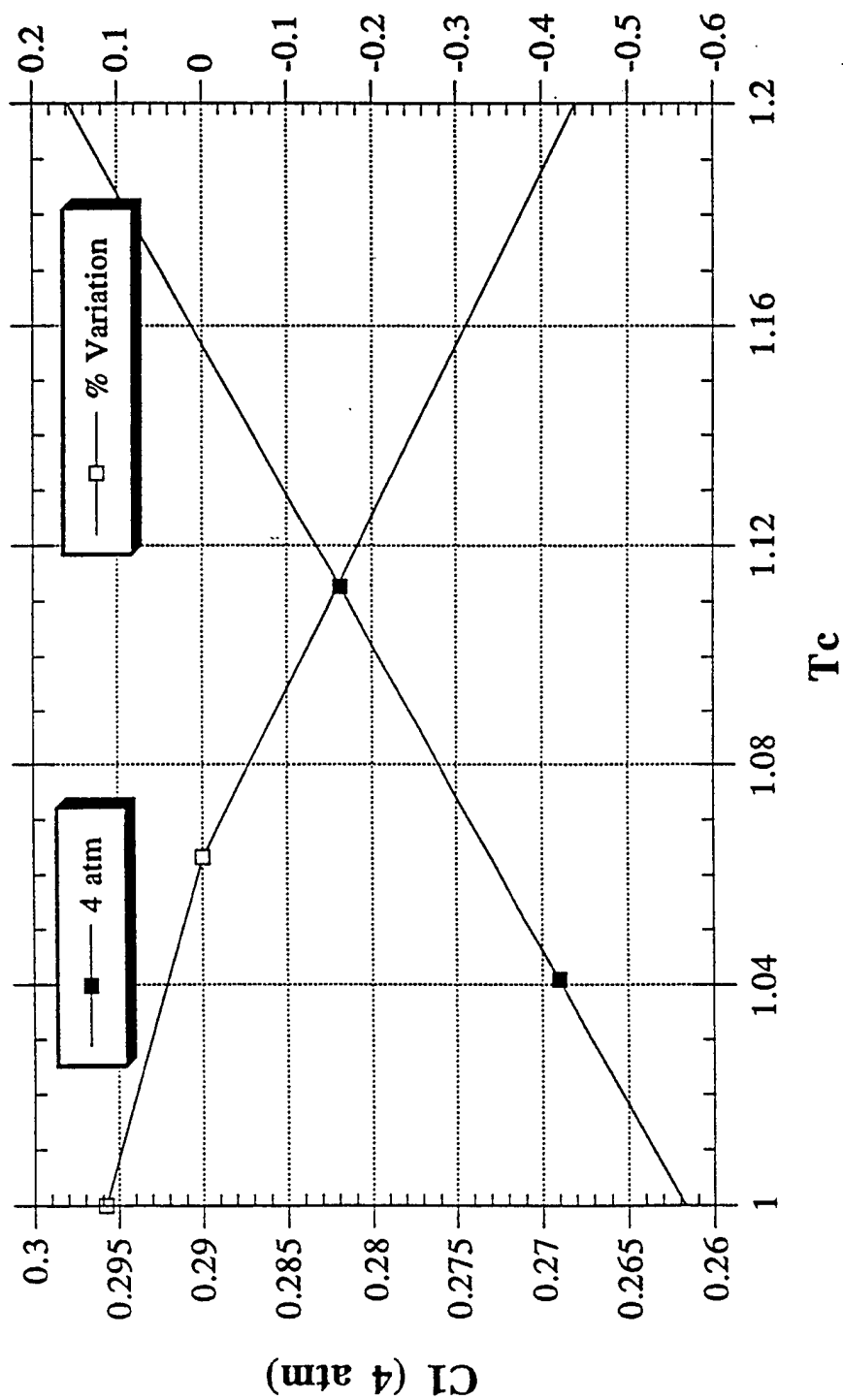
Figure C-7
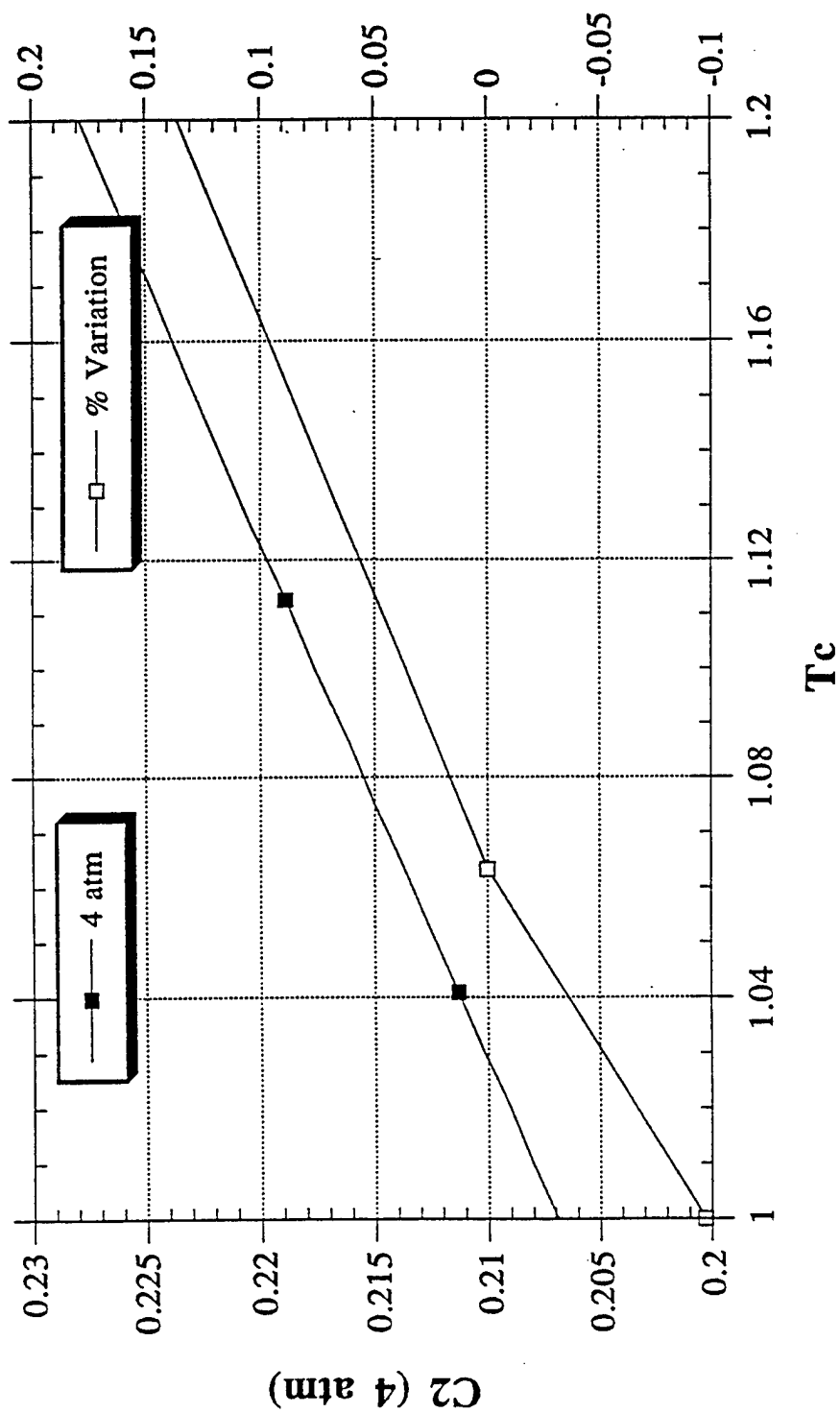
% Variation in Actual C2 from C2 at 4 atm
(approximation)

Figure C-8
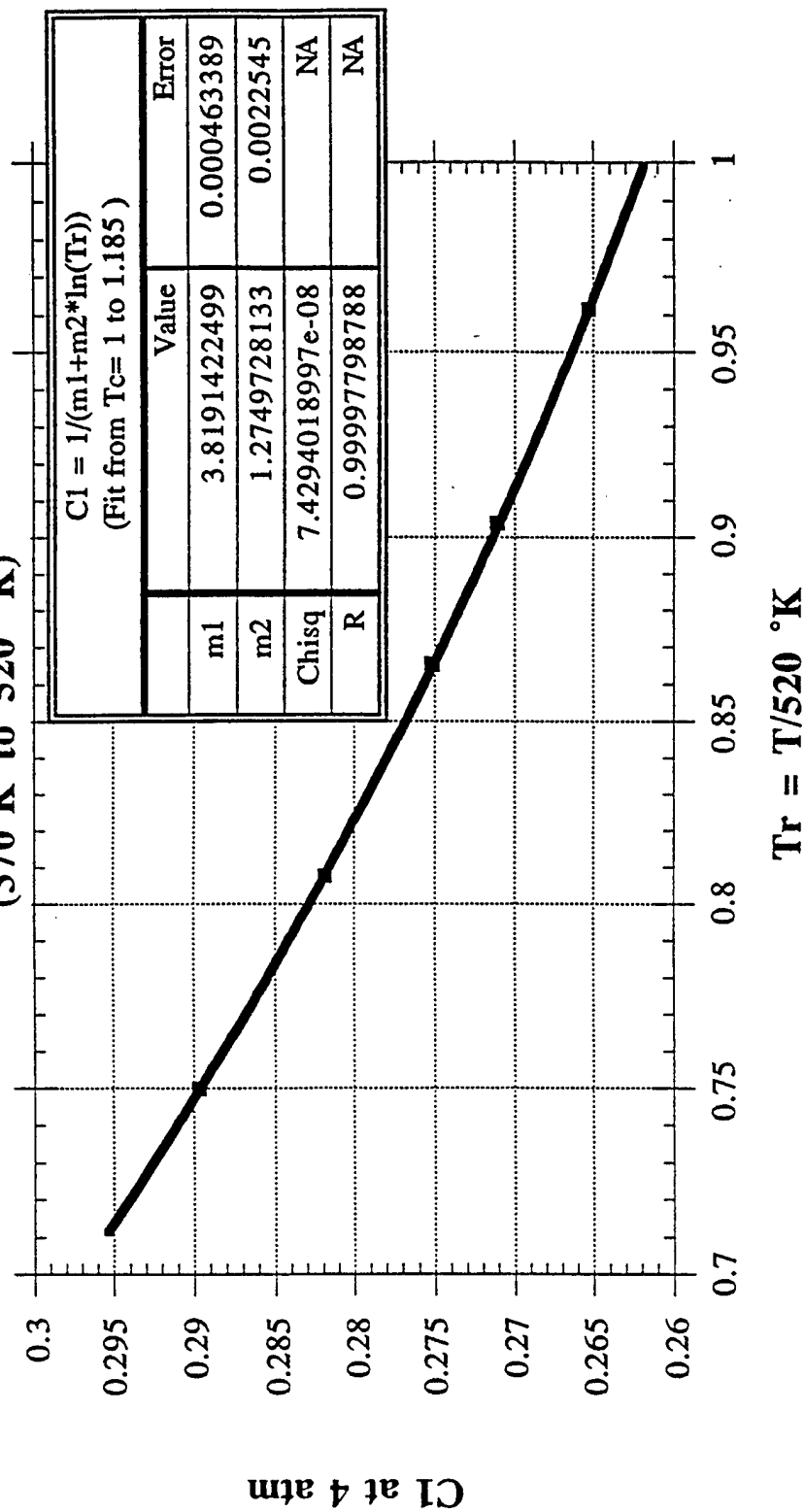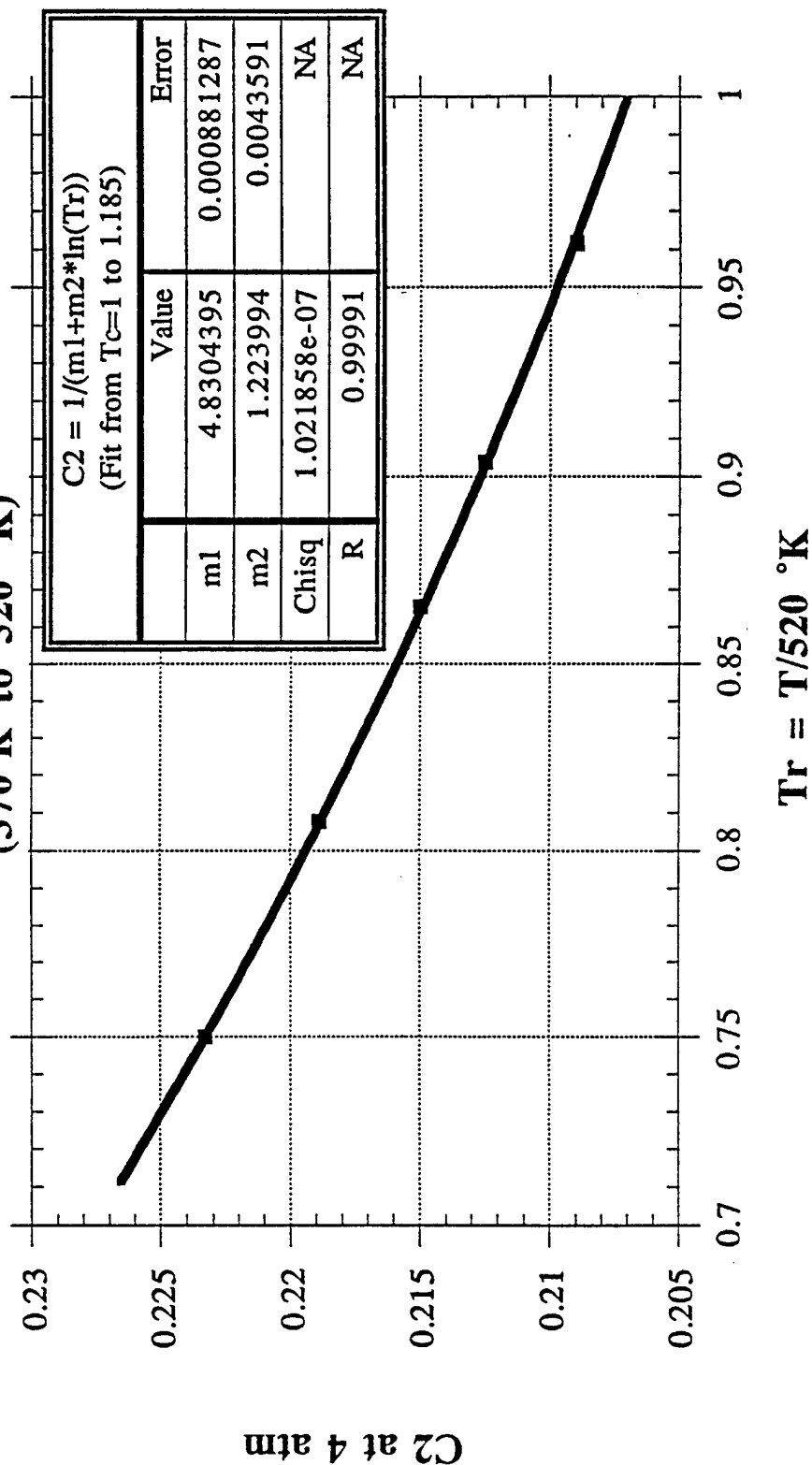## 1/log fit for C1 versus Tr (=T/T$_0$)
(370°K to 520 °K)

		Value	Error
	C1 = 1/(m1+m2*ln(Tr))		
	(Fit from Tc= 1 to 1.185)		
m1		3.8191422499	0.000463389
m2		1.2749728133	0.0022545
Chisq		7.4294018997e-08	NA
R		0.9999798788	NA

C1 at 4 atm (vertical axis)

Tr = T/520 °K (horizontal axis)

Figure C-9
1/log fit for C2 versus Tr ($=T/T_0$)
(370°K to 520 °K)

		Value	Error
$C2 = 1/(m1+m2*\ln(Tr))$ (Fit from Tc=1 to 1.185)	m1	4.8304395	0.00081287
	m2	1.223994	0.0043591
	Chisq	1.021858e-07	NA
	R	0.99991	NA

Tr = T/520 °K

C2 at 4 atm

Figure C-10
% Variation Between C1 and 1/log fit of C1

149

Figure C-11
% Variation Between C2 and 1/log fit of Cl^2
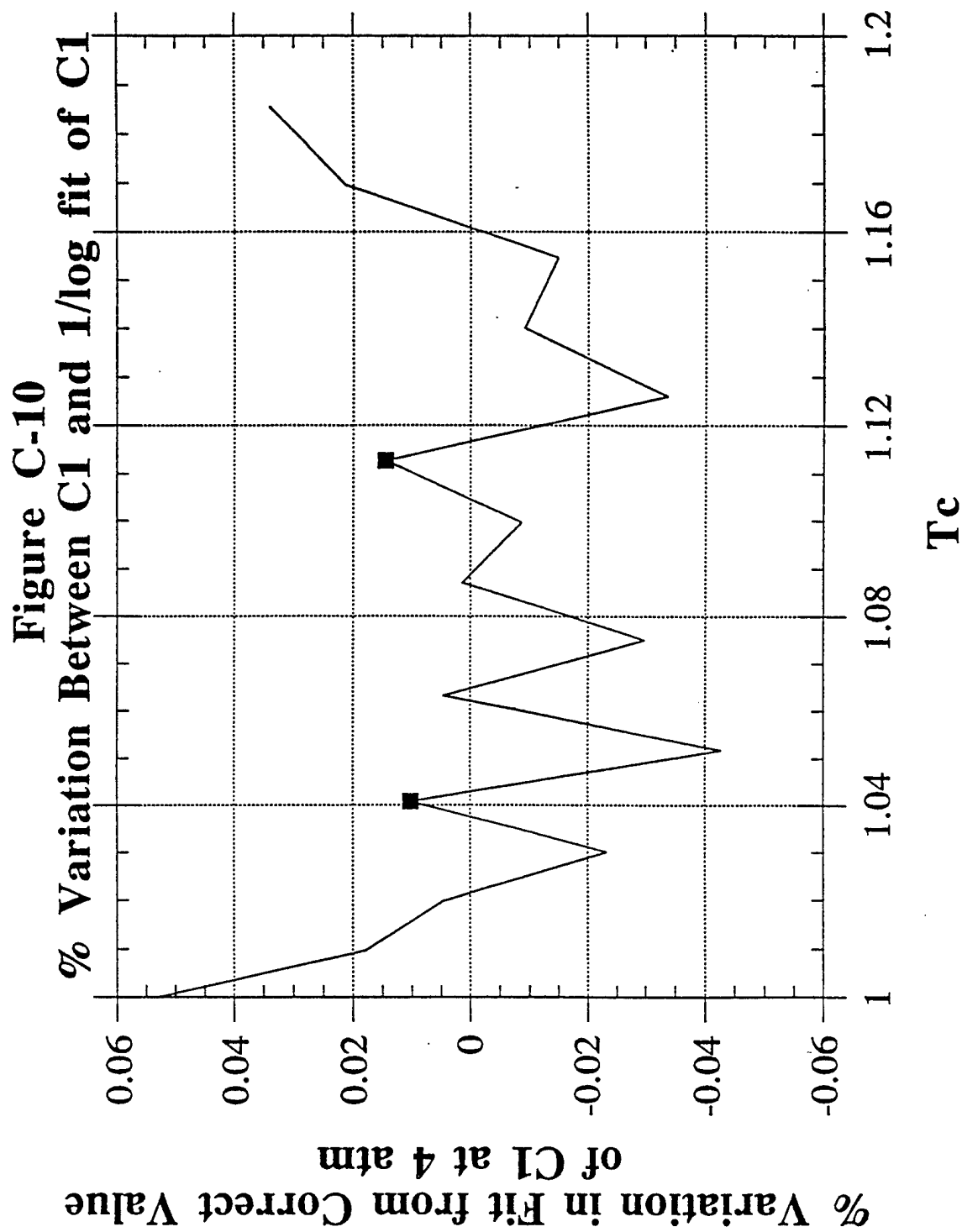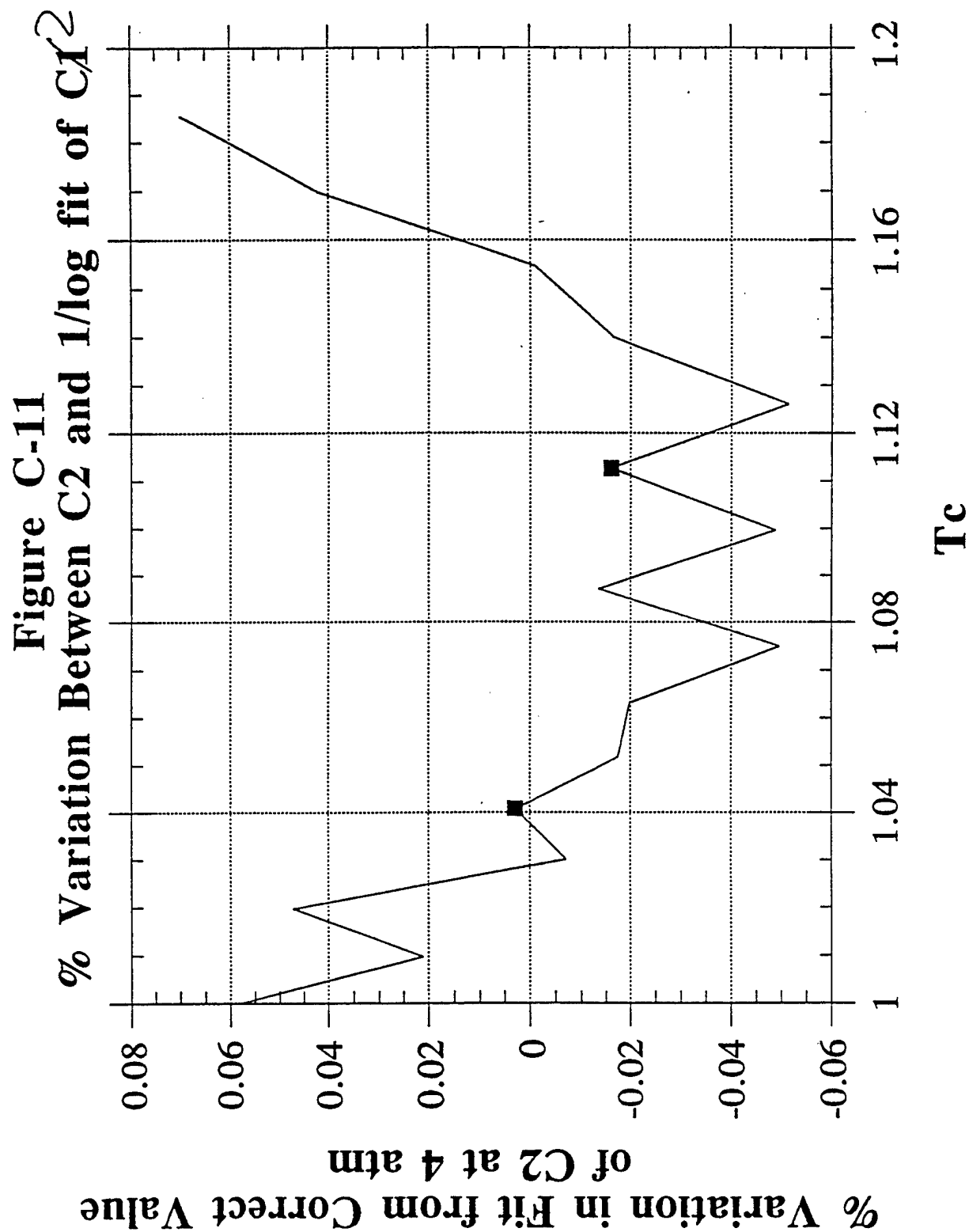
Figure C-12
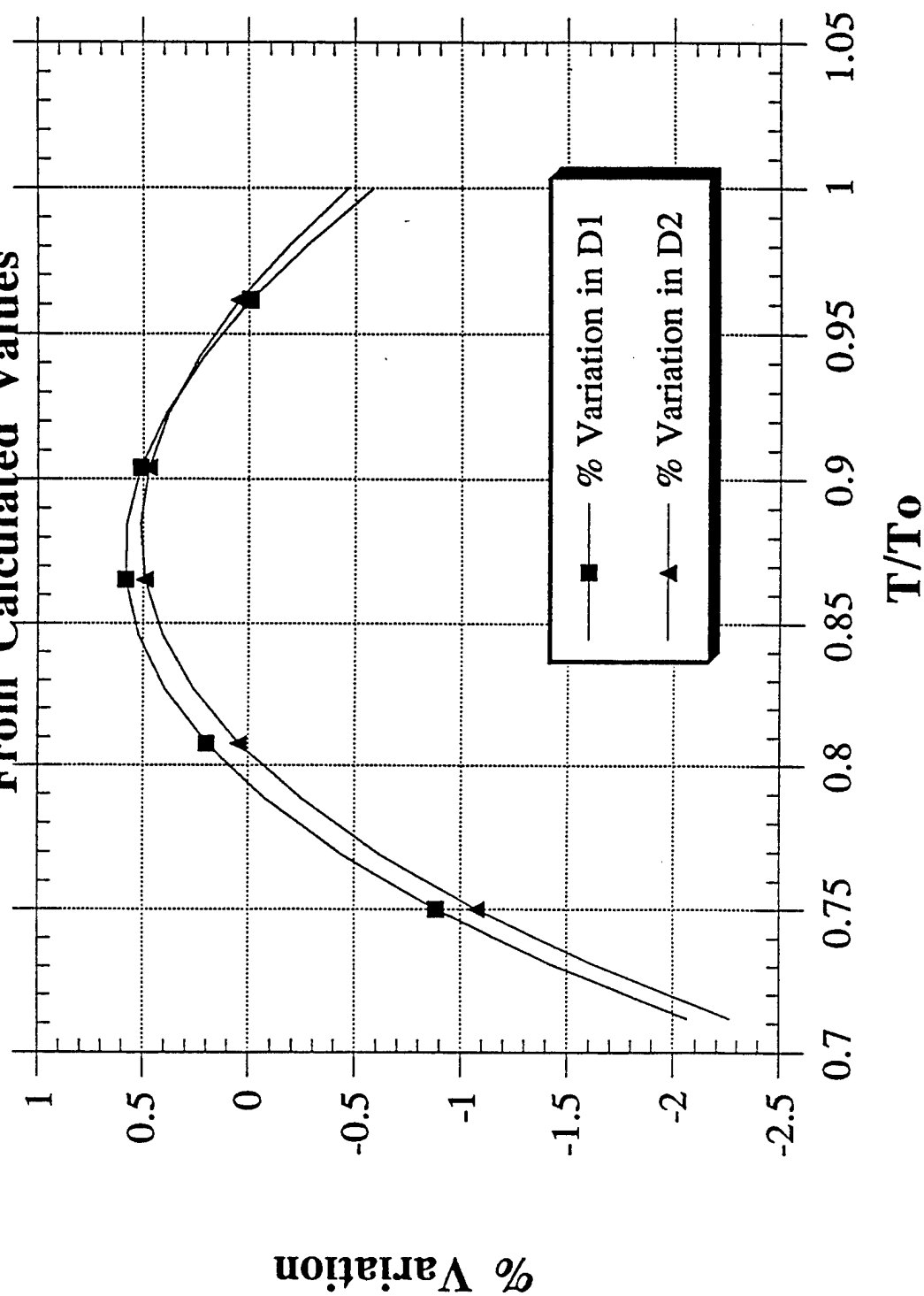Variation in Fits of D1 and D2
From Calculated Values

Figure C-13

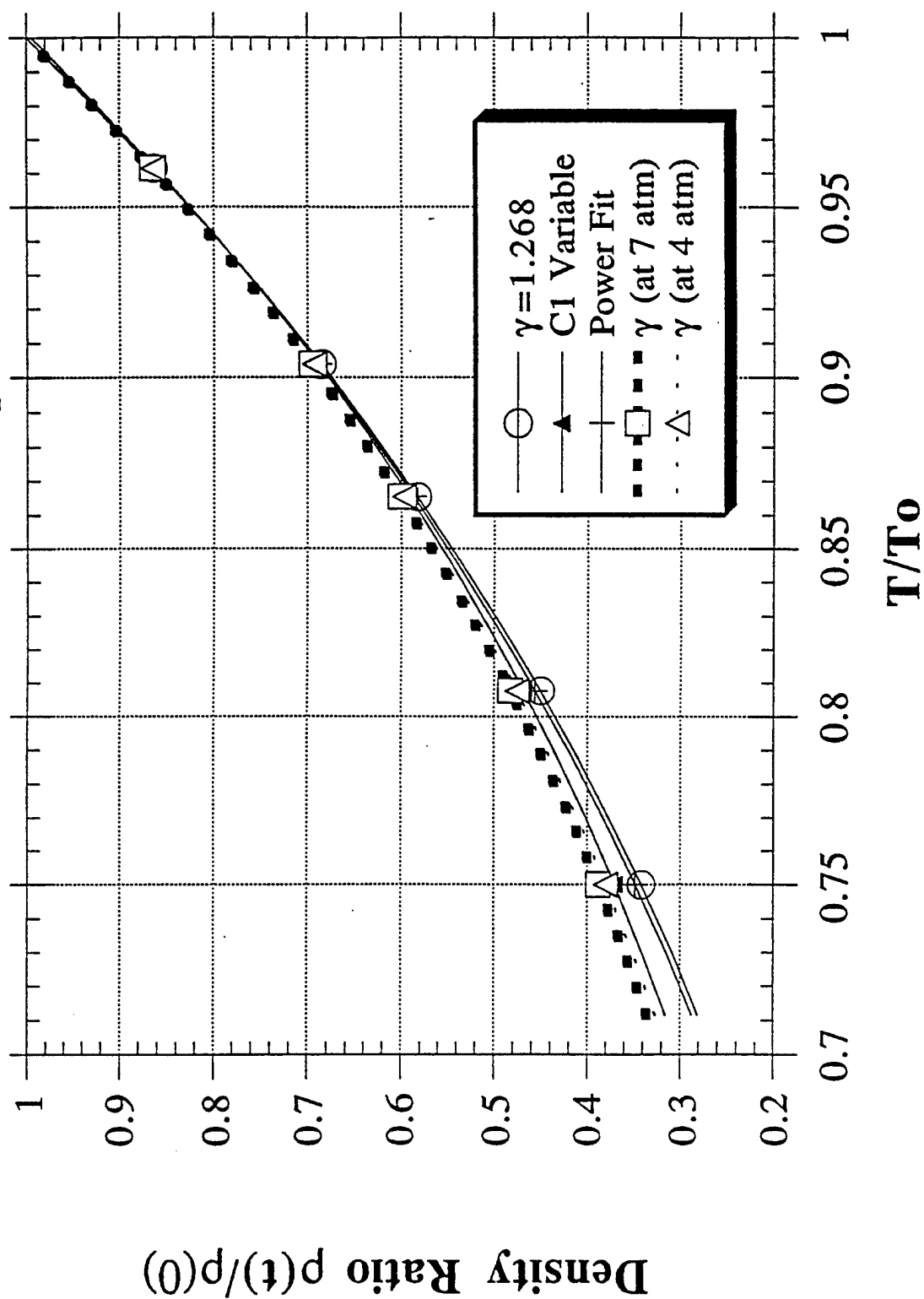**Different Ways of Calculating the Density Ratio as a Function of the Temperature Ratio**

Figure C-13a
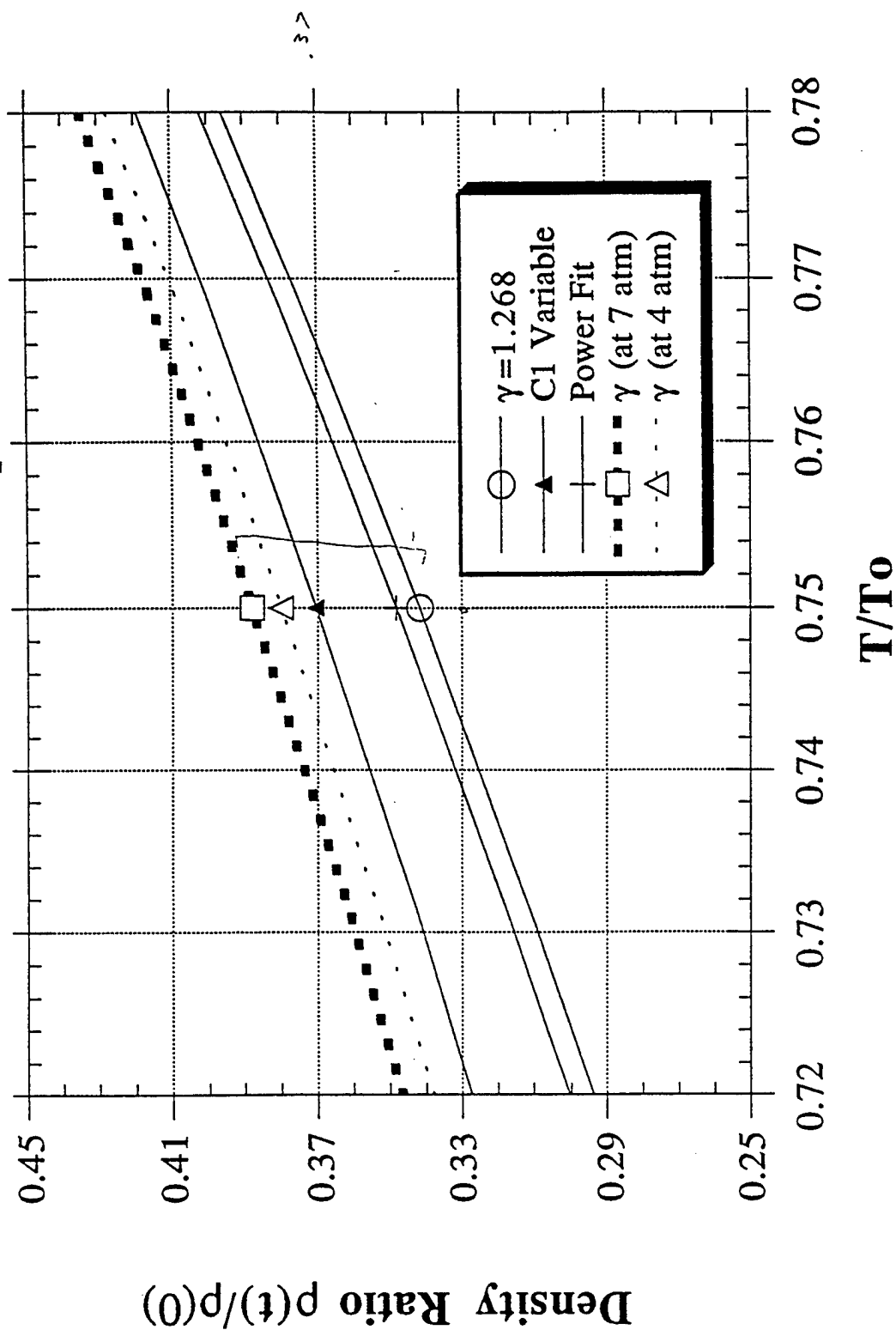## Different Ways of Calculating the Density Ratio as a Function of the Temperature Ratio

Figure C-14
Variation in Methods for Calculating the Density Ratio

Figure C-15
Difference in Density Ratio Based on
C1 and γ (Indep. of Press.)

Figure C-15a
Difference in Density Ratio Based on
C1 and γ (Indep. of Press.)